UNIVERSITETET
I OSLO

PHD THESIS

Transient glacier dynamics and subglacial hydro-mechanical processes

Candidate:
Coline BOUCHAYER

Supervisors:
Prof. Thomas V. SCHULER
Dr. Ugo NANNI
Prof. François RENARD
Dr. Kjetil THØGERSEN

A thesis submitted in fulfillment of the requirements for the degree of Philosophiae Doctor

at

University of Oslo

Pour toi, Bonpapa.

Series of dissertations submitted to the
Faculty of Mathematics and Natural Sciences, University of Oslo
No. 2692

ISSN 1501-7710

Cover: UiO.
Print production: Graphic center, University of Oslo.

Abstract

The Cryosphere, comprising components such as sea ice, permafrost, snow, mountain glaciers, Arctic and Antarctic glaciers, and ice sheets, faces a significant threat due to ongoing climate change. The present and future evolution of these cryospheric components hold the potential to profoundly impact Earth ecosystems, human lives, and livelihoods. To comprehend and accurately project their future trajectory and consequential effects, an improved understanding of the dynamics governing these systems is imperative. This understanding is pivotal for informing mitigation strategies and urgent policy decisions.

Within the realm of the Cryosphere, the flow of glaciers and ice sheets presents a critical concern for future sea-level rise. Futhermore, the intricate transient velocity dynamics exhibited by some glaciers remain inadequately understood, despite their capacity to dramatically alter projections of future sea-level rise. This doctoral research aims at enhancing our comprehension of the underlying processes governing transient glacier flow dynamics by delving into the subglacial hydrological and mechanical feedback mechanisms. The investigation primarily centers around surge-type glaciers. These glaciers exhibit cyclic patterns of rapid flow for brief duration, bounded with extended periods of slow movement. I performed a comprehensive analysis spanning multiple scales: regional examination across the Svalbard archipelago, glacier-specific investigation of Kongsvegen glacier within the same region, and localized assessments within this glacier. This research encompasses various temporal scales, ranging from timeless analyses to studies extending over several years. Employing a multidisciplinary approach, the research integrates glacier flow, subglacial hydrology, subglacial mechanics, and a diverse array of methodologies including data mining, machine learning modeling, field observations, and cryoseismology.

The research findings offer several insights. First, I show that surge-type glaciers demonstrate distinctive geometrical attributes, including increased thickness and width, coupled with a low surface slope. However, these characteristics are non-uniformly distributed across the entire glacier, instead localizing to specific regions that correspond to zones where instability can be triggered. These triggering zones serve as a starting point for an instability to eventually propagate and influence parts or the entire glacier. Moreover, the research underscores the interplay between crevasse formation, efficient conveyance of surface water to the subglacial environment, augmented basal slip and sediment deformation, and subsequent glacier flow enhancement, in turn, opening more crevasses. This hydro-mechanical feedback mechanism emerges as the fundamental driver behind the buildup of glacier surge fronts. Lastly, the intricate relationship between the configuration of the subglacial drainage system,

hydraulic connectivity, and the mechanical properties of subglacial sediment is highlighted as a crucial factor for transient acceleration.

In summary, this work discuss the interplay between ice flow, basal friction, subglacial drainage system, and subglacial sediment mechanic at different spatio-temporal scale orchestrating transient glacier dynamics and highlight future research directions.

Sammendrag

Kryosfæren, som omfatter komponenter som sjøis, permafrost, snø, og isbreer i fjell og polare områder, samt de store innlandsisene, står overfor en betydelig trussel på grunn av pågående klimaendringer. Den nåværende og fremtidige utviklingen av kryosfæren har potensial til å påvirke jordens økosystemer, menneskeliv og levebrød på en dyp måte. Det er nødvending med en forbedret forståelse av dynamikken som styrer disse systemene for å nøyaktig forutsi deres fremtidige utvikling og dens konsekvenser. Denne forståelsen er essensiell for å informere tiltakstrategier og presserende politiske beslutninger. En potensiell akselerasjon av isstrømning i breer og innlandsis vekker bekymring for fremtidig havnivåstigning. Det fins betydelige kunnskapshull knyttet til dynamikken under transiente forhold, til tross for at de involverte prosessene har potensialet til dramatisk å endre projeksjoner for fremtidig havnivåstigning.

Denne doktorgradsavhandlingen har som mål å forbedre vår forståelse av de underliggende prosessene som styrer dynamikken i transient brebevegelse, med særlig fokus på breer av surgetype. Ved å fokusere på subglasial hydrologi og mekaniske prosesser, vil avhandlingen belyse kompleksiteten som resulterer av koblingen mellom de ulike prosessene. Undersøkelsen fokuserer primært på breer av surgetype. Disse breene er karakterisert av sykliske mønstre med rask bevegelse i korte perioder, avbrutt av lange perioder med sakte bevegelse. Jeg utførte en omfattende analyse som strekker seg over flere skalaer: en regional undersøkelse av hele Svalbard-a, en bre-spesifikk undersøkelse av Konsgsvegen-breen innenfor samme region, og lokale undersøkelser på denne breen. Denne forskningen omfatter ulike tidsskalaer, alt fra analyser uten tidsdimensjon til studier som strekker seg over flere år. Ved å bruke en tverrfaglig tilnærming, integrerer forskningen subglasial hydrologi, mekanikk og en mangfoldig rekke metoder, inkludert datamining, maskinlæringsmodellering, feltobservasjoner og kryoseismologi.

Forskningsfunnene gir flere innsikter. Først viser breer av surgetype karakteristiske geometriske egenskaper, inkludert økt tykkelse og bredde, kombinert med en lav overflatehelling. Disse egenskapene er imidlertid ikke jevnt fordelt over hele breens areal, men er heller lokalisert til spesifikke deler som tilsvarer soner der ustabilitet kan utløses. Disse utløsningssonene har potensial til å initiere forstyrrelser som kan propagere, og dermed påvirke hele breen. Videre understreker forskningen samspillet mellom dannelse av sprekker, effektiv transport av overflatevann til brebunnen, økt basal glidning og deformasjon av sedimenter, og etterfølgende akselerasjon av brebevegelsen, som igjen åpner opp for flere sprekker. Denne hydro-mekaniske tilbakekoblingsmekanisme framstår som den grunnleggende driveren bak oppbyggingen av instabiliteter.

Til slutt fremheves det intrikate forholdet mellom konfigurasjonen av det subglasiale dreneringssystem, hydraulisk konnektivitet og mekaniske egenskaper av bunnsedimenter som en avgjørende faktor for transient akselerasjon.

Oppsummert diskuterer dette arbeidet samspillet mellom isflyt, bunnfriksjon, det subglasiale dreneringssystemet og mekanikken i bunnsedimenter på ulike romlige og tidsmessige skalaer understreker dens betydning for å forstå transient brebevegelse og fremhever fremtidige forskningsretninger.

Acknowledgements

On the 28th of August 2023

Four years of research on glaciers. It is the culmination of a long ascent that began with my innocent childhood steps on the snowy mountains of the Alps, followed by the pursuit of a dream when I discovered the profession of glaciologist. The mountains are not climbed alone, and numerous people have contributed to this ascent.

Most of my childhood souvenirs are in the mountains, skiing, hiking, climbing, with my family. You were my ever first rope guides. You introduced me to the mountains from my first steps (maybe you did not even wait for that), then passed on your passion for vast spaces, the beauty of summits, and the thirst for adventures, along with Jul's and Nono, my first (and still!) rope companions. You have always supported my professional and personal choices (how strange they may be) and advised me with kindness. Thank you for everything, Maman, Papa, Grand-Pere, Mathy, Malili, and Bonpapa.

Then, my training initiated in Grenoble, where I met my first professional rope guides, Christian and Vincent. I was barely aware that glaciologist was even a thing that I embarked into a steep learning process where you taught me everything that a beginner needs to know about glaciers with patience, humor, and passion. Our regular discussions and your advice guided me to grow, as a glaciologist and as a person, and to pursue a PhD in this field. My will to continue in academia has as well strengthened with Vincent and Pascal during my Master thesis. I learned a lot about snow and sharpened my academic skills working with you. Even if I came back to the glaciers topic, I thank you deeply for having inspired me to become a researcher.

From the Alps to Norway, my PhD advisors took over the relay and guided me for four years through the path to reach this new summit, the PhD degree. Thomas, thank you for giving me the opportunity to climb this peak by accepting me and my French character to work jointly with you during these four years. When not in the office, we shared many successful field campaigns in Svalbard and for a fellowship that was not originally supposed to involve any fieldwork, I was able to extensively discover and enjoy the wonders of the Arctic. Thank you for these adventures! Francois, you kept a cool head when mine was boiling, always calm and serene in guiding me back on track when I faltered. Your passion for research and dedication for your students are inspiring, and I felt greatly supported working alongside you. Kjetil, your physicist perspective on glaciology has enlightened and challenged me in approaching glaciology today. You showed me that bridging different field is a strength, even if understanding each others jargon and backgrounds requires

effort. I learned that even coming from a different background, everything can be learned, but with more or less effort (guess who needed to put the most effort). Ugo, it is hard to know where to begin. You have always accompanied and supported me, starting from our Master together in Grenoble. Who would have thought that five years later we would work together again and that you would take on this supervisory role after all? Our mutual experiences has over time forged a professional partnership that elevates us to achieve our individual goals while continuing to nurture a strong friendship. Thank you for your honnest feedback, the trust you give me on the field, your repeated explanations over and over again of basic principles that I have not understand, the numerous discussions about our future aspirations and so much more. In brief, thank you for being a loyal work companion and a very good friend.

I also would like to deeply thank my opponents, Tavi Murray, Martin Truffer, and Mathew Domeier, for agreeing to meet me at the summit and evaluate the effort put into these four years of research. Your time is precious and your expertise, flawless. I am honored to share the end of this journey with you.

I would like to deeply thank my rope companions. You have contributed to the progress towards the summit, keeping the rope taught to jump over crevasses, helping and teaching me to tie knots, turning back when the weather was unfavorable, and starting anew the next morning. Thanks to all my co-authors, John, Kjetil, Francois, Thomas, Andreas, PiM, John, Louise. This journey has been also yours and I would not have succeeded without you.

To prepare for the ascent and gather precious data for my thesis, we needed a very skilled and experienced person. John, whether it is conceptualizing new instruments, engaging in mechanics, electro-mechanics, plumbing, welding, sharing a beer, or competing in an underwater breath-holding competition in a jacuzzi (that, btw, you remember that you lost?), you are truly THE indispensable person in the field and it was a pleasure working and spending time with you! In addition to the core MAMMAMIA group, we needed even more reinforcement. So, during our Arctic expeditions, we had the support of exceptional field assistants. Thanks to Wenxue (the best Arctic co-pilote), Basile (the Ny-Ålesund king of the shorts), Adrien (the real mountaineer), Urs (Mr ploughmeter) and Ashley (the British tea drinker) for their invaluable and energetic help during the Arctic field campaigns. In addition, a lot a unpredictable things happen when it comes to ice borehole drilling and we would not have manage to overcome these challenges without the generous help of the NP crew, especially Cat', Ceslav, Simon, PiM, Jack, Svein, JC and Steve,!! I was always so happy to go up to Ny-Ålesund to retrieve you, guys, and share coffees, discussion, snowy, icy and safari expeditions, parties at Mellagret, sauna, jacuzzi and so much more! Last but not least, thanks to the permanent or seasonal team in Ny-Ålesund, especially those from King's Bay, NP,

the blue house, Corbel, and Italy, for your work in the town and on the field and more importantly, for making these visits to Ny-Ålesund unforgettable.

I would like as well to thank the incredible Alaskan team for having taking me on the same rope as yours during this incredible McCarthy summer school! I will never forget this experience. A massive thank you for organising this amazing summer school and for creating a close-knit community bounded around your passion for glaciers and the unwavering commitment to pass on your skills. A big shoutout to Regine, Martin, Andy, Mark, Ed, Eric, Sarah, Aleah and of course, all my buddies, especially Tess, Yoram and Victor!

Eager for glacier, snow-covered, rocky, or explosive summits, colleagues from GeoHyd and Njord have been by my side, sharing similar passions and troubles. Whether in hallway discussions or spirited debates, snowy or maritime and forest adventures, beach barbecues or dinners at each other's places, and daily lab lunches inside looking at the Norwegian rain or on the terrace enjoying the sun, LønningsPils or spontaneous afterwork beer, you have always been there to discuss, debate, laugh, share, care and create a joyful work atmosphere, which is so important to ascend our summits with (almost) serenity. Thank you all!

I also want to give a special thank to Lea and Juditha, my friends, with whom I began my thesis journey simultaneously. We were not part of the same rope team, but we had the same summit in mind, the PhD. Like mountaineers returning to the base camp after each expedition step, we debriefed our experiences over numerous coffees and deep discussions, learning from each other. Though seemingly trivial, I believe all these discussions have truly contributed significantly to accomplishing this project. From colleagues, we became super good friends, sharing many hours outside the lab to talk (yes, again!), ski (or fall), have dinners (or a drink), play coinche with Ole, meet up (at two or three), complain (a lot), laugh (even more), and forget (or celebrate) the long day that we had all just gone through! My time with you, girls, has been amazing so far and I am sure it will continue, no matter what is the next challenge, thank you so much!

After each ascent attempt, whether successful or unsuccessful, I found comfort with my friends in the valley. First, I want to thank you, my ever-present French friends, even though thousands of kilometers separate us. We have taken different paths and have different mountains to climb, but between summits, we always find time to reconnect, call each other, and support each other through life's challenges. Thank you to the sport gang, Zazou, Marie, Axou, Riss, Thomas, Jo, Roche, Bib; the Beauvais crew, Camie, Flo, Alice, Camille, Paul, Marion, Cons and the 077 promotion; and lifelong friends from Lyon, Minette, Mome, Marie, Bere, Tif. You have always been here, merci!!

In this initially unknown land, I finally found a new cocoon in Norway,

thanks to you, my friends here, and especially Thea, whom I met in Svalbard. I owe much of my social integration in this culturally different country to you. You took me under your wing and opened my eyes to the many advantages of life in Norway. Apparently, you did not only convince me, but Cat' too! The Ny-Ålesund alchemy among us three adventurous girls keeps its vibes alive here in Oslo! We have gathered already so many souvenirs of unforgettable escapades and the excitement of the train shows no signs of stopping. Shoutout to Simon, PiM, John, Marius and Chris for occasionally jumping aboard and joining our wild ride. Big thanks to all of you!

My social ascent in Norway lead me to find an intimate rope companion, Carlo, with whom I share my life. You have managed to tie in with me to build our cocoon in Oslo which provided me with comfort, attention, magical moments, fantastic adventures, laughter, discussions and so much more. Coming home in the evening and being by your side significantly contributed to this journey. Thank you Bebe!

I want to re-iterate my thank to each and everyone of you for being by my side throughout the journey towards the summit, because I won't lie – it did not always feel like an easy walk in the park!

Coline

Preface

During the duration of my PhD, significant global events have occurred, including the worldwide Covid-19 pandemic and the resurgence of conflicts in Europe. However, this section does not intend to provide an exhaustive list or elaborate on these events. Simultaneously, significant advancements in technology have taken place, and I have had the opportunity to witness and utilize them. One of the latest advancements that I would like to briefly discuss is the introduction in November 2022 of the pre-trained ChatGPT (3.5, 2023) model developed by OpenAI (Brown et al., 2020). This powerful tool has sparked extensive discussions and raised important concerns within the scientific community. Questions have arisen regarding the role of AI in assisting with paper writing, whether ChatGPT should be acknowledged as a co-author, and potential issues related to plagiarism (Aczel and Wagenmakers, 2023).

In light of the controversies surrounding the usage of ChatGPT in academic writing, I have made a conscious decision to be transparent about my utilization of the tool in the composition of my PhD thesis[1]. I want to clarify that while I extensively utilized ChatGPT during my research, none of the information presented in this thesis is sourced directly from ChatGPT's responses to my inquiries. Instead, the majority of the text generated by ChatGPT was employed as a reference point for me to improve and refine my own writing. Specifically, phrases such as "re-write that in a better way: [my text]" were used as prompts to enhance the clarity and coherence of my work.

In addition to using ChatGPT for enhancing my writing, I also leveraged its capabilities as a synthetic tool. At times, my writing could become convoluted and maintaining a clear narrative thread that keeps the reader engaged proved to be a challenge. To address this, I employed ChatGPT to assist in synthesizing ideas and extracting keywords from my paragraphs, aiding in the restructuring and refinement of my text. Through prompts such as "shorten this paragraph, extracting the main important information: [my text]" or "extract the key words from: [text]," I utilized ChatGPT's capabilities to streamline and condense my writing, ensuring that the essential information was conveyed effectively. It served as a valuable resource to help me distill complex concepts and communicate them more concisely, enabling me to maintain a coherent and reader-friendly flow throughout my work.

I utilized ChatGPT primarily as a tool to facilitate organized thinking throughout the process of writing my PhD thesis. I firmly maintain that the content presented in this thesis represents my original work, and the thoughts and

[1]The University of Oslo lacks specific guidelines regarding the use of ChatGPT as a tool for aiding in the writing of PhD theses. However, there is an agreement with the faculty that this particular PhD thesis will serve as a pilot study to inform future decisions.

ideas developed herein are entirely my own. However, much like attributing acknowledgment to Prof. X or Y for reviewing and providing feedback on a research paper, I wanted to ensure transparency regarding the significant improvements made to the text with the assistance of ChatGPT. While the core concepts and analysis remain my intellectual property, it is important to recognize that the text itself has undergone substantial refinement through the use of ChatGPT. This preface is intended to give credit to the role of ChatGPT in enhancing the clarity and cohesiveness of the written material, while affirming my ownership of the ideas and arguments presented in this thesis.

Contents

List of Figures

Chapter 1

Introduction

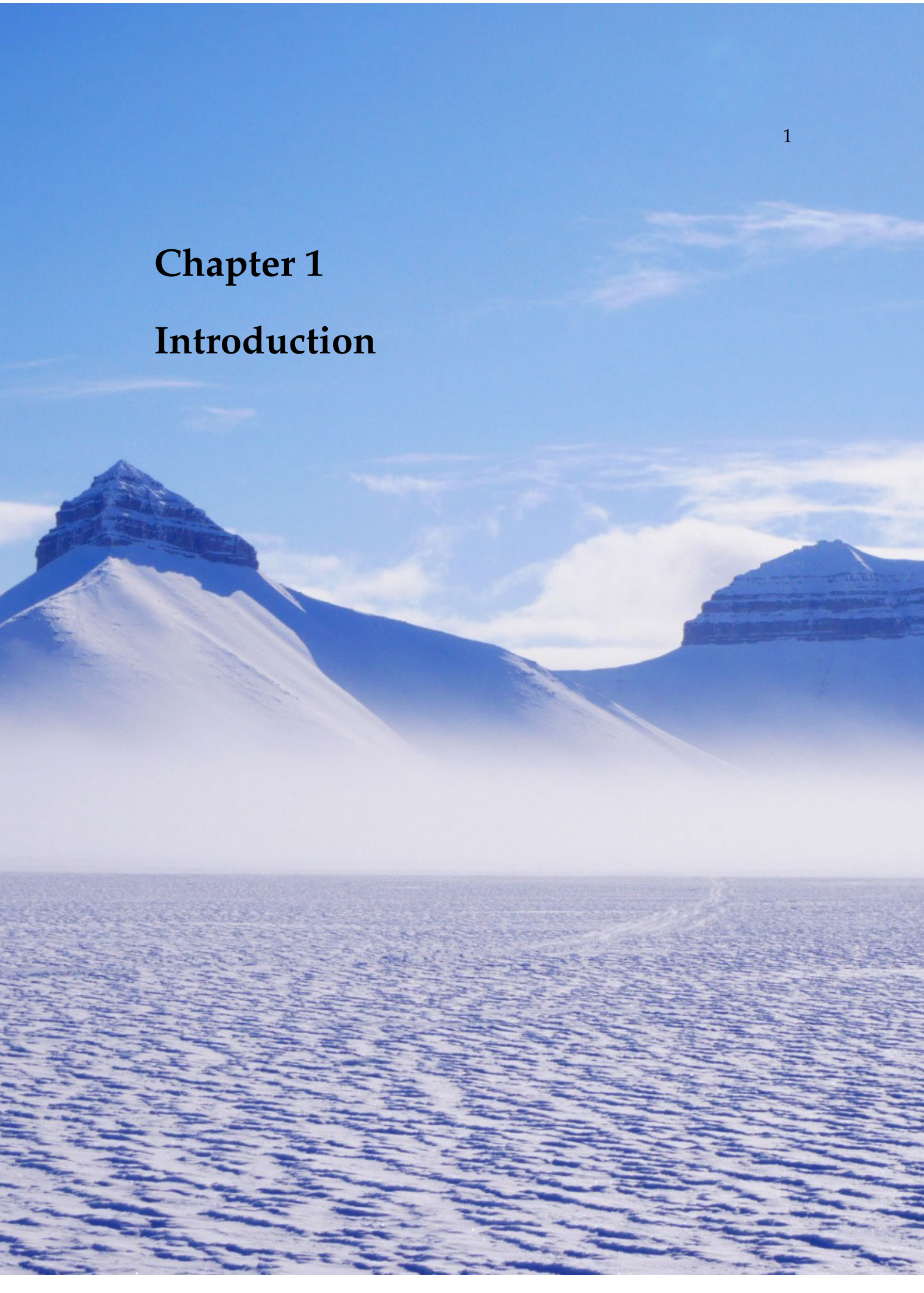

"Learn from yesterday, live for today, hope for tomorrow. The important thing is not to stop questioning." - Albert Einstein

1.1 Anthropogenic climate change

The world is currently undergoing unprecedented and rapid changes caused by climate change, posing a significant threat to the ecosystems (Grimm et al., 2013; Malhi et al., 2020), lives and livelihood (McMichael et al., 2006; Ravindra et al., 2019), and the cryosphere (IPCC, 2021; ICCI, 2022; Rounce et al., 2023). Analysis of past CO2 concentrations from paleo-archives such as ice cores and sediment cores from ancient lakes (Burke et al., 2018) has revealed that during Ice Age periods, CO2 levels were consistently around 180 ppm, while warmer inter-glacial periods saw levels around 280 ppm, going back 3 million years (Rapp et al., 2009). Over the last 10 000 years, Earth CO2 concentration remained relatively stable, at 280-285 ppm until 1850. However, with the burning of fossil fuels associated with the begin of the industrial era, CO2 levels began to rise, reaching 320 ppm by 1920, 320 ppm by 1960, and surpassing 400 ppm around 2015 (ICCI, 2022). In 2022, CO2 levels exceeded 422 ppm twice in daily averages, and the average CO2 level for 2023, measured at the Mauna Loa observatory, is projected to reach 420.2 ± 0.5 ppm (US Department of Commerce, 2005). This will be the first time that the average annual CO2 concentration surpasses 420 ppm (MetOfficeUK, 2022). Despite climate pledges aligned with the 2015 Paris Agreement, the concentration of CO2 continues to increase by 2 to 3 ppm annually, surpassing expectations of reaching peak emissions by 2020 (ICCI, 2022).

Through the continuous emission of CO2 and other greenhouse gases, the world is pushing the planet beyond anything experienced in the past 3 million years. The Intergovernmental Panel on Climate Change has projected future carbon emission pathways based on the adoption of different climate policies and mitigation measures (IPCC, 2018; IPCC, 2021). Based on these scenarios, the future of the cryosphere can be anticipated. These reports emphasize that only the two lowest emission pathways offer a chance to prevent long-lasting impacts on the cryosphere, as the processes involved cannot easily reverse within a timeframe shorter than centuries to tens of thousands of years. The importance of adhering to these lower emission pathways becomes apparent when considering the irreversible consequences that could otherwise occur (ICCI, 2022). Even by staying in the lowest emission pathways scenarios, the world has already committed to see the disappearance of some component of the cryosphere (e.g., the summer Arctic sea ice, Kim et al., 2023).

1.2 Sea level rise and the cryosphere in a changing climate

Transient glacier dynamic examples

- Marine Ice sheet instabilities: rapid changes in marine-based ice sheets, like in Antarctica and Greenland, caused by interactions between ice, bedrock, and ocean. They lead to increased ice flow, discharge into the ocean, and rising sea levels. Key factors include ice shelf retreat and grounding line collapse, impacting ice sheet dynamics and global sea-level rise predictions.
- Glacier lake outburst flood: sudden release of a large amount of water stored in or under a glacier or ice cap. This can occur due to various triggers, such as the melting of ice, volcanic activity, or the collapse of an ice dam.
- Glacier surges: rapid and temporary accelerations in the flow of certain glaciers. During a surge, a glacier can suddenly increase its speed by several orders of magnitude compared to its normal flow. These events are typically characterized by a rapid advance of the glacier's terminus followed by a period of slower movement or stagnation. Surges are caused by complex interactions between the glacier, its underlying bed, and the presence of water at the base of the glacier (see as well Sect. 1.4).
- Glacier collapses: abrupt and extensive retreats or disintegration of glaciers, where large sections of ice detach and rapidly move or break apart. These collapses can be triggered by various factors, including warming temperatures, increased meltwater, ocean interactions, and underlying geothermal activity.

Presently, approximately one billion individuals reside in areas situated less than 10 m above the current high tide lines, with 230 million people living within 1 m, representing 13% of the global population at risk (McGranahan et al., 2007; Neumann et al., 2015). Sea-level rise disproportionately affects low-income communities and people of color, exacerbating climate justice concerns and impacting those who are the least responsible for greenhouse gases emissions (Pettit, 2004; Schlosberg and Collins, 2014; Davis and Todd, 2017). The consequences of rising sea levels extend beyond social and environmental implications; they also carry significant economic costs. Without adaptation measures, a sea-level rise of 1 to 2 meters by 2100 could result in economic losses ranging from $14 trillion to $27 trillion globally (Kirezci et al., 2020).

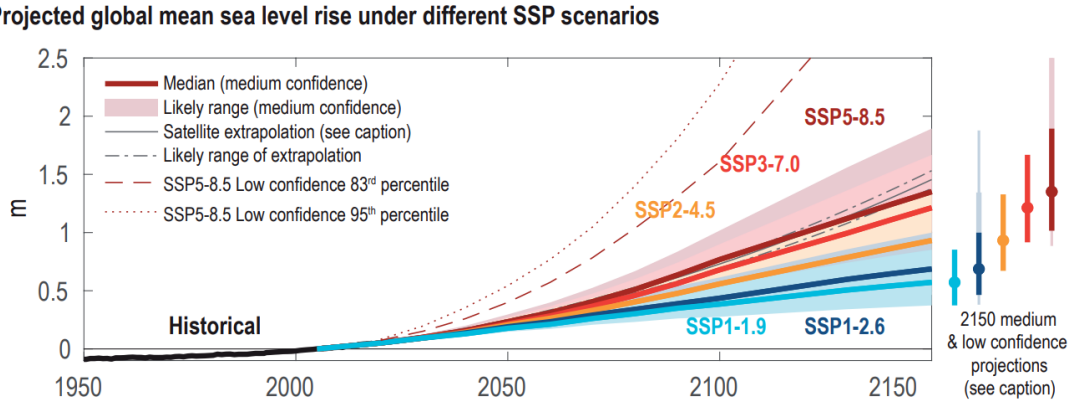

FIGURE 1.1: Projected global mean sea level rise under different Shared Socio-economic Pathway (SSP) scenarios. Projections and likely ranges at 2150 are shown on right for each scenarios. Lightly shaded ranges and thinner lightly shaded ranges on the right show the 17th–83rd and 5th–95th percentile ranges for projections including low confidence processes e.g. ice-sheet instabilities for SSP1-2.6 and SSP5-8.5 only. Including instabilities can change drastically future global mean sea level rise projections, modified after IPCC (2021).

Sea-level rise is currently primarily driven by two factors: the expansion of warmer seawater (due to its increased volume, e.g., Llovel et al., 2019; Zanna et al., 2019; Frederikse et al., 2020) and the loss of mass from glaciers (e.g., Zemp et al., 2019; Hugonnet et al., 2021; Rounce et al., 2023). From 1901 to 2018, these factors contributed 38% and 41% to the overall sea-level rise, respectively (IPCC, 2021). Glaciers are sensitive to climate variability and respond by expanding or shrinking in size (Harrison, 2013; Roe and Baker, 2016; Marzeion et al., 2018). Glaciers lose mass by melting and sublimation. For glaciers terminated in ocean and lakes, they also lose mass by frontal ablation/calving. Modification in glacier geometry under current climate change affect back these processes, e.g., glacier melt amplification as the glacier ice reaches lower altitude due to reduce thickness, and glacier flow accelerations that can amplify the calving rate. Consequently, these changes circle back to impact the glacier geometry and its responsiveness to shifts in climate conditions. Most of the world glaciers are out of balance with the present climate and projections suggest that glaciers could lose 26 ± 6% (in scenarios with the lowest greenhouse gas emissions) to 41 ± 11% (in scenarios with the highest greenhouse gas emissions) of their mass by 2100 compared to 2015 levels, contributing to a sea-level equivalent of 0.90 m ± 0.26 m to 1.54 m ± 0.44 m (Rounce et al., 2023). Although ice sheets currently do not play a dominant role in global

sea-level rise, their contributions have increased fourfold from 2010-2019 compared to 1992-1999 (Bamber et al., 2018; Mouginot et al., 2019; Otosaka et al., 2022). Their future contribution to sea-level rise is expected to become dominant. Greenland contribution to sea level rise is estimated to be 0.3 m ± 0.07 m sea-level rise regardless of the carbon emission pathways (Box et al., 2022).

Overall, in the past century, global sea level has risen by 0.16 to 0.210 m, (Frederikse et al., 2020). Even with immediate and substantial reductions in carbon emissions, projections indicate that sea level will continue to rise between 0.37 m (in scenarios with very low greenhouse gas emissions) and close to 2 m by 2150 (in scenarios with very high greenhouse gas emissions) compared to the 1995-2014 baseline (Fig. 1.1, light blue and dark red curves, respectively, IPCC, 2021). The future picture of sea-level rise can however be much more dramatic (approaching 2 meters by 2100 and 5 meters by 2150, Fig. 1.1, dashed dark red curve, IPCC, 2021) under very high greenhouse gas emissions scenarios considering glaciers and ice-sheet instabilities and their responses to changing conditions, processes that are still currently not well understood (IPCC, 2021; Golledge and Lowry, 2021; González-Herrero et al., 2022; Box et al., 2022).

General goal of my doctoral research: One critical question that the scientific community must address to better constrain the future projection of sea-level rise is the processes driving short-term changes of glaciers and ice sheets in response to varying environmental conditions, referred to as transient glacier and ice sheet dynamics (Fig. 1.1, DeConto et al., 2021; Bamber et al., 2022). The most striking examples of such dynamic are e.g., marine ice sheet instabilities, glacial lake outburst floods, glacier collapses and surges. These events are driven by the complex interplay between changes in subglacial hydrological conditions and mechanical processes in response to climate variability. My doctoral research aims at refining the comprehension of these mechanisms and their interconnections by adopting a multi-observational approach performed at different spatio-temporal scales. The investigation centers on characterising unstable zones within glaciers, comprehending the hydro-mechanical interplay governing the propagation of instabilities, and examining the alterations within the subglacial hydrology and sediment mechanics induced by forcing, e.g., surface melt water, variations.

1.3 Glaciology: a short recap'

Note to the reader: Much of the information presented in this section draws from the book Cuffey and Paterson (2010). Therefore, unless otherwise stated, the information

can be attributed to this source.

Before delving into the complex processes associated with transient glacier dynamics, I provide in this Section a concise description of glacier dynamics that applies broadly to all glaciers. I first take a step back and define what is a glacier (Sect. 1.3.1). Then, I dive into the different components of glacier hydraulics (Sect. 1.3.2) before dissecting the different processes driving glacier flow (Sect. 1.3.3). Within each section, I provide a description of the fundamental basis of our current knowledge, while also spotlighting unresolved enigmas. The purpose of these subsequent portions is not to offer a complete overview but rather to accentuate the perplexities I tackle within this thesis.

Some useful definitions

- Overburden pressure: pressure caused by the weight of the overlying material at specific depth.
- Normal stress: force acting perpendicular to the surface, here the stress applied by ice overburden pressure times the sinus of the surface slope.
- Shear stress: forces that cause deformation of a material by sliding, here stress applied by overburden pressure times the sinus of the surface slope.
- Effective stress: normal stress minus pore-water pressure.
- Shear strength: the ability of a material to resist forces that cause the material internal structure to slide against itself.
- Strain rate: amount of deformation caused as a result of stress.
- Effective pressure: the difference between the overburden pressure and the basal water pressure.
- Rate-strengthening friction: the steady-state frictional resistance increases with sliding velocity.
- Rate-weakening friction: the steady-state frictional resistance decreases with sliding velocity.

1.3.1 What is a glacier?

"This huge ice is, in my opinion, nothing but snow, which... is only a little dissolved to moisture, whereby it becomes more compact..." wrote William Baffin

in his note on his search for the North-West passage (Fotherbye, 1881). He then believed that a glacier originates from compacted snow that undergoes various processes involving the percolation of water. While the concept of glacier may appear straightforward, the reality is more complex, although William Baffin was not far from the truth. Glacier ice is indeed sourced from snow through e.g., snowfall, avalanches, snow drift. At the surface, snow metamorphoses due to surrounding temperature changes and interactions with the atmosphere (Dadic et al., 2010; Chen and Baker, 2010). Beneath the surface, the compaction of snow occurs in three successive stages (Herron and Langway, 1980; Arnaud et al., 2000). Initially, near the surface, grain growth and realignment arise from grain boundary sliding, leading to compaction (Alley, 1987). Subsequently, compaction intensifies as rising overburden pressure which induces creep deformation and the emergence of inter-granular bonds (Wilkinson and Ashby, 1975; Wilkinson, 1988; Spencer et al., 2001). Ultimately, interconnected pores close, and air bubble compression drives the final compaction phase (Alley and Bentley, 1988; Salamatin et al., 1997; Gregory et al., 2014). In environments where water is present, compaction combines the dry snow compaction mechanisms just mentioned, with water refreezing, which can augment or hinder the densification process (Colbeck, 1976; Machguth et al., 2016; Meyer and Hewitt, 2017). Glacier ice contains approximately 10% air bubbles that are trapped within the matrix. These air bubbles serve as preserved samples of the atmosphere from the time of their formation and subsequently provide a unique record of past climates (Jouzel and Masson-Delmotte, 2010).

A glacier is often sub-divided into two areas: the accumulation area and the ablation area. The former refers to the broad upper region of the glacier that experiences a yearly mass gain (yearly mass balance is positive) and where snow is still found at the end of the ablation seasons. The latter refers to the broad lower region where the yearly mass budget is in deficit (yearly mass balance is negative) covered by bare ice at the end of the ablation seasons. The altitude separating these two zones (and where the yearly mass balance is zero) is often conceptualised as a line called the equilibrium line altitude (hereafter, referred to as ELA). Accumulation is made by snowfall, avalanche deposition, refreezing of water and wind deposition. Ablation happens by melt, sublimation and calving/frontal processes. In terms of mass balance, a glacier is considered at equilibrium when the yearly mass accumulated equals the yearly mass lost. Overall, only a tiny fraction of the glaciers worldwide remains currently at equilibrium (IPCC, 2021; Rounce et al., 2023). Glaciers and ice sheets flow to transport accumulated mass from higher elevations to lower ablation areas. This flow is determined by the balance between driving stresses, such as gravitational forces that pull the glacier downhill, and resisting stresses, including

shear stress along the bed, lateral drag along the sides, longitudinal stress gradients that exert pulls and pushes, and buttressing effect of the ice-shelves (Nye, 1952, see also Sect. 1.3.3). Glaciers and ice sheets are considered to be in dynamic equilibrium when the forces are balanced. The two major ice sheets are out of dynamic equilibrium mainly caused by the thinning and break-up of their ice-shelves leading to the acceleration of ice flow from the land into the sea and the calving rate, having catastrophic effect for the sea-level rise (e.g., Mouginot et al., 2015; Reese et al., 2018; Gudmundsson et al., 2019; Banwell et al., 2021; Greene et al., 2022)

1.3.2 Glacial hydrology

Glaciers and ice sheets are made of frozen mostly pure water on Earth. Liquid water flows on, through and under them through what is commonly called supra-, en-, and sub-glacial drainage system, respectively. The surface water that access the glacier bed follows a complex journey through the internal pathways of the glacier. It resurfaces at the glacier front, where it feeds rivers or releases freshwater into the ocean. Glacier hydrology encompasses the transportation and storage of the water on and within the glaciers and under the glacier, detailed in Section 1.3.2, which has major implication for glacier dynamic (Fig. 1.3).

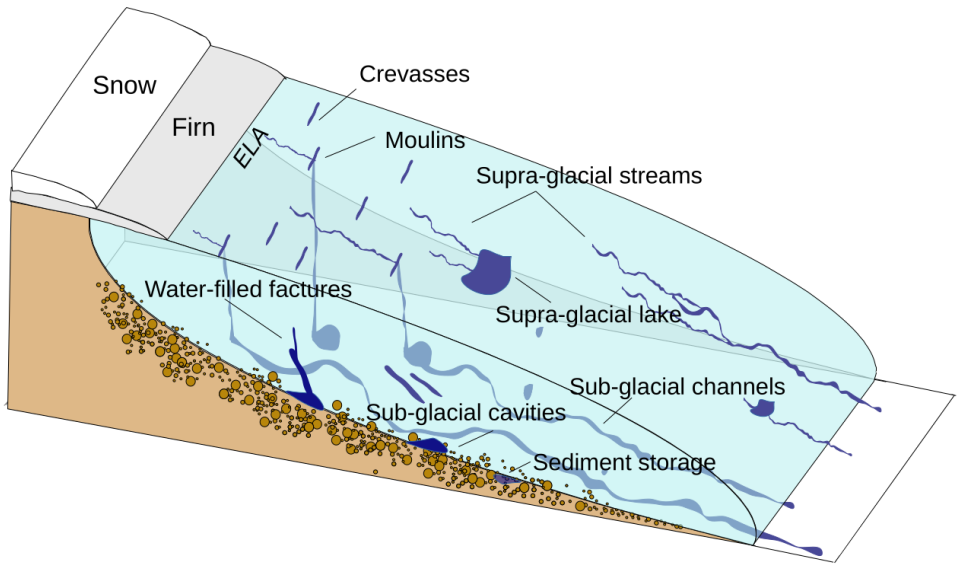

FIGURE 1.2: Schematic figure of the glacial hydrological system.

A journey from the surface to glacier bed

Water at the surface originates from rainfall events and melting processes. Additionally, as the ice deforms, the friction between ice grains generates water (e.g. Clarke et al., 1977). At the base of the glacier, water is introduced through frictional heating (e.g., Schäfer et al., 2014) and geothermal heating (e.g., Larour et al., 2012). The internal- and bed-generated water production generally remains constant over time, but the input of water at the surface varies both in space and time. As water travels along the glacier surface, it acts like a river, gradually eroding the ice creating supra-glacial rivers and lakes (e.g., Das et al., 2008; Smith et al., 2015, Fig. 1.3). It exploits vulnerabilities to seep into the glacier, thereby vanishing from the surface. Crevasses serve as pathways for water to penetrate the interior of the glacier by hydro-fracturing (e.g., Van der Veen, 1998; Colgan et al., 2016, Fig. 1.3) as well as vertical shafts called moulins that act as water highways, connecting the glacier surface to its bed (e.g., Nienow et al., 1998; Covington et al., 2020, Fig. 1.3).

Subglacial hydrology

Water that does not run off along the surface or within glacier eventually reaches the glacier bed, contributing to the formation of the subglacial drainage system (Shreve, 1972). The subglacial drainage system comprises channels, cavities, and conduits through which water flows beneath a glacier at varying basal water pressure (Fig. 1.3). The basal water pressure exerts significant influence on the mechanical coupling between the ice and the glacier bed (referred to as ice-bed coupling), which, in turn, impacts glacier sliding velocity (Weertman, 1957; Lliboutry, 1968; Budd et al., 1979; Iken, 1981; Bindschadler, 1983; Boulton and Hindmarsh, 1987; Fowler, 1987; Kamb, 1991; Hooke et al., 1997). Basal water pressure hinges on the balance between the rate of water supply to the glacier bed and the subglacial drainage system capacity to accommodate it. Basal water pressure decreases when the water supply to the glacier bed occurs at a rate that equals or is lower than the rate at which the subglacial drainage system configuration can evolve to accommodate it. In this configuration, the subglacial drainage system evolution is at equilibrium with the water supply and results in increasing ice-bed coupling and till shear strength in the adjacent areas under the ice. In the reverse scenario, the subglacial drainage system is out of equilibrium with the water supply resulting in decreasing ice-bed coupling and till shear strength in the adjacent areas under the ice (Shoemaker, 1986; Boulton and Hindmarsh, 1987; Rempel, 2009). Therefore, this interplay can drive shifts in glacier stress balance, driving significant rearrangements in ice sheet flow patterns (Tulaczyk et al., 2000; Boulton et al., 2009; Piotrowski et al., 2009; Bougamont et al., 2003; Bougamont et al., 2015;

Elsworth and Suckale, 2016). In the following, we investigate the subglacial drainage system configurations for glaciers resting on solid bed rock, i.e. hard-bed glaciers, and for those resting on subglacial deformable granular material so-called till, i.e. soft-bed glaciers, while addressing the unresolved enigmas.

On one hand, in hard-bed glaciers, two types of subglacial drainage system are generally distinguished: channelised and distributed drainage system. In channelized systems, water is concentrated in well-defined channels that efficiently transport water downstream. The channels form by melting the ice roof by turbulent dissipation of heat, referred to as R-type channels (Röthlisberger, 1972), or by eroding the underlying bedrock, referred to as N-type channels (Nye, 1965). Both types close by creep of the ice. In this configuration, the water is often conveyed efficiently resulting in a relatively low basal water pressure inside the channel. In distributed systems, water is dispersed across a broad area, often in a network of e.g. interconnected cavities, tunnels, sheet. As ice slides over a rough bed, cavities form on the downstream sides of bumps (Lliboutry, 1968). These cavities become filled with water and are interconnected through narrow orifices and water paths within the bed (Walder and Hallet, 1979). This results in a complex network of hydraulic connections where water flows both across and down the glacier. The size and geometry of these cavities is influenced by the melting of ice walls and ice sliding, while closure occurs due to ice creep (Kamb and Engelhardt, 1987). These cavity-like systems usually operate at relatively high basal water pressure resulting from inefficient routing of the water in this configuration. Recent observational studies have added complexity to our understanding of the cavity system by categorizing it into two subtypes based on the linkage between cavities (Andrews et al., 2014; Rada and Schoof, 2018; Rada Giacaman and Schoof, 2023). These studies indicate the existence of hydraulic disconnection between cavities. In these areas, cavities may exist, but they are not sufficiently numerous or large enough to be extensively connected, preventing the flow of water between them. Instead, these cavities potentially act as water storage that can drain during winter, leading to increases in glacier speed during that season (e.g., Vincent et al., 2022).

On the other hand, at present, the understanding of the configuration of the subglacial drainage system in soft-bed glaciers is limited. Initial attempts regarded the subglacial drainage system as an aquifer, where porous flow governed water drainage (Shoemaker, 1986; Lingle and Brown, 1987). While water percolation into the till affects basal resistance and ice flow (Tulaczyk et al., 2000; Bougamont et al., 2003), water transport through the till, predominantly clay-rich, is likely inefficient due to low permeability (Alley et al., 1989; Iverson et al., 1997; Iverson et al., 1998). Subsequent models abandoned the notion of Darcian-type water transport to advocate the presence of a macro-porous

horizon in which the water flow (Weertman and Birchfield, 1982; Alley et al., 1989; Le Brocq et al., 2009; Kyrke-Smith and Fowler, 2014). According to this concept, the macro-porous horizon constitutes a thin, permeable layer of water and sediment, encompassing pore spaces, thin films, cavities, or larger gaps at the ice-till interface. This flow within the macro-porous horizon critically influences basal sliding and till deformation, given its extensive ice contact area. This hypothesis may be less applicable to till consisting of fine grains. Inspired by hard-bed scenarios where subglacial water flow eventually erodes the ice to form an efficient channel, Walder and Fowler (1994), Ng (2000a), and Damsgaard et al. (2017) proposed that a soft-bed efficient system can be carved into the till, called canals. The dynamics of the till, particularly till erosion and deformation, emerged as pivotal for canal sustainability (Walder and Fowler, 1994). Steady-state conditions were investigated by Walder and Fowler (1994) and Ng (2000a), revealing that canals remain separate and resemble cavities in hard-bed contexts. However, Walder and Fowler (1994) ignored that till is known to deform only above a certain threshold, and parameterized till to continuously creep toward the channel and counteract fluvial erosion. Recently, investigations into deglaciated landscapes, focusing on landform and sediment records, aims at investigating subglacial fluvial erosion, deposition, and sediment mobility (Damsgaard et al., 2017; Beaud et al., 2018; Hewitt and Creyts, 2019; Vérité et al., 2022; Kirkham et al., 2022), to further constrain the complex configuration and evolution of the subglacial drainage system on soft-bed glaciers.

In both hard- and soft-bed glaciers, the subglacial drainage system is dynamic and constantly adjusts in accordance with variations in water input: (i) canals embedded in till can erode and deform, while channels undergo expansion due to heat generated through friction against their walls; (ii) channels contract under the influence of ice movement, (iii) cavities within the system enlarge due to sliding effects and reduce by creep, (iv) the orifices connecting them enlarge through both sliding forces and the dissipation of heat and close by creep (Clarke, 1996; Kessler and Anderson, 2004). Therefore, the configuration of the subglacial drainage system cannot be regarded alone and its evolution needs to be coupled with glacier flow, basal sliding and subglacial till deformation and transport (Sect. 1.3.3), detailed in the sections below.

1.3.3 How do glaciers flow?

Glaciers can be viewed as solid rivers in that their flow is the result of (i) ice deformation (Fig. 1.3a), (ii) basal sliding (Fig. 1.3b) and (iii) bed deformation if at all (Fig. 1.3c). The combination of these processes allows the accumulated ice in the upper accumulation areas to flow downhill, ultimately reaching the

lower ablation areas. The velocity of glaciers can vary greatly, ranging from nearly stationary (few meters per year, e.g., Meserve glacier, Cuffey et al., 2000) to speeds on the order of several kilometers per year (e.g., Jakobshavn glacier, Joughin et al., 2004). Glacier velocities can also change over time due to seasonal fluctuations (e.g., Bingham et al., 2003; Moon et al., 2014), long-term climate trends (e.g., Oerlemans, 2001), or transient events like glacier surges (Meier and Post, 1969; Truffer et al., 2021). The wide-spectrum of glacier velocity observed emerges from e.g., the diverse glacier geometries, the characteristics of their bed, and the climatic conditions in the glacier surroundings. In the following sections, we explore in more details the processes regulating glacier flow.

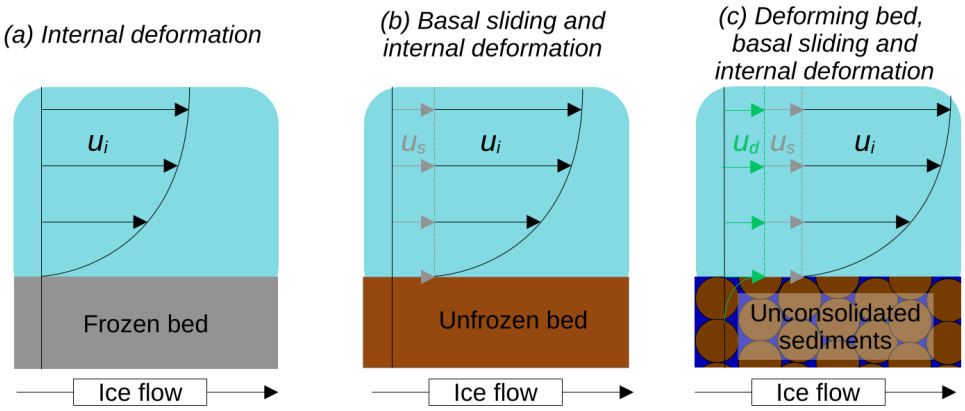

FIGURE 1.3: Schematic of processes driving ice flow. a) Ice deformation, b) basal sliding and internal deformation, c) bed deformation, basal sliding and internal deformation.

Ice deformation

Glacier ice undergoes a gradual and constant deformation in response to applied stress, referred to as creep (Glen, 1955; Weertman, 1983). This process involves the mutual displacement of ice crystals due to shear stress, resulting in a gradual forward movement in the direction of the ice-surface slope. In cases where ice creep alone cannot accommodate the internal stresses, folding and faulting become prevalent (e.g., Nye, 1952; Meier et al., 1974; Hambrey and Dowdeswell, 1994; Hambrey and Lawson, 2000; Colgan et al., 2016). The rate of creep diminishes with depth. Surface areas experience the swiftest ice motion, whereas the base and valley sides exhibit slower or negligible movement due to the substantial resistive forces (Jiskoot, 2011). When subjected

to substantial stress, the ice can fracture in a brittle manner, leading to the formation of surface and basal crevasses (e.g., Colgan et al., 2016). The behavior of ice material, a combination of deformation and fracturing, is intermediate between viscous rheology, i.e., where stress and deformation rate are proportional, and plastic rheology, i.e., deformation occurs only beyond a critical stress threshold (Duval et al., 2010).

Basal sliding

Basal ice is at the pressure melting point when the pressure at the glacier bed is exceeded by the ice overburden pressure. Pioneers in glaciology recognise that this condition allows the ice to slide over the glacier bedrock (De Saussure, 1796; Forbes, 1843). Wet ice on a smooth surface exhibits slipperiness, facilitating the sliding motion at the interface between the ice and the bed. In combination with the subglacial water control, the sliding behavior at the ice-bed interface is influenced by e.g., refreezing of the ice at the bed (e.g., Hubbard and Sharp, 1993), the roughness of the bed (e.g., Hoffman et al., 2022) and the amount of rock debris within the glacier ice (e.g., Iverson et al., 2003). Understanding the mechanics of basal sliding in glaciers remains a significant challenge in the field of glacier physics.

One of the primary obstacles is the absence of a universally applicable sliding law. A sliding law is a mathematical relationship that connects the shear stress, denoted as τ_b, with the sliding velocity u_b and other variables, e.g. the basal water pressure. This relationship takes the form of a function that captures the intricate interplay between these variables:

$$\tau_b = f(u_b, ...) \tag{1.1}$$

Accurately formulating a sliding law is crucial for predicting the movement of glaciers and their response to environmental changes. The velocity of Antarctic ice streams, for instance, is largely attributed to basal sliding, which leads to the draining of ice from the continent (Kamb, 1991; Kamb, 2001). This mechanism is also believed to play a significant role in transient glacier dynamics, e.g., glacier surges (Truffer et al., 2021). Therefore, understanding the underlying processes at the glacier base and determining the parameters for a universal friction law are crucial for e.g., predicting the potential disintegration of the West Antarctic Ice Sheet, the occurrence of glacier surges, and the rate of glacial erosion. Currently, encouraging progress has been made to develop a universal sliding law but whether the sliding rate of most glaciers can ever be predicted is an open question (Minchew and Joughin, 2020).

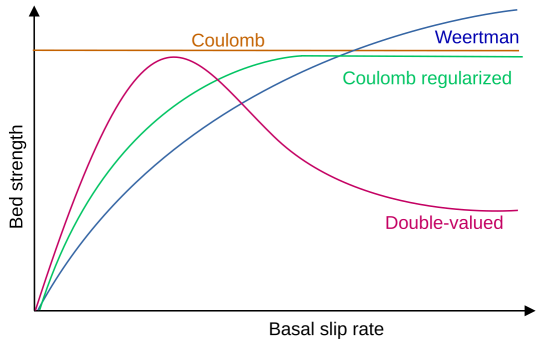

FIGURE 1.4: Representation of the classical sliding laws. The orange curve corresponds to the Coulomb-plastic law, in green, the regularised Coulomb-plastic law, in blue, Weertman's sliding law and in pink, rate-depending friction law.

The study of sliding laws gained significant momentum with the seminal work of Weertman (1957), who introduced the concept of sliding around obstacles. Weertman proposed that glacier sliding is a complex interplay of two processes: regelation around obstacles and creep. According to his hypothesis, sliding occurs as a result of increased deformation caused by stress concentration at these obstacles (Fig. 1.4, blue curve).

A counterpoint to the earlier sliding law formulation was presented by Lliboutry (1968), who raised concerns about the unrealistic nature of a monotonically increasing relationship between basal sliding and shear stress. Lliboutry argued that such a formulation fails to account for intra-annual variations in glacier speed and does not provide reasonable sliding speeds for realistic obstacle sizes. To address these shortcomings, Lliboutry proposed a modified formulation that incorporates a third mechanism: cavity opening. According to Lliboutry's proposition, when basal water pressure beneath the glacier is high, the glacier has the ability to detach from the bed, leading to the opening of cavities. These cavities predominantly form on the lee side of the obstacles, where the basal water pressure is lowest. As the cavities grow, they engulf parts of the obstacles and diminish the apparent roughness of the bed, resulting in increased basal sliding for the glacier.

One of the persistent challenges in understanding this sliding law was the lack of a bound on the shear stress (τ_b), which meant that it could potentially increase without limit. To address this issue, Iken (1981) demonstrated that the growth of cavities imposes an upper bound on the quantity $\tau_b/(p_i - p_w)$, where p_i is the ice overburden pressure and p_w is the basal water pressure. This upper bound is proportional to the maximum slope of the glacier bed, later generalised by Schoof (2005). Building upon these insights, Gagliardini et al. (2007) developed a friction law that incorporates the role of cavities and

includes the Iken's bound, based on the development of Fowler (1987) and Schoof (2005). Depending on an index that characterizes the steepness of obstacles for a given roughness, the Gagliardini law incorporates different sliding laws. It includes a regularized Coulomb-plastic friction law (Fig. 1.4, green curve) and a double-valued law (Fig. 1.4, pink curve) that incorporates rate-strengthening and rate-weakening friction. However, in this configuration, sustained rate-weakening friction is an unstable situation and, in the absence of any controlling mechanism, can lead to infinitely high velocities. This unrealistic behavior contradicts our observations of glacier motion, where glaciers typically exhibit bounded velocities and are subject to various constraints imposed by their environment. Current research focuses on incorporating additional mechanisms or processes that can stabilize the sliding behavior and prevent uncontrolled acceleration. These may include factors such as subglacial hydrology, basal till properties, or the glacier bed topography.

As discussed here and in the subglacial hydrology section (Sect. 1.3.2), basal sliding controls the subglacial drainage system configuration and vice versa, so this coupling effect has significant impact on the glacier dynamic. Several models aim at incorporating this coupling in a two-way fashion to simulate glacier velocity variations and understand better their driving mechanisms (e.g., Hewitt, 2013; Hoffman and Price, 2014; Gagliardini and Werder, 2018; Sommers et al., 2018; Brinkerhoff et al., 2021) but they often (i) use two distinct parametrisations to describe the influence on subglacial drainage system on basal sliding and the subglacial drainage system evolution, (ii) built the model with a sliding law that neglect the rate-weakening friction, and (iii) assume that the subglacial drainage system evolves a similar timescale as that of the water pressure variations, a condition often not fulfilled. Recent modeling effort aims at resolving these challenges and proposes a fully friction-drainage coupled model to simulate glacier flow (Gilbert et al., 2022). Their framework is able to simulate with accuracy variations in observed glacier flow while understanding the subglacial hydro-mechanical feedback that drives such variations. Despite the crucial insights that this model gives, the authors emphasize that friction-drainage coupling parameters related to, e.g. bed geometry, the presence of till, and their dependencies on the subglacial drainage system is lacking as this coupling has received so far little experimental and observational attention. They emphasize that constraining these parameters can allow to simulate a wide-range of glacier velocity variations.

Apart from recent modelling efforts, the Weertman's sliding law (Weertman, 1957) is the most widely used in glacier-flow models which has been developed for hard-bed glaciers. However, the dependencies between viscous drag and regelation/creeping flow when the ice passes obstacles contradicts

experimental results showing that the shear stress in the presence of till is either independent of its deformation rate or highly sensitive to it and that the till shear strength increases linearly with effective stress (Iverson, 2010). Additionally, modelling and observational studies on soft-bed glaciers shows that a Coulomb sliding law is more appropriate (Minchew et al., 2016; Vallot et al., 2017; Stearns and Van der Veen, 2018; Joughin et al., 2019) which motivates certain glacier-flow models to implement it (Bougamont et al., 2011; Pattyn, 2017). However, Zoet and Iverson (2020) claim that glacier sliding over till encompasses hard-bed sliding processes and till deformation, and so, a sliding relationship merging both processes was still lacking. Therefore, based on experimental results, they reconciled both mechanisms into a single framework valid for soft-bed glaciers relating shear stress, sliding velocity, and basal water pressure. They show that until reaching a threshold velocity, the glacier slides across its bed in a hard-bed fashion, but above it, the till shears at its shear strength. Building upon the development of a separate sliding law for hard-bed (Gagliardini et al., 2007) and soft-bed (Zoet and Iverson, 2020) glaciers, Beaud et al. (2022) reconcile these two frameworks and propose a sliding law valid for both soft- and hard-bed glaciers into a single framework. However, the sliding relationship parameters still need to be quantitatively constrained by acquiring better surface and bed geometry. As mentioned in this last paragraph, formulating an appropriate sliding law for soft-bed glaciers lies on understanding the deformation and transport of the till, processes that are discussed in the next section.

Bed deformation and transport

The till underlying soft-bed glaciers has the ability to deform, enhancing the glacier flow velocity (Fig. 1.3c, Blankenship et al., 1986; Alley et al., 1986; Boulton and Hindmarsh, 1987; Murray, 1997). Till deformation is particularly pronounced for glaciers and ice sheets resting on permeable, high porosity till (Blankenship et al., 1986; Reinardy et al., 2011; Stokes, 2018). The depth of its deformation directly governs both the rate and magnitude of till deformation, exerting a direct influence on the velocity at which glaciers or ice sheets shape their bed morphology (Hindmarsh, 1998; Alley, 2000; Fowler, 2000; Schoof, 2007). The resultant landforms from this bed reshaping process induce localized alterations in ice dynamics and till deformation by modifying bed gradients, redirecting subglacial drainage system, and potentially creating obstacles to ice motion (Walder and Fowler, 1994; Alley et al., 2007; Kyrke-Smith and Fowler, 2014; Flowers, 2015; Stokes, 2018; Lipovsky et al., 2019).

While the deformation of till was hypothesized upon the examination of folded drumlin, i.e., elongated geomorphological feature formed by glacial ice

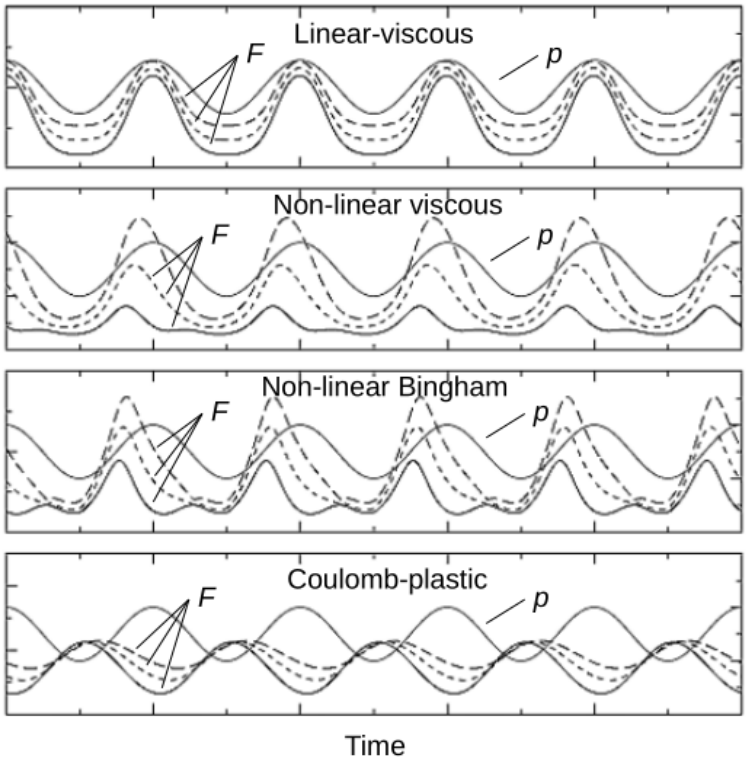

FIGURE 1.5: Modelled output for water pressure (p) and ploughmeter force (F) for different till rheology. a) Linear viscous, b) non-linear viscous, c) non-linear Bingham, d) Coulomb-plastic. The dashed line for the ploughmeter force corresponds to different insertion depth of the ploughmeter tip into the till (0.10 cm: solid line, 0.20 cm: short-dashed line, 0.30 cm: dashed-line. Modified after Kavanaugh and Clarke (2006).

sliding on till, cores in the early 20th century, conclusive evidence of its deformation emerged only in the 1970s through detailed process observations (Boulton, 1986). This breakthrough led to the investigation of a flow law governing till behavior, with a pivotal advancement achieved through subglacial experiments at the shear margin of Breidamerkurjökull, Iceland (Boulton and Hindmarsh, 1987). These experiments involved direct access to unfrozen subglacial till via tunnels excavated into the glacier front, wherein strain markers were positioned at varying depths through four boreholes. Monitoring these markers unveiled a pattern of downward displacement, with upper markers displaying greater movement. These observations incited Boulton and collaborators to formulate the first foundational flow law for till (Boulton, 1979; Boulton and Jones, 1979; Boulton and Hindmarsh, 1987). They stipulate that the till viscosity depends on the shear stress and effective pressure. Notably,

this implied a near-independent till viscosity with strain rate, featuring either a slightly non-linear viscous or a Bingham-type viscous rheology (Fig. 1.5b and c). The recognition of saturated and weak sediment beneath Ice Stream B in West Antarctica (Blankenship et al., 1986; Alley et al., 1986; Alley, 1987) indicated that till deformation occurs also at the ice sheet scale, significantly influencing fast ice flow. Contrary to the earlier proposed non-linear viscous or Bingham-type rheology, it was discerned that till behaves plastically (Fig. 1.5b and c). A plastic rheology means that the till starts to deform when the stresses applied, here the normal and shear stresses, exceed the shear strength of the till (well represented by the Coulomb failure criterion), correlated with the effective pressure, the till porosity, the volume fraction of fines and the strain history (Iverson et al., 1998). Currently, the nearly-plastic till behavior has been largely accepted as it is known from fundamental granular and soil mechanics (e.g., Schofield and Wroth, 1968; Nedderman et al., 1992; Terzaghi et al., 1996; Mitchell, Soga, et al., 2005), field measurements on subglacial till deformation (Hooke et al., 1997; Kavanaugh and Clarke, 2006), laboratory deformation experiments on till (e.g., Kamb, 1991; Iverson et al., 1998; Tulaczyk et al., 2000; Iverson et al., 2007), inversion of subglacial mechanics from ice-surface velocities (e.g., Tulaczyk et al., 2000; Walker et al., 2012; Goldberg et al., 2014; Minchew et al., 2016; Gillet-Chaulet et al., 2016) and numerical experiments (Iverson and Iverson, 2001; Kavanaugh and Clarke, 2006; Damsgaard et al., 2013; Damsgaard et al., 2016, see also, Sect. 1.3.3).

Despite numerous insights gained since the development of the first flow law for till, the response of the till to variations in glacier flow and subglacial water is not fully understood. It is directly linked to the complex mechanical coupling between the glacier ice and the till, which determines its mobilisation beneath the ice-bed interface (Iverson and Semmens, 1995; Fischer and Clarke, 1997; Boulton et al., 2001; Mair et al., 2003; Iverson, 2010). The ice-bed coupling is influenced by e.g., the presence of clasts in the glacier ice that plough through the uppermost till layer (Tulaczyk et al., 2001; Fischer et al., 2001; Iverson et al., 2003; Iverson and Hooyer, 2004; Thomason and Iverson, 2008; Zoet and Iverson, 2020), regelation processes incorporating the till into the basal ice (Iverson et al., 2007), the deformation profile of the till at the depth (Hindmarsh, 1998; Alley, 2000; Fowler, 2000; Schoof, 2007), the permeability of the till matrix (Zoet et al., 2023). However, inconsistent spatio-temporal observations highlight the current incomplete understanding of the feedbacks between ice motion, till deformation and subglacial water at the ice-till interface and storage inside it (Damsgaard et al., 2020). Continuous and multi-scale observations are needed to capture the observed, large variability of the ice-meltwater-till system at a single point measurement approach does not always provide sufficient constraints to assess the evolution of basal sliding and

till transport (Damsgaard et al., 2020; Zoet et al., 2023).

1.4 Transient glacier dynamics: the example of glacier surges

In the preceding section, I emphasized a number of unresolved questions that demand further exploration. Primarily, the intricate relationships among glacier dynamics, subglacial drainage systems, basal sliding, and till deformation still require more precise delineation, given that their interplay fundamentally steers the overall glacier dynamic. Furthermore, alterations in these conditions possess the capacity to trigger glaciers and ice sheets destabilization, so there is a need for a better comprehension of these processes as they have the potential to drastically change sea-level rise projections. To address these questions, my doctoral research is centered on investigating the subglacial hydro-mechanical processes at different spatio-temporal scales driving a particular case of transient glacier dynamic, glacier surges. In this section, I first define glacier surges (Sect. 1.4.1) before pointing out their spatial distribution (Sect. 1.4.2) and controls (Sect. 1.4.3). Wrapping up this section, I accentuate the existing challenges associated with discerning such behaviors and elaborate on how I tackle these issues in the scope of my doctoral research. Later, I describe the primary theories aiming at explaining glacier surges and the current state of knowledge (Sect. 1.4.4). At the end of the section, I address their short-comings and how my doctoral research contributes to resolving some of these.

1.4.1 Definition

Glacier surges represent one facet of the broader range of instabilities observed in glaciers and ice sheets. They are intriguing phenomena that defy the steady flow behavior commonly observed in glaciers. They are characterized by significant ice flow accelerations often accompanied by sudden and rapid advances of glaciers (Truffer et al., 2021). The period between two surges, known as the quiescent phase, is marked by a stagnant lower part of the glacier while the upper part acts as an ice reservoir. During the quiescent phase, the glacier gradually accumulates ice in the upper area, leading to the thickening of the glacier and the steepening of the surface slope. As a result, the shear stress, $\tau_d = \rho g H \sin\alpha$ (ρ is the ice density, g, the standard acceleration due to gravity, H, the glacier thickness and α, the glacier surface slope), increases. Eventually, the glacier reaches a critical profile at which the surge is triggered. The ice stored in the upper area rapidly propagates downward towards the receiving zone, often resulting in substantial advances of the glacier front (Truffer et al.,

2021). Surge-type glaciers represent only a small fraction, approximately 1% (Jiskoot et al., 1998), of glaciers worldwide, but they exhibit diverse behavior (Herreid and Truffer, 2016). While surges occur at quasi-regular intervals, the duration of surge cycles, i.e. a single cycle being characterized by a surge followed by a period of quiescence, can vary greatly. Some surge cycles, such as the Turner Glacier in Alaska, can last for less than a decade (Nolan et al., 2021). On the other hand, surges cycles in regions like Svalbard have been documented to last for centuries (Dowdeswell et al., 1991). The ice velocity associated with the active surge phase also exhibits a wide range of variability. During the surge phase, the ice velocity can be on the order of tens of meters per year in some cases (e.g., Trapridge glacier, Frappé and Clarke, 2007), while in other instances it may be on the scale of hundreds of meters per day (e.g., Medvezhiy Glacier, Kotlyakov et al., 2008).

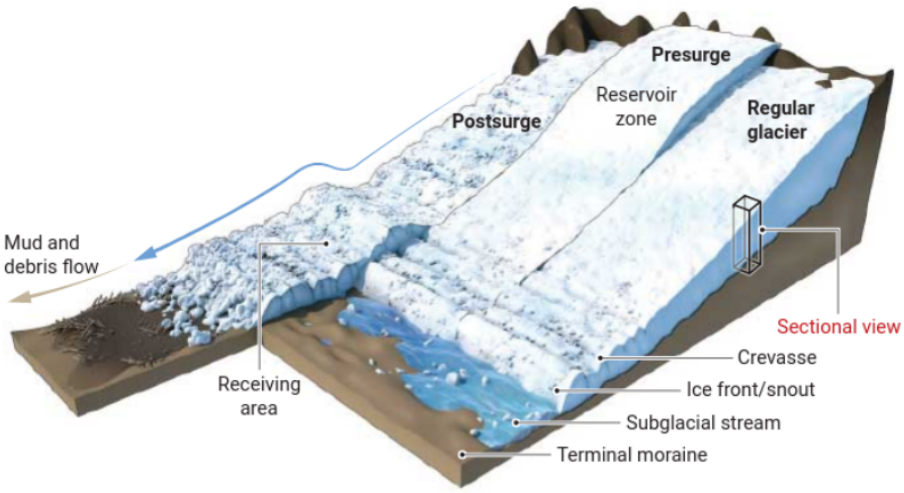

FIGURE 1.6: Representation of a surge cycle (Credits: C. Bikel/Science, Qiu, 2017)

1.4.2 Spatial distribution

Surge-type glaciers are not randomly distributed across glaciated regions of the world, but rather follow specific climatic patterns (Sevestre and Benn, 2015). They are primarily found in two main regions: the Arctic ring, which includes areas like Alaska, Yukon Territory, Arctic Canada, Greenland, Iceland, Svalbard, and Novaya Zemlya (Post, 1969; Fischer et al., 2003; Copland et al., 2003; Jiskoot et al., 2003; Grant et al., 2009; Citterio et al., 2009; Yde and Knudsen, 2007), and Western Central Asia, encompassing the Karakoram, Pamirs, and

western Tien Shan mountain ranges (Hewitt, 1969; Hewitt, 1998; Kotlyakov et al., 2008; Copland et al., 2009; Copland et al., 2011). Additionally, a smaller number of surge-type glaciers can be found in regions such as the Caucasus, parts of the Andes, Russian high Arctic, Kamchatka, and Tibet (Dolgoushin, 1975; Espizua and Bengochea, 1990; Dowdeswell and Williams, 1997; Casassa et al., 1998; Kotlyakov et al., 2004). Sevestre and Benn (2015) conducted statistical analyses and identified a well-defined climatic envelope that bounds the occurrence of surge-type glaciers. This envelope is determined by specific temperature and precipitation thresholds. Their findings provide valuable insights into two aspects: firstly, the non-random distribution of surges across different regions, and secondly, the historical presence of surge-type glaciers in certain areas, such as the European Alps, which may no longer support such glaciers due changes in climatic settings. While climate change has inhibited the surging potential of some glaciers, some studies suggest that glaciers currently flowing at steady-flow could become surge-type under changing climate (Thøgersen et al., 2019) suggesting that surge behaviour could become widespread in some areas.

1.4.3 Controls on the distribution

Through various statistical studies, significant progresses have been made in identifying the geometric and geological factors that enhance the surging potential of some glaciers. Firstly, surge-type glaciers tend to be longer and/or wider compared to non-surging glaciers (Barrand and Murray, 2006; Clarke et al., 1986; Clarke and Blake, 1991; Jiskoot et al., 1998; Sevestre and Benn, 2015). Additionally, the surface slope of surge-type glaciers is generally lower (Clarke and Blake, 1991; Sevestre and Benn, 2015). Surge-type glaciers often have more branches, particularly in regions like Alaska and Yukon Sevestre and Benn (2015). The composition of the glacier bed also plays a role. Surge-type glaciers are more likely to have beds consisting of younger and mechanically weaker lithologies (till), in contrast to hard-bedded glaciers (Jiskoot et al., 1998; Jiskoot et al., 2000). Lastly, in specific regions like Svalbard, surge-type glaciers are more commonly polythermal, meaning that their glacier ice is composed of ice with temperatures equal to (temperate ice) or below (cold ice) the melting point (Jiskoot et al., 2000). Temperate ice allows for the presence of liquid water within the glacier body, even during the cold winter period.

Problem addressed in this thesis 1 : Most studies to date have focused on identifying surge-type versus non-surge type glaciers based on features integrated over the entire glacier area. Recent research has revealed that glacier surges are triggered in localized areas of instability, with this instability subsequently propagating up and/or down the glacier, culminating in a surge (Thøgersen et al., 2019). Therefore, it is crucial to consider distributed geometric and climatic parameters that capture specific glacier zone characteristics in order to identify the unstable region within a glacier accurately. Integrated parameters such as average slope, width, and thickness across the entire glacier are insufficient for this purpose.

→ **One of the objectives of my doctoral research is to develop a comprehensive framework for assessing multiple machine learning models performance in determining the probability for glaciers to be surge-type based on discretized features within glaciers. By interpreting the model decision process, the aim is to identify the particular regions within glaciers that have the characteristics required to undergo a transition into an unstable regime. This entails determining the geometric and climatic attributes associated with these areas (*Paper I*)**.

1.4.4 Physical processes driving glacier surges

The wide range of behaviors observed in glacier surges has led to ongoing debates and discussions regarding the underlying processes that trigger these events. Unifying theories that can comprehensively explain the mechanisms behind glacier surges has been a subject of debate for a long time (described later in this section and in the persepective study of Terleth et al., 2021), and continues to be a topic of active research and inquiry in the present day.

Initial theories attempting to explain glacier surges suggested a possible connection to tectonic activities or volcanic processes (Tarr and Martin, 1906; Nielsen, 1937). However, subsequent observational studies have provided evidence that glaciers can undergo surges even in the absence of active tectonic or volcanic settings (Post, 1969; Thorarinsson, 1969). Since then, numerous efforts have been made to develop a comprehensive model that can explain the diverse range of behaviors exhibited by glacier surges. Below, we provide a brief overview of these theories along with their limitations.

The thermal switch mechanism

The role of ice temperature in triggering glacier instabilities was first proposed by Robin (1955). This study proposed that a transition from sub-freezing temperatures to temperate ice at the base of glaciers and ice sheets could induce transient dynamic episodes. This so-called thermal switch, driven by feedback between increasing shear stress and ice deformation below the reservoir zone, would initiate the surge. Schytt (1969) further developed this theory by suggesting that the cold ice present at the glacier base would act as a dam, amplifying basal water pressure and facilitating surging. However, the thermal switch mechanism fell out of favor for nearly two decades due to studies indicating that it would result in longer surge cycles than observed (Clarke, 1976). Additionally, the thermal switch mechanism would lead to the release of significant volumes of water during the surge which was not detected during the in-depth investigation of surges of Trapridge and Variegated glaciers in Alaska (Clarke et al., 1984; Bindschadler, 1997). The thermal switch mechanism was reevaluated with extensive observations of the surge of Bakaninbreen glacier in Svalbard, which revived interest in this theory (Murray et al., 2000; Fowler et al., 2001). These observations suggested that the thermal switch mechanism is relevant for polythermal glacier surges, but it does not explain the surging behavior of temperate glaciers, also known to exist. As a result, alternative physical mechanisms to account for glacier surging have been inspected, including variations in the configuration of the subglacial drainage system.

The hydraulic switch mechanism

Early studies suggested that water present at the glacier base may play a crucial role in glacier surges (Röthlisberger, 1969; Thorarinsson, 1969). The in-depth investigation of the Variegated glacier surge played a pivotal role in the development of the hydrologic switch mechanism (Kamb et al., 1985). Through extensive field measurements, it was discovered that during the quiescent phase, the subglacial drainage system effectively drained the water, resulting in low basal water pressure. In contrast, during the surge phase, the basal water pressure remained high, indicating the presence of a dispersed and distributed subglacial drainage system (Björnsson, 1998). Building upon these observations, Kamb et al. (1985) proposed that the surge is triggered by a switch from an efficient subglacial drainage system to an inefficient one. This transition is accompanied by extensive cavitation of water over the bed, leading to ice-bedrock separation and the development of high glacier velocities. Surges may initiate when a channel-like system collapses into a linked cavities-like system,

which is then stabilized by high flow velocities and a low hydraulic gradient (Kamb and Engelhardt, 1987). The connection between cavities can be enlarged by significant water inputs, switching the drainage system to conduits. While the termination processes of surges are well-understood, the conceptualization of how channels would transition to linked cavities during surge initiation remains challenging. In addition, the principle of cavities apply for hard-bed glaciers while surge-type glaciers mainly lay on soft, deformable sediments (Jiskoot et al., 1998; Jiskoot et al., 2000).

Towards unifying a surge model

Like a quasi-regular surge cycle of twenty years, it is after four decades since the introduction of the hydraulic switch theory and two decades since the revival of the thermal switch mechanism that the scientific community has rekindled the debate by proposing four distinct models based on different assumptions in an attempt to unify the theories of glacier instabilities. First, a model proposed by Benn et al. (2019) suggests that the stability of a glacier is governed by the equilibrium between variations in enthalpy at the glacier bed and variations in ice mass. A rise in enthalpy, influenced by geothermal and frictional heating, and losses in enthalpy, by conduction and loss of meltwater exiting the system, impact the glacier flow. When the ice mass and enthalpy budgets are out of equilibrium, the glacier undergoes alternating periods of quiescence and surge phases. Second, Thøgersen et al. (2019) developed an evolution model for subglacial friction based on the rate-and-state friction law (Dieterich, 1992; Ruina, 1983), commonly used in studies of sliding on tectonic faults. They demonstrate that large enough perturbations drive the transition from rate-strengthening to rate-weakening friction combined with a characteristic length scale for the evolution of subglacial cavities. This framework can simulate the initiation of the initiation of the surge and its propagation. Building upon the recent friction-drainage coupled model proposed by Gilbert et al. (2022), the model of Thøgersen et al. (2019) has been extended to fully couple the interplay between basal friction and the subglacial drainage system (Thøgersen et al., 2021) through a rate-and-state friction-drainage description. This allows the simulation of a wide range of glacier instabilities, e.g. fast-flow, aborted surges, regular and irregular surge cycles. Thirdly, few models consider that most surge-type glaciers rest on till, which is likely to control shear stress (Zoet and Iverson, 2020). Using also the rate-and-state friction framework, Minchew and Meyer (2020) put forth a model describing the mechanical evolution of till, considering internal friction, porosity, and pore water pressure, as the glacier flows. They suggest that changes in the hydro-mechanical properties of the sediment layer and variations in glacier thickness may play a role in controlling surge behavior. Finally, Beaud et al. (2022) use a generalised

sliding law valid for both hard-bed and soft-bed glaciers to simulate the surge of an analytical glacier and provide a first-order assessment of these sliding law parameters using remote sensing data.

Problem addressed in this thesis 2 : Despite the crucial insights that these models give, many processes are loosely constrained due to the lack of observational data. In the frameworks of Thøgersen et al. (2019), Thøgersen et al. (2021), and Gilbert et al. (2022), the friction-drainage coupling parameters related to, e.g. bed geometry, the presence of till, and their dependencies on the subglacial drainage system are lacking. Indeed, this coupling has received so far little experimental and observational attention. However, achieving this goal could significantly improve our ability to predict glacier velocity variations. Beaud et al. (2022) conclude their study the same way, advocating for more field insights to allow the quantification of the sliding relationship parameters of their generalised sliding law. Finally, Minchew and Meyer (2020) suggest that the interplay between till rheology and pore water pressure activates or desactivates the surge phase, but this hypothesis needs to be validated against field observation.

→ **One of my doctoral research objectives is to provide observational insights on the interplay between subglacial drainage system evolution and subglacial processes driving glacier flow and surge initiation (*Paper II* and *Paper III*). Additionally, by simultaneously monitoring variations in basal water pressure and till mechanics, I aim at constraining bed property characteristics and dependencies with variations in the subglacial drainage system (*Paper III*)**.

1.5 The challenging observation of the subglacial environment

Studying glaciers is already a challenging task due the frequently severe conditions of their environment. However, the observation of surge-type glaciers presents even greater difficulties as the timing of surges is unpredictable. Furthermore, the subglacial environment, hidden beneath hundreds of meters of ice, is particularly challenging to observe and understand. Despite these challenges, it is crucial to gather observations in order to advance our knowledge of transient glacier dynamics. Current observations often center on assessing

subglacial drainage efficiency, e.g., via (i) point-scale measurements of subglacial water pressure within boreholes (e.g., Hubbard and Sharp, 1993; Andrews et al., 2014; Rada and Schoof, 2018), (ii) spatially integrated measurements using dye tracing and remote sensing (e.g., Tranter et al., 1993; Fricker et al., 2010; Chandler et al., 2013; Jouvet et al., 2018), (iii) static spatially discretized measurements using ground penetrating radar (e.g., Moorman and Michel, 2000; Church et al., 2021). These investigations have provided valuable insights on subglacial hydrology. One key observation is the highly heterogeneous nature of the glacier bed, with some areas connected to active drainage systems while others remain isolated, resulting in spatial variations in water pressure even at small scales (e.g., Murray and Clarke, 1995; Iken and Truffer, 1997; Gordon et al., 1998; Kavanaugh and Clarke, 2000; Fudge et al., 2008; Andrews et al., 2014; Hoffman et al., 2016; Rada and Schoof, 2018; Rada Giacaman and Schoof, 2023). Furthermore, temporal variations have been observed in the organization of the subglacial drainage system (Gordon et al., 1998; Kavanaugh and Clarke, 2000). Therefore, these findings cannot be readily extrapolated to the entire glacier scale nor used to predict the subglacial hydrology evolution temporally, as they have revealed the simultaneous occurrence of diverse processes within the subglacial environment.

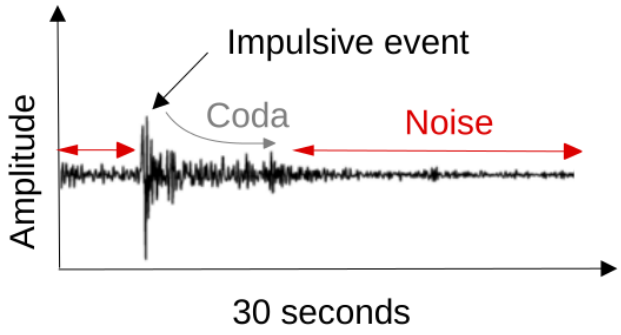

FIGURE 1.7: Representation and decomposition of a seismic wave.

In recent years, cryoseismology has emerged as a complementary tool to study the characteristics of the subglacial drainage system (Podolskiy and Walter, 2016). Any seismology method utilizes seismic waves generated by various sources that propagate through the medium and are recorded by receivers. These seismic signals can be divided into two categories: impulsive events and background noise (Fig. 1.7). The background noise represents continuous signals present on Earth, which arise from natural and human activities. The

study of the seismic noise has evolved into a distinct field called environmental seismology and is used to investigate a wide range of phenomena, including ocean waves, atmospheric disturbances, volcanic activity, glacial processes, and even human-induced vibrations (Larose et al., 2015). For glaciers, the main source of seismic noise is turbulent water flow. Indeed, as for a river, turbulent water flow generates seismic tremor at high frequency (>1 Hz) and thus can be used to quantify relative changes in the subglacial drainage system conditions (Bartholomaus et al., 2015; Gimbert et al., 2016; Nanni et al., 2020; Lindner et al., 2020; Labedz et al., 2022). The recorded seismicity is mainly dominated by the strongest seismic sources and thus often represents the most active part of the drainage system (Nanni et al., 2021).

Few studies have complemented the hydrological analysis with investigations of the mechanical properties of the till, via (i) instrumenting boreholes with ploughmeter, drag spool or tiltmeters (Fischer and Clarke, 1994; Fischer et al., 1998; Fischer et al., 1999; Fischer et al., 2001; Porter et al., 1997; Kavanaugh and Clarke, 2000; Kavanaugh and Clarke, 2006) or (ii) by deriving subglacial shear stresses from seismic observations (Hudson et al., 2020; Gräff and Walter, 2021). The former method allows to retrieve the shear stress, basal displacement and depth-deformation profile into the till, and associated changes caused by variations in the basal water pressure. The latter is based on the detection of seismic impulsive events which have traditionally received more attention with the study of earthquakes and correspond to short-lived but intense events. In glaciology, these impulsive events are often attributed to crevasse openings (Hudson et al., 2020; Walter et al., 2008), calving events (Köhler et al., 2012) or basal stick-slip (Gräff and Walter, 2021; Gräff et al., 2021).

Problem addressed in this thesis 3 : These studies have given precious insights into the subglacial environment mechanisms and interplay that take place between subglacial hydrology and till mechanics. However, most of these studies are either point-scale observations or integrated measurements over a large spatial scale. The ones that are spatially discretised focused either on the glacier subglacial hydrology or the subglacial till properties. To understand the heterogeneous nature of the feedbacks between ice motion, till deformation, the subglacial drainage system at the ice-till interface and storage inside it, multi-spatio-temporal scale analysis needs to be performed (Damsgaard et al., 2020; Zoet et al., 2023).

→ **One of my doctoral research objectives is to explore the spatio-temporal evolution of hydro-mechanical conditions along the glacier flow-line and from the surface to the glacier bed leading to surge-build-up using cryoseismology *Paper II*. Additionally, I aim at reconciling point-scale measurements and local integrated observations to constrain runoff-induced changes in subglacial hydrology and till mechanics. Finally, by the simultaneous observation of subglacial hydrology and till mechanics, I explore these systems dependencies and influence on the overall glacier dynamic *Paper III*.**

1.6 Research questions and outlines

The previous sections provide an overview of the current state of knowledge within the scientific community regarding transient glacier dynamics and the subglacial hydro-mechanical mechanisms at play during these events and the numerous remaining unresolved questions. Gaining a deeper understanding of these processes is crucial to predict the occurrence of transient glacier dynamics, assess their impact on sea-level rise, and evaluate potential hazards for nearby populations. Here, I summarize the key thematic questions that are at the center of my doctoral research to contribute to the resolution of these challenging issues:

Thematic questions

1. **Glacier surges:** What are the characteristics of glaciers exhibiting transient dynamics compared to others?
2. **Hydro-mechanical conditions:** What is the interplay between ice flow, basal friction and subglacial drainage system and how do they influence the glacier-wide dynamic?
3. **Till mechanics:** How does the till adapt to changes in subglacial hydrological conditions?

In order to address these questions, several methodological considerations needed to be explored, which are summarized as follows:

Methodological questions

1. **Machine learning practices:** How well does machine learning inform quantitatively on the wide-spectrum of transient glacier dynamics?
2. **Seismic instrumentation - from the glacier bed to surface:** What hydro-mechanical information do we learn by co-locating geophones at the glacier surface and close to the glacier bed?
3. **Multi-scales multi-instruments framework :** To which extent a multi-instruments multi-scale framework helps at understanding the different subglacial hydro-mechanical conditions happening at different areas of the bed?

This PhD thesis is designed to address both thematic and methodological questions. To this end, Chapter 2 provides an overview of the study area. This begins with an overview of the umbrella project underpinning my doctoral research — the MAMMAMIA project (Sect. 2.1). Subsequently, the focus narrows onto the Svalbard archipelago, renowned for its dense cluster of surge-type glaciers (Sect. 2.2). Within this context, particular emphasis is placed on the surge-type glacier Kongsvegen in Svalbard suspected to be on the verge of a surge event (Sect. 2.3). Chapters 3, 4, and 5 each corresponds to a research step taken over the course of my doctoral research, culminating in a published, soon-to-be submitted and in-review article, respectively. These Chapters are structured to lead the reader through an insightful progression across varying spatial scales. The journey commences with a regional analysis of the Svlabard

archipelago before gradually focusing on the intricate dynamics of Kongsvegen glacier, and ultimately narrows in a detailed exploration of a specific area within this glacier.

Chapter 3 presents the regional investigation conducted in Svalbard to understand the factors influencing surge-type glaciers and gain insights into surge theories. The Chapter begins with a preface (Sect. 3.1) describing the custom-built database created for the study (Sect. 3.1.1) and provides a brief overview of the three machine learning models used (Sect. 3.1.2). The subsequent section presents the summary and key findings of *Paper I* (Sect. 3.2).

Chapter 4 focuses on a zoomed-in investigation of one surge-type glacier, Kongsvegen glacier in Svalbard to understand the interplay between ice flow, subglacial hydrological and mechanical processes over the course of three melt seasons, focusing on the surge initiation at Kongsvegen in Svalbard. The Chapter begins with a preface (Sect. 4.1) that highlights the deployment of a multi-scale multi-instrument network on Kongsvegen, with a focus on the seismic installations (Sect. 4.1.1). It then describes the cryoseismology steps performed to derive the mechanical processes (Sect. 4.1.2) and hydrological variables (Sect. 4.1.3). Later, it presents the summary and key findings of *Paper II* (Sect. 4.2).

In Chapter 5, the focus narrows even further onto Kongsvegen glacier, aiming at understanding the variations in hydro-mechanical conditions induced by runoff examined at the local scale spanning approximately 1 km^2 close to the ELA. The Chapter starts with a preface (Sect. 5.1) aiming at first describing the additional data collected on the field to complement the seismic investigation (Sect. 5.1.1). It then describes the theoretical relationships used to assess the regime in which the subglacial system developed and its stage of equilibrium that we compare to our seismic observations and derived variables (Sect. 5.1.2). Later, I present the summary and key findings of *Paper III* (Sect. 5.2).

In Chapter 6, I answer the thematic and methodological questions addressed in the introduction (Sect. 6.1) and suggests future research directions (Sect. 6.2.

Finally, Chapter 7 includes the complete versions of the three articles incorporated in the thesis:

- *Paper I*: Bouchayer, C., Aiken, J. M., Thøgersen, K., Renard, F., Schuler, T. V. (2022). A Machine Learning Framework to Automate the Classification of Surge-Type Glaciers in Svalbard. *Journal of Geophysical Research: Earth Surface*, 127(7);

- *Paper II*[1]: Bouchayer, C., Nanni, U., Köhler A., Mannerfelt E., Renard F.,

[1]In this paper, Ugo Nanni and I both share the first co-authorship as we have made an equal contribution to the work.

Lefeuvre, P. M., Hulth, J., Schuler, T.V. Acceleration of an Arctic glacier triggered by climate warming and hydro-mechanical feedback. *In preparation for submission in Geophysical Research Letters*.

- *Paper III*: Bouchayer, C., Nanni, U., Lefeuvre, P. M., Hulth, J., Schmidt, L.S., Kohler, J., Renard, F., Schuler, T. V. Multi-scale variations of hydro-mechanical conditions at the base of the surge-type glacier Kongsvegen, Svalbard. In review in *The Cryosphere*;

Appendix A includes two additional articles that I have contributed to over the course of my doctoral research. Appendix B draws the list of the talks, posters, outreach communications and scientific services done during my PhD fellowship.

Chapter 2

Study area

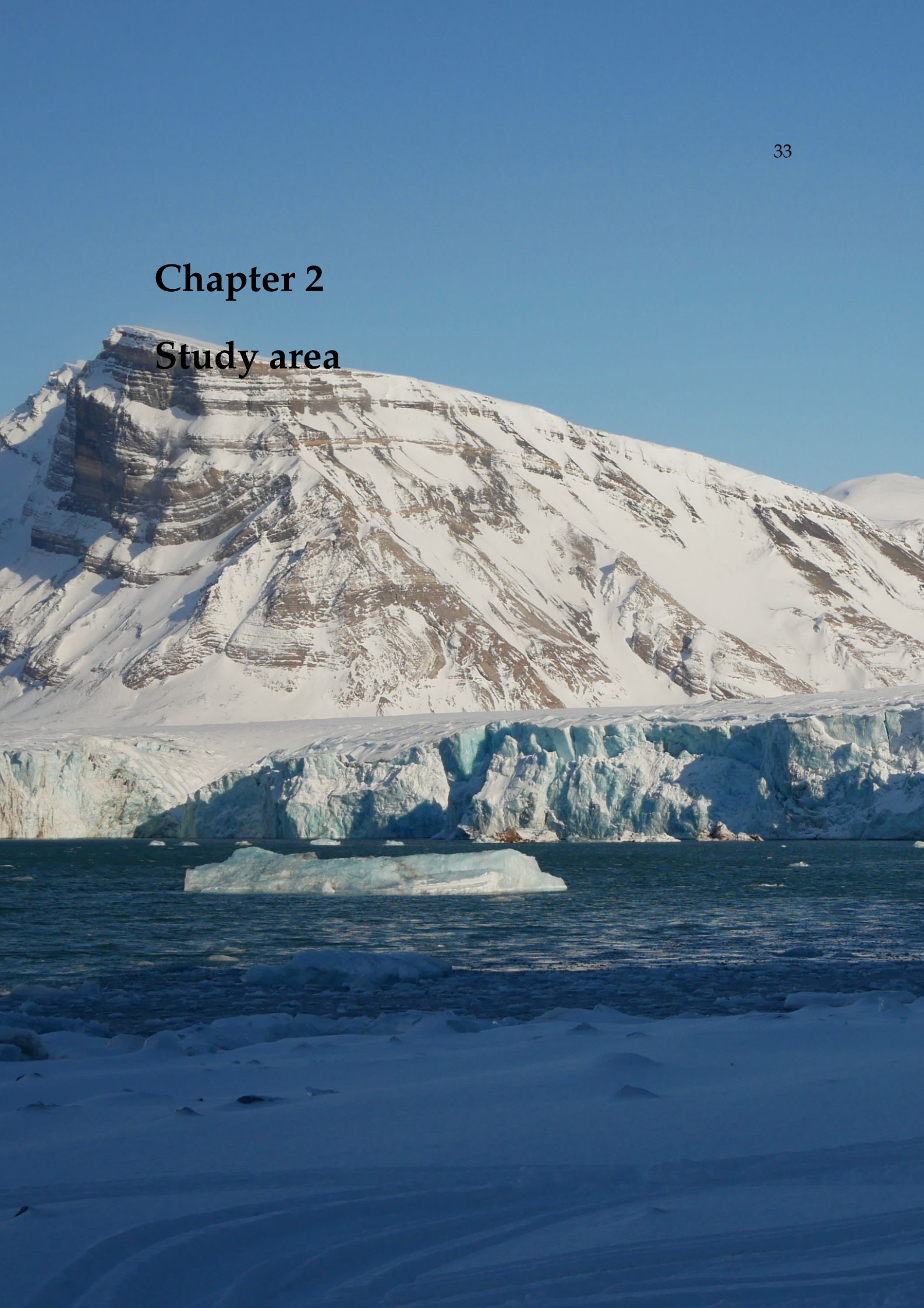

"Why then do we feel this strange attraction for these Polar Regions, a feeling so powerful and lasting, that when we return home we forget the mental and physical hardships, and want nothing more than to return to them?" - Jean-Baptiste Charcot

I used the natural laboratory environment that offers the region of Svalbard to study the subglacial hydro-mechanical processes that drive transient glacier dynamics. To do so, I focus on understanding the factors that lead certain glaciers to exhibit surge-type behavior while others do not. The research then zooms in on Kongsvegen glacier, which is a surge-type glacier and has recently displayed indications of an impending fast-flow event. This Chapter aims to provide an overview of the umbrella project under which I did my doctoral research, MAMMAMIA (Sect. 2.1) and outlines the regional (Sect. 2.2) and local areas of investigation (Sect. 2.2).

2.1 The MAMMAMIA project

During my PhD fellowship, I actively contributed to the MAMMAMIA project, which stands for "Multi-scAle-Multi-Method Analysis of Mechanisms causing Ice Acceleration.". Funded by the Research Council of Norway through the FRIPRO program (project number 301837) and led by Prof. T.V. Schuler, the project aims at investigating the subglacial dynamics of polar glaciers, with a specific focus on thermal conditions, subglacial friction, and fine-scale ice dynamics in response to changes in meltwater supply.

Employing a multi-method approach, the MAMMAMIA team seeks to collect synchronized and high-resolution data on ice velocity, alongside cryoseismicity, subglacial hydrology and mechanics measurements to gain insights into the interface dynamics at the glacier base. By combining this comprehensive dataset with advanced modeling techniques, the project aims at analyzing glacier subglacial hydrology, basal friction, and ice flow in a coordinated manner. This integrated approach enables a deeper understanding of transient velocity dynamics and the conditions under which local perturbations can trigger widespread glacier accelerations. The project is structured into two main components: collecting a comprehensive dataset of glacier motion at different spatio-temporal scales, and using a multiple model approach to simulate glacier hydraulics, basal friction, and ice flow for interpretation and validation against observations.

The field site for this project is located in Kongsfjorden, Svalbard, near the

Ny-Ålesund research station (Fig. 2.1a). Over the course of five field campaigns spanning from 2021 to 2023, I actively participated in instrument deployment, maintenance, and data collection on Kongsvegen glacier in Svalbard. My primary contributions to the project involved collecting and processing data, constructing a multi-scale multi-method dataset, and using/developing diverse methodologies to investigate the glacier hydraulics, basal friction, till deformation, surface/basal crevasses, their interactions and consequences for the overall glacier dynamic, as detailed in *Paper II and Paper III* (see also, Chapter 4 and 5).

2.2 Regional investigation: Svalbard archipelago

2.2.1 Historical and environmental settings

Svalbard, a Norwegian archipelago located in the Arctic Ocean, lies between the northern coast of Norway and the North Pole. It is believed to mean "the cold coast" or "the cold edge," and it first appears in Icelandic annals from 1194 in connection with a brief mention, such as *Svalbaði fundinn*. However, the exact discovery of Svalbard is uncertain, with the Icelanders or the Pomors (people from the White Sea region) being the two candidates. What is certain is that when Willem Barents and the members of the Dutch Expedition were in search of the northeast passage to China and India in 1596, they stumbled upon Bjørnøya and later the fragmented west coast of Spitsbergen. There is no evidence to suggest that they had prior knowledge of Svalbard. In fact, they even assumed that these lands were part of Greenland (Hisdal, 1998). The history of Svalbard includes its use as a base by whalers in the 17th and 18th centuries, followed by the establishment of coal mining communities in the early 20th century (Hisdal, 1998). Sovereignty over the Svalbard archipelago in the Arctic Ocean was granted to Norway at the Versailles peace conference in 1920.

The Svalbard archipelago ranges from 74° to 81° north latitude and 10° to 35° east longitude, with Spitsbergen as the largest island followed by Nordaustlandet and Edgeøya (Fig. 2.1). Despite its high latitude, Svalbard experiences milder temperatures compared to other regions at similar latitudes, due to its Arctic climate influenced by the warming effects of the North Atlantic drift (Svendsen et al., 2002; Sato et al., 2014). The environmental conditions, including the long period of midnight sun compensating for the polar night, have shaped a resilient flora adapted to live in this challenging environment.

However, Svalbard has not been immune to the effects of global warming. Between 1970 and 2020, the average temperature on Svalbard rose by 4°C, with winter months experiencing a significant increase of 7°C (Hanssen-Bauer

et al., 2019). These changes have major implications for the delicate balance in which the ecosystem evolves and highlight the urgency of understanding and mitigating the impacts of climate change on the archipelago. Among the most striking examples of the dramatic changes initiated by climate change is the decline in the polar bear population in Svalbard, a symbol of the area. Female polar bears in the European Arctic now have only 33% of the denning habitat available compared to the 1980s, as numerous areas have become inaccessible within the critical timeframe for maternity denning. This reduction is particularly pronounced in Svalbard and Novaya Zemlya until 2020. Furthermore, projections indicate that by the 2090s, all areas will likely be inaccessible to pregnant bears, posing a severe threat to their reproductive success (Merkel and Aars, 2022). Glaciers, another iconic feature of Svalbard, are also experiencing a decline, as I detail in the following section.

2.2.2 Svalbard glaciers

Svalbard, with its total land area of approximately 60 000 km^2, features a glacier coverage of about 34 000 km^2, accounting for 57% of its total land area (Nuth et al., 2013). This constitutes nearly 10% of the Arctic glacier area, excluding the Greenland ice sheet. The archipelago hosts 1 615 individual glaciers (Fig. 2.1), encompassing a diverse range of glacier types. These include small cirque glaciers and valley glaciers that predominantly terminate on land, as well as large ice fields and ice caps, some of which span up to approximately 8 000 km^2, feeding multiple outlet glaciers.

Remarkably, a significant proportion of Svalbard glaciers, around 15% in terms of number and up to 60% in terms of area (Błaszczyk et al., 2009), are tidewater glaciers. These glaciers reach the fjords or ocean waters, introducing freshwater into the marine environment through subglacial channels, submarine melting, and calving icebergs.

Most of the glaciers in Svalbard exhibit a polythermal nature (Hagen et al., 1993), characterized by the coexistence of cold and temperate ice. This thermal heterogeneity results in a considerable retention capacity of these glaciers (Christianson et al., 2015). Large amounts of meltwater can refreeze in the porous snow and firn. Because of climate change, firn refreezing capacity has been reduced, and more surface meltwater exits the glacier as runoff (Østby et al., 2017; Van Pelt et al., 2019).

Estimating the total ice volume of Svalbard has been the subject of various studies, yielding divergent results. Estimates range from 4 000 to 9 600 km^3, but most studies (Hagen et al., 1993; Fürst et al., 2018) converge on a value of approximately 6 200 km^3. This corresponds to a sea-level equivalent of 0.015 m. Recently, Schuler et al. (2020) estimated that the surface mass balance (the

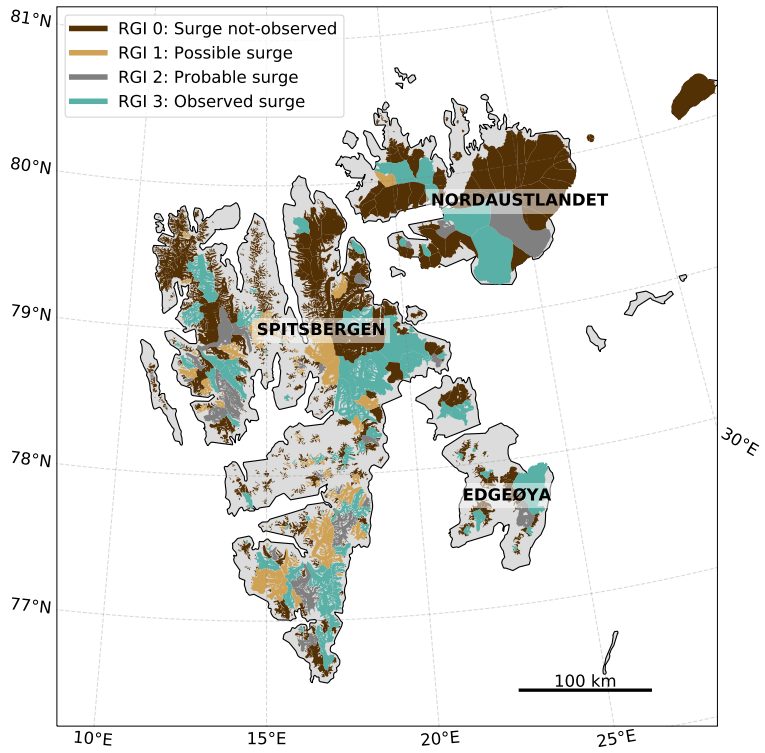

FIGURE 2.1: Classification of glaciers in Svalbard in the Randolph Glaciological Inventory database (RGI, 2017). This database contains five classes that characterize the surge potential of glaciers (Sevestre and Benn, 2015): Not observed (0), Possible (1), Probable (2), Observed (3), Not assigned (9). The class 9 is not represented in the Svalbard region.

net mass gained or loss at the surface of the glacier only,) of Svalbard between 2000 and 2019 to be -6.50 ± 3.71 Gt a^{-1}, and the total mass balance (total mass gained or loss including ice lost due to calving and thinning from contact with warm ocean waters), to be -8.28 ± 6.05 Gt a^{-1}. The difference between these values represents the sum of frontal ablation and the combined uncertainty, totaling -1.78 ± 7.33 Gt a^{-1} (the error margin is calculated from the root sum of squares of the estimated climatic mass balance and the total mass balance errors). The uncertainties primarily arise from our limited knowledge of calving processes, surge dynamics, and their influence on the overall mass balance of the region (Schuler et al., 2020).

Surge-type glaciers, although representing only 1% of the world glaciers (Jiskoot et al., 1998), are prominently found in Svalbard, making it a region with the highest concentration of such glaciers (Fig. 2.1, Sevestre and Benn, 2015). Estimations regarding the prevalence of surge-type glaciers in Svalbard

vary, ranging from 13% (Jiskoot et al., 2000), 34% (Hamilton and Dowdeswell, 1996), to as high as 90% (Lefauconnier and Hagen, 1991) of the glaciers. This distinction sets Svalbard apart from other regions worldwide. In comparison to glaciers in other parts of the world, surge cycles in Svalbard tend to be longer, lasting anywhere from 30 to 500 years (Hagen et al., 1993; Błaszczyk et al., 2009). The active surge period typically spans around six years (Lefauconnier and Hagen, 1991; Hagen et al., 1993), although longer surges of up to 12 years have been observed (Błaszczyk et al., 2009). The prolonged surge cycle duration can be attributed to the relatively low accumulation rates experienced by Svalbard glaciers compared to glaciers in other regions (Dowdeswell et al., 1991).

2.3 Local investigation: Kongsvegen glacier, Svalbard

Kongsvegen glacier, Svalbard is situated near the Ny-Ålesund research station on the northwest coast of Svalbard (78° 48'N, 12° 59' E, Fig. 2.2a). With an area of approximately 108 km^2 and a length of about 25.5 km (as of 2010, RGI, 2017), the glacier thickness is around 350 m around the long-term ELA (78° 18'N, 17° 13' E). Its surface slope varies between 0.5° and 2.5°, predominantly oriented in a northwestern direction (Hagen et al., 1993). As is common for Arctic glaciers, Kongsvegen glacier has a polythermal structure, characterized by a temperate base and an upper layer of cold ice measuring 50-130 m in thickness. The basal ice is at the pressure melting point along the entire glacier flowline (Sevestre et al., 2015). The glacier rests on fine-grained sandstone and sand/silt glacio-marine sediment (Hjelle, 1993; Murray and Booth, 2010).

Notably, Kongsvegen glacier is a surge-type glacier, having experienced surges in the past, including occurrences around 1800, 1869, and 1948 (Liestøl, 1988; Woodward et al., 2002). Currently, the glacier is in a quiescent phase following its most recent surge and displays relatively low velocities, averaging around 3 $m.a^{-1}$. Research conducted by Melvold and Hagen (1998) revealed that the mass transported down the glacier during this phase amounts to only 3-20% of the annual mass gained in the accumulation area, which is typical for a surge-type glacier in a quiescent phase gaining mass in the ice reservoir. Recent measurements of surface velocities near the equilibrium line suggest that the glacier has been accelerating since 2014, indicating the possibility of an impending fast-flow event (Fig. 2.2 b and c).

To gather data and monitor Kongsvegen glacier, we employed a range of instrumentation techniques. Specifically, we placed a total of 19 geophones on the surface of the glaciers (Fig.2.2a). Additionally, we drilled two boreholes,

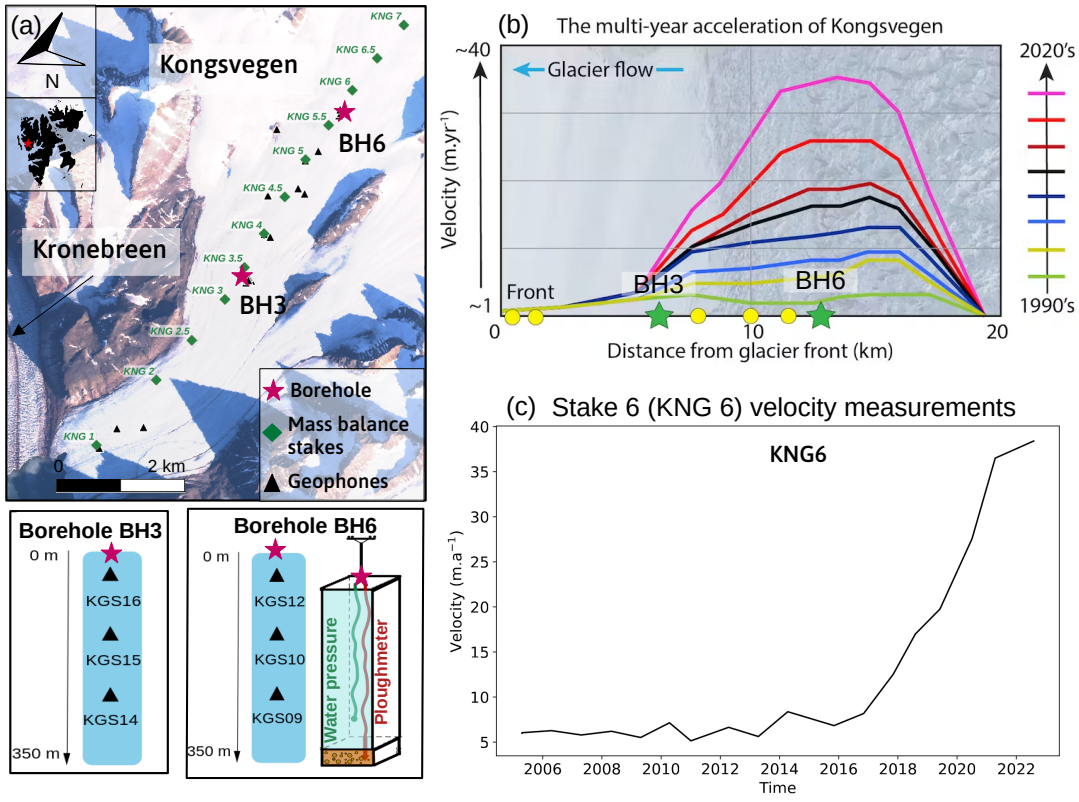

FIGURE 2.2: Location of Kongsvegen, Svalbard, and measurement sites. (a) The map illustrates the location of Kongsvegen in Svalbard, along with the corresponding surface instrumentation. Green diamonds indicate the positions of mass balance stakes, black triangles locate the surface geophones and the red starts indicate the two borehole sites, which installation is detailed below(b) The long-term velocity of Kongsvegen, measured by the Norwegian Polar Institute from the 1990's to recent times, is displayed in this figure. It was published in a popular science article, providing an overview of our work within the MAMMAMIA project (Nanni, 2023). (c) The long-term velocity at KNG6, located near the Equilibrium Line Latitude of the glacier, is depicted in this figure.

one near the long-term ELA of the glacier (BH6: 78° 47'N, 13° 07'E) and the other in the glacier ablation area (BH3: 78° 48'N 12° 54'E), each equipped with three borehole seismometers (Fig.2.2a). The ice thickness measures approximately 349 m at BH6 and 340 m at BH3. At the BH6 site, we also installed another borehole equipped with sensors for direct measurements of subglacial

hydrology (water pressure) and subglacial mechanics (ploughmeter). Furthermore, a GNSS (Global Navigation Satellite System) was positioned ~700 m from BH6 (78° 47'N, 13° 09'E) to record the surface velocity (Fig.2.2c). For more detailed information about the instruments used, we refer the reader to Chapter 4 and 5.

Chapter 3

Surge-type glaciers at regional scale: controls and characteristics of glacier instability

This Chapter is centered on Paper I: Bouchayer, C., Aiken, J. M., Thøgersen, K., Renard, F., & Schuler, T. V. (2022). A Machine Learning Framework to Automate the Classification of Surge-Type Glaciers in Svalbard. Journal of Geophysical Research: Earth Surface, 127(7), e2022JF006597. The complete article can be found in Chapter 7, Section 7.1. The primary focus of this Chapter is to address the following research and thematic questions:

Thematic question 1: Glacier surges: What are the characteristics of glaciers exhibiting transient dynamics compared to others?

Methodological question 1: Machine learning practices: How well does machine learning inform quantitatively on the wide-spectrum of transient glacier dynamics?

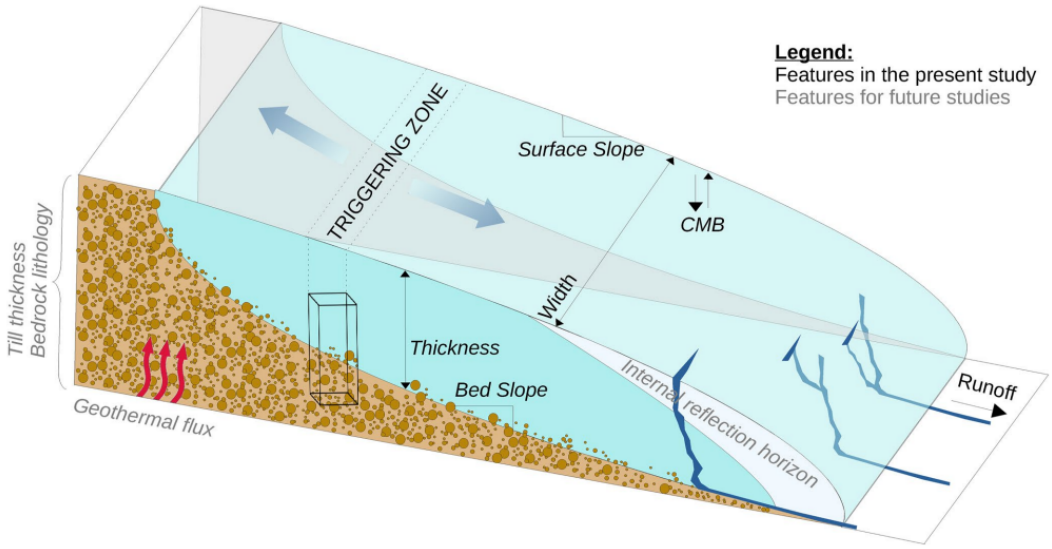

FIGURE 3.1: Sketch of the features that we used and combined in a custom-built data set to investigate the potential for the glaciers in Svalbard to be surge-type.

"The way to get started is to quit talking and begin doing." - Walt Disney

The initial phase of my doctoral research was intended to rely on the data obtained from fieldwork conducted in 2020 as part of the MAMMAMIA project. Unfortunately, the outbreak of the COVID-19 pandemic necessitated the cancellation of the fieldwork campaign, resulting in the unavailability of new data. However, this challenge prompted me to explore existing data sources to gain a deeper understanding of surge-type glaciers, specifically investigating why certain glaciers in the relatively homogeneous climate region of Svalbard exhibit surges while others do not. Additionally, my objective was to enhance the understanding of unstable regions within glaciers and characterized the key attributes of these areas. To begin, I provide an overview of the custom-built database I compiled and the employment of machine learning models to analyze the data. These preliminary steps laid the foundation for the subsequent section, where I summarise *Paper I* and present the key findings.

3.1 Preface

3.1.1 A regional custom built database for surging

To examine the surge potential of glaciers in Svalbard, I have compiled a database that integrates various geometric and climatic features. The database incorporates geometrical features from the Open Global Glacier Model (Maussion et al., 2019) and SVIFT1.0 (Fürst et al., 2018), i.e., the bed elevation and slope, the surface elevation and slope, the thickness and the glacier width, and climatic features computer by Van Pelt et al. (2019), i.e., the runoff and climatic mass balance.

By leveraging the centerlines computed with the Open Global Glacier Model, we have discretized all the features along these centerlines. This allows the interpolation or extrapolation of the data along the coordinates of the centerlines, resulting in a discretised representation of the glaciers in the custom-built database. Additionally to the eight features described above, I added so-called combined features, i.e., the glacier width divided by its thickness and the driving stress at each centerline points.

As a result, our database encompasses 981 glaciers, with their respective features discretized along 97 140 points (Fig. 3.2).

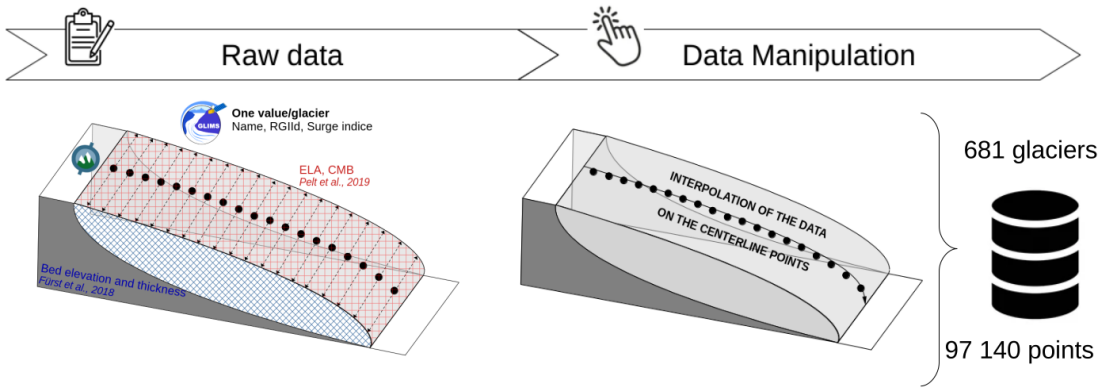

FIGURE 3.2: Workflow to create the custom-built database to evaluate the potential of surging for Svalbard glaciers. Once the raw data are collected, the features are interpolated along the centerlines points.

3.1.2 The machine learning models

The Randolph Glacier Inventory (hereafter RGI, RGI, 2017) categorizes each glacier worldwide with a surge index, indicating the glacier surging potential. These indices have been incorporated into RGI based on the extensive bibliography review and statistical analysis performed by Sevestre and Benn (2015). In RGI, the glaciers worldwide are classified into four categories: Class 0 (surges not observed), Class 1 (possible surge), Class 2 (probable surge), and Class 3 (observed surge). I use these indices to train three machine learning models. For our model training, we focused on the classes where we have the highest confidence, classes 0 and 3, as they are observation-based classes. For Svalbard glaciers, the resultant custom-built dataset is highly unbalanced, with nearly seven times more glaciers that have never been observed surging compared to those that have been observed surging. This severe class imbalance can potentially lead to classification problems in statistical analysis. To address this challenge, I under-sampled the majority class (glaciers that have never been observed surging) to create a balanced dataset. Subsequently, the resampled dataset was divided into a training set (70% - 687 glaciers) and a testing set (30% - 294 glaciers) to evaluate the performance of our models. In this study, three machine learning models, namely logistic regression, random forest, and Extreme Gradient Boosting (XGBoost), are trained using the surge indices from RGI (2017) to evaluate the potential for glaciers in Svalbard to be surge-type (Fig. 3.3). These models are commonly employed for classification tasks and, here, are used to determine the probability of each centerline point to be classified as surge-type or non-surge-type. The models are briefly described hereafter (Fig. 3.3):

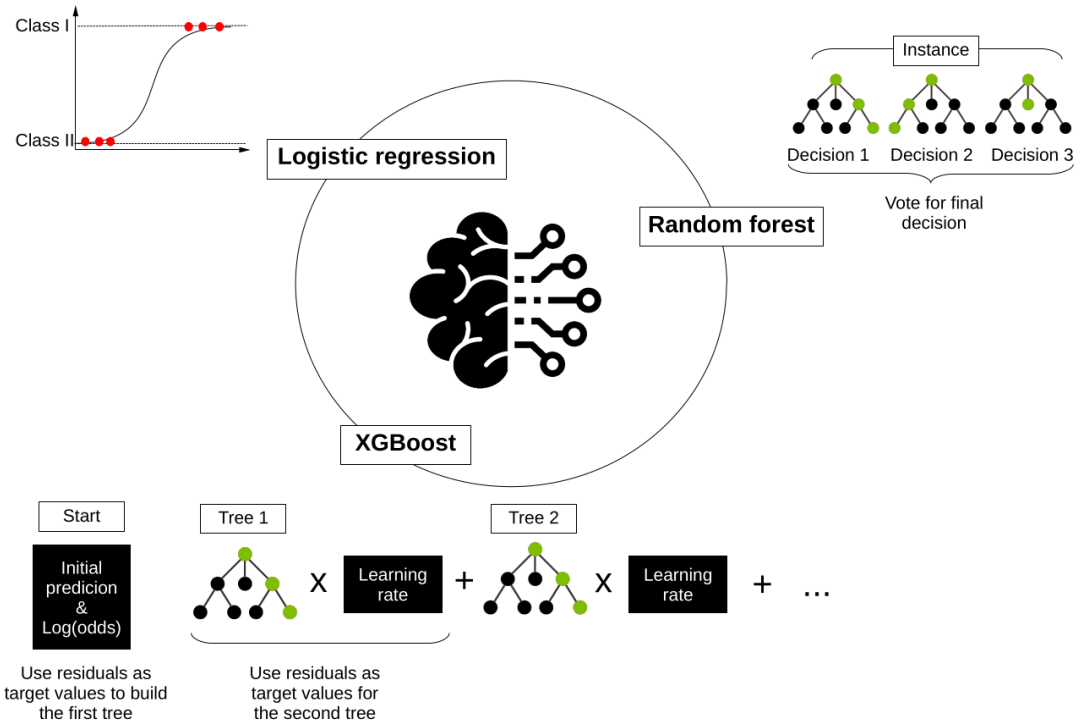

FIGURE 3.3: Schematic overview of the three machine learning models employed in *Paper I*: logistic regression, random forest, and XGBoost.

- Logistic regression (Nelder and Wedderburn, 1972) is a statistical model that predicts the probability of an event to occur based on a set of input features. It estimates the relationship between the dependent variable and independent variables by fitting a logistic function to the data. It works well for linearly separable problems and provides interpretable coefficients that indicate the influence of each feature on the outcome. Logistic regression is a parametric model that assumes a linear relationship between independent features and the log-odds of the outcome, i.e., logarithmic of the probability of success/failure (Fig. 3.3).

- Random forest (Breiman, 2001) is an ensemble learning method that combines multiple decision trees to make predictions. It creates a forest of decision trees, where each tree is trained on a random subset of the data and features. The final prediction is determined by aggregating the predictions of all individual trees. Random forest can handle non-linear relationships, high-dimensional data, and is robust against overfitting (Fig. 3.3).

- XGBoost (Chen and Guestrin, 2016) is another ensemble learning algorithm

that iteratively trains weak prediction models, such as decision trees, in a gradient boosting framework. It uses a gradient descent algorithm to minimize a loss function and optimize the model performance. In other words, XGBoost focuses on boosting weak models. XGBoost employs a regularization technique to prevent overfitting and provides better accuracy and faster training times compared to other boosting methods and random forest (Fig. 3.3).

After evaluating the performance of the three machine learning models, we determined that XGBoost outperforms the others. Consequently, we utilized this model to delve into the prediction process and gain valuable insights into the distinguishing characteristics of surge-type glaciers, described more in details in the following section.

3.2 Summary of *Paper I*

Surge-type glaciers represent only 1% of the world's glaciers (Jiskoot et al., 1998) and they are part of the wide spectrum of glacier instabilities. Understanding these instabilities is essential for accurate sea-level rise projections and effective hazard mitigation (IPCC, 2021; Truffer et al., 2021). However, important questions remain unanswered: What causes some glaciers to surge while others remain stable? How and where does the instability start before propagating throughout the entire glacier? Previous statistical studies have identified certain characteristics that the surge-type glaciers seems to have in common, such as certain length, width, bed composition, and climatic distribution (Clarke et al., 1986; Clarke and Blake, 1991; Hamilton and Dowdeswell, 1996; Jiskoot et al., 1998; Jiskoot et al., 2000; Barrand and Murray, 2006; Sevestre and Benn, 2015). Yet, these studies have limitations. They consider features integrated over the entire glacier area, which present challenges to identify specific triggering zones within a glacier. Additionally, they do not compare different types of models.

To address these limitations, we have developed a machine learning framework for classifying surge-type and non surge-type glaciers in Svalbard. This region provides a relatively homogeneous climate, allowing us to focus on the geometric characteristics of surge-type glaciers and relate our findings to existing surge theories. Our framework consists of a custom-built database, machine learning model training following best practices, evaluation methods for model outputs (here the output being the probability of a glacier to be classified as surge-type), and a method for mapping the surge probability of Svalbard glaciers. The database comprises various data points collected

across Svalbard glaciers, including width, bed and surface elevations, thickness, bed and surface slopes, runoff, and climatic mass balance. Each feature is resampled onto glacier centerline coordinates computed with Open Global Glacier Model (Maussion et al., 2019). We train three different models (logistic regression, random forest and XGBoost), but find that XGBoost outperforms the others. Although all models perform better than a random guess, XGBoost have the highest precision (0.85) and the lowest false positive results (0.23). Lastly, our model demonstrates robustness by correctly identifying glaciers as surge-type that were not initially labeled as such in RGI but have been observed surging recently (Schellenberger et al., 2017; Benn et al., 2019; Leclercq et al., 2021). Consequently, we utilize this model to gain insights into the distinguishing characteristics of surge-type glaciers.

Our findings reveal that glacier width, ice thickness, and surface slope are the primary features driving a glacier to be classified as surge-type or not. A thicker and wider glacier with a low surface slope has a higher probability of being classified as surge-type, aligning well with existing surge theories (Kamb and Engelhardt, 1987; Fowler, 1989; Benn et al., 2019; Thøgersen et al., 2019). Additionally, we have generated the first map quantifying the surge probability of glaciers on Svalbard. This map, along with associated probabilities, provides new information for the Randolph Glacier Inventory surging classes. Moving beyond a binary distinction between surge-type and non-surge-type glaciers, our approach quantifies these classes along a continuous scale using robust statistical methods. It is important to note that the model assesses surge-like probability at each centerline point, implying that the probability of surging within the glacier is not necessarily constant. This opens up avenues for further research in terms of local predictions and the identification of unstable zones within a glacier (triggering zones that can propagate throughout the entire glacier), likely to be precursory for surge triggering (Thøgersen et al., 2019).

To gain a deeper understanding of glacier surges, additional observations could be considered and could be integrated into the framework. These include the thickness and lithology of the underlying till, the analysis of internal reflection horizons that indicate the transition between cold and temperate ice, the basal temperature and geothermal gradient, all considered pivotal in enhancing glacier instability (Benn et al., 2019; Minchew and Meyer, 2020; Zoet et al., 2023). By incorporating these factors, we can enhance our comprehension of glacier surge dynamics. Furthermore, the current custom-built database provides a static snapshot of the glaciers, but it would be beneficial to include multi-temporal data for certain features. Incorporating a time component would enable us to study the build-up, trigger and termination of a surge

and better understand the surge cycle evolution over time. In terms of predictions, instead of simply averaging the probability computed for every centerline point to obtain a glacier-wide prediction, more advanced methods could be employed, e.g. meta-learning techniques. These sophisticated techniques could account for spatial variations and provide more accurate and detailed predictions of surge probabilities within glaciers.

In conclusion, the machine learning framework developed in this study has the potential to be applied to assess the surge probability of glaciers in other regions worldwide. It can be expanded as new data becomes available and can even be adapted for use in other fields, such as studying landslides or earthquake dynamics.

Chapter 4

Surge-type glaciers at glacier scale: surge initiation driven by hydro-mechanical feedback

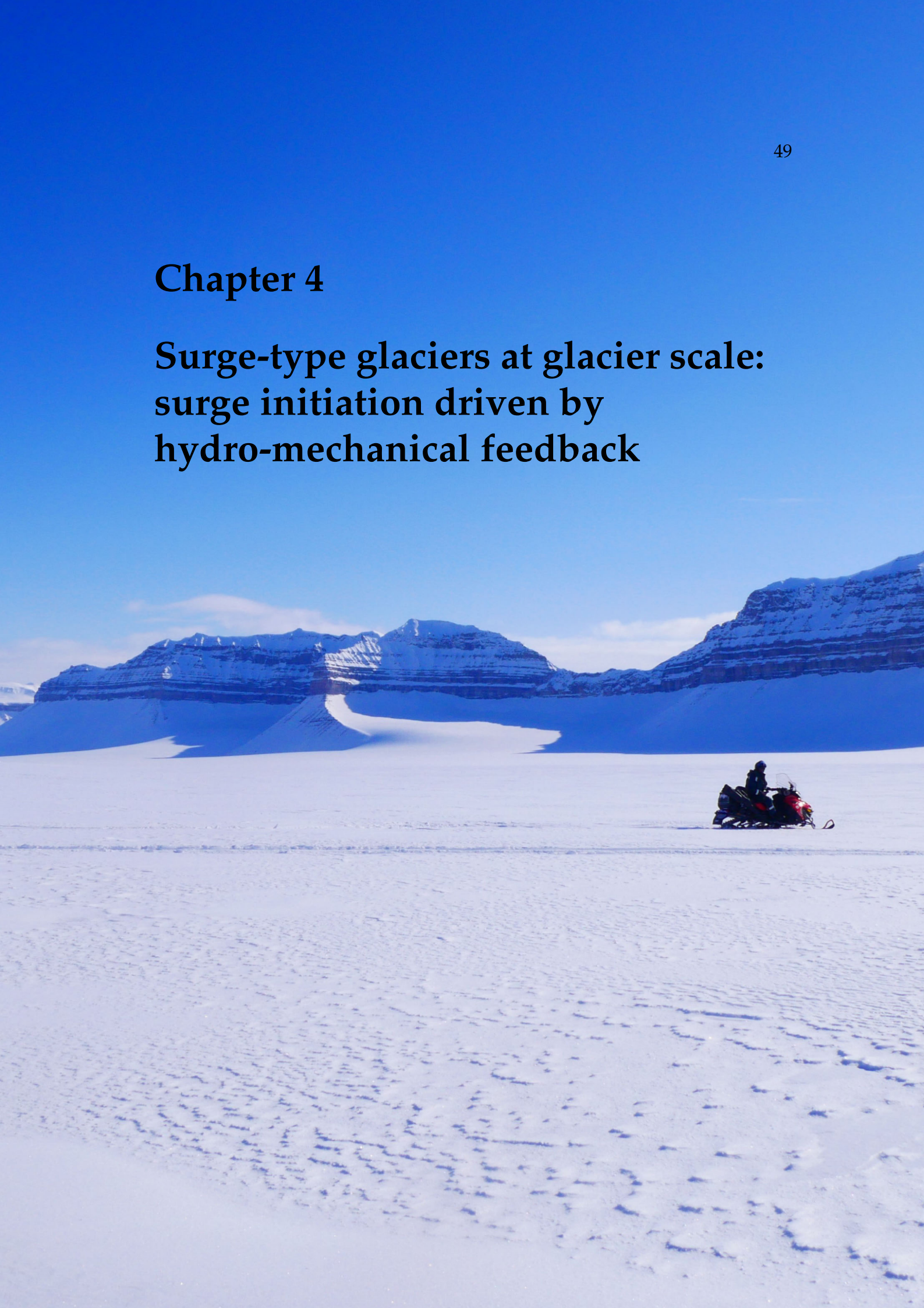

This Chapter is centered on Paper II[1]*: Bouchayer, C., Nanni, U., Köhler A., Mannerfelt E., Lefeuvre P.M., Renard F., Hulth, J., Schuler, T.V. Acceleration of an Arctic glacier triggered by climate warming and hydro-mechanical feedback. In preparation for submission in Geophysical Research Letters. The complete article can be found in Chapter 7, Section 7.2. The primary focus of this Chapter is to address the following research and thematic questions:*

Thematic question 2: Hydro-mechanical conditions: What is the interplay between ice flow, basal friction and subglacial drainage system and how do they influence the glacier-wide dynamic?

Methodological question 2: Seismic instrumentation - from the glacier bed to surface: What hydro-mechanical information do we learn by co-locating geophones at the glacier surface and close to the glacier bed?

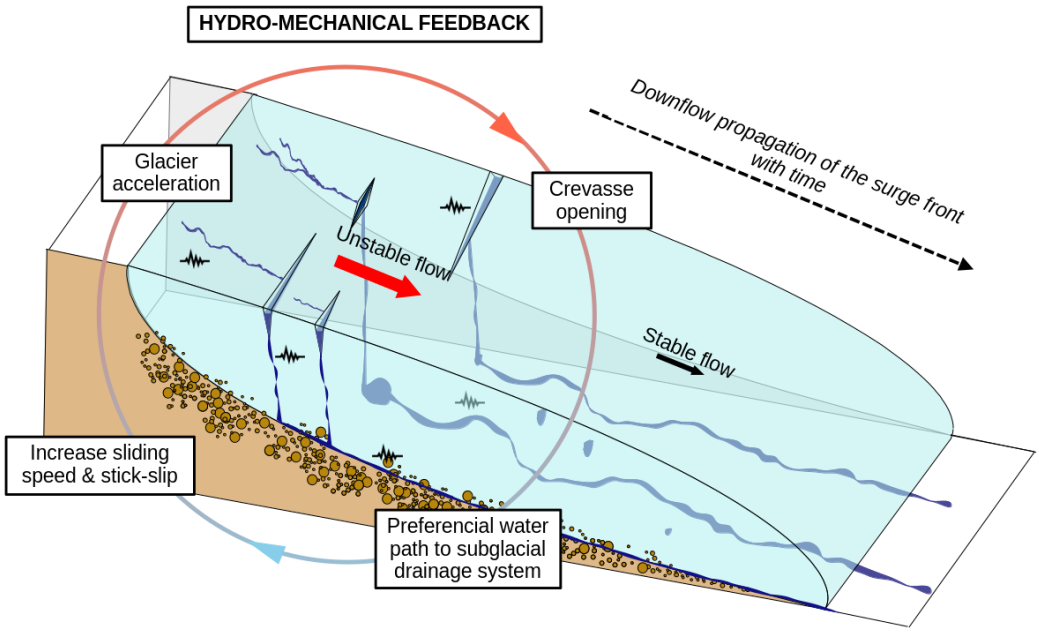

FIGURE 4.1: Sketch of the hydro-mechanical feedback at place during Kongsvegen surge front built-up.

[1]In this paper, Ugo Nanni and I both share the first co-authorship as we have made an equal contribution to the work.

"The Earth has music for those who listen." - William Shakespeare

Cryoseismology can be viewed as listening to the glaciers with the use of seismometers. By analysing the seismic signals, we can understand the hydrological and mechanical processes that happen at the glacier surface and base, spatially and temporally. As part of the MAMMAMIA project that started in 2021, the team and I continued the deployment of surface and borehole seismometers that had started in 2018, as part of another project led by A. Köhler. Throughout my my doctoral research, I conducted a total of five field campaigns, with three specifically dedicated to drilling at different sites on the glacier and deploying surface geophones (Fig. 4.2). The remaining campaigns focused on instrument maintenance and data collection. With the seismic data collected, I derived subglacial drainage system capacity and the icequakes occurrence and amplitude and aim at understanding the hydro-mechanical feedback at play during the build-up of Kongsvegen. In this section preface, I provide a description of the seismic network and an overview of the data analysis methodology. Subsequently, I summarize *Paper II* and present the key findings.

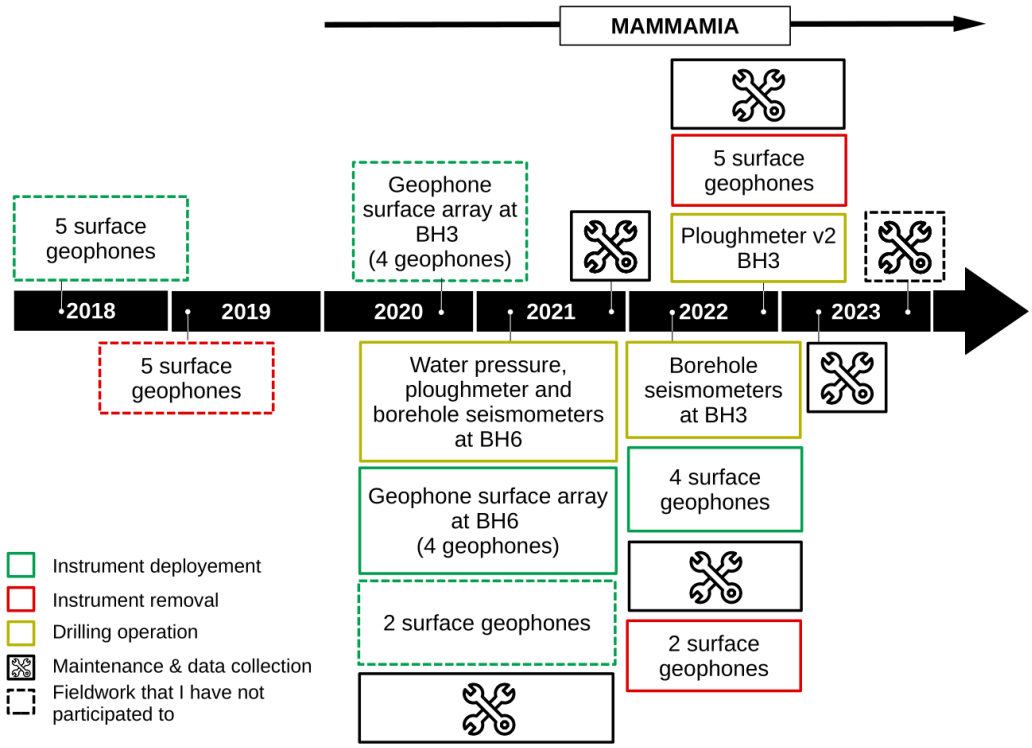

FIGURE 4.2: Calendar of all the field campaigns realised to collect the dataset used in *Paper II* and *Paper III*.

4.1 Preface

4.1.1 The multi-scale multi-instrument network - Part I: the seismic network

The MAMMAMIA project employs a variety of instruments with the goal of combining different sensors to effectively capture a wide range of spatial scales where subglacial processes occur. To achieve this project goal, two main approaches have been employed: the deployment of geophones at the glacier surface and the drilling and instrumentation of boreholes for direct access to the subglacial environment with ploughmeter, vibrating wire pressure sensor and geophones. In this section, we focus on the seismic installation both at the surface and within the borehole as we used exclusively this network for *Paper II*. Further details on the other instruments can be found in the following Chapter 5, Section 5.1.1.

At the surface, numerous geophones have been installed (DiGOS, 4.5 Hz). The initial geophones were stand-alone stations installed in 2018, but they were removed in 2019 as part of a separate project unrelated to MAMMAMIA. The first geophones installed specifically for the MAMMAMIA project were two 3D geophones arrays (four geophones at each site), at the BH3 and BH6 sites (Figs. 4.3 and 4.2). Subsequently, between 2021 and 2023, additional stand-alone stations were gradually installed (Figs. 4.3 and 4.2). Overall, we have so far monitored 19 locations at the glacier surface, some intermittently and others continuously (Fig. 4.2). Currently, ten locations are still monitored by the surface network.

One of the drill sites drilled in 2021 (BH6, Fig. 4.2) is strategically located at the long-term equilibrium line altitude of the glacier. This particular area has shown an acceleration in the velocity of Kongsvegen glacier since 2014, indicating an active surge buildup. There, the borehole is equipped with three borehole geophones (HG-6 OB, 14 Hz, 375 Ω), placed at varying distances from the glacier bed (the closest to the bed being 263 m beneath the surface, 86 m above the glacier bed). The same operation has been done on a second drill site drilled in 2022 (BH3, Fig. 4.2), located in the ablation zone of the glacier. In this area, the glacier velocity remains low, indicating that it has not yet been affected by the surge buildup. The lowest geophone is located 262 m below the glacier surface and 78 m above the glacier bed.

In addition, we use the model output from Schmidt et al. (2023) that simulate the surface runoff across Kongsvegen glacier.

The dataset used for *Paper II* then consists of the seismic records of the surface and borehole geophones, and the runoff model output. From these

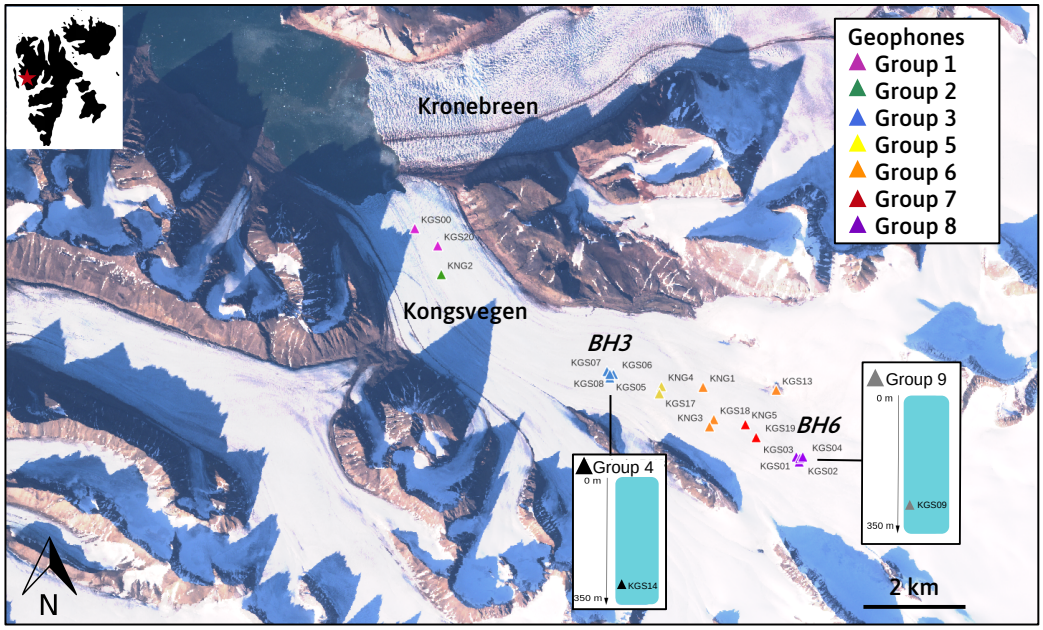

FIGURE 4.3: Location of the cryoseismic network on Konsgsvegen. The different groups correspond to geophones located at close proximity (<1 km) their records are merged to maximize the continuity and data quality.

records, we derive icequakes occurrence and amplitude and subglacial drainage system properties, described below.

4.1.2 Icequakes occurrence and amplitude

Impulsive seismic event serve as a valuable indicator of icequakes activity, which in turn is a signature of localized stress variations (Hudson et al., 2020). Between 2018 and 2022, we assessed icequake occurrences by detecting impulsive seismic event through comparing a running 0.25-second short-term average (STA) and a five-second long-term average (LTA) of the vertical component of ground velocity, specifically above the 25 Hz frequency range (Withers et al., 1998; Trnkoczy, 2009; Beyreuther et al., 2010). Event onset is recognized when the STA/LTA ratio surpasses a value of four, while event cessation is determined when the ratio reaches two. The amplitude of an event is computed as the 99th percentile of the waveform envelope spanning from

0.5 seconds prior to event initiation until its conclusion. Our parameter selection for detecting impulsive seismic events has been tailored to focus on short-term impulsive phenomena such as crevasse opening (attributed to alterations in tensile stress, Nye, 1955) and stick-slip occurrences (i.e., friction behavior when surfaces alternate between sticking and sliding over each other, with a corresponding change in the force of friction Byerlee, 1970). Additionally, the parameter choice minimizes the influence of tremor-like signals like calving events and water flow effects (Podolskiy and Walter, 2016). Catalogs derived from surface measurements predominantly capture surface crevasses (Walter et al., 2008), whereas those derived from borehole measurements primarily detect basal events such as basal crevasses and/or stick-slip events (Gräff and Walter, 2021; Gräff et al., 2021).

4.1.3 Studying the subglacial hydrology with cryoseismology: derived variables

To study the subglacial hydraulic properties of the subglacial drainage system, we adopt the framework developed by Gimbert et al. (2016) linking the seismic power, P and the subglacial water discharge, Q. This theoretical framework allows to derive the relative changes in hydraulic radius, denoted as R, which represents the ratio of the cross-sectional area of channel flow to its wet perimeter and scales with flow depth in open channel flow (Fig. 4.4). The hydraulic pressure gradient, denoted as S, depends on both the rate of change of water pressure in the flow direction and the bed slope (Fig. 4.4).

The relative changes in R and S can be derived as:

$$S/S_{ref} = \frac{P}{P_{ref}}^{24/41} \frac{Q}{Q_{ref}}^{-30/41} \frac{N}{N_{ref}}^{6/41} \tag{4.1}$$

$$R/R_{ref} = \frac{P}{P_{ref}}^{-9/82} \frac{Q}{Q_{ref}}^{21/41} \frac{N}{N_{ref}}^{-33/82} \tag{4.2}$$

where the subset denoted as ref represents a reference state, defined over the same time period for both P and Q, although not necessarily for R and S. This framework has been formulated to encompass conduits that can be established within ice, sediments, and/or bedrock. Additionally, a sensitivity analysis has indicated that fluctuations in relative bed roughness, relative to the water flow depth of 3% to 10% (as typically encountered in setups similar to ours, Mankoff et al., 2017), may introduce uncertainties ranging from 10% to 25% and from 0% to 5% in the estimation of S and R, respectively (Gimbert et al., 2016). In addition, alterations in the number of conduits, even within an order of magnitude (a range that exceeds expectations in Kongsvegen glacier,

Scholzen et al., 2021), do not significantly impact the accuracy of S and R estimation (Nanni et al., 2020). In *Paper II* and *Paper III*, we assume a constant number of channels, resulting in the omission of the latter terms in both equations.

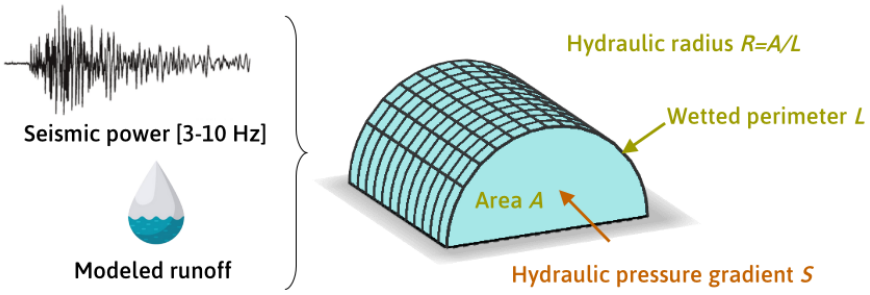

FIGURE 4.4: Schematic representation of subglacial channel-flow-induced seismic noise. Representation of an idealized conduit of hydraulic radius R and hydraulic pressure gradient S.

To apply this framework, we calculate the seismic power using the vertical component of the ground velocity through Welch's method over a two-second time window with a 50% overlap (Welch, 1967; Beyreuther et al., 2010) within the frequency band 5 to 10 Hz. Our choice of these frequencies is based on the premise that it is dominated by the subglacial turbulent-water-flow-induced seismic noise (Bartholomaus et al., 2015; Gimbert et al., 2016; Nanni et al., 2020; Nanni et al., 2022), as previously observed in numerous glacial settings (e.g., Preiswerk and Walter, 2018; Lindner et al., 2020; Labedz et al., 2022; Clyne et al., 2023). To maximize sensitivity to continuous background noise while mitigating the influence of impulsive short-lived events, we apply a rolling minimum over a five-minute time window within the decimal logarithmic space. Subsequently, we define P as the median seismic power within the 5-10 Hz frequency band, which best encapsulates the seismic noise generated by subglacial turbulent water flow, given that higher-frequency seismic signals primarily stem from bedload sediment transport (Gimbert et al., 2016).

Additionally, we use the surface runoff modelled on Kongsvegen glacier by Schmidt et al. (2023) to estimate the subglacial discharge, denoted as Q. The model incorporates a percolation scheme to account for snow and firn transfer times, coupled with a horizontal delay scheme that accommodates local topographical variations. Through validation against in-situ observations, the model proficiency in accurately representing daily discharge at the catchment scale has been established (Schmidt et al., 2023). To establish a connection between alterations in runoff and fluctuations in subglacial discharge, we assume

a consistent and efficient englacial transfer of the water from the glacier surface to the subglacial environment. This hypothesis is substantiated by in-situ investigations conducted on glaciers within a polythermal regime similar to that of Kongsvegen glacier (Benn et al., 2009; Gulley, 2009; Bælum and Benn, 2011; Irvine-Fynn et al., 2011).

4.2 Summary of *Paper II*

Climate change has increased surface melt in almost all the glaciated areas (e.g. Wille et al., 2019; Thomson et al., 2021; Hugonnet et al., 2021; Stokes et al., 2022; Johnson et al., 2022). These have implications on the ice-bed interface coupling and so on the flow and stability of glaciers and ice sheets (Weertman, 1957; Lliboutry, 1968; De Fleurian et al., 2014; Thøgersen et al., 2019; Gilbert et al., 2022). On glaciers and ice sheets, water from melt and precipitation is conveyed to the subglacial environment through crevasses, moulins, and englacial features (Shreve, 1972). Different parts of the subglacial drainage system exhibit distinct behavior: the water is drained efficiently in localised channels, flowing under reduced water pressure (Röthlisberger, 1972; Hubbard et al., 1995; Schoof, 2010) while in the inefficient parts, the water is drained over distributed segments operating at higher water pressure (Lliboutry, 1968; Kamb, 1987). The basal water pressure significantly influences the ice-bed coupling, ultimately affecting glacier sliding and stability (Iken and Truffer, 1997; Davison et al., 2019; Stevens et al., 2023). The interplay between the subglacial drainage capacity and mechanical processes plays a major role in glaciers exhibiting transient dynamic such as glaciers surges but is yet not well understood due to the challenging access to the subglacial environment (Thøgersen et al., 2019; Benn et al., 2019; Minchew and Meyer, 2020; Gimbert et al., 2021; Fleurian et al., 2022; Maier et al., 2022; Nanni et al., 2023). This study delves into the response of an Arctic glacier to the increase in intensity and spatial extent of surface melt.

Our study employs a network of strategically positioned seismometers to analyze both the spatial and temporal evolution of icequake activity and subglacial hydraulic conditions. From 2018, we progressively and intermittently deployed 19 three-components geophones positioned along flow from the glacier front and spanning up to a distance of 13 km, near the equilibrium line altitude and two seismometers placed close to the ice-bed interface (~80 m above the glacier bed) at 6 km and 13 km from the glacier front. We derive the icequakes occurrence and amplitude from the seismic signal (i.e., crevasses openings and stick-slip motion, Withers et al., 1998; Trnkoczy, 2009; Beyreuther et al., 2010). Additionally, we compute the seismic power within the 5 to 10 Hz frequency band (a frequency band generally dominated by turbulent water

flow, Bartholomaus et al., 2015; Gimbert et al., 2016; Nanni et al., 2020; Nanni et al., 2022). Combining the seismic power with the subglacial discharge derived from the surface runoff, we derive the hydraulic capacity and the water pressure conditions of the subglacial drainage system (Preiswerk and Walter, 2018; Lindner et al., 2020; Nanni et al., 2020; Labedz et al., 2022; Clyne et al., 2023).

We show that having seismometers positioned at the glacier surface and close to the glacier bed provide unique opportunity to discuss the potential combined contributions of supra-, en- and sub-glacial turbulent water flow to the seismic power, often attributed to subglacial turbulent water flow only. The hydraulic capacity, i.e., R, and water pressure, i.e. S, derived from the co-located instruments shows similar trends but slight differences in their values. Our findings reinforce the suitability of using the seismic power measured both at the surface and within boreholes to investigate subglacial hydraulic properties as the fluctuations recorded are alike. However, surface measurements tend to underestimate the decrease of subglacial water pressure and the increase in the subglacial drainage capacity at the peak of the melt season, as they are potentially also influenced by the development of step-pool sequences and large bends in the supra- and en- glacial system as observed in similar glacier settings (Piho et al., 2022). Additionally, the presence of higher amplitude icequakes recorded close to the glacier bed compared to the glacier surface reinforces that instruments placed close to the glacier bed are more sensitive to basal events such as stick slip (Gräff and Walter, 2021; Gräff et al., 2021) while instruments close to the glacier surface are more sensitive to crevasse opening (Hudson et al., 2020), a dominant process into most icequake catalog.

Furthermore, at the seasonal scale, the subglacial drainage system evolution and icequake activity reveals contrasting dynamics between glacier bed regions located below sea level and those above sea level. For the former case, despite increased drainage capacity, high basal water pressure persists throughout all the melt season. This is coupled with relatively low icequake rates but an increasing icequake amplitude with increasing runoff, indicating enhanced ice-bed mechanical decoupling and local tensile stress amplification. Conversely, glacier beds above sea-level exhibit an upglacier development in the subglacial drainage system. As runoff rises (falls), drainage capacity increases (decreases) and basal water pressure decreases (increases). This coincides with a rise in icequake activity as basal water pressure drops, indicating enhanced ice-bed mechanical coupling during the peak of the melt season. These patterns align with expectations for marine-terminating glaciers below sea-level (Moon et al., 2014) and land-terminating glaciers above sea-level (Röthlisberger, 1972; Ng, 2000b; Davison et al., 2019; Nanni et al., 2023),

elucidating their transient responses to changing subglacial discharge.

We suggest that Kongsvegen glacier is undergoing destabilisation following two main mechanisms both driven by the increase in intensity and spatial extent of the surface melt. On one hand, we suggest that the glaciers geometry at lower elevation is highly impacted by climate change leading to the steepening of this area while little changes are observed in higher elevation. Such steepening lead to an increase of basal shear stress in the upper part of the glacier which has led to a moderate increase ($< 40\%$) of both basal and surface glacier velocities, which is still much lower than the >500% acceleration observed. On the other hand, we observe the progression of icequake activity along the glacier flow which demonstrates a notable rise in crevasse and stick-slip phenomena in the upper glacier region consistently evident across melt seasons. The icequake catalog is dominated by surface events but the elevated icequake amplitude detected near the glacier base relative to the surface highlights the significant involvement of basal events. We suggest then that the initial acceleration is caused by local changes in the internal state of stress. Additionally, the increased runoff has allowed the formation of crevasses. The newly formed crevasses could then grow by hydrofracturing due to the increase in runoff, and favor new pathways for the surface meltwater to reach the subglacial environment. As a consequence, water is likely supplied to formerly dried areas in the bed where it could modify the ice-bed coupling and/or sediment deformation. In turn, sliding of the glacier is likely to increase in these areas, favoring the opening of new crevasses.We refer to this feedback as an hydro-mechanical feedback (Dunse et al., 2015), which has been proposed to explain other surge initiation (Dunse et al., 2014; Kääb et al., 2018; Sevestre et al., 2018). Furthermore, the over-deepening bed geometry of the glacier is favoring the glacier-wide propagation of an instability.

Our approach sheds light on glacier destabilisation mechanisms and can be adapted to study other transient earth surface processes governed by hydro-mechanical conditions, such as volcanic systems, ice falls, snow avalanches, and debris flows. To deepen our understanding, we propose complementing this approach by precisely identifying seismic noise sources (Wang et al., 2013; Chang and Nakata, 2022), exploring absolute stress changes through focal mechanisms and event localization (Hudson et al., 2020; Gräff et al., 2021), and retrieving structural changes using noise interferometry (Zhan, 2019; Guerin et al., 2021).

Chapter 5

Surge-type glaciers at local scale: runoff-induced subglacial hydro-mechanical condition variations

This Chapter is centered on Paper III: Bouchayer, C., Nanni, U., Lefeuvre, P. M., Hulth, J., Schmidt, L.S., Kohler, J., Renard, F., Schuler, T. V. Multi-scale variations of subglacial hydro-mechanical conditions at Kongsvegen, Svalbard. In review in The Cryosphere. The complete article can be found in Chapter 7, Section 7.3. The primary focus of this Chapter is to address the following research and thematic questions:

Thematic question 2: Hydro-mechanical conditions: What is the interplay between sub- glacial hydrological and mechanical processes and how do they influence the glacier-wide dynamic?

Methodological question 3: Multi-scales multi-instruments framework : To which extent a multi-instruments multi-scale framework helps at understanding the different subglacial hydro-mechanical conditions happening at different areas of the bed?

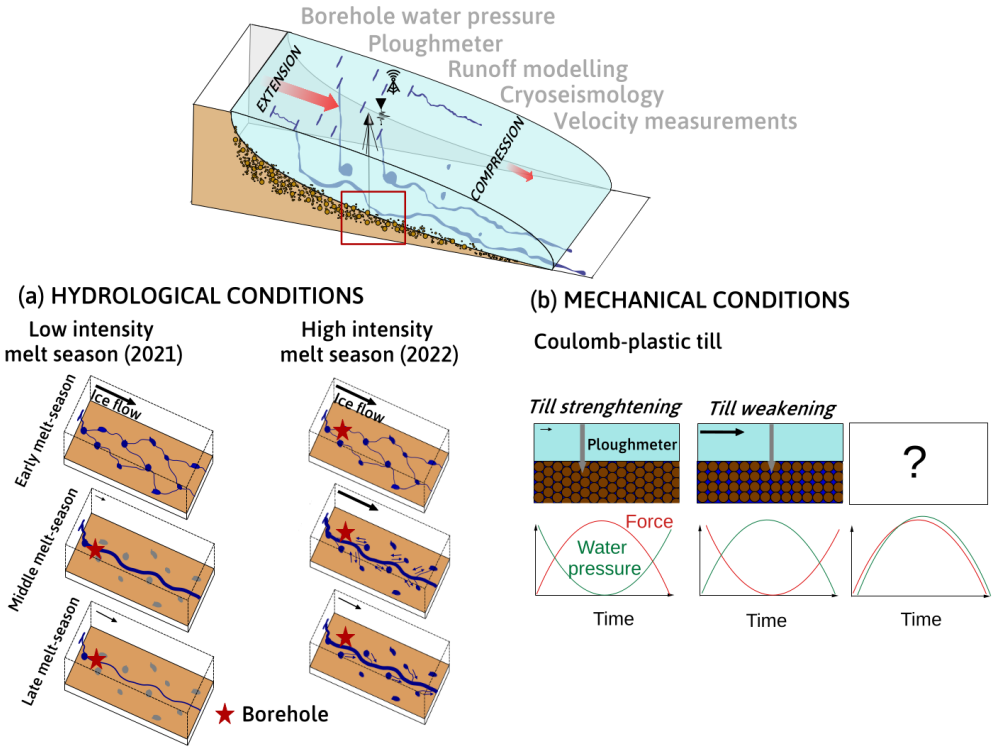

FIGURE 5.1: Sketch of the adjustment of local hydro-mechanical conditions to variations in runoff between the period spanning from June 2021 to August 2022.

"It is a capital mistake to theorize before one has data." - Sherlock Holmes, as portrayed in the writings of Arthur Conan Doyle

As said in the previous Chapter 4, the multi-scale multi-instrument network consists of more instruments than geophones (Fig. 4.2). Complementary to the seismic network, we simultaneously record at the point-scale inside a borehole changes in basal water pressure changes in till mechanics, and their interactions constrain subglacial hydro-mechanical conditions induced by runoff on Kongsvegen glacier. By combining these records with cryoseismology, I delve into the interconnected feedback mechanisms between water input, subglacial hydrology, till mechanics, and the overall dynamic of the glacier. In this section preface, I provide details on the other instruments and an overview of the data analysis methodology. Subsequently, I summarize *Paper III* and present the key findings.

5.1 Preface

5.1.1 The multi-scale multi-instrument network - Part II: point-scale instruments

In addition of the 25 seismometers deployed in the MAMMAMIA context, we instrumented the borehole with a vibrating wire pressure sensor and a ploughmeter.

At BH6 site, the vibrating wire pressure sensor (Geokon 4500SH, < 2 kPa accuracy and 10.5 kPa resolution) has been installed at ~ 1 m from the glacier bed inside the borehole. It provides quantitative information about the basal water pressure and changes occurring at the glacier bed. We use the basal water pressure data recorded without any further post-processing. The ploughmeter, consisting of a 1.4 m steel rod equipped with pairs of strain gauges, is inserted into the sediments with its upper part trapped in the ice. By measuring the bending of the strain gauges on the ploughmeter caused by the movement of the glacier ice and the resisting forces of the till, we can capture changes in the sliding velocity of the glacier and/or in the till conditions. We convert the changes in voltage induced by the ploughmeter bending recorded into a variable known as the force applied to the till by the ploughmeter, F.

At BH3 site, the borehole houses an improved version of the ploughmeter used at BH6 that had onboard water pressure sensors among other sensors. Unfortunately, despite its successful performance during lab calibration and testing, this instrument failed to operate in the borehole, resulting in the absence of data.

In addition, the glacier daily velocity near BH6 site has been continuously monitored for a significant period with Global Navigation Satellite System (GNSS). Data are recorded at five-seconds interval continuously between April 1st and September 1st when there is enough sun for the solar panels, and to conserve battery power, only for one hour per day during the rest of the year. Static post-processing is applied to the GNSS data, assuming that the rover station is static for one hour due to the relatively low speed of the glacier. The Norwegian Mapping Authority permanent network base station in Ny-Ålesund is used as reference.

In *Paper III*, we use the central surface geophone from the 3D geophone array located at BH6, the water pressure from the vibrating wire pressure sensor and force applied to the till by the ploughmeter. We examine the response of these data to modelled runoff forcing (Schmidt et al., 2023). To inspect the response-forcing relationship, using the same method as in *Paper II* (see also Sect. 4.1.3), we derive the seismic power derived from 3 to 10 Hz, P, the subglacial hydraulic radius, R and subglacial hydraulic pressure gradient, S. We use the glacier daily velocity to study the response of runoff induced changes in hydro-mechanical conditions on the glacier dynamic. All the variables are averaged in a 3-hours time window.

5.1.2 Studying the subglacial hydrology with cryoseismology: theoretical scaling

We compare the recorded seismic power, P to the theoretical scaling relationship between P and subglacial water discharge, Q, derived by Gimbert et al. (2016) to determine the regime in which subglacial channels develop, considering two end-members: (i) channels with a fixed hydraulic radius and varying hydraulic pressure (Fig. 5.2a), or (ii) channels controlled by a constant hydraulic pressure gradient with varying hydraulic radius (Fig. 5.2b). These relationships are based on two key assumptions. On one hand, the source-to-station distance is considered constant. On the other hand, all channels have equal hydraulic radius and hydraulic pressure gradient, indicating similarity in size and position compared to the seismic stations. For channels evolving under a constant hydraulic radius (with varying hydraulic pressure gradient), the scaling relationship is as follows (Fig. 5.2a):

$$P \propto Q^{14/3} \tag{5.1}$$

In contrast, if the channels evolve under a constant hydraulic pressure gradient and varying hydraulic radius (Fig. 5.2b), the scaling relationship is:

$$P \propto Q^{5/4} \tag{5.2}$$

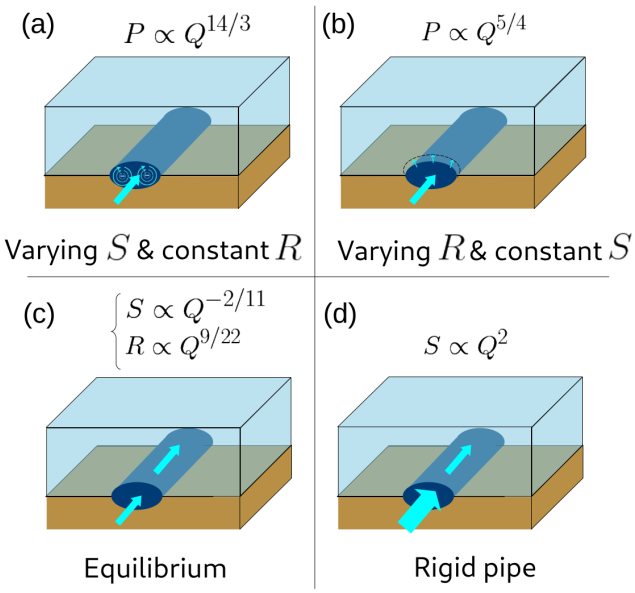

FIGURE 5.2: Schematic of the theoretical scaling relation between the seismic power P, the hydraulic radius R and the hydraulic pressure gradient S with the runoff Q. (a) The channels controlled by a constant hydraulic radius with varying hydraulic pressure gradient. (b) The channels controlled by a constant hydraulic pressure gradient with varying hydraulic radius. (c) The channel geometry changes can accommodate the rate at which water is supplied to the system. (d) The channels exhibit rigid pipe behavior.

Furthermore, in accordance with the Röthlisberger R-channel theory (Röthlisberger, 1972), channels can either evolve at equilibrium or out of equilibrium with the water input. Nanni et al. (2020) derived the equations from Röthlisberger (1972)'s theory to assess the relationships between the hydraulic radius, R, the hydraulic pressure gradient, S, and the subglacial water discharge, Q, which describe the equilibrium state in which the channels develop. A channel is considered to be at equilibrium with Q when the rate at which the channel geometry changes can accommodate the rate at which water is supplied to the system (Fig. 5.2c). If this condition is not met, the channels evolve out of equilibrium and behave similar to a rigid pipe, with an increase in pressure resulting from the influx of water (Fig. 5.2d). For the former case, the scaling relationships are as follows:

$$R \propto Q^{9/22} \tag{5.3}$$

$$S \propto Q^{-2/11} \tag{5.4}$$

The channels exhibit rigid pipe behavior if:

$$S \propto Q^2 \tag{5.5}$$

5.2 Summary of *Paper III*

Glacial flow is influenced by ice deformation, basal sliding at the ice-bed interface, and subglacial sediment deformation (Cuffey and Paterson, 2010). Changes in subglacial environment conditions can lead to unstable glacier flow. However, limited access to the subglacial environment has resulted in a lack of data to effectively constrain models and understand glacier instabilities (Thøgersen et al., 2019; Gilbert et al., 2022). Previous studies have used different approaches to study these processes. One approach involves the instrumentation of boreholes with vibrating wire pressure sensors to monitor point-scale changes in subglacial hydrology (e.g. Andrews et al., 2014; Doyle et al., 2018; Rada and Schoof, 2018; Sugiyama et al., 2019), as well as ploughmeters, tiltmeters, or drag spools to gain local insights into subglacial till mechanics (Fischer and Clarke, 1994; Porter et al., 1997; Kavanaugh and Clarke, 2000). Another approach involves studying seismic noise to investigate spatially integrated development of the subglacial drainage system (Bartholomaus et al., 2015; Gimbert et al., 2016; Nanni et al., 2020; Lindner et al., 2020; Labedz et al., 2022). However, these techniques are typically used separately, which hinders a simultaneous study of different areas within the subglacial environment and their interactions.

To overcome these challenges, we have assembled a comprehensive dataset that combines subglacial variables, i.e., the basal water pressure from the vibrating wire pressure sensor, force applied to the till by the ploughmeter, the seismic power derived from 3 to 10 Hz, P, the subglacial hydraulic radius, R and subglacial hydraulic pressure gradient, S. Additionally, we measure the daily glacier velocity and modelled the surface runoff. This surge-type glacier has shown accelerations since 2014, indicating an upcoming fast-flow event. The records cover two contrasting melt seasons from June 2021 to August 2022, the former is short (67 days) accompanied by low runoff input (lower than 20 $m^3\ s^{-1}$), while the latter is long (at least 83 days) with high runoff input (higher than 20 $m^3\ s^{-1}$). By analyzing the responses of subglacial variables recorded in our study, we characterize the response of the subglacial environment to runoff. We examine the forcing-response relationships between these variables and runoff at different glaciologically significant time scales: seasonal, multi-day, and diurnal. We also compare the response of the seismic power, hydraulic radius and hydraulic pressure gradient, to runoff, using established theoretical scaling relationships (Gimbert et al., 2016; Nanni et al., 2020).

During the short and less intensive melt season 2021, we conjecture that our borehole intersected a well-connected part of the subglacial drainage system. In contrast, in the longer and intensive melt season 2022, the borehole records are characteristic of a poorly connected subdomain of the subglacial drainage system. Nevertheless, seismological records indicate the development of an efficient drainage system during both melt seasons as they progressed. Our findings derived from different records sometimes led to ambiguities and inconsistencies. These discrepancies raise questions about the underlying factors contributing to such differences. We interpret that these differences can be caused by the existence of different hydraulic connections within the subglacial drainage system captured by the different instrument footprints. Indeed, the subglacial water pressure is recorded inside the borehole and gives a very local (point-scale) representation of the subglacial environment, giving the opportunity to be one year placed in a preferential channel axis while during another season be in an isolated part of the subglacial drainage system, as we observe. On the other hand, the records from cryoseismology are integrated measurements over a km^2-scale. The latter is dominated by high turbulent water flow (main active part of the subglacial drainage system), hiding the potential presence of low turbulent water flow in other areas of the subglacial drainage system.

The multi-instrument approach then captures different areas of the subglacial drainage system and highlights the simultaneous presence of different hydraulic connections. We then can observe that the isolated part of the subglacial drainage system increase in basal water pressure when the main active channels operate at high basal water pressure during high runoff input. During these events, we conjecture that the drainage capacity of the preferential drainage axis is exceeded, promoting the extent of the hydraulically connected regions and locally ice-bed decoupling promoting sliding.

Our study also sheds light on the complex rheology of the till. While a consensus appears to be forming around its Coulomb-plastic characteristics, our findings contribute to this understanding at the seasonal scale. We indeed observe a Coulomb-plastic behavior in the till at this time-scale, aligning well with contemporary modeling, experimental data, and in-situ observations. However, at shorter time scales, it exhibits apparent characteristics of a viscous material, especially during glacier accelerations, albeit inconsistently. We propose that different mechanisms, e.g. till loaded towards their yield strength, variations in the mobilization of the till at depth, and the presence of clasts help to reconcile the apparent contradiction we observed in our results concerning Coulomb-plastic rheology. However, how these processes explain our results remains unclear and require further investigations.

Overall, our study emphasizes the importance of a multi-sensor and multi-scale approach to investigate the heterogeneous subglacial drainage system and the interactions of its different parts. In addition, we show that we can gain insights on the Coulomb-plastic till rheology and study more in depth the subglacial hydro-mechanical variations leading to glacier-wide dynamic. To go further, the precise location of the active and less active part of the subglacial drainage system could be inferred from a dense seismic array (Nanni et al., 2021) and the changes in till behaviour assessed with the ploughmeter records could be complemented by assessing changes in till properties using seismic noise interferometry (Zhan, 2019).

Chapter 6

Conclusions and perspectives

"Humanity will draw more good than evil from new discoveries" - Marie Curie

The understanding of transient glacier dynamics is crucial for accurately projecting future global sea-level rise. However, many aspects of the governing processes behind glacier instabilities remain poorly understood. Throughout my doctoral research, I undertook a comprehensive investigation of glacier instabilities, examining multiple scales of analysis encompassing regional, glacier-specific, and localized areas within approximately 1 km^2 (Fig. 6.1). This work spanned a range of temporal scales, from studies without a specific time component to investigations extended over multiple years and those focused on a single year (Fig. 6.1). This interdisciplinary thesis crosses various fields within glaciology, bridging subglacial hydrology and mechanics. I used diverse methodologies, including data mining and machine learning modeling, field observations and cryoseismology. In this section, I answer the research questions addressed at the beginning of this thesis. Later, I propose future research directions to deepen our understanding on glacier transient dynamic and subglacial hydro-mechanical processes building upon the findings of my doctoral research.

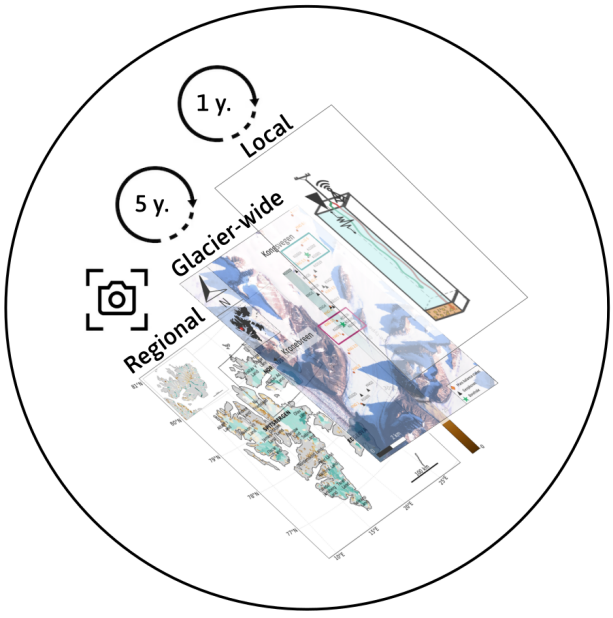

FIGURE 6.1: Visualizing the spatio-temporal scale investigated during my doctoral research.

6.1 Answers to the research questions

6.1.1 Thematic questions

Glacier surges: What are the characteristics of glaciers exhibiting transient dynamic compared to others?

I show that glaciers possessing greater thickness and width, coupled with a low surface slope, exhibit an elevated probability of being categorized as surge-type glaciers, a result which is in agreement with existing surge theories (Kamb and Engelhardt, 1987; Fowler, 1989; Benn et al., 2019; Thøgersen et al., 2019). However, notably, I highlight a unique aspect: these discerning characteristics are not uniformly distributed across the entirety of the glacier, but rather localized to specific regions. I propose that these localized sectors within a glacier could be designated as "triggering zones." These zones serve as points of origin for the initiation of an instability phenomenon to occur, subsequently propagating throughout the glacier and leading to its partial or complete destabilisation as in Thøgersen et al. (2019). Historically, glaciers have been categorized as either non-surge or surge-type, with additional subdivisions like Alaskan or Svalbard types. However, recent research (Herreid and Truffer, 2016; Thøgersen et al., 2021; Benn et al., 2023), including the study presented in this thesis, proposes a more nuanced viewpoint. According to this perspective, glacier instability is better understood as a continuous spectrum, contingent on how instability propagates and impacts different glacier sections or the entirety of glaciers. This spectrum culminates with the most extreme expressions of instability: glacier surges and collapses.

Hydro-mechanical conditions: What is the interplay between ice flow, basal friction and the subglacial drainage system and how do they influence the glacier-wide dynamic?

I demonstrate that the initiation of glacier surges can occur through a hydro-mechanical feedback mechanism. Crevasses within the glacier open preferential routes for the infiltration of surface runoff into the subglacial environment. This process amplifies sliding and glacier acceleration, consequently leading to the formation of additional crevasses. Modern models are currently coupling basal friction with subglacial hydrology to explain glaciers surges (Thøgersen et al., 2021; Beaud et al., 2022) but omit that ice flow acceleration causes additionally surface crevasses, leading to an additional supply of water to the subglacial environment. This process appears pivotal from the results presented in my thesis. Additionally, I show that slip acceleration can be caused by the interplay between hydraulically active and less active sections of the

subglacial drainage system. By demonstrating the simultaneous presence of different hydraulic connections in the subglacial drainage system, I emphasise the necessity of transcending the conventional dichotomy of the subglacial drainage system, consisting often of only two components. Instead, I advocate for a shift towards recognizing the subglacial drainage system as a collection of entities, each of these maintaining different equilibrium state with respect to runoff, and having the potential to evolve independently but with the ability to establish hydraulic connections and influence glacier-wide dynamic, as advocated by Schoof (2023a) and Schoof (2023b).

Till mechanics: How does the till adapt to changes in subglacial hydrological conditions?

I show that, at seasonal scale, the till behaves as Coulomb-plastic material, weakening during relatively pressurized conditions and strengthening during less pressurized conditions, as currently demonstrated by several other studies (e.g., Schofield and Wroth, 1968; Kamb, 1991; Nedderman et al., 1992; Hooke et al., 1997; Tulaczyk et al., 2000; Iverson and Iverson, 2001; Kavanaugh and Clarke, 2006; Iverson et al., 2007; Gillet-Chaulet et al., 2016; Damsgaard et al., 2016). However, at shorter time-scale, the till layer exhibits characteristics indicative of a viscous rheology. I suggest to approach this conclusion with caution, as several factors might come into play i.e., ice-decoupling phenomena, the depth dependency of the till deformation, occurrences of refreezing, and the presence of clasts within the upper till layer, which can modify the observed behavior while not inherently contradicting the Coulomb-plastic rheology. The present work provides more constraints on the till response to changes in ice flow and subglacial water pressure, as suggested by other recent studies (Damsgaard et al., 2017; Zoet et al., 2023).

6.1.2 Methodological questions

Machine learning practices: How well does machine learning inform quantitatively on the wide-spectrum of transient glacier dynamics?

I show that discretizing glacier characteristics along their centerlines as machine learning model input to calculate surging probabilities acknowledges the complexity of natural systems, preventing oversimplification through integrated features and highlight preferential triggering zones where the instability could initiate, therefore arguing for a more continuous scale of glaciers instabilities rather than a binary classification. Using this method, I propose the first map that quantifies the probability for every glacier in Svalbard to

be surge-type and the location of the potential triggering zones. The method shows robustness by classifying some glaciers surge-type, which, although previously not identified as such in global inventories, have been observed surging. The models performance, although considered good, is influenced by the quality and uncertainty of input features, which are mostly derived from numerical simulations. Spatial resolution differences and temporal snapshots of features introduce variability and potential inaccuracies.

Seismic instrumentation - from the glacier bed to surface: What hydro-mechanical information do we learn from geophones positioned at the surface compared to close to the glacier bed?

I show that the co-location of instruments, positioned both at the glacier surface and at its base allows for an easier segregation between icequakes originated by surface events, and icequakes originated by basal events. Additionally, I quantify that while surface and basal geophones are appropriate to retrieve subglacial drainage system properties, the hydraulic properties inferred from the surface instrumentation are most likely influenced by supra-glacial drainage system such as step-pools sequences and large bends formation. I estimate that the hydraulic pressure gradient is likely overestimated by 9-16% and the subglacial drainage capacity is likely underestimated by 23-40% when inferred from surface measurements during the peak melt season.

Multi-scales multi-instruments framework: To which extent a multi-instruments multi-scale framework helps at understanding the different subglacial hydro-mechanical conditions happening at different areas of the bed?

The simultaneous recording of the basal water pressure and till mechanics provide some useful insights into the complex subglacial hydro-mechanical coupling at local scales. Additionally, discrepancies in the subglacial drainage system characteristics derived between the sensors, i.e., basal water pressure and geophones, can be viewed as a positive result. Indeed, the instruments have different footprints and so I justify that we are able to record simultaneously hydraulically active and less active/isolated parts of the subglacial drainage system. However, the inconsistencies within our subglacial hydrology records present challenges in making accurate extrapolations. Indeed, these discrepancies raise questions about potential human influence, considering that the act of drilling boreholes might have introduced biases into the recorded information. Additionally, in the study setting, a variety of till processes could have resulted in comparable observations. Consequently, the

multi-method approach adopted in my thesis falls short of providing a definitive means of distinguishing between these processes.

6.2 Outlook

The insights gained from studying glacier instabilities during my doctoral research open up exciting research opportunities. Here, I suggest future research directions to continue improving our understanding of transient glacier dynamics:

1. The database compiled for investigating the probability of glaciers to be surge-type and their characteristics in Svalbard holds the promise of expansion to encompass other surge clusters across the globe. This expansion would facilitate a broader comprehension of these phenomena and potentially move away from the dichotomy of non-surge and surge-type glacier in favor of a more continuous scale of instability, also suggested by Herreid and Truffer (2016), Thøgersen et al. (2021), and Benn et al. (2023).

2. The observations of different hydraulic connections and the potential hydraulic disconnection in the subglacial system reinforce the need for further modelling effort to incorporate these elements as they can drive glacier wide acceleration, not implemented in most current models (Schoof, 2005; Gagliardini et al., 2007; Werder et al., 2013; Sommers et al., 2018; Helanow et al., 2020; Helanow et al., 2021).

3. Even by coupling several instruments, the interplay between basal water pressure and till mechanics is complex since many processes such as ploughing clasts, refreezing processes, location of the shear band, and till characteristics influence the till deformation. Further experimental and observation efforts should be conducted to disentangle where and how these processes affect the till over large spatio-temporal scale as they are likely to control basal drag (Zoet and Iverson, 2020) and such observations would help their parametrization in soft-bed surge models (Minchew and Joughin, 2020; Beaud et al., 2022).

4. Current models focus on coupling basal friction with subglacial drainage system (Thøgersen et al., 2021; Gilbert et al., 2022), which constitute a major step forward to model transient velocity variations. Future research should as well incorporate feedback between ice flow acceleration and crevasse openings, providing preferential pathways for surface water to access the

subglacial environment, which in turn affect the friction-drainage coupling and the overall propagation of instabilities.

Half a century has passed since the pioneering studies of glacier surges (Dolgushin et al., 1964; Meier and Post, 1969) but much remains to be understood. Obtaining field data on unstable glaciers is challenging and so field observations are scarce, making the dataset collected and used during my doctoral research precious. Nevertheless, as emphasized in the suggested outlook, these datasets play a pivotal role in guiding the parametrization of models, validating the results produced by models, proposing supplementary coupling processes, and illuminating significant processes that the modeling community should aim to integrate into their models. While simplified frameworks can effectively encapsulate some observations, the multifaceted nature of transient glacier dynamics rests upon an intricate interplay among numerous processes. These interactions frequently resist simplification and demand a more detailed description for a complete grasp of the phenomenon. It is therefore essential that future scientific efforts, supported by appropriate financial and political decisions, are directed towards bridging the modelling community and the observational based approach to better understand transient glacier dynamics and their subglacial hydro-mechanical processes.

Bibliography

Aczel, Balazs and Eric-Jan Wagenmakers (2023). "Transparency guidance for ChatGPT usage in scientific writing". In: *PsyArXiv*.

Alley, RB (1987). "Texture of polar firn for remote sensing". In: *Annals of Glaciology* 9, pp. 1–4.

Alley, Richard B (2000). "Continuity comes first: recent progress in understanding subglacial deformation". In: *Geological Society, London, Special Publications* 176.1, pp. 171–179.

Alley, Richard B and Charles R Bentley (1988). "Ice-core analysis on the Siple Coast of West Antarctica". In: *Annals of Glaciology* 11, pp. 1–7.

Alley, Richard B et al. (1986). "Deformation of till beneath ice stream B, West Antarctica". In: *Nature* 322.6074, pp. 57–59.

Alley, Richard B et al. (1989). "Sedimentation beneath ice shelves—the view from ice stream B". In: *Marine Geology* 85.2-4, pp. 101–120.

Alley, Richard B et al. (2007). "Effect of sedimentation on ice-sheet grounding-line stability". In: *Science* 315.5820, pp. 1838–1841.

Andrews, Lauren C et al. (2014). "Direct observations of evolving subglacial drainage beneath the Greenland Ice Sheet". In: *Nature* 514.7520, pp. 80–83.

Arnaud, Laurent, Jean M Barnola, and Paul Duval (2000). "Physical modeling of the densification of snow/firn and ice in the upper part of polar ice sheets". In: *Physics of ice core records*. Hokkaido University Press, pp. 285–305.

Bælum, K and DI Benn (2011). "Thermal structure and drainage system of a small valley glacier (Tellbreen, Svalbard), investigated by ground penetrating radar". In: *The Cryosphere* 5.1, pp. 139–149.

Bamber, JL et al. (2022). "Ice sheet and climate processes driving the uncertainty in projections of future sea level rise: Findings from a structured expert judgement approach". In: *Earth's Future* 10.10.

Bamber, Jonathan L et al. (2018). "The land ice contribution to sea level during the satellite era". In: *Environmental Research Letters* 13.6.

Banwell, Alison F et al. (2021). "The 32-year record-high surface melt in 2019/2020 on the northern George VI Ice Shelf, Antarctic Peninsula". In: *The Cryosphere* 15.2, pp. 909–925.

Barrand, Nicholas E and Tavi Murray (2006). "Multivariate controls on the incidence of glacier surging in the Karakoram Himalaya". In: *Arctic, Antarctic, and Alpine Research* 38.4, pp. 489–498.

Bartholomaus, Timothy C et al. (2015). "Subglacial discharge at tidewater glaciers revealed by seismic tremor". In: *Geophysical research letters* 42.15, pp. 6391–6398.

Beaud, Flavien, Gwenn E Flowers, and Jeremy G Venditti (2018). "Modeling sediment transport in ice-walled subglacial channels and its implications for esker formation and proglacial sediment yields". In: *Journal of Geophysical Research: Earth Surface* 123.12, pp. 3206–3227.

Beaud, Flavien et al. (2022). "Surge dynamics of Shisper Glacier revealed by time-series correlation of optical satellite images and their utility to substantiate a generalized sliding law". In: *The cryosphere* 16.8, pp. 3123–3148.

Benn, DI et al. (2019). "A general theory of glacier surges". In: *Journal of Glaciology* 65.253, pp. 701–716.

Benn, Douglas et al. (2009). "Englacial drainage systems formed by hydrologically driven crevasse propagation". In: *Journal of Glaciology* 55.191, pp. 513–523.

Benn, Douglas I, Ian J Hewitt, and Adrian J Luckman (2023). "Enthalpy balance theory unifies diverse glacier surge behaviour". In: *Annals of Glaciology*, pp. 1–7.

Beyreuther, Moritz et al. (2010). "ObsPy: A Python toolbox for seismology". In: *Seismological Research Letters* 81.3, pp. 530–533.

Bindschadler, Robert (1983). "The importance of pressurized subglacial water in separation and sliding at the glacier bed". In: *Journal of Glaciology* 29.101, pp. 3–19.

— (1997). "Actively surging West Antarctic ice streams and their response characteristics". In: *Annals of Glaciology* 24, pp. 409–414.

Bingham, Robert G, Peter W Nienow, and Martin J Sharp (2003). "Intra-annual and intra-seasonal flow dynamics of a High Arctic polythermal valley glacier". In: *Annals of Glaciology* 37, pp. 181–188.

Björnsson, Helgi (1998). "Hydrological characteristics of the drainage system beneath a surging glacier". In: *Nature* 395.6704, pp. 771–774.

Blankenship, D Do et al. (1986). "Seismic measurements reveal a saturated porous layer beneath an active Antarctic ice stream". In: *Nature* 322.6074, pp. 54–57.

Błaszczyk, Małgorzata, Jacek Jania, and Jon Ove Hagen (2009). "Tidewater glaciers of Svalbard: Recent changes and estimates of calving fluxes". In.

Bougamont, M et al. (2011). "Dynamic patterns of ice stream flow in a 3-D higher-order ice sheet model with plastic bed and simplified hydrology". In: *Journal of Geophysical Research: Earth Surface* 116.F4.

Bougamont, Marion, Slawek Tulaczyk, and Ian Joughin (2003). "Response of subglacial sediments to basal freeze-on 2. Application in numerical modeling of the recent stoppage of Ice Stream C, West Antarctica". In: *Journal of Geophysical Research: Solid Earth* 108.B4.

Bougamont, Marion et al. (2015). "Reactivation of Kamb Ice Stream tributaries triggers century-scale reorganization of Siple Coast ice flow in West Antarctica". In: *Geophysical Research Letters* 42.20, pp. 8471–8480.

Boulton, GS (1979). "Processes of glacier erosion on different substrata". In: *Journal of glaciology* 23.89, pp. 15–38.

— (1986). "Push-moraines and glacier-contact fans in marine and terrestrial environments". In: *Sedimentology* 33.5, pp. 677–698.

Boulton, GS, KE Dobbie, and S Zatsepin (2001). "Sediment deformation beneath glaciers and its coupling to the subglacial hydraulic system". In: *Quaternary International* 86.1, pp. 3–28.

Boulton, GS and RCA Hindmarsh (1987). "Sediment deformation beneath glaciers: rheology and geological consequences". In: *Journal of Geophysical Research: Solid Earth* 92.B9, pp. 9059–9082.

Boulton, GS and AS Jones (1979). "Stability of temperate ice caps and ice sheets resting on beds of deformable sediment". In: *Journal of Glaciology* 24.90, pp. 29–43.

Boulton, GS et al. (2009). "Drainage beneath ice sheets: groundwater–channel coupling, and the origin of esker systems from former ice sheets". In: *Quaternary Science Reviews* 28.7-8, pp. 621–638.

Box, Jason E et al. (2022). "Greenland ice sheet climate disequilibrium and committed sea-level rise". In: *Nature Climate Change* 12.9, pp. 808–813.

Breiman, Leo (2001). "Random forests". In: *Machine learning* 45, pp. 5–32.

Brinkerhoff, Douglas, Andy Aschwanden, and Mark Fahnestock (2021). "Constraining subglacial processes from surface velocity observations using surrogate-based Bayesian inference". In: *Journal of Glaciology* 67.263, pp. 385–403.

Brown, Tom et al. (2020). "Language models are few-shot learners". In: *Advances in neural information processing systems* 33, pp. 1877–1901.

Budd, WF, PL Keage, and NA Blundy (1979). "Empirical studies of ice sliding". In: *Journal of glaciology* 23.89, pp. 157–170.

Burke, Kevin D et al. (2018). "Pliocene and Eocene provide best analogs for near-future climates". In: *Proceedings of the National Academy of Sciences* 115.52, pp. 13288–13293.

Byerlee, JD (1970). "The mechanics of stick-slip". In: *Tectonophysics* 9.5, pp. 475–486.

Casassa, Gino et al. (1998). "Glaciers in south America". In: *Studies and reports in hydrology* 56, pp. 125–146.

Chandler, DM et al. (2013). "Evolution of the subglacial drainage system beneath the Greenland Ice Sheet revealed by tracers". In: *Nature Geoscience* 6.3, pp. 195–198.

Chang, Hilary and Nori Nakata (2022). "Investigation of time-lapse changes with DAS borehole data at the brady geothermal field using deconvolution interferometry". In: *Remote Sensing* 14.1, p. 185.

Chen, S and I Baker (2010). "Observations of the morphology and sublimation-induced changes in uncoated snow using scanning electron microscopy". In: *Hydrological processes* 24.14, pp. 2041–2044.

Chen, Tianqi and Carlos Guestrin (2016). "Xgboost: A scalable tree boosting system". In: *Proceedings of the 22nd acm sigkdd international conference on knowledge discovery and data mining*, pp. 785–794.

Christianson, Knut et al. (2015). "Dynamic perennial firn aquifer on an Arctic glacier". In: *Geophysical Research Letters* 42.5, pp. 1418–1426.

Church, Gregory et al. (2021). "Ground-penetrating radar imaging reveals glacier's drainage network in 3D". In: *The Cryosphere* 15.8, pp. 3975–3988.

Citterio, Michele et al. (2009). "Remote sensing of glacier change in West Greenland: accounting for the occurrence of surge-type glaciers". In: *Annals of Glaciology* 50.53, pp. 70–80.

Clarke, Garry KC (1976). "Thermal regulation of glacier surging". In: *Journal of Glaciology* 16.74, pp. 231–250.

— (1996). "Lumped-element analysis of subglacial hydraulic circuits". In: *Journal of Geophysical Research: Solid Earth* 101.B8, pp. 17547–17559.

Clarke, Garry KC and Erik W Blake (1991). "Geometric and thermal evolution of a surge-type glacier in its quiescent state: Trapridge Glacier, Yukon Territory, Canada, 1969–89". In: *Journal of Glaciology* 37.125, pp. 158–169.

Clarke, Garry KC, Sam G Collins, and David E Thompson (1984). "Flow, thermal structure, and subglacial conditions of a surge-type glacier". In: *Canadian Journal of Earth Sciences* 21.2, pp. 232–240.

Clarke, Garry KC, Uzi Nitsan, and WSB Paterson (1977). "Strain heating and creep instability in glaciers and ice sheets". In: *Reviews of geophysics* 15.2, pp. 235–247.

Clarke, Garry KC et al. (1986). "Characteristics of surge-type glaciers". In: *Journal of Geophysical Research: Solid Earth* 91.B7, pp. 7165–7180.

Clyne, Elisabeth et al. (2023). "Glacial hydraulic tremor on Rhonegletscher, Switzerland". In: *Journal of Glaciology* 69.274, pp. 370–380.

Colbeck, Samuel C (1976). "An analysis of water flow in dry snow". In: *Water Resources Research* 12.3, pp. 523–527.

Colgan, William et al. (2016). "Glacier crevasses: Observations, models, and mass balance implications". In: *Reviews of Geophysics* 54.1, pp. 119–161.

Copland, Luke, Martin J Sharp, and Julian A Dowdeswell (2003). "The distribution and flow characteristics of surge-type glaciers in the Canadian High Arctic". In: *Annals of Glaciology* 36, pp. 73–81.

Copland, Luke et al. (2009). "Glacier velocities across the central Karakoram". In: *Annals of Glaciology* 50.52, pp. 41–49.

Copland, Luke et al. (2011). "Expanded and recently increased glacier surging in the Karakoram". In: *Arctic, Antarctic, and Alpine Research* 43.4, pp. 503–516.

Covington, MD et al. (2020). "Moulin volumes regulate subglacial water pressure on the Greenland Ice Sheet". In: *Geophysical Research Letters* 47.20, e2020GL088901.

Cuffey, KM et al. (2000). "Entrainment at cold glacier beds". In: *Geology* 28.4, pp. 351–354.

Cuffey, Kurt M and William Stanley Bryce Paterson (2010). *The physics of glaciers*. Academic Press.

Dadic, R et al. (2010). "Wind influence on snow depth distribution and accumulation over glaciers". In: *Journal of Geophysical Research: Earth Surface* 115.F1.

Damsgaard, Anders, Liran Goren, and Jenny Suckale (2020). "Water pressure fluctuations control variability in sediment flux and slip dynamics beneath glaciers and ice streams". In: *Communications Earth & Environment* 1.1, p. 66.

Damsgaard, Anders et al. (2013). "Discrete element modeling of subglacial sediment deformation". In: *Journal of Geophysical Research: Earth Surface* 118.4, pp. 2230–2242.

Damsgaard, Anders et al. (2016). "Ice flow dynamics forced by water pressure variations in subglacial granular beds". In: *Geophysical Research Letters* 43.23, pp. 12–165.

Damsgaard, Anders et al. (2017). "Sediment behavior controls equilibrium width of subglacial channels". In: *Journal of Glaciology* 63.242, pp. 1034–1048.

Das, Sarah B et al. (2008). "Fracture propagation to the base of the Greenland Ice Sheet during supraglacial lake drainage". In: *Science* 320.5877, pp. 778–781.

Davis, Heather and Zoe Todd (2017). "On the Importance of a Date, or Decolonizing the Anthropocene". In: *ACME* 16.4, pp. 761–780.

Davison, Benjamin Joseph et al. (2019). "The influence of hydrology on the dynamics of land-terminating sectors of the Greenland ice sheet". In: *Frontiers in Earth Science* 7, p. 10.

De Fleurian, B et al. (2014). "A double continuum hydrological model for glacier applications". In: *The Cryosphere* 8.1, pp. 137–153.

De Saussure, Horace Benedict (1796). *Voyages dans les Alpes: précédés d'un essai sur l'histoire naturelle des environs de Genève*. Vol. 3. Chez Samuel Fauche.

DeConto, Robert M et al. (2021). "The Paris Climate Agreement and future sea-level rise from Antarctica". In: *Nature* 593.7857, pp. 83–89.

Dieterich, James H (1992). "Earthquake nucleation on faults with rate-and state-dependent strength". In: *Tectonophysics* 211.1-4, pp. 115–134.

Dolgoushin, D (1975). "Glacier surges and the problem of their forecasting". In: *IAHS publication* 104, pp. 292–304.

Dolgushin, Leonid Dmitrievich et al. (1964). *The recent advance of the Medvezhii Glacier*. Directorate of Scientific Information Services, DRB Canada.

Dowdeswell, Julian A, Gordon S Hamilton, and Jon Ove Hagen (1991). "The duration of the active phase on surge-type glaciers: contrasts between Svalbard and other regions". In: *Journal of Glaciology* 37.127, pp. 388–400.

Dowdeswell, Julian A and Meredith Williams (1997). "Surge-type glaciers in the Russian High Arctic identified from digital satellite imagery". In: *Journal of Glaciology* 43.145, pp. 489–494.

Doyle, Samuel H et al. (2018). "Physical conditions of fast glacier flow: 1. Measurements from boreholes drilled to the bed of Store Glacier, West Greenland". In: *Journal of Geophysical Research: Earth Surface* 123.2, pp. 324–348.

Dunse, Thorben et al. (2014). "Destabilisation of an Arctic ice cap triggered by a hydro-thermodynamic feedback to summer-melt". In: *The Cryosphere Discussions* 8, pp. 2685–2719.

Dunse, Thorben et al. (2015). "Glacier-surge mechanisms promoted by a hydro-thermodynamic feedback to summer melt". In: *The Cryosphere* 9.1, pp. 197–215.

Duval, Paul et al. (2010). "Creep and plasticity of glacier ice: a material science perspective". In: *Journal of Glaciology* 56.200, pp. 1059–1068.

Elsworth, Cooper W and Jenny Suckale (2016). "Rapid ice flow rearrangement induced by subglacial drainage in West Antarctica". In: *Geophysical Research Letters* 43.22, pp. 11–697.

Espizua, Lydia E and Jorge D Bengochea (1990). "Surge of Grande del Nevado Glacier (Mendoza, Argentina) in 1984: its evolution through satellite images". In: *Geografiska Annaler: Series A, Physical Geography* 72.3-4, pp. 255–259.

Fischer, Andrea, Helmut Rott, and Helgi Björnsson (2003). "Observation of recent surges of Vatnajökull, Iceland, by means of ERS SAR interferometry". In: *Annals of Glaciology* 37, pp. 69–76.

Fischer, URS H and Garry KC Clarke (1994). "Ploughing of subglacial sediment". In: *Journal of Glaciology* 40.134, pp. 97–106.

Fischer, Urs H and Garry KC Clarke (1997). "Stick–slip sliding behaviour at the base of a glacier". In: *Annals of Glaciology* 24, pp. 390–396.

Fischer, Urs H, Garry KC Clarke, and Heinz Blatter (1999). "Evidence for temporally varying "sticky spots" at the base of Trapridge Glacier, Yukon Territory, Canada". In: *Journal of Glaciology* 45.150, pp. 352–360.

Fischer, Urs H et al. (1998). "Estimation of hydraulic properties of subglacial till from ploughmeter measurements". In: *Journal of Glaciology* 44.148, pp. 517–522.

Fischer, Urs H et al. (2001). "Hydraulic and mechanical properties of glacial sediments beneath Unteraargletscher, Switzerland: implications for glacier basal motion". In: *Hydrological Processes* 15.18, pp. 3525–3540.

Fleurian, Basile de, Richard Davy, and Petra M Langebroek (2022). "Impact of runoff temporal distribution on ice dynamics". In: *The Cryosphere* 16.6, pp. 2265–2283.

Flowers, Gwenn E (2015). "Modelling water flow under glaciers and ice sheets". In: *Proceedings of the Royal Society A: Mathematical, Physical and Engineering Sciences* 471.2176, p. 20140907.

Forbes, JD (1843). "Fourth letter on glaciers. Geneva, 5 October 1842". In: *Edinburgh New Philosophical Journal*, 34, p. 1.

Fotherbye, Ro. (1881). "THE THIRD RECORDED VOYAGE OF WILLIAM BAFFIN". In: *Voyages of William Baffin, 1612–1622*. Ed. by Clements R.Editor Markham. Cambridge Library Collection - Hakluyt First Series. Cambridge University Press, pp. 80–102.

Fowler, AC (1987). "A theory of glacier surges". In: *Journal of Geophysical Research: Solid Earth* 92.B9, pp. 9111–9120.

— (1989). "A mathematical analysis of glacier surges". In: *SIAM Journal on Applied Mathematics* 49.1, pp. 246–263.

— (2000). "An instability mechanism for drumlin formation". In: *Geological Society, London, Special Publications* 176.1, pp. 307–319.

Fowler, AC, Tavi Murray, and FSL Ng (2001). "Thermally controlled glacier surging". In: *Journal of Glaciology* 47.159, pp. 527–538.

Frappé, Tom-Pierre and Garry KC Clarke (2007). "Slow surge of Trapridge Glacier, Yukon Territory, Canada". In: *Journal of Geophysical Research: Earth Surface* 112.F3.

Frederikse, Thomas et al. (2020). "The causes of sea-level rise since 1900". In: *Nature* 584.7821, pp. 393–397.

Fricker, Helen Amanda et al. (2010). "Synthesizing multiple remote-sensing techniques for subglacial hydrologic mapping: application to a lake system beneath MacAyeal Ice Stream, West Antarctica". In: *Journal of Glaciology* 56.196, pp. 187–199.

Fudge, TJ et al. (2008). "Diurnal fluctuations in borehole water levels: configuration of the drainage system beneath Bench Glacier, Alaska, USA". In: *Journal of Glaciology* 54.185, pp. 297–306.

Fürst, Johannes J et al. (2018). "The ice-free topography of Svalbard". In: *Geophysical Research Letters* 45.21, pp. 11–760.

Gagliardini, Olivier and Mauro A Werder (2018). "Influence of increasing surface melt over decadal timescales on land-terminating Greenland-type outlet glaciers". In: *Journal of Glaciology* 64.247, pp. 700–710.

Gagliardini, Olivier et al. (2007). "Finite-element modeling of subglacial cavities and related friction law". In: *Journal of Geophysical Research: Earth Surface* 112.F2.

Gilbert, Adrien et al. (2022). "A Consistent Framework for Coupling Basal Friction With Subglacial Hydrology on Hard-Bedded Glaciers". In: *Geophysical Research Letters* 49.13, e2021GL097507.

Gillet-Chaulet, F et al. (2016). "Assimilation of surface velocities acquired between 1996 and 2010 to constrain the form of the basal friction law under Pine Island Glacier". In: *Geophysical Research Letters* 43.19, pp. 10–311.

Gimbert, F et al. (2021). "Do existing theories explain seasonal to multi-decadal changes in glacier basal sliding speed?" In: *Geophysical Research Letters* 48.15, e2021GL092858.

Gimbert, Florent et al. (2016). "Subseasonal changes observed in subglacial channel pressure, size, and sediment transport". In: *Geophysical Research Letters* 43.8, pp. 3786–3794.

Glen, John W (1955). "The creep of polycrystalline ice". In: *Proceedings of the Royal Society of London. Series A. Mathematical and Physical Sciences* 228.1175, pp. 519–538.

Goldberg, Daniel, Christian Schoof, and Olga Sergienko (2014). "Supporting Material for Stick-slip motion of an Antarctic Ice Stream: the effects of viscoelasticity". In.

Golledge, Nicholas R and Daniel P Lowry (2021). "Is the marine ice cliff hypothesis collapsing?" In: *Science* 372.6548, pp. 1266–1267.

González-Herrero, Sergi et al. (2022). "Climate warming amplified the 2020 record-breaking heatwave in the Antarctic Peninsula". In: *Communications Earth & Environment* 3.1, p. 122.

Gordon, Shulamit et al. (1998). "Seasonal reorganization of subglacial drainage inferred from measurements in boreholes". In: *Hydrological Processes* 12.1, pp. 105–133.

Gräff, Dominik and Fabian Walter (2021). "Changing friction at the base of an Alpine glacier". In: *Scientific Reports* 11.1, p. 10872.

Gräff, Dominik et al. (2021). "Fine structure of microseismic glacial stick-slip". In: *Geophysical Research Letters* 48.22, e2021GL096043.

Grant, Katie L, Chris R Stokes, and Ian S Evans (2009). "Identification and characteristics of surge-type glaciers on Novaya Zemlya, Russian Arctic". In: *Journal of Glaciology* 55.194, pp. 960–972.

Greene, Chad A et al. (2022). "Antarctic calving loss rivals ice-shelf thinning". In: *Nature* 609.7929, pp. 948–953.

Gregory, SA, MR Albert, and I Baker (2014). "Impact of physical properties and accumulation rate on pore close-off in layered firn". In: *The Cryosphere* 8.1, pp. 91–105.

Grimm, Nancy B et al. (2013). "The impacts of climate change on ecosystem structure and function". In: *Frontiers in Ecology and the Environment* 11.9, pp. 474–482.

Gudmundsson, G Hilmar et al. (2019). "Instantaneous Antarctic ice sheet mass loss driven by thinning ice shelves". In: *Geophysical Research Letters* 46.23, pp. 13903–13909.

Guerin, Gauthier et al. (2021). "Frictional origin of slip events of the Whillans Ice Stream, Antarctica". In: *Geophysical Research Letters* 48.11, e2021GL092950.

Gulley, Jason (2009). "Structural control of englacial conduits in the temperate Matanuska Glacier, Alaska, USA". In: *Journal of Glaciology* 55.192, pp. 681–690.

Hagen, Jon Ove et al. (1993). *Glacier atlas of Svalbard and jan mayen*. Ed. by Annernor Brekke. Norsk Polarinstitutt.

Hambrey, Michael J and Julian A Dowdeswell (1994). "Flow regime of the Lambert Glacier-Amery Ice Shelf system, Antarctica: structural evidence from Landsat imagery". In: *Annals of Glaciology* 20, pp. 401–406.

Hambrey, Michael J and Wendy Lawson (2000). "Structural styles and deformation fields in glaciers: a review". In: *Geological Society, London, Special Publications* 176.1, pp. 59–83.

Hamilton, Gordon S and Julian A Dowdeswell (1996). "Controls on glacier surging in Svalbard". In: *Journal of Glaciology* 42.140, pp. 157–168.

Hanssen-Bauer, I et al. (2019). "Climate in Svalbard 2100 - a knowledge base for climate adaptation". In: *NCCS report* 1/2019, p. 208.

Harrison, WD (2013). "How do glaciers respond to climate? Perspectives from the simplest models". In: *Journal of Glaciology* 59.217, pp. 949–960.

Helanow, Christian et al. (2020). "Sliding relations for glacier slip with cavities over three-dimensional beds". In: *Geophysical Research Letters* 47.3, e2019GL084924.

Helanow, Christian et al. (2021). "A slip law for hard-bedded glaciers derived from observed bed topography". In: *Science Advances* 7.20, eabe7798.

Herreid, Sam and Martin Truffer (2016). "Automated detection of unstable glacier flow and a spectrum of speedup behavior in the Alaska Range". In: *Journal of Geophysical Research: Earth Surface* 121.1, pp. 64–81.

Herron, Michael M and Chester C Langway (1980). "Firn densification: an empirical model". In: *Journal of Glaciology* 25.93, pp. 373–385.

Hewitt, Ian J and Timothy T Creyts (2019). "A model for the formation of eskers". In: *Geophysical Research Letters* 46.12, pp. 6673–6680.

Hewitt, IJ (2013). "Seasonal changes in ice sheet motion due to melt water lubrication". In: *Earth and Planetary Science Letters* 371, pp. 16–25.
Hewitt, Kenneth (1969). "Glacier surges in the Karakoram Himalaya (central Asia)". In: *Canadian Journal of Earth Sciences* 6.4, pp. 1009–1018.
— (1998). "Glaciers receive a surge of attention in the Karakoram Himalaya". In: *Eos, Transactions American Geophysical Union* 79.8, pp. 104–105.
Hindmarsh, Richard CA (1998). "The stability of a viscous till sheet coupled with ice flow, considered at wavelengths less than the ice thickness". In: *Journal of Glaciology* 44.147, pp. 285–292.
Hisdal, Vidar (1998). *Svalbard: nature and history*. Ed. by Annemor Brekke. Norsk Polarinstitutt.
Hjelle, Audun (1993). *Geology of Svalbard*. Norsk Polarinstitutt.
Hoffman, Andrew O et al. (2022). "The impact of basal roughness on inland Thwaites Glacier sliding". In: *Geophysical Research Letters* 49.14, e2021GL096564.
Hoffman, Matthew and Stephen Price (2014). "Feedbacks between coupled subglacial hydrology and glacier dynamics". In: *Journal of Geophysical Research: Earth Surface* 119.3, pp. 414–436.
Hoffman, Matthew J et al. (2016). "Greenland subglacial drainage evolution regulated by weakly connected regions of the bed". In: *Nature communications* 7.1, p. 13903.
Hooke, Roger LeB et al. (1997). "Rheology of till beneath Storglaciären, Sweden". In: *Journal of Glaciology* 43.143, pp. 172–179.
Hubbard, BP et al. (1995). "Borehole water-level variations and the structure of the subglacial hydrological system of Haut Glacier d'Arolla, Valais, Switzerland". In: *Journal of Glaciology* 41.139, pp. 572–583.
Hubbard, Bryn and Martin Sharp (1993). "Weertman regelation, multiple refreezing events and the isotopic evolution of the basal ice layer". In: *Journal of Glaciology* 39.132, pp. 275–291.
Hudson, Thomas Samuel et al. (2020). "Icequake source mechanisms for studying glacial sliding". In: *Journal of Geophysical Research: Earth Surface* 125.11, e2020JF005627.
Hugonnet, Romain et al. (2021). "Accelerated global glacier mass loss in the early twenty-first century". In: *Nature* 592.7856, pp. 726–731.
ICCI (2022). *State of the Cryosphere 2022 – Growing Losses, Global Impacts*. Stockholm, Sweden: International Cryosphere Climate Initiative (ICCI).
Iken, Almut (1981). "The effect of the subglacial water pressure on the sliding velocity of a glacier in an idealized numerical model". In: *Journal of Glaciology* 27.97, pp. 407–421.
Iken, Almut and Martin Truffer (1997). "The relationship between subglacial water pressure and velocity of Findelengletscher, Switzerland, during its advance and retreat". In: *Journal of Glaciology* 43.144, pp. 328–338.

IPCC (2018). *Global warming of 1.5°C. An IPCC Special Report on the impacts of global warming of 1.5°C above pre-industrial levels and related global greenhouse gas emission pathways, in the context of strengthening the global response to the threat of climate change, sustainable development, and efforts to eradicate poverty [V. Masson-Delmotte, P. Zhai, H. O. Pörtner, D. Roberts, J. Skea, P.R. Shukla, A. Pirani, W. Moufouma-Okia, C. Péan, R. Pidcock, S. Connors, J. B. R. Matthews, Y. Chen, X. Zhou, M. I. Gomis, E. Lonnoy, T. Maycock, M. Tignor, T. Waterfield (eds.)]* Vol. In Press.

— (2021). *Climate Change 2021: The Physical Science Basis. Contribution of Working Group I to the Sixth Assessment Report of the Intergovernmental Panel on Climate Change*. Vol. In Press. Cambridge, United Kingdom and New York, NY, USA: Cambridge University Press.

Irvine-Fynn, Tristram DL et al. (2011). "Polythermal glacier hydrology: A review". In: *Reviews of Geophysics* 49.4.

Iverson, Neal R (2010). "Shear resistance and continuity of subglacial till: hydrology rules". In: *Journal of Glaciology* 56.200, pp. 1104–1114.

Iverson, Neal R, Robert W Baker, and Thomas S Hooyer (1997). "A ring-shear device for the study of till deformation: tests on tills with contrasting clay contents". In: *Quaternary Science Reviews* 16.9, pp. 1057–1066.

Iverson, Neal R and Thomas S Hooyer (2004). "Estimating the sliding velocity of a Pleistocene ice sheet from plowing structures in the geologic record". In: *Journal of Geophysical Research: Earth Surface* 109.F4.

Iverson, Neal R, Thomas S Hooyer, and Robert W Baker (1998). "Ring-shear studies of till deformation: Coulomb-plastic behavior and distributed strain in glacier beds". In: *Journal of Glaciology* 44.148, pp. 634–642.

Iverson, Neal R and Richard M Iverson (2001). "Distributed shear of subglacial till due to Coulomb slip". In: *Journal of Glaciology* 47.158, pp. 481–488.

Iverson, Neal R and Darius J Semmens (1995). "Intrusion of ice into porous media by regelation: A mechanism of sediment entrainment by glaciers". In: *Journal of Geophysical Research: Solid Earth* 100.B6, pp. 10219–10230.

Iverson, Neal R et al. (2003). "Effects of basal debris on glacier flow". In: *Science* 301.5629, pp. 81–84.

Iverson, Neal R et al. (2007). "Soft-bed experiments beneath Engabreen, Norway: regelation infiltration, basal slip and bed deformation". In: *Journal of Glaciology* 53.182, pp. 323–340.

Jiskoot, Hester (2011). "Dynamics of glaciers". In: *physical Research* 92.B9, pp. 9083–9100.

Jiskoot, Hester, Paul Boyle, and Tavi Murray (1998). "The incidence of glacier surging in Svalbard: evidence from multivariate statistics". In: *Computers & Geosciences* 24.4, pp. 387–399.

Jiskoot, Hester, Tavi Murray, and Paul Boyle (2000). "Controls on the distribution of surge-type glaciers in Svalbard". In: *Journal of Glaciology* 46.154, pp. 412–422.

Jiskoot, Hester, Tavi Murray, and Adrian Luckman (2003). "Surge potential and drainage-basin characteristics in East Greenland". In: *Annals of Glaciology* 36, pp. 142–148.

Johnson, Andrew, Regine Hock, and Mark Fahnestock (2022). "Spatial variability and regional trends of Antarctic ice shelf surface melt duration over 1979–2020 derived from passive microwave data". In: *Journal of Glaciology* 68.269, pp. 533–546.

Joughin, Ian, Waleed Abdalati, and Mark Fahnestock (2004). "Large fluctuations in speed on Greenland's Jakobshavn Isbrae glacier". In: *Nature* 432.7017, pp. 608–610.

Joughin, Ian, Benjamin E Smith, and Christian G Schoof (2019). "Regularized Coulomb friction laws for ice sheet sliding: Application to Pine Island Glacier, Antarctica". In: *Geophysical research letters* 46.9, pp. 4764–4771.

Jouvet, Guillaume et al. (2018). "Short-lived ice speed-up and plume water flow captured by a VTOL UAV give insights into subglacial hydrological system of Bowdoin Glacier". In: *Remote sensing of environment* 217, pp. 389–399.

Jouzel, Jean and Valérie Masson-Delmotte (2010). "Paleoclimates: what do we learn from deep ice cores?" In: *Wiley Interdisciplinary Reviews: Climate Change* 1.5, pp. 654–669.

Kääb, Andreas et al. (2018). "Massive collapse of two glaciers in western Tibet in 2016 after surge-like instability". In: *Nature Geoscience* 11.2, pp. 114–120.

Kamb, Barclay (1987). "Glacier surge mechanism based on linked cavity configuration of the basal water conduit system". In: *Journal of Geophysical Research: Solid Earth* 92.B9, pp. 9083–9100.

— (1991). "Rheological nonlinearity and flow instability in the deforming bed mechanism of ice stream motion". In: *Journal of Geophysical Research: Solid Earth* 96.B10, pp. 16585–16595.

— (2001). "Basal zone of the West Antarctic ice streams and its role in lubrication of their rapid motion". In: *The West Antarctic ice sheet: behavior and environment* 77, pp. 157–199.

Kamb, Barclay and Hermann Engelhardt (1987). "Waves of accelerated motion in a glacier approaching surge: the mini-surges of Variegated Glacier, Alaska, USA". In: *Journal of Glaciology* 33.113, pp. 27–46.

Kamb, Barclay et al. (1985). "Glacier surge mechanism: 1982-1983 surge of Variegated Glacier, Alaska". In: *Science* 227.4686, pp. 469–479.

Kavanaugh, Jeffrey L and Garry KC Clarke (2000). "Evidence for extreme pressure pulses in the subglacial water system". In: *Journal of Glaciology* 46.153, pp. 206–212.

— (2006). "Discrimination of the flow law for subglacial sediment using in situ measurements and an interpretation model". In: *Journal of Geophysical Research: Earth Surface* 111.F1.

Kessler, Mark A and Robert S Anderson (2004). "Testing a numerical glacial hydrological model using spring speed-up events and outburst floods". In: *Geophysical Research Letters* 31.18.

Kim, Yeon-Hee et al. (2023). "Observationally-constrained projections of an ice-free Arctic even under a low emission scenario". In: *Nature Communications* 14.1, p. 3139.

Kirezci, Ebru et al. (2020). "Projections of global-scale extreme sea levels and resulting episodic coastal flooding over the 21st Century". In: *Scientific reports* 10.1, p. 11629.

Kirkham, James D et al. (2022). "Tunnel valley formation beneath deglaciating mid-latitude ice sheets: Observations and modelling". In: *Quaternary Science Reviews*, p. 107680.

Köhler, Andreas et al. (2012). "Autonomous detection of calving-related seismicity at Kronebreen, Svalbard". In: *The Cryosphere* 6.2, pp. 393–406.

Kotlyakov, Vladimir M, OV Rototaeva, and GA Nosenko (2004). "The September 2002 Kolka glacier catastrophe in North Ossetia, Russian Federation: evidence and analysis". In: *Mountain Research and Development* 24.1, pp. 78–83.

Kotlyakov, VM, GB Osipova, and DG Tsvetkov (2008). "Monitoring surging glaciers of the Pamirs, central Asia, from space". In: *Annals of Glaciology* 48, pp. 125–134.

Kyrke-Smith, TM and AC Fowler (2014). "Subglacial swamps". In: *Proceedings of the Royal Society A: Mathematical, Physical and Engineering Sciences* 470.2171, p. 20140340.

Labedz, Celeste R et al. (2022). "Seismic mapping of subglacial hydrology reveals previously undetected pressurization event". In: *Journal of Geophysical Research: Earth Surface* 127.3, e2021JF006406.

Larose, Eric et al. (2015). "Environmental seismology: What can we learn on earth surface processes with ambient noise?" In: *Journal of Applied Geophysics* 116, pp. 62–74.

Larour, E et al. (2012). "Ice flow sensitivity to geothermal heat flux of Pine Island Glacier, Antarctica". In: *Journal of Geophysical Research: Earth Surface* 117.F4.

Le Brocq, Anne M et al. (2009). "A subglacial water-flow model for West Antarctica". In: *Journal of Glaciology* 55.193, pp. 879–888.

Leclercq, Paul Willem, Andreas Kääb, and Bas Altena (2021). "Brief communication: Detection of glacier surge activity using cloud computing of Sentinel-1 radar data". In: *The Cryosphere* 15.10, pp. 4901–4907.

Lefauconnier, Bernard and Jon Ove Hagen (1991). *Surging and calving glaciers in eastern Svalbard*. Norsk Polarinstitutt.

Liestøl, Olav (1988). "The glaciers in the Kongsfjorden area, Spitsbergen". In: *Norsk Geografisk Tidsskrift-Norwegian Journal of Geography* 42.4, pp. 231–238.

Lindner, Fabian et al. (2020). "Glaciohydraulic seismic tremors on an Alpine glacier". In: *The Cryosphere* 14.1, pp. 287–308.

Lingle, Craig S and Timothy J Brown (1987). "A subglacial aquifer bed model and water pressure dependent basal sliding relationship for a West Antarctic ice stream". In: *Dynamics of the West Antarctic Ice Sheet: Proceedings of a Workshop held in Utrecht, May 6–8, 1985*. Springer, pp. 249–285.

Lipovsky, Bradley Paul et al. (2019). "Glacier sliding, seismicity and sediment entrainment". In: *Annals of Glaciology* 60.79, pp. 182–192.

Lliboutry, Louis (1968). "General theory of subglacial cavitation and sliding of temperate glaciers". In: *Journal of Glaciology* 7.49, pp. 21–58.

Llovel, William et al. (2019). "Global ocean freshening, ocean mass increase and global mean sea level rise over 2005–2015". In: *Scientific reports* 9.1, p. 17717.

Machguth, Horst et al. (2016). "Greenland meltwater storage in firn limited by near-surface ice formation". In: *Nature Climate Change* 6.4, pp. 390–393.

Maier, Nathan, Florent Gimbert, and Fabien Gillet-Chaulet (2022). "Threshold response to melt drives large-scale bed weakening in Greenland". In: *Nature* 607.7920, pp. 714–720.

Mair, Douglas et al. (2003). "Hydrological controls on patterns of surface, internal and basal motion during three "spring events": Haut Glacier d'Arolla, Switzerland". In: *Journal of Glaciology* 49.167, pp. 555–567.

Malhi, Yadvinder et al. (2020). "Climate change and ecosystems: Threats, opportunities and solutions". In: *Philosophical Transactions of the Royal Society B* 375.1794, p. 20190104.

Mankoff, Kenneth D et al. (2017). "Roughness of a subglacial conduit under Hansbreen, Svalbard". In: *Journal of Glaciology* 63.239, pp. 423–435.

Marzeion, Ben et al. (2018). "Limited influence of climate change mitigation on short-term glacier mass loss". In: *Nature Climate Change* 8.4, pp. 305–308.

Maussion, Fabien et al. (2019). "The open global glacier model (OGGM) v1. 1". In: *Geoscientific Model Development* 12.3, pp. 909–931.

McGranahan, Gordon, Deborah Balk, and Bridget Anderson (2007). "The rising tide: assessing the risks of climate change and human settlements in low elevation coastal zones". In: *Environment and urbanization* 19.1, pp. 17–37.

McMichael, Anthony J, Rosalie E Woodruff, and Simon Hales (2006). "Climate change and human health: present and future risks". In: *The Lancet* 367.9513, pp. 859–869.

Meier, Mark F and Austin Post (1969). "What are glacier surges?" In: *Canadian Journal of Earth Sciences* 6.4, pp. 807–817.

Meier, Mark F et al. (1974). "Flow of Blue Glacier, Olympic Mountains, Washington, USA". In: *Journal of Glaciology* 13.68, pp. 187–212.

Melvold, Kjetil and Jon Ove Hagen (1998). "Evolution of a surge-type glacier in its quiescent phase: Kongsvegen, Spitsbergen, 1964–95". In: *Journal of Glaciology* 44.147, pp. 394–404.

Merkel, Benjamin and Jon Aars (2022). "Shifting polar bear Ursus maritimus denning habitat availability in the European Arctic". In: *Polar Biology* 45.3, pp. 481–490.

MetOfficeUK (2022). *Mauna Loa Carbon dioxide forecast for 2023*. URL: https://www.metoffice.gov.uk/research/climate/seasonal-to-decadal/long-range/forecasts/co2-forecast-for-2023#:~:text=As%20a%20result%2C%20we%20forecast,concentration%20to%20be%20419.2%20ppm.

Meyer, Colin R and Ian J Hewitt (2017). "A continuum model for meltwater flow through compacting snow". In: *The Cryosphere* 11.6, pp. 2799–2813.

Minchew, Brent and Ian Joughin (2020). "Toward a universal glacier slip law". In: *Science* 368.6486, pp. 29–30.

Minchew, Brent et al. (2016). "Plastic bed beneath Hofsjökull Ice Cap, central Iceland, and the sensitivity of ice flow to surface meltwater flux". In: *Journal of Glaciology* 62.231, pp. 147–158.

Minchew, Brent M and Colin R Meyer (2020). "Dilation of subglacial sediment governs incipient surge motion in glaciers with deformable beds". In: *Proceedings of the Royal Society A* 476.2238, p. 20200033.

Mitchell, James Kenneth, Kenichi Soga, et al. (2005). *Fundamentals of soil behavior*. Vol. 3. John Wiley & Sons New York.

Moon, Twila et al. (2014). "Distinct patterns of seasonal Greenland glacier velocity". In: *Geophysical research letters* 41.20, pp. 7209–7216.

Moorman, Brian J and Frederick A Michel (2000). "Glacial hydrological system characterization using ground-penetrating radar". In: *Hydrological Processes* 14.15, pp. 2645–2667.

Mouginot, Jeremie et al. (2015). "Fast retreat of zachariæ isstrøm, northeast Greenland". In: *Science* 350.6266, pp. 1357–1361.

Mouginot, Jérémie et al. (2019). "Forty-six years of Greenland Ice Sheet mass balance from 1972 to 2018". In: *Proceedings of the national academy of sciences* 116.19, pp. 9239–9244.

Murray, Tavi (1997). "Assessing the paradigm shift: deformable glacier beds". In: *Quaternary Science Reviews* 16.9, pp. 995–1016.

Murray, Tavi and Adam D Booth (2010). "Imaging glacial sediment inclusions in 3-D using ground-penetrating radar at Kongsvegen, Svalbard". In: *Journal of Quaternary science* 25.5, pp. 754–761.

Murray, Tavi and Garry KC Clarke (1995). "Black-box modeling of the subglacial water system". In: *Journal of Geophysical Research: Solid Earth* 100.B6, pp. 10231–10245.

Murray, Tavi et al. (2000). "Glacier surge propagation by thermal evolution at the bed". In: *Journal of Geophysical Research: Solid Earth* 105.B6, pp. 13491–13507.

Nanni, Ugo (2023). *Listening to the song of Melting Glaciers*. URL: https://theconversation.com/listening-to-the-song-of-melting-glaciers-191041.

Nanni, Ugo et al. (2020). "Quantification of seasonal and diurnal dynamics of subglacial channels using seismic observations on an Alpine glacier". In: *The Cryosphere* 14.5, pp. 1475–1496.

Nanni, Ugo et al. (2021). "Observing the subglacial hydrology network and its dynamics with a dense seismic array". In: *Proceedings of the National Academy of Sciences* 118.28, e2023757118.

Nanni, Ugo et al. (2022). "Dynamic Imaging of Glacier Structures at High-Resolution Using Source Localization With a Dense Seismic Array". In: *Geophysical Research Letters* 49.6, e2021GL095996.

Nanni, Ugo et al. (2023). "Climatic control on seasonal variations in mountain glacier surface velocity". In: *The Cryosphere* 17.4, pp. 1567–1583.

Nedderman, Ronald Midgley et al. (1992). *Statics and kinematics of granular materials*. Vol. 352. Cambridge University Press Cambridge.

Nelder, John Ashworth and Robert WM Wedderburn (1972). "Generalized linear models". In: *Journal of the Royal Statistical Society Series A: Statistics in Society* 135.3, pp. 370–384.

Neumann, Barbara et al. (2015). "Future coastal population growth and exposure to sea-level rise and coastal flooding-a global assessment". In: *PloS one* 10.3, e0118571.

Ng, Felix SL (2000a). "Canals under sediment-based ice sheets". In: *Annals of Glaciology* 30, pp. 146–152.

— (2000b). "Coupled ice–till deformation near subglacial channels and cavities". In: *Journal of Glaciology* 46.155, pp. 580–598.

Nielsen, Niels (1937). "A volcano under an ice-cap. Vatnajökull, Iceland, 1934-36". In: *Geographical Journal*, pp. 6–20.

Nienow, Peter, Martin Sharp, and Ian Willis (1998). "Seasonal changes in the morphology of the subglacial drainage system, Haut Glacier d'Arolla, Switzerland". In: *Earth Surface Processes and Landforms: The Journal of the British Geomorphological Group* 23.9, pp. 825–843.

Nolan, Andrew et al. (2021). "Kinematics of the exceptionally-short surge cycles of Sıt'Kusá (Turner Glacier), Alaska, from 1983 to 2013". In: *Journal of Glaciology* 67.264, pp. 744–758.

Nuth, Christopher et al. (2013). "Decadal changes from a multi-temporal glacier inventory of Svalbard". In: *The Cryosphere* 7.5, pp. 1603–1621.

Nye, JF (1965). "The flow of a glacier in a channel of rectangular, elliptic or parabolic cross-section". In: *Journal of glaciology* 5.41, pp. 661–690.

Nye, John F (1952). "The mechanics of glacier flow". In: *Journal of Glaciology* 2.12, pp. 82–93.

— (1955). "Comments on Dr. Loewe's letter and notes on crevasses". In: *Journal of Glaciology* 2.17, pp. 512–514.

Oerlemans, Johannes (2001). *Glaciers and climate change*. CRC Press.

Østby, Torbjørn Ims et al. (2017). "Diagnosing the decline in climatic mass balance of glaciers in Svalbard over 1957–2014". In: *The Cryosphere* 11.1, pp. 191–215.

Otosaka, Inès N et al. (2022). "Mass balance of the Greenland and Antarctic ice sheets from 1992 to 2020". In: *Earth System Science Data Discussions* 2022, pp. 1–33.

Pattyn, Frank (2017). "Sea-level response to melting of Antarctic ice shelves on multi-centennial timescales with the fast Elementary Thermomechanical Ice Sheet model (f. ETISh v1. 0)". In: *The Cryosphere* 11.4, pp. 1851–1878.

Pettit, Jethro (2004). "Climate justice: A new social movement for atmospheric rights". In: *IDS Bulletin* 35.3.

Piho, Laura, Andreas Alexander, and Maarja Kruusmaa (2022). "Topology and spatial-pressure-distribution reconstruction of an englacial channel". In: *The Cryosphere* 16.9, pp. 3669–3683.

Piotrowski, Jan A, Piotr Hermanowski, and Agnieszka M Piechota (2009). "Meltwater discharge through the subglacial bed and its land-forming consequences from numerical experiments in the Polish lowland during the last glaciation". In: *Earth Surface Processes and Landforms* 34.4, pp. 481–492.

Podolskiy, Evgeny A and Fabian Walter (2016). "Cryoseismology". In: *Reviews of geophysics* 54.4, pp. 708–758.

Porter, Philip R, Tavi Murray, and Julian A Dowdeswell (1997). "Sediment deformation and basal dynamics beneath a glacier surge front: Bakaninbreen, Svalbard". In: *Annals of Glaciology* 24, pp. 21–26.

Post, Austin (1969). "Distribution of surging glaciers in western North America". In: *Journal of Glaciology* 8.53, pp. 229–240.

Preiswerk, Lukas E and Fabian Walter (2018). "High-Frequency (> 2 Hz) Ambient Seismic Noise on High-Melt Glaciers: Green's Function Estimation and Source Characterization". In: *Journal of Geophysical Research: Earth Surface* 123.8, pp. 1667–1681.

Qiu, J. (2017). *Why slow glaciers can sometimes surge as fast as a speeding train - wiping out people in their path*. URL: https://www.science.org/content/article/why-slow-glaciers-can-sometimes-surge-fast-speeding-train-wiping-out-people-their-path.

Rada, Camilo and Christian Schoof (2018). "Channelized, distributed, and disconnected: subglacial drainage under a valley glacier in the Yukon". In: *The Cryosphere* 12.8, pp. 2609–2636.

Rada Giacaman, Camilo Andrés and Christian Schoof (2023). "Channelized, distributed, and disconnected: spatial structure and temporal evolution of the subglacial drainage under a valley glacier in the Yukon". In: *The Cryosphere* 17.2, pp. 761–787.

Rapp, Donald et al. (2009). "Ice ages and interglacials". In: *Measurement, interpretation and models*.

Ravindra, Khaiwal et al. (2019). "Generalized additive models: Building evidence of air pollution, climate change and human health". In: *Environment international* 132, p. 104987.

Reese, Ronja et al. (2018). "The far reach of ice-shelf thinning in Antarctica". In: *Nature Climate Change* 8.1, pp. 53–57.

Reinardy, Benedict TI et al. (2011). "Streaming flow of an Antarctic Peninsula palaeo-ice stream, both by basal sliding and deformation of substrate". In: *Journal of Glaciology* 57.204, pp. 596–608.

Rempel, Alan W (2009). "Transient effective stress variations forced by changes in conduit pressure beneath glaciers and ice sheets". In: *Annals of Glaciology* 50.52, pp. 61–66.

RGI, Consortium (2017). *Randolph Glacier Inventory (RGI) - A dataset of Global Glacier Outlines: Version 6.0*. URL: http://www.glims.org/RGI/randolph60.html.

Robin, G de Q (1955). "Ice movement and temperature distribution in glaciers and ice sheets". In: *Journal of glaciology* 2.18, pp. 523–532.

Roe, Gerard H and Marcia B Baker (2016). "The response of glaciers to climatic persistence". In: *Journal of Glaciology* 62.233, pp. 440–450.

Röthlisberger, H (1969). "Evidence for an ancient glacier surge in the Swiss Alps". In: *Canadian Journal of Earth Sciences* 6.4, pp. 863–865.

Röthlisberger, Hans (1972). "Water pressure in intra-and subglacial channels". In: *Journal of Glaciology* 11.62, pp. 177–203.

Rounce, David R et al. (2023). "Global glacier change in the 21st century: Every increase in temperature matters". In: *Science* 379.6627, pp. 78–83.

Ruina, Andy (1983). "Slip instability and state variable friction laws". In: *Journal of Geophysical Research: Solid Earth* 88.B12, pp. 10359–10370.

Salamatin, Andrey N, Vladimir Ya Lipenkov, and Paul Duval (1997). "Bubbly-ice densification in ice sheets: I. Theory". In: *Journal of Glaciology* 43.145, pp. 387–396.

Sato, Kazutoshi, Jun Inoue, and Masahiro Watanabe (2014). "Influence of the Gulf Stream on the Barents Sea ice retreat and Eurasian coldness during early winter". In: *Environmental Research Letters* 9.8, p. 084009.

Schäfer, Martina et al. (2014). "Assessment of heat sources on the control of fast flow of Vestfonna ice cap, Svalbard". In: *The Cryosphere* 8.5, pp. 1951–1973.

Schellenberger, Thomas et al. (2017). "Multi-year surface velocities and sea-level rise contribution of the Basin-3 and Basin-2 surges, Austfonna, Svalbard". In: *The Cryosphere Discussions* 2017, pp. 1–27.

Schlosberg, David and Lisette B Collins (2014). "From environmental to climate justice: climate change and the discourse of environmental justice". In: *Wiley Interdisciplinary Reviews: Climate Change* 5.3, pp. 359–374.

Schmidt, Louise Steffensen et al. (2023). "Meltwater runoff and glacier mass balance in the high Arctic: 1991–2022 simulations for Svalbard". In: *The Cryosphere* 17.7, pp. 2941–2963.

Schofield, Andrew Noel and Peter Wroth (1968). *Critical state soil mechanics*. Vol. 310. McGraw-hill London.

Scholzen, Chloé, Thomas V Schuler, and Adrien Gilbert (2021). "Sensitivity of subglacial drainage to water supply distribution at the Kongsfjord basin, Svalbard". In: *The Cryosphere* 15.6, pp. 2719–2738.

Schoof, Christian (2005). "The effect of cavitation on glacier sliding". In: *Proceedings of the Royal Society A: Mathematical, Physical and Engineering Sciences* 461.2055, pp. 609–627.

— (2007). "Cavitation on deformable glacier beds". In: *SIAM Journal on Applied Mathematics* 67.6, pp. 1633–1653.

— (2010). "Ice-sheet acceleration driven by melt supply variability". In: *Nature* 468.7325, pp. 803–806.

— (2023a). "The evolution of isolated cavities and hydraulic connection at the glacier bed. Part 1: steady states and friction laws". In: *EGUsphere*, pp. 1–27.

— (2023b). "The evolution of isolated cavities and hydraulic connection at the glacier bed. Part 2: a dynamic viscoelastic model". In: *EGUsphere* 2023, pp. 1–30.

Schuler, Thomas V et al. (2020). "Reconciling Svalbard glacier mass balance". In: *Frontiers in Earth Science*, p. 156.

Schytt, Valter (1969). "Some comments on glacier surges in eastern Svalbard". In: *Canadian Journal of Earth Sciences* 6.4, pp. 867–873.

Sevestre, Heıdi and Douglas Benn (2015). "Climatic and geometric controls on the global distribution of surge-type glaciers: implications for a unifying model of surging". In: *Journal of Glaciology* 61.228, pp. 646–662.

Sevestre, Heıdi et al. (2015). "Thermal structure of Svalbard glaciers and implications for thermal switch models of glacier surging". In: *Journal of Geophysical Research: Earth Surface* 120.10, pp. 2220–2236.

Sevestre, Heıdi et al. (2018). "Tidewater glacier surges initiated at the terminus". In: *Journal of Geophysical Research: Earth Surface* 123.5, pp. 1035–1051.

Shoemaker, EM (1986). "Subglacial hydrology for an ice sheet resting on a deformable aquifer". In: *Journal of Glaciology* 32.110, pp. 20–30.

Shreve, RL (1972). "Movement of water in glaciers". In: *Journal of Glaciology* 11.62, pp. 205–214.

Smith, Laurence C et al. (2015). "Efficient meltwater drainage through supraglacial streams and rivers on the southwest Greenland ice sheet". In: *Proceedings of the National Academy of Sciences* 112.4, pp. 1001–1006.

Sommers, Aleah, Harihar Rajaram, and Mathieu Morlighem (2018). "SHAKTI: subglacial hydrology and kinetic, transient interactions v1. 0". In: *Geoscientific Model Development* 11.7, pp. 2955–2974.

Spencer, MK, Richard B Alley, and Timothy T Creyts (2001). "Preliminary firn-densification model with 38-site dataset". In: *Journal of Glaciology* 47.159, pp. 671–676.

Stearns, LA and CJ Van der Veen (2018). "Friction at the bed does not control fast glacier flow". In: *Science* 361.6399, pp. 273–277.

Stevens, Nathan T et al. (2023). "Multi-decadal basal slip enhancement at Saskatchewan Glacier, Canadian Rocky Mountains". In: *Journal of Glaciology* 69.273, pp. 71–86.

Stokes, Chris R (2018). "Geomorphology under ice streams: moving from form to process". In: *Earth Surface Processes and Landforms* 43.1, pp. 85–123.

Stokes, Chris R et al. (2022). "Response of the East Antarctic Ice Sheet to past and future climate change". In: *Nature* 608.7922, pp. 275–286.

Sugiyama, Shin, Masahiro Minowa, and Marius Schaefer (2019). "Underwater ice terrace observed at the front of Glaciar Grey, a freshwater calving glacier in Patagonia". In: *Geophysical research letters* 46.5, pp. 2602–2609.

Svendsen, Harald et al. (2002). "The physical environment of Kongsfjorden–Krossfjorden, an Arctic fjord system in Svalbard". In: *Polar research* 21.1, pp. 133–166.

Tarr, Ralph S and Lawrence Martin (1906). "Glaciers and glaciation of Yakutat Bay, Alaska". In: *Bulletin of the American Geographical Society* 38.3, pp. 145–167.

Terleth, Yoram et al. (2021). "Complementary approaches towards a universal model of glacier surges". In: *Frontiers in Earth Science* 9, p. 732962.

Terzaghi, Karl, Ralph B Peck, and Gholamreza Mesri (1996). *Soil mechanics in engineering practice*. John wiley & sons.

Thøgersen, Kjetil et al. (2019). "Rate-and-state friction explains glacier surge propagation". In: *Nature communications* 10.1, p. 2823.

Thøgersen, Kjetil et al. (2021). "Glacier surges controlled by the close interplay between subglacial friction and drainage". In: *EarthArXiv*.

Thomason, Jason F and Neal R Iverson (2008). "A laboratory study of particle ploughing and pore-pressure feedback: a velocity-weakening mechanism for soft glacier beds". In: *Journal of Glaciology* 54.184, pp. 169–181.

Thomson, Laura et al. (2021). *Observational Assessments of Glacier Mass Changes at Regional and Global Level*.

Thorarinsson, Sigurdur (1969). "Glacier surges in Iceland, with special reference to the surges of Brúarjökull". In: *Canadian Journal of Earth Sciences* 6.4, pp. 875–882.

Tranter, Martyn et al. (1993). "A conceptual model of solute acquisition by Alpine glacial meltwaters". In: *Journal of Glaciology* 39.133, pp. 573–581.

Trnkoczy, Amadej (2009). "Understanding and parameter setting of STA/LTA trigger algorithm". In: *New manual of seismological observatory practice (NMSOP)*. Deutsches GeoForschungsZentrum GFZ, pp. 1–20.

Truffer, Martin et al. (2021). "Glacier surges". In: *Snow and ice-related hazards, risks, and disasters*. Elsevier, pp. 417–466.

Tulaczyk, Slawek, W Barclay Kamb, and Hermann F Engelhardt (2000). "Basal mechanics of ice stream B, West Antarctica: 1. Till mechanics". In: *Journal of Geophysical Research: Solid Earth* 105.B1, pp. 463–481.

Tulaczyk, Slawek M, Reed P Scherer, and Christopher D Clark (2001). "A ploughing model for the origin of weak tills beneath ice streams: a qualitative treatment". In: *Quaternary International* 86.1, pp. 59–70.

US Department of Commerce, NOAA (Oct. 2005). *Global Monitoring Laboratory - Carbon Cycle Greenhouse Gases*. URL: `https://gml.noaa.gov/ccgg/trends/mlo.html`.

Vallot, Dorothée et al. (2017). "Basal dynamics of Kronebreen, a fast-flowing tidewater glacier in Svalbard: non-local spatio-temporal response to water input". In: *Journal of Glaciology* 63.242, pp. 1012–1024.

Van der Veen, CJ (1998). "Fracture mechanics approach to penetration of bottom crevasses on glaciers". In: *Cold Regions Science and Technology* 27.3, pp. 213–223.

Van Pelt, Ward et al. (2019). "A long-term dataset of climatic mass balance, snow conditions, and runoff in Svalbard (1957–2018)". In: *The Cryosphere* 13.9, pp. 2259–2280.

Vérité, Jean et al. (2022). "Formation of murtoos by repeated flooding of ribbed bedforms along subglacial meltwater corridors". In: *Geomorphology* 408, p. 108248.

Vincent, Christian et al. (2022). "Evidence of seasonal uplift in the Argentière glacier (Mont Blanc area, France)". In: *Journal of Geophysical Research: Earth Surface* 127.7, e2021JF006454.

Walder, Joseph and Bernard Hallet (1979). "Geometry of former subglacial water channels and cavities". In: *Journal of Glaciology* 23.89, pp. 335–346.

Walder, Joseph S and Andrew Fowler (1994). "Channelized subglacial drainage over a deformable bed". In: *Journal of glaciology* 40.134, pp. 3–15.

Walker, Ryan T et al. (2012). "A viscoelastic flowline model applied to tidal forcing of Bindschadler Ice Stream, West Antarctica". In: *Earth and Planetary Science Letters* 319, pp. 128–132.

Walter, Fabian, Nicholas Deichmann, and Martin Funk (2008). "Basal icequakes during changing subglacial water pressures beneath Gornergletscher, Switzerland". In: *Journal of Glaciology* 54.186, pp. 511–521.

Wang, Chen-Long et al. (2013). "Microseismic events location of surface and borehole observation with reverse-time focusing using interferometry technique". In: *Chinese Journal of Geophysics* 56.9, pp. 3184–3196.

Weertman, J and GE Birchfield (1982). "Subglacial water flow under ice streams and West Antarctic ice-sheet stability". In: *Annals of glaciology* 3, pp. 316–320.

Weertman, Johannes (1957). "On the sliding of glaciers". In: *Journal of glaciology* 3.21, pp. 33–38.

— (1983). "Creep deformation of ice". In: *Annual Review of Earth and Planetary Sciences* 11.1, pp. 215–240.

Welch, Peter (1967). "The use of fast Fourier transform for the estimation of power spectra: a method based on time averaging over short, modified periodograms". In: *IEEE Transactions on audio and electroacoustics* 15.2, pp. 70–73.

Werder, Mauro A et al. (2013). "Modeling channelized and distributed subglacial drainage in two dimensions". In: *Journal of Geophysical Research: Earth Surface* 118.4, pp. 2140–2158.

Wilkinson, David Stirling and MF Ashby (1975). "The development of pressure sintering maps". In: *Sintering and Catalysis*. Springer, pp. 473–492.

Wilkinson, DS (1988). "A pressure-sintering model for the densification of polar firn and glacier ice". In: *Journal of Glaciology* 34.116, pp. 40–45.

Wille, Jonathan D et al. (2019). "West Antarctic surface melt triggered by atmospheric rivers". In: *Nature Geoscience* 12.11, pp. 911–916.

Withers, Mitchell et al. (1998). "A comparison of select trigger algorithms for automated global seismic phase and event detection". In: *Bulletin of the Seismological Society of America* 88.1, pp. 95–106.

Woodward, John, Tavi Murray, and Andrew McCaig (2002). "Formation and reorientation of structure in the surge-type glacier Kongsvegen, Svalbard".

In: *Journal of Quaternary Science: Published for the Quaternary Research Association* 17.3, pp. 201–209.

Yde, Jacob C and N Tvis Knudsen (2007). "20th-century glacier fluctuations on Disko Island (Qeqertarsuaq), Greenland". In: *Annals of Glaciology* 46, pp. 209–214.

Zanna, Laure et al. (2019). "Global reconstruction of historical ocean heat storage and transport". In: *Proceedings of the National Academy of Sciences* 116.4, pp. 1126–1131.

Zemp, Michael et al. (2019). "Global glacier mass changes and their contributions to sea-level rise from 1961 to 2016". In: *Nature* 568.7752, pp. 382–386.

Zhan, Zhongwen (2019). "Seismic noise interferometry reveals transverse drainage configuration beneath the surging Bering Glacier". In: *Geophysical Research Letters* 46.9, pp. 4747–4756.

Zoet, LK et al. (2023). "An experimental baseline for ice-till strain indicators". In: *Canadian Journal of Earth Sciences* 60.5, pp. 537–549.

Zoet, Lucas K and Neal R Iverson (2020). "A slip law for glaciers on deformable beds". In: *Science* 368.6486, pp. 76–78.

Chapter 7

Articles

7.1 Article I: A machine learning framework to automate the classification of surge-type glaciers in Svalbard (published, 2022)

This paper has been published in *Journal of Geophysical Research: Earth Surfaces* in 2022. I played a central role in the study, conducting formal analysis, compiling a comprehensive dataset on surge-type glaciers in Svalbard, and training and evaluating machine learning models. I also assessed the significance of glacier features using the XGBoost model and developed the necessary code for analysis and figure generation. Additionally, I led the writing of the manuscript and oversaw correspondence and revisions. J. Aiken contributed to the conceptual framework and initial data exploration, providing guidance on machine learning concepts and Python implementation. He also contributed to describing the machine learning methods in the manuscript. K. Thøgersen helps at shaping the research direction at the early stage of the study conceptualisation before providing insights during the manuscript writing phase. F. Renard made valuable contributions throughout the study, shaping the research direction and providing insightful input at every stage, from conception to manuscript writing. T.V. Schuler participated in providing input at every stage and finalising the manuscript prior to submission.

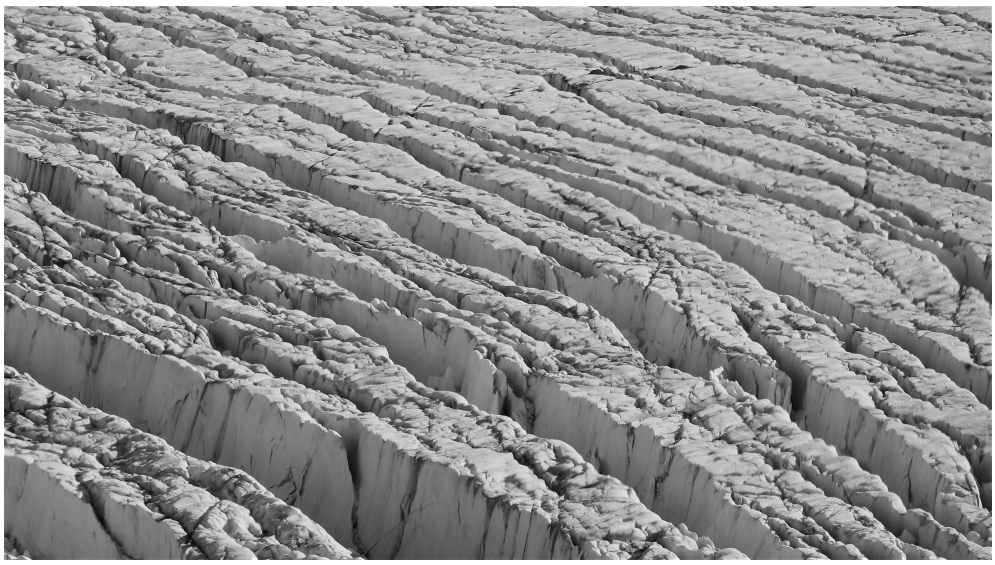

FIGURE 7.1: Navigating over expansive crevasses while flying out from Ny-Ålesund during the spring of 2022.

AGU ADVANCING EARTH AND SPACE SCIENCE

JGR Earth Surface

RESEARCH ARTICLE
10.1029/2022JF006597

A Machine Learning Framework to Automate the Classification of Surge-Type Glaciers in Svalbard

C. Bouchayer[1], J. M. Aiken[1], K. Thøgersen[1], F. Renard[1,2], and T. V. Schuler[1]

[1]The Njord Centre, Departments of Geosciences and Physics, University of Oslo, Oslo, Norway, [2]ISTerre, University Grenoble Alpes, Grenoble INP, University Savoie Mont Blanc, CNRS, IRD, University Gustave Eiffel, Grenoble, France

Key Points:

- We establish a machine learning framework to evaluate the probability of glacier surge
- We build a combined database of glaciers in Svalbard that contains thirteen features
- We compute the first map of glacier surge probability in Svalbard and we quantify the relative importance of relevant features

Correspondence to:

C. Bouchayer,
colili@uio.no

Citation:

Bouchayer, C., Aiken, J. M., Thøgersen, K., Renard, F., & Schuler, T. V. (2022). A Machine learning framework to automate the classification of surge-type glaciers in Svalbard. *Journal of Geophysical Research: Earth Surface*, *127*, e2022JF006597. https://doi.org/10.1029/2022JF006597

Received 12 JAN 2022
Accepted 27 JUN 2022

Abstract Surge-type glaciers are present in many cold environments in the world. These glaciers experience a dramatic increase in velocity over short time periods, the surge, followed by an extended period of slow movement, the quiescence. This study aims at understanding why only few glaciers exhibit a transient behavior. We develop a machine learning framework to classify surge-type glaciers, based on their location, exposure, geometry, climatic mass balance and runoff. We apply this approach to the Svalbard archipelago, a region with a relatively homogeneous climate. We compare the performance of logistic regression, random forest, and extreme gradient boosting (XGBoost) machine learning models that we apply to a newly combined database of glaciers in Svalbard. Based on the most accurate model, XGBoost, we compute surge probabilities along glacier centerlines and quantify the relative importance of several controlling features. Results show that the surface and bed slopes, ice thickness, glacier width, climatic mass balance, and runoff along glacier centerlines are the most significant features explaining surge probability for glaciers in Svalbard. A thicker and wider glacier with a low surface slope has a higher probability to be classified as surge-type, which is in good agreement with the existing theories of surging. Finally, we build a probability map of surge-type glaciers in Svalbard. The framework shows robustness on classifying surge-type glaciers that were not previously classified as such in existing inventories but have been observed surging. Our methodology could be extended to classify surge-type glaciers in other areas of the world.

Plain Language Summary 1% of the glaciers in the world exhibit intermittent phases of accelerated motion, called surge. These accelerations are not fully understood and we do not know why only few glaciers experience such behavior. Surging glaciers may lead to dramatic advances over rivers and damming up lakes that are then prone to a sudden and possibly catastrophic drainage. The Svalbard archipelago, located in the high Arctic, hosts more than one hundred surging glaciers. By analyzing statistically several data-sets, we calculate the probability for every glacier to experience surge events. Our results show that specific combinations of surface and bed slopes, glacier width and ice thickness control glacier surge probability. To a smaller extent climatic parameters such as the mass a glacier may lose or gain during the year and the amount of melt water available also contribute to the surge probability. These findings are in good agreement with existing theories explaining surge dynamics. We produce the first probabilistic map of surging for all the glaciers in Svalbard. Our classification highlights some glaciers that were not classified as surging glaciers in glacier inventories but have been observed surging, confirming the robustness of our framework. Our method is applicable to other world regions.

1. Introduction

Glacier instabilities, such as surges, are primary contributors to uncertainties of future sea-level rise projections (Ritz et al., 2015). Surge-type glaciers exhibit long periods of quiescence and short periods of accelerated motion, transferring substantial ice mass to lower elevation and thus often leading to rapid ice loss (Cuffey & Paterson, 2010; Meier & Post, 1969). They represent approximately 1% of the glaciers in the world (Sevestre & Benn, 2015) and pose a considerable hazard potential (Truffer et al., 2021). Surges can occur at quasi-regular time intervals and a huge spatial variability has been observed, with surging and non-surging glaciers located next to each other (Bhambri et al., 2017; Cuffey & Paterson, 2010; Meier & Post, 1969). Thus, identifying surge-type glaciers may contribute to a reduction in the uncertainties of future sea-level rise and may provide better hazard mitigation (e.g., surges related to glacier lake outburst floods (Bazai et al., 2021)). In the present study, we use the term surge for quasi-cyclic increases of ice flow velocity that "result from oscillations in conditions at the bed of the glacier" (Benn & Evans, 2014).

Surge dynamics is considered to be governed by changes in the sub-glacial drainage system configuration, switch in the thermal basal conditions and interactions between the hydrology and the glacier substrate (Benn et al., 2019; Cuffey & Paterson, 2010; Minchew & Meyer, 2020; Thøgersen et al., 2019, 2021). Due to the limited accessibility of subglacial environments, the physical processes at the ice-bed interface are difficult to measure. Recently, three approaches have been proposed to unify the theories of glacier instabilities. On the one hand, Benn et al. (2019) proposed that a glacier remains stable when the variations of enthalpy at the glacier bed, which impact the ice flow, are in equilibrium with the variations of ice mass. Enthalpy increases through geothermal and frictional heating and decreases by heat conduction and melt water exiting the system. If the ice mass and enthalpy budget are out of equilibrium, the glacier dynamic will alternate between periods of quiescence and surge phases. On the other hand, Thøgersen et al. (2019); Thøgersen et al. (2021) developed an evolution model for subglacial friction based on the rate-and-state friction law (Dieterich, 1992), suggesting that large enough perturbations can propagate and cause a glacier surge. They concluded that a better understanding of the feedback between the subglacial drainage and basal friction is critical to describe such perturbations. Other studies have examined the rate-and-state friction law to describe mechanical processes at the ice-bed interface (Zoet et al., 2020). Finally, Minchew and Meyer (2020) proposed a model describing the mechanical evolution of the till (internal friction, porosity and pore water pressure) while the glacier is flowing. They suggested that changes on both hydromechanical properties of the sediment layer and the thickness of the glacier may control surge behavior. Based on these three approaches, we select a series of features detailed below, which have been proposed to control the process of glacier surge. In the following, we use the term features to denominate physical parameters that may have an effect on glacier surging.

Previous studies have established that surge-type glaciers have the following properties: (a) they are more likely to be longer and/or wider (Barrand & Murray, 2006; Clarke, 1991; Clarke et al., 1986; Jiskoot et al., 1998) than non-surging glaciers. These variables are highly correlated to the bed and surface slopes of the glacier and so the relative importance of each individual feature is hard to assess (Clarke, 1991; Clarke et al., 1986); (b) their bed contains more likely younger and mechanically weaker lithologies than hard beds (Jiskoot et al., 1998, 2000); (c) they are clustered in climatic envelopes between cold-dry and warm-humid environments (Sevestre & Benn, 2015); and (d) they are more likely polythermal in Svalbard (only region where the thermal regime has been integrated into a statistical study) (Jiskoot et al., 2000). Based upon these studies, Sevestre and Benn (2015) built an entropy maximization model to qualitatively classify the glaciers in the Randolph Glacier Inventory database, RGI (2017), into five surging categories, from no surge to surge-type (Figure 1). However, statistical studies of glacier surges have two limitations: (a) they use integrated features for entire glaciers, and (b) none of them are comparing different type of models. Although Barrand and Murray (2006) explored differences between generalized linear models and the features that are included in each model, their study does not compare different types of models.

Here we address the question of why some glaciers exhibit such intermittent behavior while others do not, and whether these differences can be explained based on geometric and climatic characteristics. By limiting the geographical extent of our study area to a climatically relative homogeneous setting, we exclude overall climatic controls (Sevestre & Benn, 2015) and aim to isolate the non-climatic influences. The climate in Svalbard is assumed to be relatively homogeneous compare to other regions. Around 22% of Svalbard's glaciers are surge-type, which represents a relatively large proportion of the 1,615 glaciers of this region reported in the Randolph Glacier Inventory (RGI, 2017). We propose a framework to regularize the evaluation of several machine learning models for determining glacier surge probability. The machine learning framework aims at identifying glacier areas that might enter an unstable regime due to their geometrical and climatic configuration (Figure 2). Selecting the best performing model, the Extreme Gradient Boosting (XGBoost) (Chen & Guestrin, 2016), we identify the features that control the classification of surge-type glaciers. By applying this framework on a custom-built database, we produce a map of surge probability for Svalbard glaciers. Using this model, we demonstrate that geometrical features have a high impact on the classification, and these findings are discussed in the context of the existing glacier surge theories. The machine-learning framework can be applied for assessing the surge probability of glaciers in other regions of the world, expanded when new data are available and/or adapted to other fields (e.g., landslides, earthquakes dynamics).

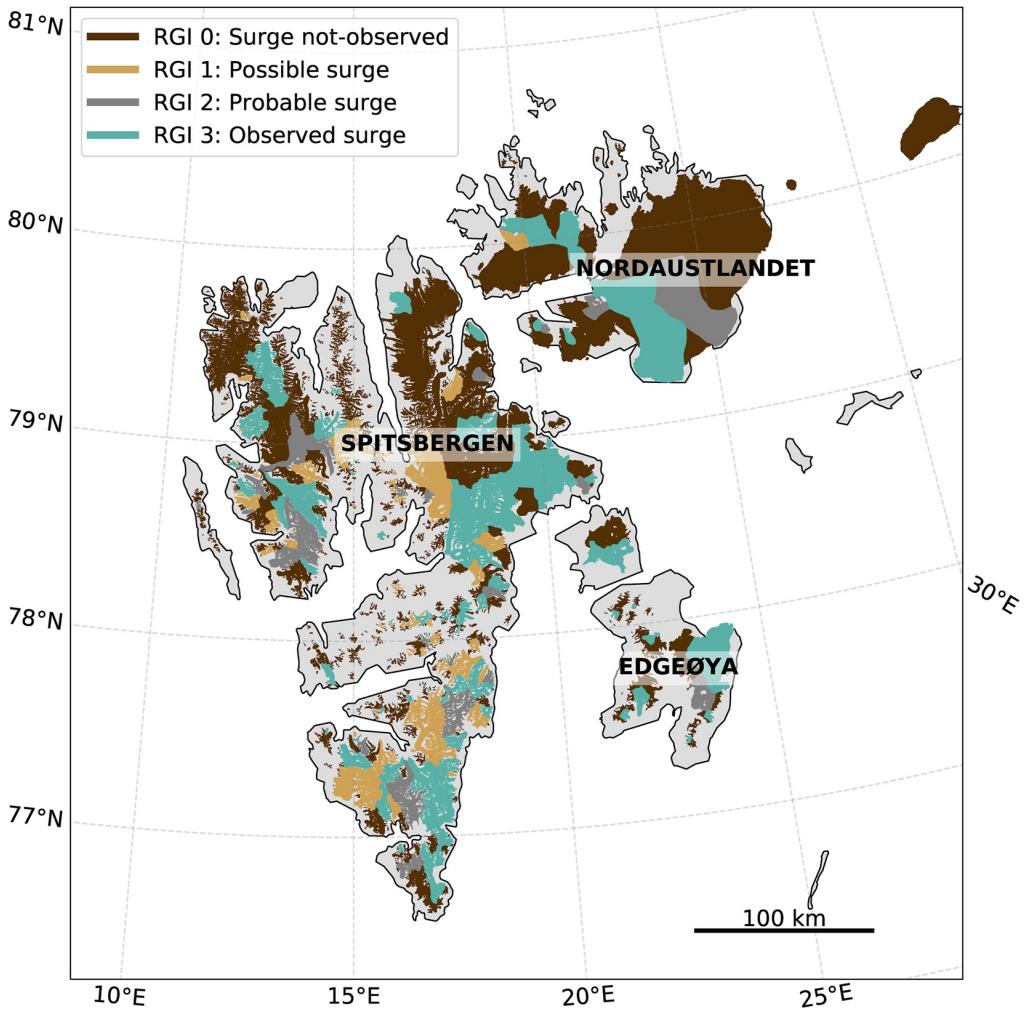

Figure 1. Classification of glaciers in Svalbard in the Randolph Glaciological Inventory database (RGI, 2017). This database contains five classes that characterize the surge potential of glaciers (Sevestre & Benn, 2015): Not observed (0), Possible (1), Probable (2), Observed (3), Not assigned (9). The class 9 is not represented in the Svalbard region.

2. Data and Methods to Assess the Surge Probability of Glaciers in Svalbard

We develop a machine learning framework for classifying surge-type glaciers. This framework includes the development of a custom-built database, a method for training machine learning models consistent with best machine learning practices, methods for evaluating the model outputs (i.e., the probability for a glacier to be classified as surge-type), and finally a method for mapping the surge probability of Svalbard glaciers. Additionally, we identify the key features that control the predictions of the models.

We build a glacier database by combining the Randolph Glacier Inventory (RGI, 2017), geometrical features (Fürst et al., 2018; Maussion et al., 2019), and climatic data (Pelt et al., 2019). These data are discretized along the glacier centerlines. After discretizing and post-processing the data, the custom-build database combines 981 glaciers which are discretized along 97,140 points over Svalbard.

The database is used in three different supervised machine learning models: logistic regression, random forest, and XGBoost. Data are split between training and testing data-sets. Training data are used to teach the machine learning models whether a glacier is surge-type. Testing data are used to evaluate the ability of the models to classify surge-type glaciers.

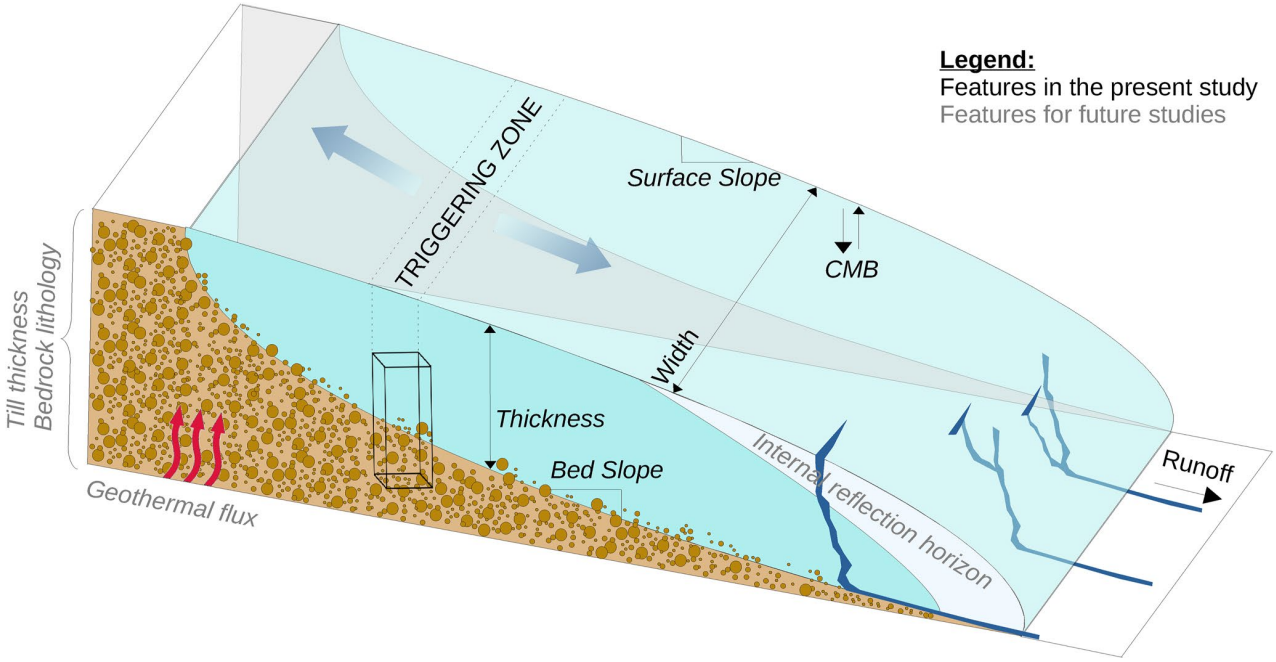

Figure 2. Sketch of the features that have been implemented in our model and new features that could be implemented for evaluating the surging potential of glaciers.

These models are evaluated using multiple statistic metrics, such as the area under the Receiver Operator Characteristic curve (Hanley & McNeil, 1982). After the models are evaluated, the best model, in our case XGBoost, is used to calculate the surge probability of each centerline point in each glacier. These values are then used to build a probability map of surge glaciers in Svalbard.

In addition to generating the probability map, we identify the features in the training data set that most strongly control the classification. We calculate the feature importance scores for each model. We also perform a recursive feature elimination to quantify the contribution of each features in the model performance (Chen & Jeong, 2007), and finally we use the Shapley Additive values (Lundberg & Lee, 2017). The sketch in Figure 3 illustrates our framework.

2.1. Data

2.1.1. Randolph Glacier Inventory Features

The Randolph Glacier Inventory (RGI, 2017) is a globally complete database of digital outlines of glaciers worldwide, excluding the ice sheets. This database was developed to provide better estimates of past and future surface mass balance of glaciers (Pfeffer et al., 2014). It includes integrated features such as glacier surface area and length. Glaciers are classified into five different surging categories: 0 - Surge not observed, 1 - Possible surge-type, 2 - Probable surge-type, 3 - Surge Observed, 9 - Not surging (Figure 1). This classification has been established following the work of Sevestre and Benn (2015). While the classes 0 and 3 are based on field observations, the classes 1 and 2 are based on statistical modeling (Sevestre & Benn, 2015). However, no quantitative predictions of surge probability are assessed.

The Randolph Glacier Inventory is distributed through the Global Land Ice Measurements from Space, and the National Snow and Ice Data Center (GLIMS/NSIDC) website (RGI, 2017). It is continuously developed and new versions are released regularly. In the present study, we use the most recent version (v6.0) for the Svalbard region, which is the region 7 in this database. From the Randolph Glacier Inventory, we use only the unique identifier allocated for each glacier in Svalbard (RGIId), the corresponding glacier name and the surging class (Figure 3). Other features present in the Randolph Glacier Inventory, such as the surface area and the length of glaciers, are

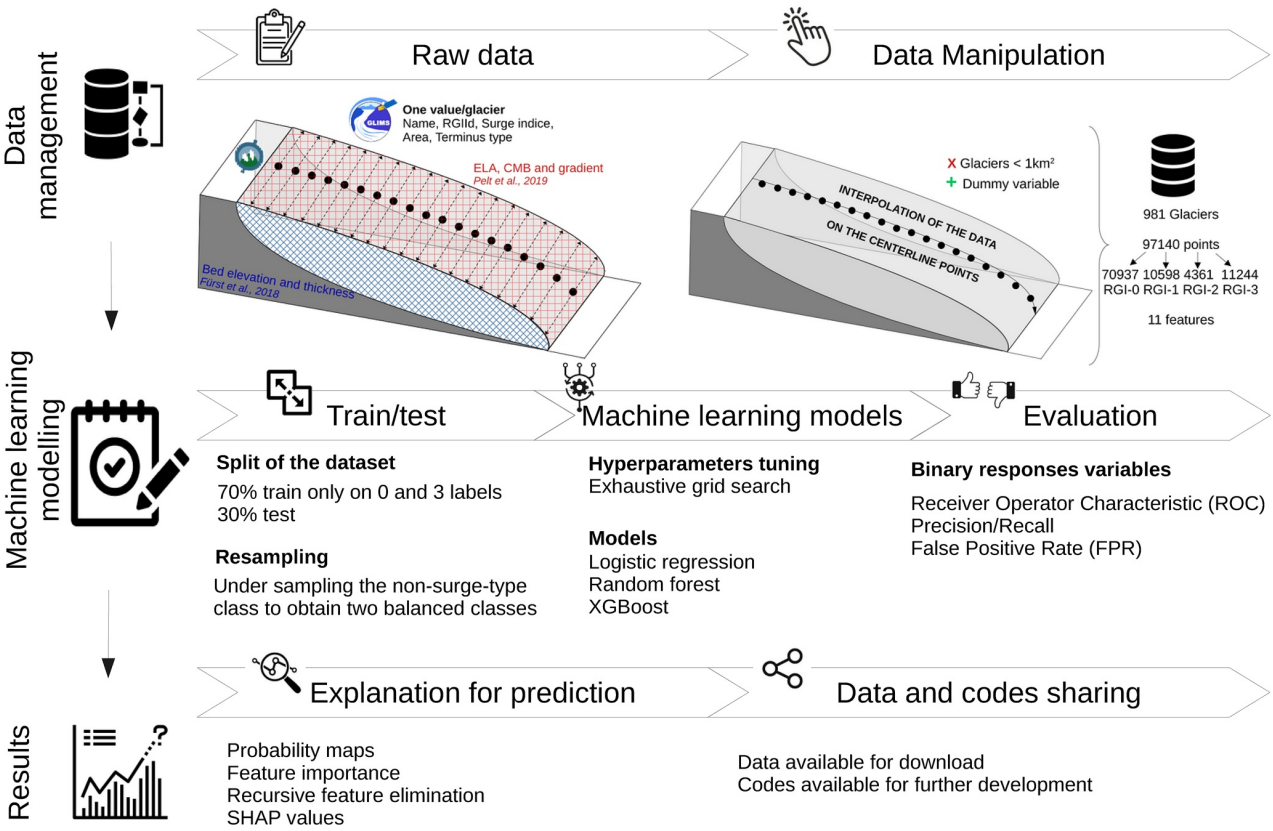

Figure 3. Workflow of the machine learning methods used to classify surge-type glaciers. Once the raw data are collected, the features are interpolated along the centerlines points. The database is then filtered and separated into a train data set and a test data set. Data are re-sampled to obtain balanced classes between surge-type and non-surge-type glaciers. The machine learning models are run and evaluated. The best model is XGBoost after evaluation. By looking at the contribution of each feature contribution in the model, the surge probability map of glaciers in Svalbard is produced.

not used because these are integrated features across each glaciers while we focus in this study on discretized variables along glacier centerlines.

2.1.2. Geometric Features

Many studies investigating glacier surges have highlighted the importance of geometrical features (Barrand & Murray, 2006; Björnsson et al., 2003; Clarke, 1991; Clarke et al., 1986; Hamilton & Dowdeswell, 1996; Jiskoot et al., 1998, 2000; Sevestre & Benn, 2015). In the present study, we include the width, the thickness, the bed elevation and the surface elevation of each glacier, and the associated bed and surface slopes. The geometrical widths have been computed using the Open Global Glacier Model (Maussion et al., 2019). This model is open-source and is partly used to simulate past and future changes of any glacier in the world. Glacier outlines are extracted from the Randolph Glacier Inventory and projected onto a local glacier grid. The spatial resolution depends on the size of the glacier (Maussion et al., 2019). The geometrical widths are computed by intersecting lines perpendicular to the flow lines at each grid point with the glacier outlines and the tributary catchment areas. The detailed workflow is described in Maussion et al. (2019).

The bed elevation and glacier thickness are retrieved from Fürst et al. (2018). These authors presented a first version of the ice-free topography (SVIFT1.0), which was computed using a mass conservation approach for mapping glacier ice thickness. This database is built from more than one million point measurements coming from radio-echo soundings. In total, it corresponds to an accumulated length of 700 km of measured thickness profiles. The ice thickness was also computed where measurements were not available and an error estimation map is available by comparing the model calculation and the observations. The reconstructed ice thickness corresponds to the status of the glaciers in year 2010 (Fürst et al., 2018). We also estimated the surface and bed slopes

by calculating the gradient between two successive points along the centerlines of the surface and bed elevation data.

2.1.3. Climatic Features

We added climatic features to the database, that is, runoff and climatic mass balance (CMB). Pelt et al. (2019) created a long-term (1957–2018) data set of CMB for the glaciers, snow conditions, and runoff with a 1 × 1 km spatial resolution and 3-hr temporal resolution over Svalbard. These authors used a coupled energy balance–subsurface model, forced with down-scaled regional climate model fields, and apply it to both glacier-covered and land areas in Svalbard. In our study, we characterize CMB by spatially distributed values of the Equilibrium Line Altitude (ELA) and mass balance gradient. The runoff is the local discharge corresponding to the available water coming from rainfall and melt at the bed after accounting for retention by refreezing and liquid water storage (Pelt et al., 2019). We use the latest computed data corresponding to the year 2018.

2.2. Data Management

2.2.1. Discretization

Using the Open Global Glacier Model, we computed the centerline coordinates for each glacier in Svalbard with the algorithm developed by Kienholz et al. (2014) and modified by Maussion et al. (2019). Once the termini and the heads of each glacier are identified, the least-cost route is calculated to derive the centerlines. The centerline points are not equidistant after this calculation. Then, the centerlines points are interpolated to be equidistant from each other. Depending on the size of each glacier, the distance between successive points varies between 20 and 400m for different glaciers. Some glacier catchments contain a main glacier accompanied by its tributary glaciers and so several centerlines are computed for the same catchment. In our study, we use the longest centerline as the main centerline of the principal glacier. Once the centerlines have been extracted, we interpolate or extrapolate all other data along the centerlines coordinates.

2.2.2. Custom-Built Database of Svalbard Glaciers

The database is the combination of all the features discretized along the centerlines. Since the climatic data have a spatial resolution of 1 × 1 km, we exclude all the glaciers with a surface area less than 1 km^2 and a length less than one km.

As a consequence, our custom-built database contains 981 glaciers which are discretized along 97,140 points: 70,937 points belong to the class "Not Observed Surging," 10,598 belong to the class "Possible Surge," 4,361 belong to the class"Probable Surge-type," and 11,244 belong to the class "Observed Surging." The surge class of an entire glacier is assigned to every points discretized along the centerline of this glacier. Eleven features are used to train the statistical models: the surging class (1), the bed elevation and slope (2, 3), the surface elevation and slope (4, 5), the thickness (6), the CMB (7), the glacier width (8), the width divided by the thickness (9), and the driving stress (10). A random number is also added as a dummy feature (11) that does not have a physical interpretation and is used here to compare the importance of the other features to a random value (McBeck et al., 2020). The final database contains as well the Randolph Glacier Inventory identifier and the corresponding glacier name.

Figure 4 displays the correlations between these features. The features clustered in the upper left corner of the correlation matrix show high positive or negative correlations. Following the diagonal of the matrix toward the lower right corner, the correlations are decreasing. The bed elevation, thickness, width, runoff, bed and surface slope are highly correlated with each other. The driving stress, width times thickness (W × H), and the dummy features show correlation values close to 0, indicating that they are not correlated to other features.

2.3. Machine Learning Modeling

2.3.1. Training and Testing Data Sets

The training data set is organized in the following ways: (a) only glaciers classified as Not-Observed surge (class 0) or Observed surge (class 3) in the Randolph Glacier Inventory are used; (b) the training data set is resampled such that it contains an equal number of surge-type and non-surge-type glaciers; and (c) the training and testing

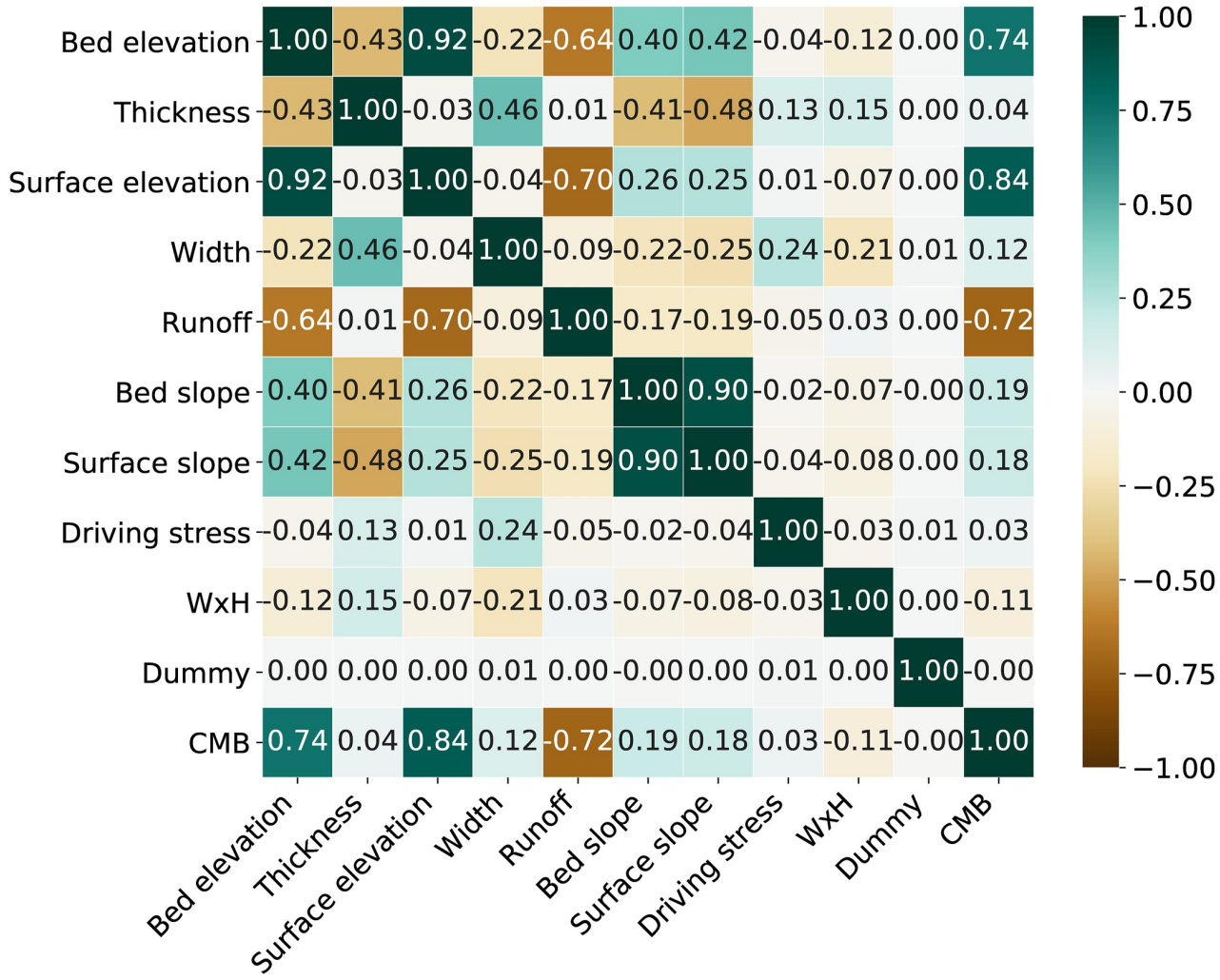

Figure 4. Correlation matrix between the most important features using only the training data. The colors shows the value of the coefficient of correlation.

data-sets are split such that all the data of a given glacier belong either to the training data set or to the testing data set, but not to both. We only use glaciers from the classes Not-Observed (0) and Observed (3) surge to avoid systematic errors that may be associated with glaciers labeled in the Randolph Glacier Inventory as having some likelihood to be surge-type but no direct evidence of surging behavior has been observed (i.e., Possible surge (1) and Probable surge (2) classes). We train the data considering only two classes, surge-type or not surge-type (class 0 and 3 of the RGI classification). Every point along the centerline will then be assigned to a 100% probability to be classified as surge-type or 100% probability to be classified as not-surge type. The results of the statistical modeling will however assess the probability for each point in the centerline of a glacier to be classified as surge-type or not rather than a binary class allocation for the entire glacier.

The glaciers classes are highly unbalanced with almost seven times more glaciers of the Not-Observed surge class than Observed surge class. An unbalanced training data set can lead to erroneous results in classification problems (Ganganwar, 2012). Therefore, we under-sampled the Not-Observed surge glaciers such that the data set contains a 50%–50% distribution of non-surging and surging glaciers. This data set is then split into a training and a testing set, respectively 70% and 30% of the database. We justify this split by running ten different models trained with a split between 10% and 90% for the training data set. The values of the Area Under The Curve (AUC) is acceptable when 70% of the database is used for training, while higher proportion might lead to overfitting model. A precise description of the analysis is presented in the appendix (Appendix A, Figure A1).

2.3.2. Machine Learning Models

We use three different supervised machine learning models: logistic regression, random forest and Extreme Gradient Boosting (hereafter, XGBoost). Logistic regression is based on the maximum likelihood and was used in previous glaciological statistical studies (Jiskoot et al., 1998, 2000), while random forest is a commonly used tree-based ensemble model. XGBoost is a new tree ensemble model that is leading machine learning competitions (e.g., Kaggle). We choose to compare traditionally used models in the glaciology community, with commonly used models in other scientific communities and a new leading model. Using a data set with a known outcome (i.e., whether a glacier is surge-type or not), we train models to identify this outcome. Each model requires selecting at least one hyperparameter (e.g., the depth of decision trees used in a random forest). We selected the values of the hyperparameters after an exhaustive grid search (Appendix C, Table C1).

2.3.2.1. *Logistic Regression*

Logistic regression is commonly used in machine learning for classification tasks. This algorithm produces a probabilistic estimate of whether a particular set of input features belongs to a class or not. Logistic regression has been used in several studies in glaciology to better understand glacier surges (e.g., Jiskoot et al. (2000); Barrand and Murray (2006)). We used the logistic regression equation (Nelder & Wedderburn, 1972):

$$\ell = \log\frac{p}{1-p} = \beta_0 + \beta_1 x_1 + \beta_2 x_2 + \cdots + \beta_M x_M = \boldsymbol{\beta}\cdot\mathbf{X} \tag{1}$$

where $\boldsymbol{\beta} = \{\beta_0, \beta_1, \ldots, \beta_M\}$ is the vector containing the model parameters that weight the impact of the input features containing in the vector $\mathbf{X} = \{x_0, x_1, \ldots, x_M\}$. $p = P(Y = 1)$ is the response of one binary feature Y. We implemented this method using the scikit-learn library in Python (Pedregosa et al., 2011). The inverse regularization length C is set to 1×10^{-5} and the penalty to L2 (Appendix C, Table C1).

2.3.2.2. *Random Forest*

Random forest is a tree-based ensemble machine learning technique that is constructed by a multitude of decision trees. Each tree in the random forests is producing a class prediction and the class with the most votes becomes the model prediction (Breiman, 1999). We implemented the random forest models with the scikit-learn library of Python (Pedregosa et al., 2011), and using the Gini impurity:

$$\text{Gini} = \sum_{i=1}^{C} f_i\,(1 - f_i) \tag{2}$$

where f_i is the frequency of the label i at a node and C is the number of unique labels. We used 1000 trees in the forests with a maximum depth of 2 and the number of features to consider when looking at the best split is the square root of the number of features (Appendix C, Table C1).

2.3.2.3. *Extreme Gradient Boosting - XGBoost*

Boosting is an ensemble technique where new models are added to correct the errors made by pre-existing models. The models are added sequentially until no further improvements is made. The algorithm attributes more weights to the misclassified data to improve the predictions. To minimize the loss function, the algorithm uses gradient descent (Hastie et al., 2009). We use a specific implementation of gradient boosting called Extreme Gradient Boosting (XGBoost) (Chen & Guestrin, 2016). XGBoost is an implementation of a stochastic gradient boosting machine (Friedman, 2001; Friedman, 2002; T. Chen et al., 2015; Chen & Guestrin, 2016). XGBoost can use a variety of learners as its base learners such as linear models or decision trees (Chen & Guestrin, 2016). We use decision trees as the base learners. The gradient boosted equation is formulated as follows:

$$\log\frac{p}{1-p} = F_0 + \sum_{m=1}^{M} r_m(\mathbf{X})F_m(\mathbf{X}) \tag{3}$$

where m is the iteration index over M maximum iterations. $F_m(\mathbf{X})$ is the current iteration fitted to the previous iterations residuals $r_m(\mathbf{X})$. F_0 is the base estimate.

We implemented XGBoost using the xgboost library in Python (Chen & Guestrin, 2016). The objective is the logistic regression, we define 20,000 boosting learners, trees have a maximum depth of 2, and the minimum child weight is 1 (Appendix C, Table C1).

2.3.3. Evaluation of the Models

We use evaluation metrics based on comparison to random chance. These evaluation metrics include the Area Under The Curve (AUC) (Hanley & McNeil, 1982), the precision and recall, and the F1-score. Each of these metrics is used widely in machine learning studies (Hastie et al., 2009).

The AUC value is within the range [0.5–1.0], where the minimum value represents the performance of a random classifier and the maximum value would correspond to a perfect classifier. A value of 0.5 would suggest no discrimination between surge-type and no surge-type glaciers. AUC values between 0.70 and 0.80 are considered acceptable for classification (Hosmer Jr et al., 2013).

The receiver operating characteristic curve is the true positive rate TP_{rate} against the false positive rate FP_{rate}:

$$TP_{rate} = \frac{TP}{TP + TN} \tag{4}$$

$$FP_{rate} = \frac{FP}{FP + FN} \tag{5}$$

where TP stands for true positive, TN for true negative, FP for false positive and FN for false negative. False positive indicates predictions that have been labeled as surge-type while the true label should have been non-surge-type. The true positives correspond to surge-type glaciers that have been labeled correctly. The same logic applies for false negative and true negative rates.

The performance of a classifier with respect to test data can be assessed by the value of the precision, which is the ratio of correctly predicted positive observations to the total predicted positive observations:

$$\text{Precision} = \frac{TP}{TP + FP} \tag{6}$$

and the value of the recall, which is the ratio of correctly predicted positive observations to the all observations in an actual class:

$$\text{Recall} = \frac{TP}{TP + FN} \tag{7}$$

The models have been trained fifty times with different training sets randomly picked and then tested in fifty different testing sets. The corresponding AUC has been calculated for each of these models. The method and results are presented in Appendix B. In addition, a K-Fold cross-validation has been performed to evaluate the model performance stability. A detailed description of the method and the results is discussed in the appendix Appendix B.

2.4. Explanation for Prediction

We examine how the eleven features impact model decision in several ways: (a) we compute the relative feature importances across all models and compare them, (b) we examine two feature importances relevant to XGBoost (gain and weight), the model that has the highest performance, (c) we calculate the Shapely Additive values for the XGBoost model.

We compare the feature importances of three models in a stacked diagram (Figure 8). For each model, the features importance score is calculated and the scores are summed together for the three models. The feature importance score informs on the gain of information a feature gives to the model for classification (a detailed description of the feature importances can be found in Appendix D). For comparison purpose, we normalized all the scores using a min-max normalization. To add more weight on best performing models, the feature importance scores are multiplied by the AUC of each corresponding models. For XGBoost, only the gain scores are taken into account.

Another way to evaluate the feature contributions to the model predictions is to compute the Shapley Additive exPlanations (SHAP) values (Lundberg & Lee, 2017). SHAP values quantify the impact of having a certain value for a given feature in comparison to the prediction the model would have made if that feature had some baseline value. SHAP values allow for (a) a global interpretation of the predictions by analyzing how much each predictor contributes positively or negatively to the target feature; (b) a local interpretation because each observation gets its own SHAP value while most of the traditional feature importance algorithms only show results across an entire class. Based on the value of the features, SHAP analysis allocates a positive or a negative impact on the model output, for example, a high value of a certain feature has a positive impact on the model output meaning that a high value will influence the model toward a high potential of surging.

2.5. Interpolation of a Surge Probability Map

The surge probability is assessed for each discrete centerline point of a glacier using the XGBoost model. Only the XGBoost model is used to produce the map because results show it is the best-fit model (see Section 3 for more details). We average the centerline points probabilities to produce a single probability per glacier centerline. If the average probability along the centerline is under 0.5, the glacier is not considered to be surge-type. If the average probability along the centerline is equal or larger than 0.5 the glacier is considered to be surge-type. The Randolph Glacier Inventory surge-type classes are shown in the map of Figure 1. The average probability per glacier calculated in the present study is shown in the map of Figure 6. We also examine a subset of discretized glacier centerlines in Nordaustlandet Island (Figure 6, inset). This step is useful to show that surge probabilities are varying along the centerline of a glacier, highlighting the potential triggering zone where a surge may develop.

3. Results

3.1. Machine Learning Models Evaluation

All three models (logistic regression, random forest, XGBoost) perform better than random chance (Figure 5a) with testing AUC values ranging from 0.69 to 0.74 (mean AUCs calculated for 50 different training and testing data-sets). XGBoost shows the highest precision (0.85, Figure 5b) and lowest False Positive Rate (0.23, Figure 5d) of all the models. This model demonstrates a lower recall (0.63) than logistic regression (0.68) and random forest (0.69) (Figure 5c). Given these superior fit statistics for XGBoost, we choose this model to calculate the probabilities along glacier centerlines and to produce the surge-type glacier classification map. We perform complementary evaluations of the performance stability of XGBoost (Appendix B, Figures B1 and B2). The AUC is consistent using different training data sets picked randomly and stays stable when we perform the K-Fold cross validation. XGBoost is the best performing model in this study and its performance is stable regardless of the points used to train the models. Because of the stability of the performance, the final results are not computed using the K-Fold cross validation since it will not improve tremendously the performance of the model and we choose to establish the model stability as presented in Appendix B.

3.2. Surge Probability Map of Svalbard Glaciers

Using the XGBoost model, we compute the surge probability of glaciers in Svalbard. The predicted probability map (Figure 6) indicates the presence of surge-type glaciers in the entire archipelago. This map has been computed from averaging the probability of every point along the centerline for each glacier. The map with centerline points can be found in Appendix E (Figure E1). However, preferential zones of surge can be identified in for example, Nordaustlandet island, Torell Land. Other areas, for example, Nordenskköld Land, Andree Land, do not gather a significant number of surge-type glaciers. The XGBoost model classifies 162 glaciers as surge-type out of 981 (see Section 2.1 for more details on the data set). While some glacier centerlines present a uniform probability distribution, some others see their probabilities for surging evolve along the centerline (Figure 6, inset).

In addition to the probability map, we compare our results to the existing Randolph Glacier Inventory classifications for surge-type glaciers. Figure 7a shows the cumulative frequency distribution of probabilities to surge calculated by the XGBoost model. The cumulative frequency distributions of the two classes with low surge potential in the Randolph Glacier Inventory (0: surge not observed, 1: possible surge) appear very similar. The same observation applies for the two classes with high surge potential (2: probable surge, 3: observed surge).

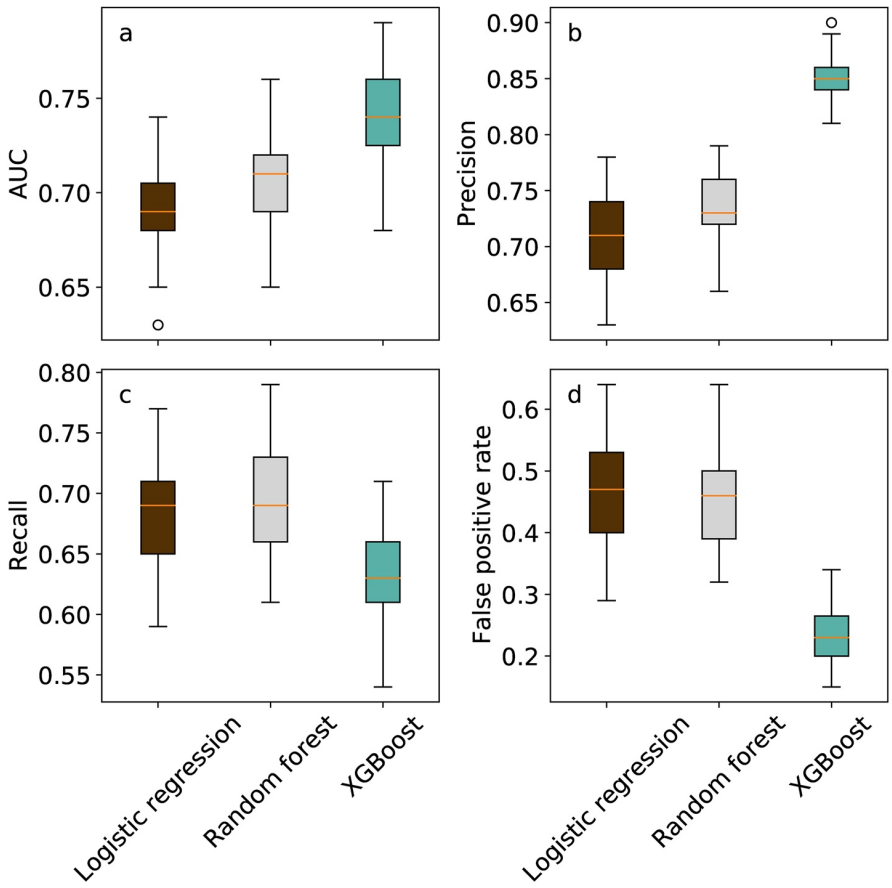

Figure 5. Boxplot representing the (a) Area Under the Curves (AUC), (b) precision score, (c) recall score, and (d) false positive rate for each of the three machine learning models. The scores have been calculated for 50 different training and testing data-sets. The orange line corresponds to the median while the box corresponds to the interquartile range. Both extremes indicates the minimum and the maximum value and the dots indicate the presence of outliers.

These results are supported by the histogram in the inset of Figure 7b which shows two distinct classes, non-surge type and surge-type glaciers. The non surge-type class is however better defined than the surge-type class.

3.3. Importance of Geometrical and Climatic Features

Figure 8 shows the combined importance for each feature used in each model (logistic regression, random forest, XGBoost). For all three models the width, thickness, and surface slope are the most important features explaining most of the models' predictions. The CMB, the width × height (W × H), the surface elevation, the driving stress, and the dummy features do not have a high impact on the model prediction. The runoff, bed elevation, and bed slope explain partially the predictions.

Beyond the comparison of features between each model, we also examine the feature importances for the best-fit model, XGBoost. Figure 9 shows the feature importance scores computed with the gain and weight implementation for the XGBoost model. The width of the glacier adds a considerable amount of information when it is selected on the trees, while the surface slope and the thickness are the features that are selected the most. The thickness, runoff, and the bed elevation add more information than the CMB, W × H, surface elevation, driving stress that are equally not significantly important to assess the surging potential of glaciers in Svalbard. The dummy feature appears in all cases to be the least important feature, as expected.

Using recursive feature elimination, we find that five to six features are needed for the model to reach the highest AUC values (Figure 10). To predict the surging potential of a glacier in Svalbard, the surface and bed slope,

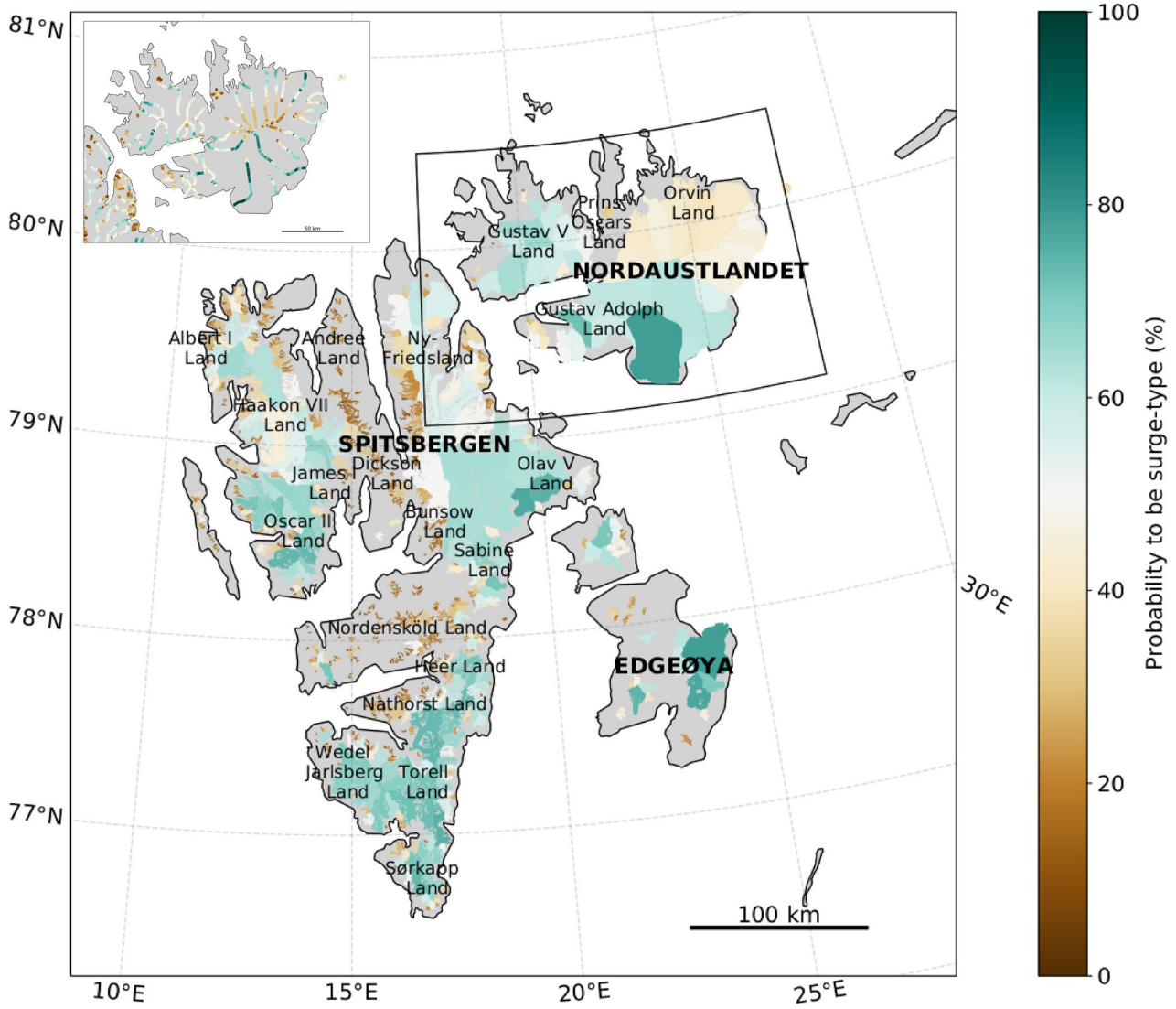

Figure 6. Averaged probability map for each glacier to be classified as surge-type in the XGBoost model. The zoom in the Austfonna ice cap shows how the average probability has been computed. First, a probability is calculated at every point along the centerline of every glacier. Then, we average the probabilities to surge of every point along the centerline to obtain an average surging probability for a given glacier.

thickness, CMB, runoff and width need to be considered. The driving stress, surface elevation and the dummy features do not have a significant impact on the model performance. All the eleven features are however used for the model final decision.

3.4. Feature Values and Local Impact on Prediction

Figure 11 shows the summary of the SHAP value analysis. While some feature values have a clear impact on the model decision, that is, the surface slope, width, others, that is, the bed and surface elevation, do not show a clear relationship between the feature values and the impact on the classification. Higher values of glacier surface slopes, CMB, and in some cases bed elevations all decrease the probability to be classified as a surge-type. Lower values of width, bed elevation, surface elevation, thickness, run off, bed slope, and W × H also decrease the probability for a glacier to be classified as surge-type. In contrast, high values of width, in some cases bed elevation, surface elevation, thickness, and W × H increase the probability for a glacier to be surge-type. Low values of surface slope and CMB are likely to increase the probability of a glacier to be classified as surge-type. Some

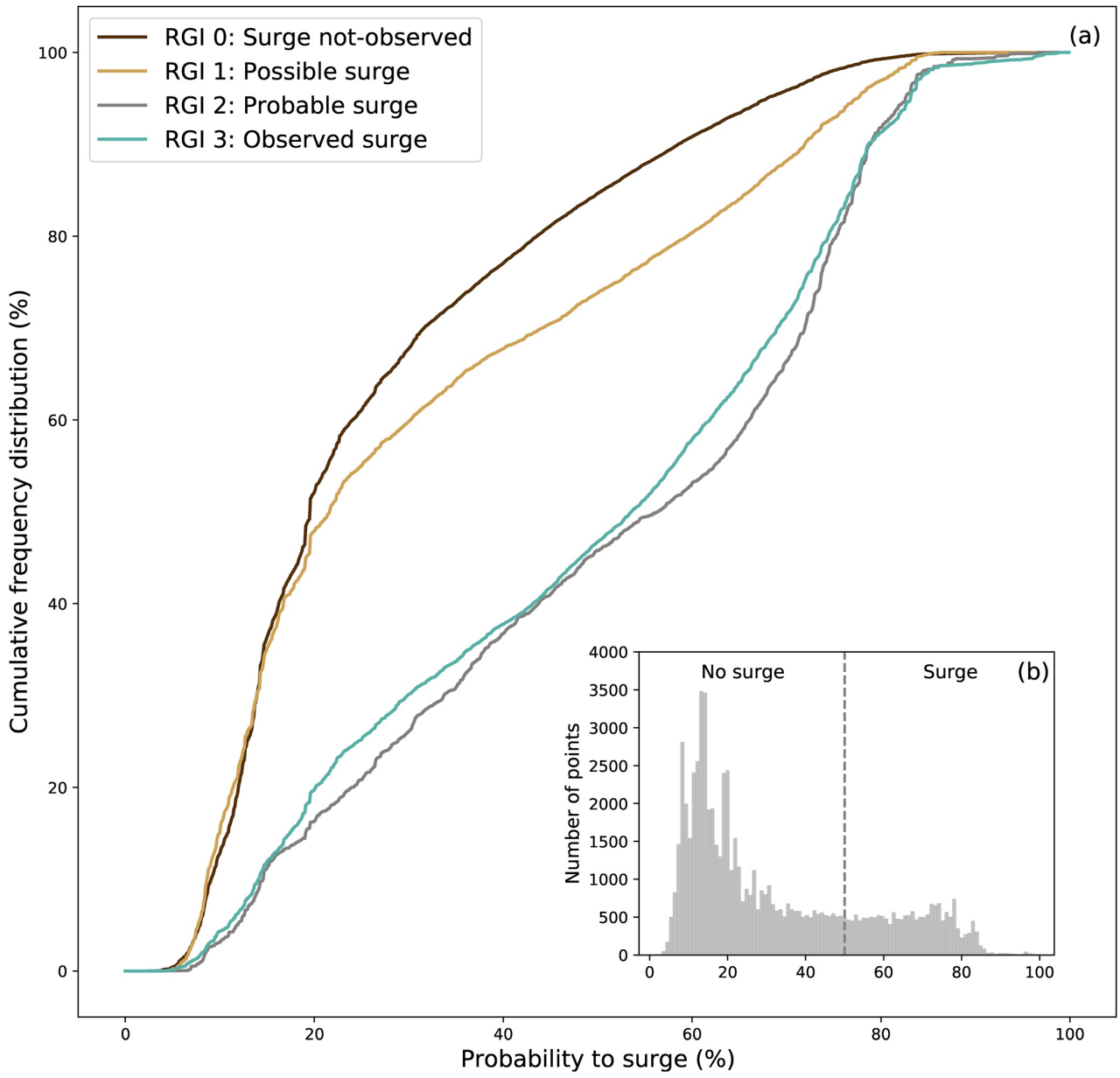

Figure 7. Cumulative frequency distribution for a glacier to be surge-type labeled by the classes defined in the Randolph Glacier Inventory. The inset shows the distribution of the probabilities. The vertical line indicates a 50% probability from which we separate surge-type from non surge-type glaciers.

features do not show clear separation between the values and the corresponding impact on the model: the bed and surface elevation, the driving stress and the dummy feature (this should be expected for the dummy feature). To summarize, a thicker and wider glacier with a low surface slope, CMB, and high runoff has more potential to be classified as surge-type.

4. Discussion

4.1. Evaluation of the Surge-Type Classification Framework

We calculate surging probabilities for glaciers in Svalbard after an evaluation of the best performing model, XGBoost. The discretization of the glaciers along centerlines increases the number of data points used to train

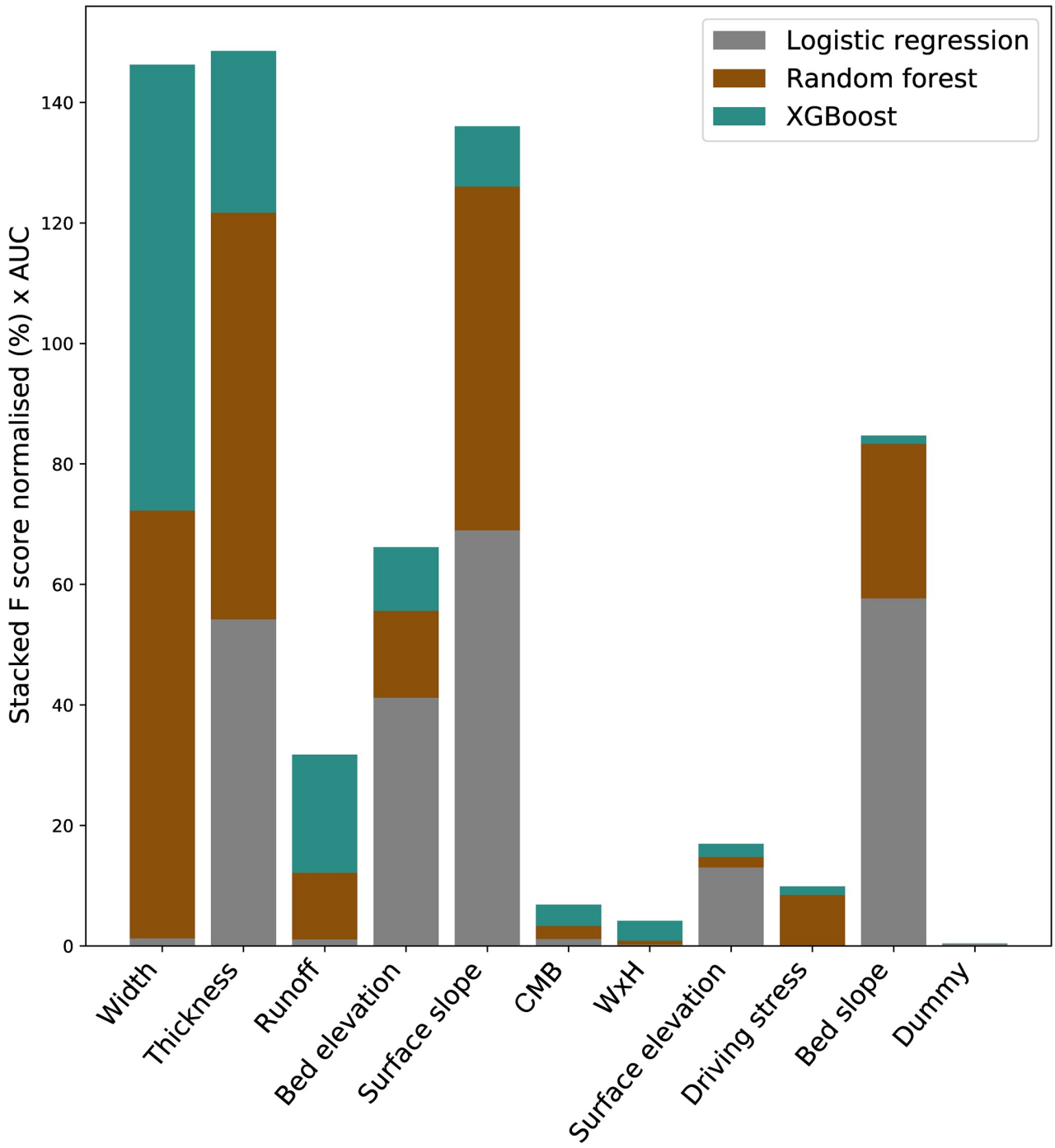

Figure 8. Feature importances for the logistic regression, random forest and XGBoost models stacked together. The F-score of each features has been normalized and multiplied by the AUC value. The features are organized from left to right from the most to the least important, according to XGBoost score.

and test models (981 glaciers corresponding to 97,140 points). The availability of data provides better insights into the relationships between features used as input for machine learning algorithms (Halevy et al., 2009). As explored in other fields (e.g., Fatichi et al. (2016)), complex natural systems cannot always be simplified using integrated features. For example, the glacier surface slope can vary along the centerline, which will change the driving stress. Averaging the slope in this case would misinform the model on changes that could impact model

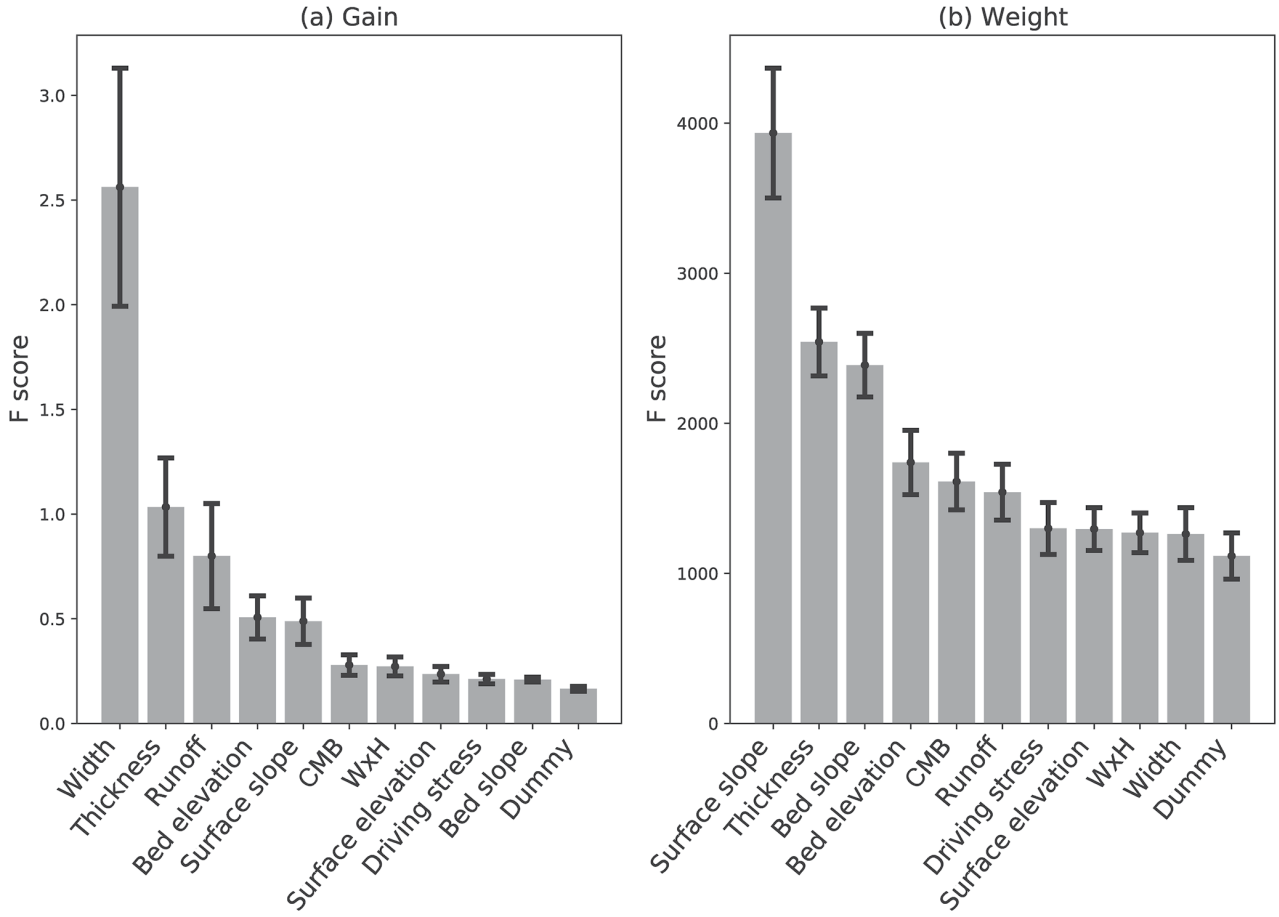

Figure 9. Feature importance of XGBoost model: (a) gain, (b) weight.

classification. In addition, discretized features enhance the spatial variability of the glaciers. A longer glacier will be constituted by a higher number of points along its centerline than a smaller glacier.

The framework presented here uses a model comparison and an evaluation method grounded in the best machine learning practices (Hastie et al., 2009). Previous statistical studies aiming at understanding surging glaciers used only one model, that is, univariate or multivariate regression (Barrand & Murray, 2006; Clarke, 1991; Clarke et al., 1986; Hamilton & Dowdeswell, 1996; Jiskoot et al., 2000) or maximum entropy (Sevestre & Benn, 2015). To our knowledge, this is the first study that compares the performances of several machine learning models to classify surge-type glaciers. Comparing models provides more confidence on the results of the best one. Numerical modeling studies have compared several models to determine the most accurate one for a defined task (e.g. (Hock et al., 2019),). The approach we take is similar. While a single model, XGBoost, is used in the final production of the classification map, we rely on the plurality of model results to support our understanding of what the models learned (e.g., Figure 8).

As with every machine learning model, the performance of XGBoost is tied to the quality of the input features. We use mostly features resulting from numerical simulations, and therefore, by nature, containing uncertainties. Pelt et al. (2019) highlights that the CMB and runoff values contain uncertainties due to (a) elevation offsets, (b) the input climatic parameters used for the simulations and (c) the modeling itself. Fürst et al. (2018) produced an error estimate map for the thickness computation that ranges from 1 to 500m. XGBoost is then trained with features that are not considered ground-truth (as opposed to field measurements). In addition, the error associated with the modeling data is unknown. Therefore, the range of resulting AUC values of XGBoost is controlled by possible bias in the input features used for training.

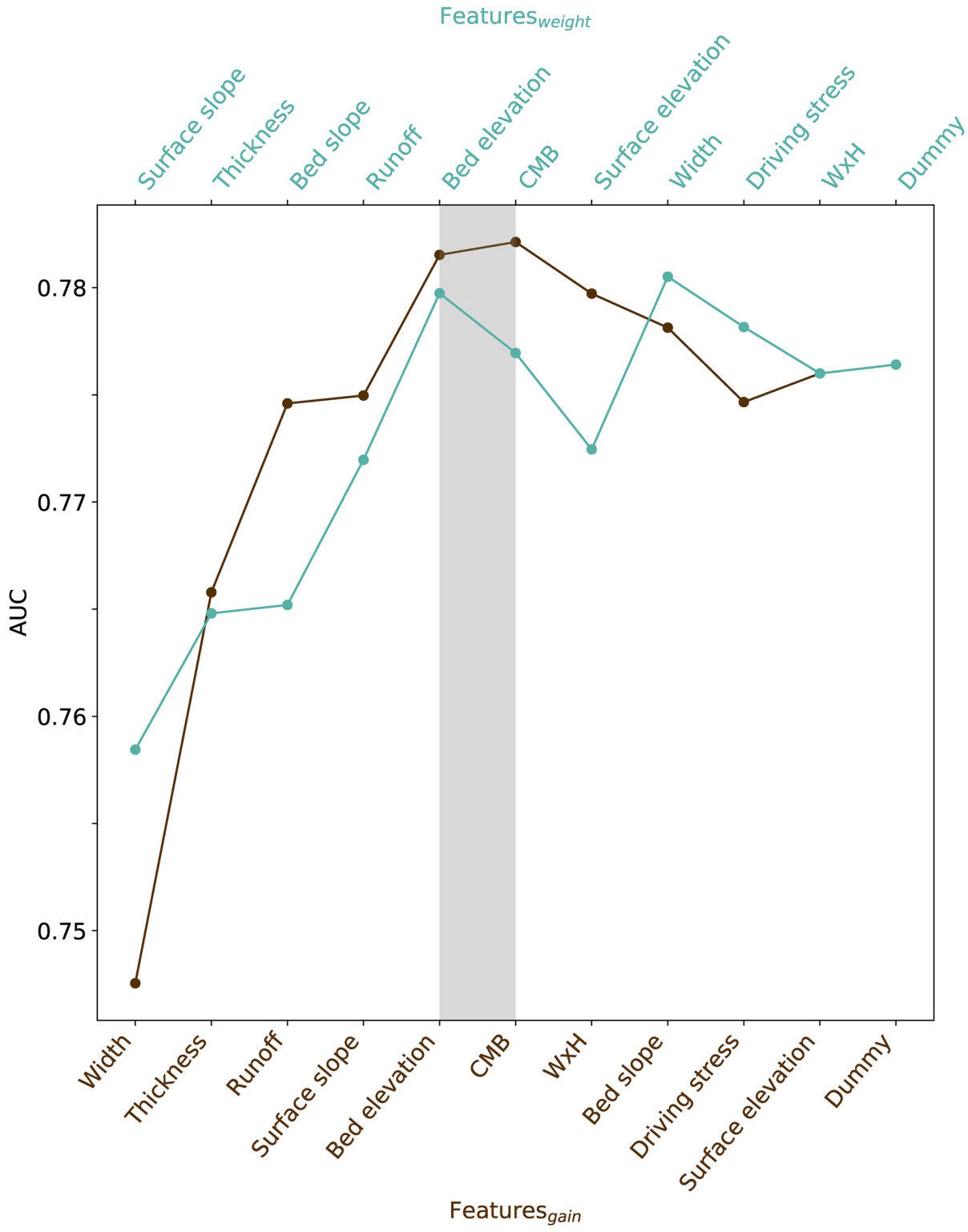

Figure 10. Results of recursive feature elimination show that four to five features explain most of the gain of information in the classification of surge-type glaciers. The number of features is added according to their order in the feature importance.

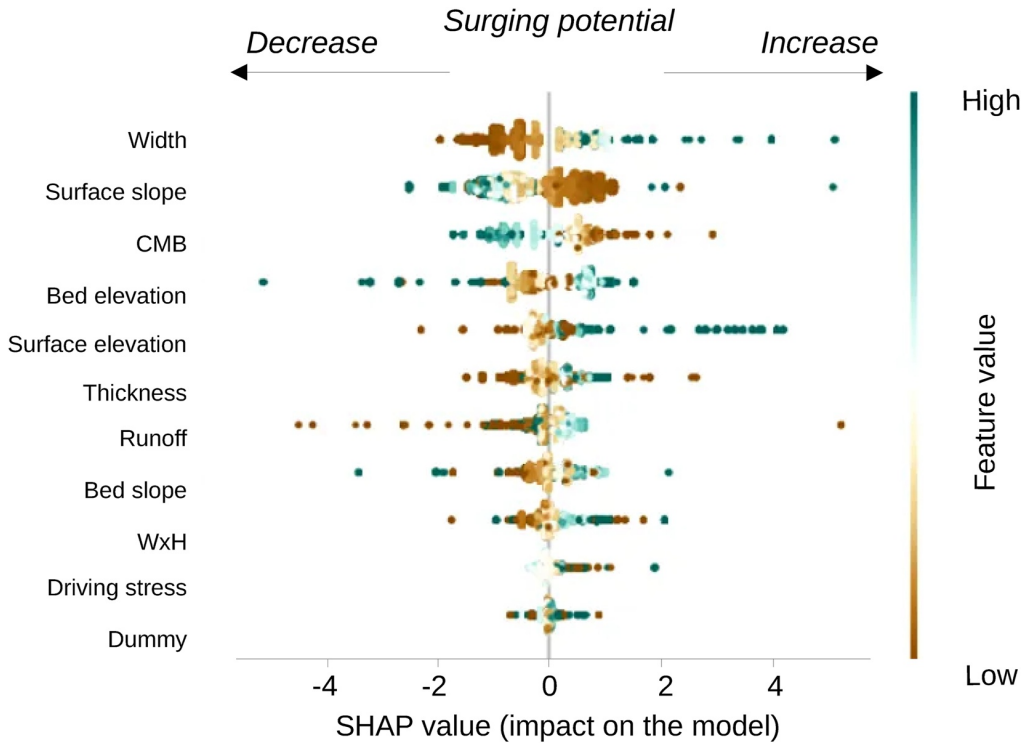

Figure 11. Summary of the SHAP values for every features at each glacier centerline point. The *x* position of each dot is the impact of the feature on the prediction of the model and the color of the dot represents the contribution of that value at each point.

In addition, the spatial resolution of individual features differs, for example, the bed elevation has been computed on a 100m resolution whereas the runoff and CMB have been calculated on a 1 km resolution grid. The features used in the models represent as well a snapshot for a particular point in time and may therefore represent different stages in the surge-cycle. While the topographic data (Fürst et al., 2018) represent the state of Svalbard in 2010, the climatic data (Pelt et al., 2019) represents the year 2018. Although we want to capture which features could cause a transient behaviour while using a snapshot in time, we consider that there are no better data available since simulating surges in real glacier geometry represents a real challenge. The current framework does not inform on the timing of the surging glacier, for example, pre-surge, post-surge. To do so, time series should be included in the framework by adding complementary types of data for example, remote sensing products. Using time series could potentially highlights an increase in probability when a glacier becomes closer to the development of a surge in the triggering zone where the surge will start to develop. However, the probability for triggering zone should always be higher than 50% since the model bases its classification on the potential of the glacier to be surge-type due to its geometrical and climatic configuration.

4.2. Feature Importance Informs on Theories of Glacier Surging

The important features in our models are the glacier width, the ice thickness, the surface and bed slopes, the runoff, and the CMB to a smaller extent (Figure 2). The width and the thickness have been shown to be important in previous statistical studies (Barrand & Murray, 2006; Clarke, 1991; Jiskoot et al., 2003) together with the surface slope (Jiskoot et al., 1998, 2000, 2003; Sevestre & Benn, 2015). Although XGBoost models predict that lower slope will drive the prediction toward increasing the probability for the point to be surge-type as in Sevestre and Benn (2015), Jiskoot et al. (1998) found the opposite. The surface and bed slopes, and the ice thickness are features controlling the dynamic of a glacier through the hydraulic gradient and the driving stress. Both are known to play a crucial role in surging theories (Benn et al., 2019; Fowler, 1989; Kamb, 1987; Thøgersen et al., 2019). Although the features controlling the surge classification are in good agreement with previous statistical studies,

the features we use in our model rely on more recent observations or modeling studies. In addition, by discretizing the features along the centerlines of the glaciers, we significantly increase the number of points, permitting a more robust statistical analysis. Thøgersen et al. (2021) highlight that in the context of a velocity weakening regime, the friction along the glacier margins is less important with an increasing glacier width. Therefore, wider glaciers should be more likely to be of surge-type which is in good agreement with the SHAP summary result (Figure 11).

To a smaller extent, the CMB is also influencing the classification. However, we are not considering that this feature is important on assessing the surge probability for glaciers due to the negligible increase of the AUC during the recursive feature elimination (Figure 10), as found in Jiskoot et al. (2000). The CMB is highly correlated to other features in the model, for example, the surface elevation and the runoff, meaning that the effect of the CMB is likely captured already into other features. However, in the interior parts of Svalbard, glaciers in drier areas show lower probabilities to be surge-type as opposed to the higher probabilities observed on the coast, in areas with more precipitation. A large glacier has a large accumulation area, receiving more precipitation than a small glacier with a small accumulation basin. Thus, the size of glaciers depends as well on the amount of precipitation they receive. Therefore, the geometrical features already account for part of the climatic influence. The relationship between the climatic and topographic variables is learned by the model and is specific to Svalbard for the trained model used in this study.

In Svalbard, we expect that climatic features are not playing a central role on the prediction compared to other regions in the world, because the climate is relatively homogeneous within the archipelago.

If more observations at the interface between the ice and the bed would become available, they could be incorporated directly into our framework, helping to assess the underlying physical processes leading to glacier surges. The framework allows to incorporate till properties if available. The change in rheological parameters, that is, the permeability and porosity of the sediment, can be responsible for a surge enhancement (Minchew & Meyer, 2020).

The complete framework develops in the present study can be directly used in other regions of the world. However, the models have been trained on Svalbard and show good performance scores. Applying the model to different regions may require a re-training. Indeed, the model in Svalbard has learned specific relation between the features that might be valid in Svalbard but different in other regions of the world. For the trained model to be directly tested in other regions of the world, every climatic-related features should be removed from the training data set in Svalbard, for example, the surface elevation which is a proxy for the mass balance and so is directly linked to the runoff as indicated previously. Due to the nature of these models, we cannot directly infer the predictive power of the topographic against the climatic features that implies a limitation for the trained-model to be directly applicable in another region.

4.3. Quantification of Surging Probabilities

To our knowledge, we produce the first map aiming at quantifying the surge probability of glaciers. The map together with the associated probabilities add new information to the Randolph Glacier Inventory surging classes. Beyond the previous binary distinction between surge-type or non surge-type glaciers, our approach quantifies these classes along a continuous scale with robust statistical methods. We propose that the four qualitative classes in Svalbard can be combined into two statistically informed classes: glaciers that have a probability to surge equal or larger than 50% can be classified as surge-type, and glaciers that present a probability lower than 50% can be classified as non-surge-type.

Our results suggest that some glaciers are misclassified in the Randolph Glacier Inventory. The glaciers listed in Table 1 have a probability higher than 50% to be surge-type in our model, while in the Randolph Glacier Inventory they are currently labeled as Not observed, Possible or Probable surge. Recent field observations have shown that all these glaciers have been seen surging, confirming the high probabilities computed in our model.

In the present study, we are averaging the probability of every points along the flowline to calculate a glacier-wide probability to be surge-type. As seen in Figure 6, some glaciers have a high probability to be surge-type on their low altitude range while other parts of the glacier have a very low probability to surge, for example, in Austfonna ice cap. In that case, to average the probability along the centerline might lead to a mis-classification of the glacier due to the averaging procedure. Further studies should be conducted on these glaciers to understand how the local

Table 1
Comparison of Several Glaciers Where Surge has Been Observed, Their Corresponding Label in the Randolph Glacier Inventory (RGI) Classification, and the Probability Estimates of Our XGBoost Model

RGIId	Name	RGI 6.0 (classes)	Probability XGBoost	Reference
RGI60–07.00276	Arnesenbreen	Possible	67%	Leclercq et al. (2021)
RGI60–07.00296	Strongbreen	Probable	72%	Leclercq et al. (2021)
RGI60–07.00440	Svalisbreen	Not Observed	64%	Leclercq et al. (2021)
RGI60–07.00241	Penckbreen	Possible	65%	Leclercq et al. (2021)
RGI60–07.00501	Aavatsmarkbreen	Possible	70%	Luckman et al. (2015)
RGI60–07.00296	Morsnevbreen	Probable	72%	Benn et al. (2019)
RGI60–07.00027	Austfonna Basin 3	Probable	71%	Schellenberger et al. (2017)

predictions are made for each point and then unravel if the evolving probability along the centerline corresponds to for example, partial surge-type glaciers and triggering zones where the surge may develop. Here, we consider that the points that have a high probability for surging correspond to zone where an instability can be triggered due to the geometrical and climatic settings. Going beyond this conclusion would require more investigations on the model prediction.

Furthermore, to average the probability along the centerline is a very basic way on representing the overall glacier potential for surging. More sophisticated methods should be investigated to represent in the best way the potential for a glacier to be surge-type for example, meta-learning techniques could be considered but would require a prior extensive data analysis.

5. Conclusions and Perspectives

We present a framework based on machine learning models as well as a newly combined database to perform probabilistic glacier hazard mapping. The framework involves discretizing features along glacier centerlines. The most important features that explain glacier surge, that is, the width, the thickness, the runoff, the surface and bed slopes and the CMB are aligned with theories of glacier surge. Our framework allows a quantitative assessment of the surge potential of glaciers in Svalbard, that complements the previously established classification in the Randolph Glacier Inventory. Several new glaciers have been identified as surging glaciers with our model and confirmed by independent observations, which strengthens the robustness of our approach. The framework includes the comparison between different machine learning models and presents an extensive evaluation of the best model stability.

To complement theories of glacier surge, new features might be added to our framework, that is, the thickness of the underlying till, the internal reflection horizons imaging the transition between cold and temperate ice, the basal temperature and geothermal gradient, and the lithology of the underlying bed. Monitoring efforts are encouraged to be pursued toward this goal (Figure 2). The present study represents a snapshot in time but future studies may include multi-temporal data of certain features to enable inclusion of a time component. Finally, future work should focus on the development of an accurate method to compute a glacier-wide probability from the centerline probabilities.

Our method to compute probabilistic glacier hazard mapping based on machine learning methods and a discretized database could also be applied to other regions of the world and/or adapted to other field (e.g., landslides and earthquakes dynamics).

Appendix A: Proportion Between the Training and Testing Data Sets

The more data is used to train the model, the better the model will become. We performed an analysis to choose the best split in the database between the points that will be used as training data and testing data. We are looking for the split that will provide the best performance of the model without overfitting. As seen in Figure A1, a split at 40% for the training data set gives a relatively high AUC value (0.77). However, a considerable proportion of ground-truth data are then dropped to train the model. A split at 70% for the training data set gives a relatively

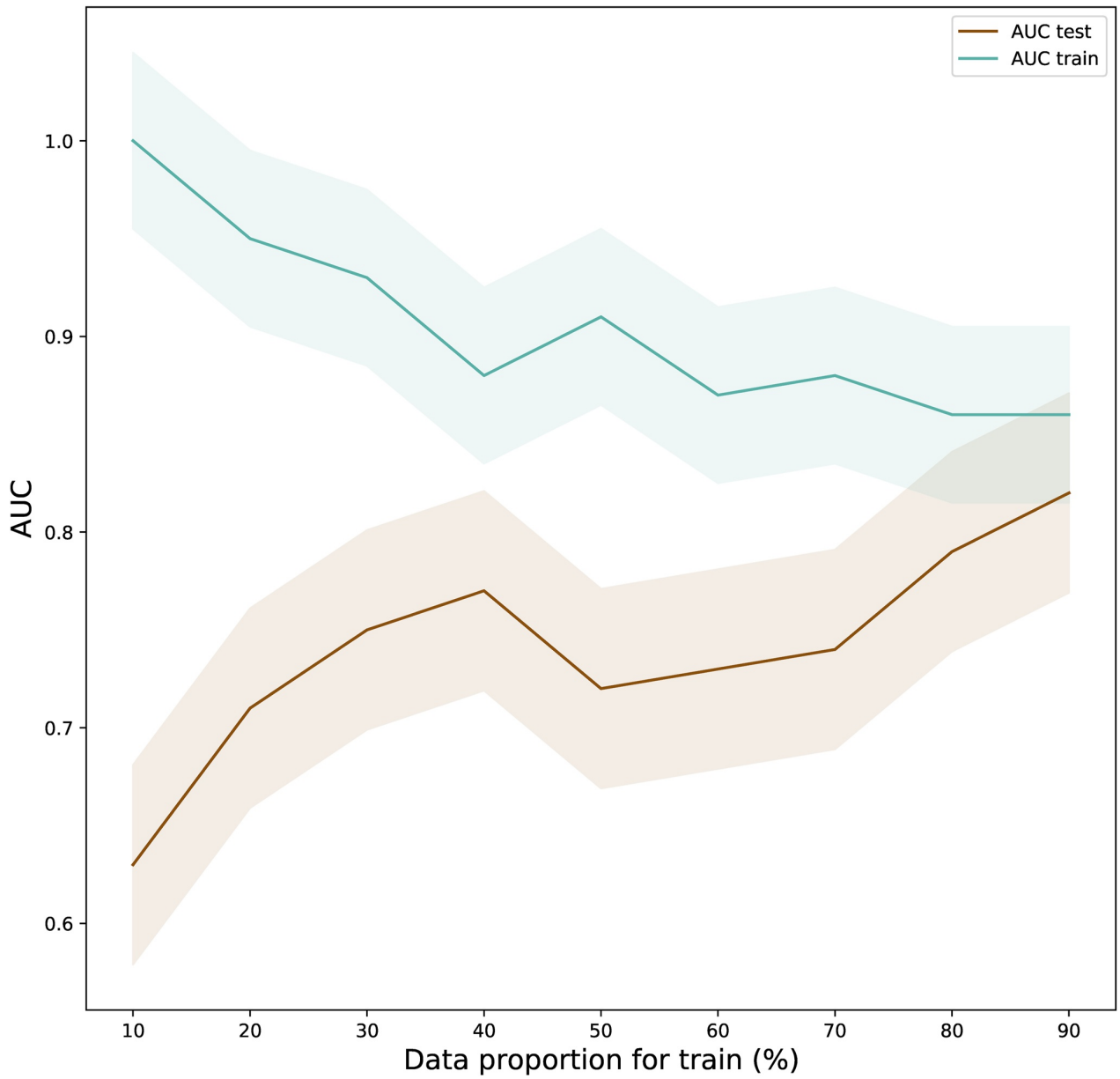

Figure A1. Evaluation of the proportion of the database to use to train the model. We trained ten models using different proportion between the training and the testing set ranging from 10% to 90%. For each models, we calculate the AUC for the training data set (blue curve) and the testing data set (brown curve).

high AUC (0.74) and use more data to train the model. If a bigger proportion of the database is used for training, the model is more sensitive to overfitting. We observe in that case that the testing AUC values might be higher that the training AUC values. For this study, we are then using a 70%–30% split for the training/testing data sets which represents a good compromise to reach good model performance and avoid overfitting.

Appendix B: Evaluation of the Model Stability

B1. Bootstrap Simulations

We performed fifty bootstrap simulations to study the consistency of the model performance among the fifty simulations. The model is trained by picking randomly the points that will be used for training. We set the

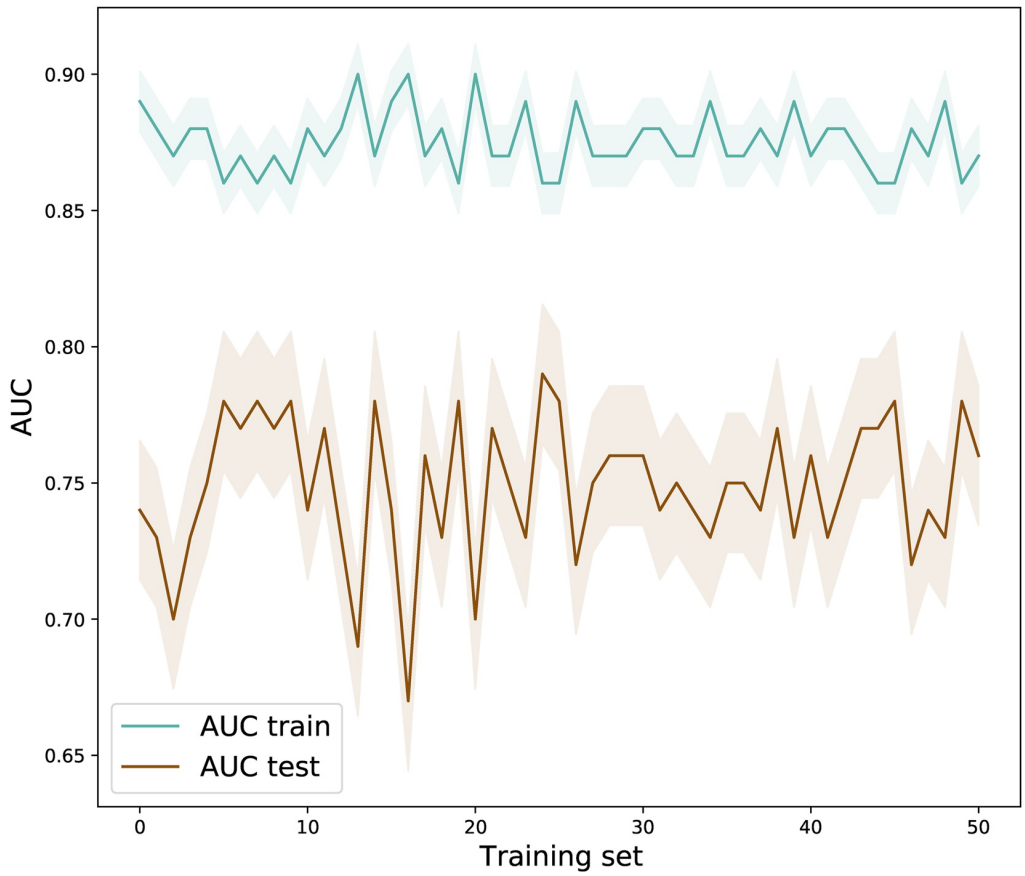

Figure B1. Evaluation of the impact of selecting fifty different training data sets on the model performance. We run the model fifty times with fifty randomly picked training data sets and computed the trained (blue) and tested (brown curve) AUCs for each of these models.

proportion for the training set at 70% of the database. To ensure that the model performance is not dependent of the training data sets that have been picked, we are training fifty different models on fifty different, randomly picked training data set and calculate the AUC for both the training data set and the testing data set. As display on Figure B1, the model remains stable with a very consistent AUC in between all the training sets.

B2. K-Fold Cross Validation

Cross-validation is a common practice in machine learning to evaluate the model performance and its performance stability. We performed a ten K-Fold cross validation for XGBoost model and calculated the corresponding AUC. In Figure B2, we observe that the model performance is relatively stable. XGBoost is robust and the performances are not affected by the quality of the training data set.

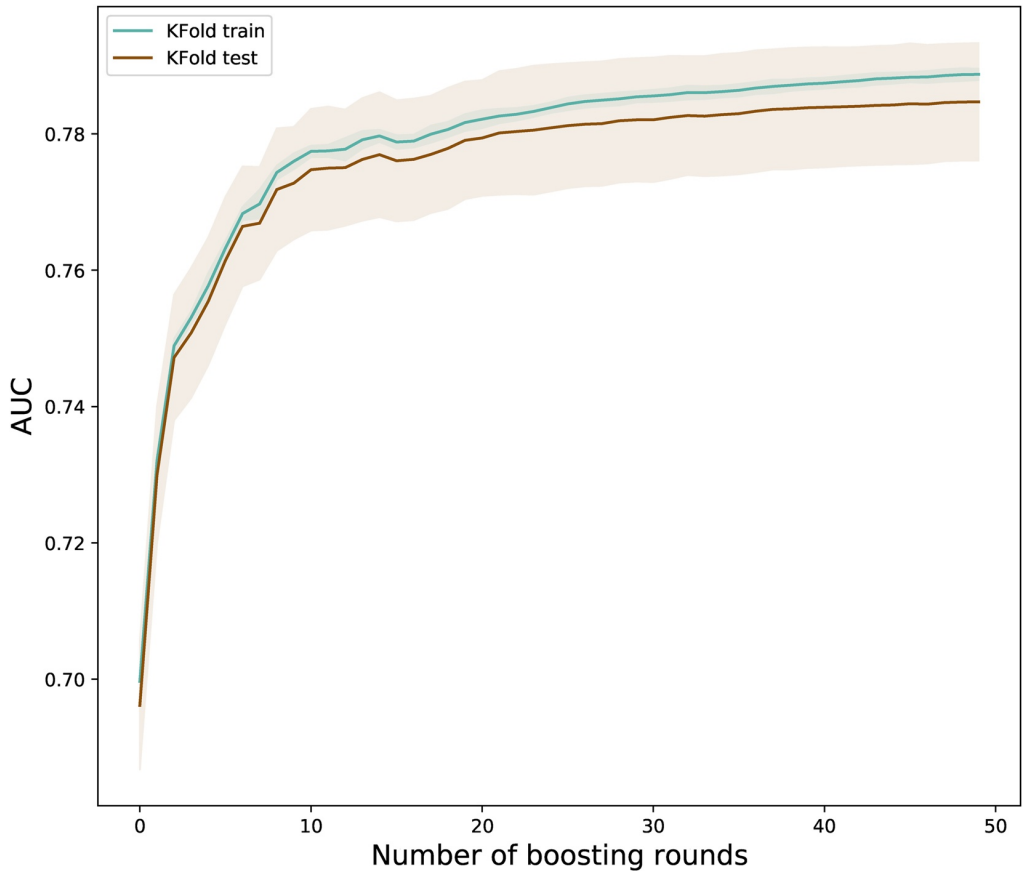

Figure B2. Evaluation of the model performances using a K-Fold cross-validation. We train the model using different 10 folds and calculated the corresponding AUC. The model uses 50 boosting rounds.

Appendix C: Exhaustive Grid search for Hyper Parameters Tuning

Hyperparameters define the structure of a model. For example, the hyperparameters of a random forest model would describe how many trees to grow, the depth of those trees, and the algorithm to use to grow the trees. Hyperparameters are separate from the data used to train the model and their values cannot be estimated from the data while they need to be set before the learning process begins. To optimize the hyperparameters we used the exhaustive grid search method. It considers several possibilities for each hyperparameters and try every combination possible before choosing the combination that returns a lower error score. This method should be guided

Table C1
Results of the Exhaustive Grid Search for Hyperparameter Tuning and the Corresponding Area Under the Curve (AUC)

Method	Hyperparameter	Best value	AUC
Logistic regression	C	1×10^{-5}	0.70
	Penalty	L2	
Random forest	Number of trees	1000	0.71
	Maximum depth	2	
XGBoost	Maximum depth	2	0.75
	Minimum child weight	1	

by cross-validation on the training set. The exhaustive grid search is run using the scikit-learn library of Python (Pedregosa et al., 2011). Table C1 displays the three different models evaluated in our study and the hyperparameters that have been selected by the exhaustive grid search. The best values for these hyperparameter are shown in the last column.

Appendix D: Detailed Description of Feature Importances

To better understand how the surge probabilities are calculated and can be correlated to surging mechanisms, the relative contribution of each feature can be analyzed by calculating the feature importance. Each one of the three machine learning models we used calculate differently the feature importances. We detail mostly how feature importance is implemented in XGBoost since this model performs the best for the assessment of surging potential for Svalbard glaciers. In XGBoost, after the trees are built, the model reports directly the feature importance instead of the coefficient values commonly reported in logistic regression. Each time a feature is used in a tree, the tree will split optimally to a certain location to increase the accuracy, so-called the gain. For each specific feature, the feature importance corresponds to the average gain across all decision making. Different implementation are proposed to estimate the contribution of each feature in the model decision. We focused on the gain and weight. The gain is the improvement in accuracy brought by a feature to the branches. A higher value implies that the feature is more important for generating a prediction. The weight corresponds to the number of times a feature is used to split the data across the tree. To assess how many features are needed to maximize the AUC, we performed a recursive feature elimination. Initially, the model is trained and tested with the features that had the highest feature importance score. Then, at every iteration, the model is trained and tested adding one more feature and this process is repeated until the maximum number of features is reached. The AUC is saved at every iteration and the recursive feature elimination is performed using the scores computed with the weight and the gain method.

Appendix E: Centerline Probability

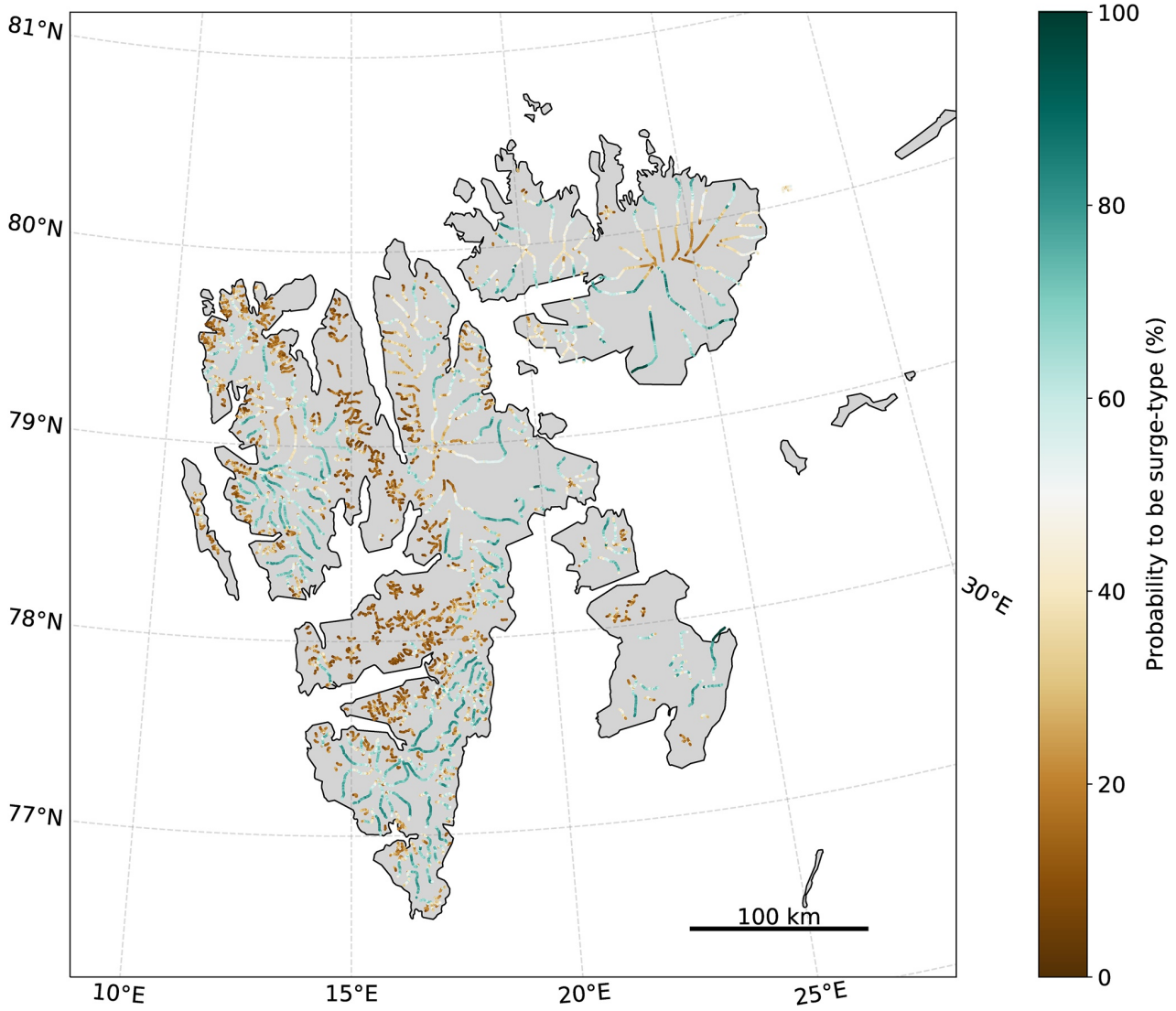

Figure E1. Probability map for each point of glacier centerlines to be classified as surge-type in the XGBoost model.

Data Availability Statement

The data and code are available in the repository https://doi.org/10.5281/zenodo.5657088 (Bouchayer, 2021).

Conflict of Interest

The authors declare no conflicts of interest relevant to this study.

Acknowledgments
This project has received support from the Norwegian Agency for International Cooperation and Quality Enhancement in Higher Education (DIKU), which supports the Center for Computing in Science Education, from the Research Council of Norway through the project MAMMAMIA (Grant No. 301837) and from the Faculty of Mathematics and Natural Sciences at the University of Oslo through the strategic research initiative EarthFlows. We thank Dr. PiM Lefeuvre and Dr. Simon Filhol for constructive insights. The authors declare no conflict of interest. The authors thank reviewer Martin Truffer, one anonymous reviewer, the Associate Editor and the Editor, Olga Sergienko, for thorough reviews that improved the manuscript.

References

Barrand, N. E., & Murray, T. (2006). Multivariate controls on the incidence of glacier surging in the karakoram himalaya. *Arctic Antarctic and Alpine Research*, *38*(4), 489–498. https://doi.org/10.1657/1523-0430(2006)38[489:mcotio]2.0.co;2

Bazai, N. A., Cui, P., Carling, P. A., Wang, H., Hassan, J., Liu, D., et al. (2021). Increasing glacial lake outburst flood hazard in response to surge glaciers in the karakoram. *Earth-Science Reviews*, *212*, 103432. https://doi.org/10.1016/j.earscirev.2020.103432

Benn, D., & Evans, D. J. (2014). *Glaciers and glaciation*. Routledge.

Benn, D., Fowler, A. C., Hewitt, I., & Sevestre, H. (2019). A general theory of glacier surges. *Journal of Glaciology*, *65*(253), 701–716. https://doi.org/10.1017/jog.2019.62

Bhambri, R., Hewitt, K., Kawishwar, P., & Pratap, B. (2017). Surge-type and surge-modified glaciers in the karakoram. *Scientific Reports*, *7*(1), 1–14. https://doi.org/10.1038/s41598-017-15473-8

Björnsson, H., Pálsson, F., Sigurđsson, O., & Flowers, G. E. (2003). Surges of glaciers in Iceland. *Annals of Glaciology*, *36*, 82–90. https://doi.org/10.3189/172756403781816365

Bouchayer, C. (2021). Colinebouch/glacier_ML: Glacier surging potential repo. *Zenodo*. https://doi.org/10.5281/zenodo.5657088

Breiman, L. (1999). Prediction games and arcing algorithms. *Neural Computation*, *11*(7), 1493–1517. https://doi.org/10.1162/089976699300016106

Chen, & Guestrin, C. (2016). Xgboost: A scalable tree boosting system. In *Proceedings of the 22nd acm sigkdd international conference on knowledge discovery and data mining* (pp. 785–794).

Chen, & Jeong, J. C. (2007). Enhanced recursive feature elimination. In *Sixth international conference on machine learning and applications* (pp. 429–435).

Chen, T., He, T., Benesty, M., Khotilovich, V., Tang, Y., & Cho, H. E. A. (2015). Xgboost: Extreme gradient boosting. *R package*, *1*(4). version 0.4-2

Clarke, G. K. (1991). Length, width and slope influences on glacier surging. *Journal of Glaciology*, *37*(126), 236–246. https://doi.org/10.3189/s0022143000007255

Clarke, G. K., Schmok, J. P., Ommanney, C. S. L., & Collins, S. G. (1986). Characteristics of surge-type glaciers. *Journal of Geophysical Research*, *91*(B7), 7165–7180. https://doi.org/10.1029/JB091iB07p07165

Cuffey, K. M., & Paterson, W. S. B. (2010). *The physics of glaciers*. Academic Press. https://doi.org/10.1016/c2009-0-14802-x

Dieterich, J. H. (1992). Earthquake nucleation on faults with rate-and state-dependent strength. *Tectonophysics*, *211*(1), 115–134. https://doi.org/10.1016/0040-1951(92)90055-B

Fatichi, S., Vivoni, E. R., Ogden, F. L., Ivanov, V. Y., Mirus, B., Gochis, D., et al. (2016). An overview of current applications, challenges, and future trends in distributed process-based models in hydrology. *Journal of Hydrology*, *537*, 45–60. https://doi.org/10.1016/j.jhydrol.2016.03.026

Fowler, A. (1989). A mathematical analysis of glacier surges. *SIAM Journal on Applied Mathematics*, *49*(1), 246–263. https://doi.org/10.1137/0149015

Friedman, J. H. (2001). Greedy function approximation: A gradient boosting machine. *Annals of Statistics*, 1189–1232.

Friedman, J. H. (2002). Stochastic gradient boosting. *Computational Statistics & Data Analysis*, *38*(4), 367–378. https://doi.org/10.1016/s0167-9473(01)00065-2

Fürst, J. J., Navarro, F., Gillet-Chaulet, F., Huss, M., Moholdt, G., Fettweis, X., et al. (2018). The ice-free topography of svalbard. *Geophysical Research Letters*, *45*(21), 11–760. https://doi.org/10.1029/2018gl079734

Ganganwar, V. (2012). An overview of classification algorithms for imbalanced datasets. *International Journal of Emerging Technology and Advanced Engineering*, *2*(4), 42–47.

Halevy, A., Norvig, P., & Pereira, F. (2009). The unreasonable effectiveness of data. *IEEE Intelligent Systems*, *24*(2), 8–12. https://doi.org/10.1109/mis.2009.36

Hamilton, G. S., & Dowdeswell, J. A. (1996). Controls on glacier surging in svalbard. *Journal of Glaciology*, *42*(140), 157–168. https://doi.org/10.3189/s0022143000030616

Hanley, J. A., & McNeil, B. J. (1982). The meaning and use of the area under a receiver operating characteristic (roc) curve. *Radiology*, *143*(1), 29–36. https://doi.org/10.1148/radiology.143.1.7063747

Hastie, T., Tibshirani, R., & Friedman, J. (2009). *The elements of statistical learning: Data mining, inference, and prediction*. Springer Science & Business Media.

Hock, R., Bliss, A., Marzeion, B., Giesen, R. H., Hirabayashi, Y., Huss, M., et al. (2019). Glaciermip–a model intercomparison of global-scale glacier mass-balance models and projections. *Journal of Glaciology*, *65*(251), 453–467. https://doi.org/10.1017/jog.2019.22

Hosmer, D. W., Jr., Lemeshow, S., & Sturdivant, R. X. (2013). *Applied Logistic Regression* (Vol. 398). John Wiley & Sons.

Jiskoot, H., Boyle, P., & Murray, T. (1998). The incidence of glacier surging in svalbard: Evidence from multivariate statistics. *Computers & Geosciences*, *24*(4), 387–399. https://doi.org/10.1016/s0098-3004(98)00033-8

Jiskoot, H., Murray, T., & Boyle, P. (2000). Controls on the distribution of surge-type glaciers in svalbard. *Journal of Glaciology*, *46*(154), 412–422. https://doi.org/10.3189/172756500781833115

Jiskoot, H., Murray, T., & Luckman, A. (2003). Surge potential and drainage-basin characteristics in east Greenland. *Annals of Glaciology*, *36*, 142–148. https://doi.org/10.3189/172756403781816220

Kamb, B. (1987). Glacier surge mechanism based on linked cavity configuration of the basal water conduit system. *Journal of Geophysical Research*, *92*(B9), 9083–9100. https://doi.org/10.1029/jb092ib09p09083

Kienholz, C., Rich, J., Arendt, A., & Hock, R. (2014). A new method for deriving glacier centerlines applied to glaciers in Alaska and northwest Canada. *The Cryosphere*, *8*(2), 503–519. https://doi.org/10.5194/tc-8-503-2014

Leclercq, P. W., Kääb, A., & Altena, B. (2021). Brief communication: Detection of glacier surge activity using cloud computing of sentinel-1 radar data. *The Cryosphere*, *15*(10), 4901–4907. https://doi.org/10.5194/tc-15-4901-2021

Luckman, A., Benn, D. I., Cottier, F., Bevan, S., Nilsen, F., & Inall, M. (2015). Calving rates at tidewater glaciers vary strongly with ocean temperature. *Nature Communications*, *6*(1), 1–7. https://doi.org/10.1038/ncomms9566

Lundberg, S. M., & Lee, S.-I. (2017). A unified approach to interpreting model predictions. In I. Guyon, U. Von Luxburg, S. Bengio, H. Wallach, R. Fergus, S. Vishwanathan & R. Garnett. (Eds.). *Advances in neural information processing systems* (Vol. 30). Curran Associates, Inc. Retrieved from https://urldefense.com/v3/__https://proceedings.neurips.cc/paper/2017/file/8a20a8621978632d76c43dfd28b67767-Paper.pdf__;!!N11eV2iwtfs!oRJsIOuE_6L1YRA_NoSYpMObcUTMcdfBQje1BwWFkyejc0nSpZ3R-Tk3DuUIt7GYsZCdVEBHYXin13YEq-saTh8V6zaF1$

Maussion, F., Butenko, A., Champollion, N., Dusch, M., Eis, J., Fourteau, K., et al. (2019). The open global glacier model (oggm) v1. 1. *Geoscientific Model Development*, *12*(3), 909–931. https://doi.org/10.5194/gmd-12-909-2019

McBeck, J. A., Aiken, J. M., Mathiesen, J., Ben-Zion, Y., & Renard, F. (2020). Deformation precursors to catastrophic failure in rocks. *Geophysical Research Letters*, *47*(24), e2020GL090255. https://doi.org/10.1029/2020gl090255

Meier, M. F., & Post, A. (1969). What are glacier surges? *Canadian Journal of Earth Sciences*, *6*(4), 807–817. https://doi.org/10.1139/e69-081

Minchew, B. M., & Meyer, C. R. (2020). Dilation of subglacial sediment governs incipient surge motion in glaciers with deformable beds. *Proceedings of the Royal Society A*, *476*(2238), 20200033. https://doi.org/10.1098/rspa.2020.0033

Nelder, J. A., & Wedderburn, R. W. (1972). Generalized linear models. *Journal of the Royal Statistical Society: Series A*, *135*(3), 370–384. https://doi.org/10.1007/978-1-4612-4380-9_39

Pedregosa, F., Varoquaux, G., Gramfort, A., Michel, V., Thirion, B., Grisel, O., et al. (2011). Scikit-learn: Machine learning in Python. *Journal of Machine Learning Research*, *12*, 2825–2830.

Pelt, W. V., Pohjola, V., Pettersson, R., Marchenko, S., Kohler, J., Luks, B., et al. (2019). A long-term dataset of climatic mass balance, snow conditions, and runoff in svalbard (1957–2018). *The Cryosphere*, *13*(9), 2259–2280. https://doi.org/10.5194/tc-13-2259-2019

Pfeffer, W. T., Arendt, A. A., Bliss, A., Bolch, T., Cogley, J. G., Gardner, A. S., et al. (2014). The randolph glacier inventory: A globally complete inventory of glaciers. *Journal of Glaciology*, *60*(221), 537–552. https://doi.org/10.3189/2014jog13j176

RGI, C. (2017). Randolph glacier inventory (rgi) - a dataset of global glacier outlines. Version 6.0. Retrieved from http://www.glims.org/RGI/randolph60.html

Ritz, C., Edwards, T. L., Durand, G., Payne, A. J., Peyaud, V., & Hindmarsh, R. C. (2015). Potential sea-level rise from Antarctic ice-sheet instability constrained by observations. *Nature*, *528*(7580), 115–118. https://doi.org/10.1038/nature16147

Schellenberger, T., Dunse, T., Kääb, A., Schuler, T. V., Hagen, J. O., & Reijmer, C. H. (2017). Multi-year surface velocities and sea-level rise contribution of the basin-3 and basin-2 surges, austfonna, svalbard. *The Cryosphere Discussions*, 1–27.

Sevestre, H., & Benn, D. I. (2015). Climatic and geometric controls on the global distribution of surge-type glaciers: Implications for a unifying model of surging. *Journal of Glaciology*, *61*(228), 646–662. https://doi.org/10.3189/2015jog14j136

Thøgersen, K., Gilbert, A., Bouchayer, C., & Schuler, T. V. (2021). Glacier surges controlled by the close interplay between subglacial friction and drainage. *Journal of Geophysical Research* (in review). https://doi.org/10.31223/x5jg87

Thøgersen, K., Gilbert, A., Schuler, T. V., & Malthe-Sørenssen, A. (2019). Rate-and-state friction explains glacier surge propagation. *Nature Communications*, *10*(1), 1–8. https://doi.org/10.1038/s41467-019-10506-4

Truffer, M., Kääb, A., Harrison, W. D., Osipova, G. B., Nosenko, G. A., Espizua, L., et al. (2021). Glacier surges. In *Snow and ice-related hazards, risks, and disasters* (pp. 417–466). Elsevier.

Zoet, L., Ikari, M., Alley, R. B., Marone, C., Anandakrishnan, S., Carpenter, B., & Scuderi, M. M. (2020). Application of constitutive friction laws to glacier seismicity. *Geophysical Research Letters*, *47*(21), e2020GL088964. https://doi.org/10.1029/2020gl088964

7.2 Article II: Acceleration of an Arctic glacier triggered by climate warming and hydro-mechanical couplings (in preparation)

In this manuscript, our collaborative effort with U. Nanni culminates in a jointly shared first co-authorship. From the fieldwork campaigns, the conceptualisation of the study to the data post-processing, figure design, and drafting, we have closely worked together, often sharing the same computer desk. A. Köhler initiated the seismic recordings on Kongsvegen glacier in 2018 and developed the original codes for analyzing icequake characteristics via the STA/LTA method. E. Mannerfelt provided yearly DEM of the study area. All authors including F., Renard, and T.V. Schuler actively contributed ideas and offered valuable insights throughout the entirety of the study. The version I present within this thesis is nearly ready for submission to *Geophysical Research Letters*. We have now included the seismic data of 2023 and we are waiting for the associated velocity before publication.

FIGURE 7.2: The stunning landscape of Svalbard emerging from the clouds.

7.3 Article III: Multi-scale variations of subglacial hydro-mechanical conditions at Kongsvegen glacier, Svalbard (in review, 2023)

This paper has been submitted in *The Cryosphere* in April 2023 and we received both reviews on the 9th of August 2023. I actively participated in multiple field campaigns, contributing to instrument deployment, data collection, and post-processing of ploughmeter and seismic data. I combined the dataset and developed the codes and figures for the study. I took the lead in writing the original manuscript and worked closely with U. Nanni and T.V. Schuler to finalize the manuscript. U. Nanni provided valuable insights, guidance, and expertise throughout the study, particularly in seismic data analysis and post-processing. P.M. Lefeuvre and J. Kohler contributed velocity data and offered valuable ideas and insights during the initial phase of the study. J. Hulth built the ploughmeter. L. Schmidt contributed with simulated surface runoff. T.V. Schuler initiated the field project, participated in all field campaigns, and played a pivotal role in designing and planning the project. I am presently working in addressing the peer reviews. The version presented here is close to be re-submitted as almost all the comments from the reviewers have now been addressed. We plan on submitting the answers to reviews before the defense accompanied by a version very close to the present one.

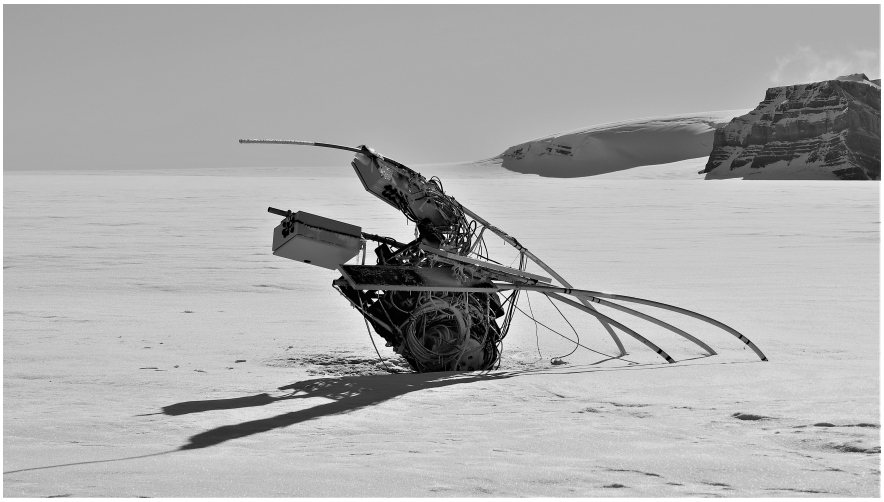

FIGURE 7.3: The condition of the surface instrumentation in 2022 prior to maintenance.

Appendix A

Contributions to other articles

A.1 Numerical modeling of the dynamics of the Mer de Glace glacier, French Alps: comparison with past observations and forecasting of near-future evolution (published, 2020)

My initial steps into the field of glaciology took place in Grenoble, France, which serves as a prominent hub for glaciological research. During my time at engineering school, we were required to undertake a three-month internship as part of our bachelor program. Intrigued by the captivating nature of ice and snow, I embarked on a search for opportunities related to the study of these elements. It was during this exploration that I discovered that *glaciologist* was a thing.

After exchanging emails and attending interviews, I started an internship supervised by Prof. Christian Vincent and Dr. Vincent Peyaud. Although I initially envisioned spending my days exploring glaciers and mountains, I found myself delving into programming and modeling using Elmer/Ice—a delightful surprise that I thoroughly enjoyed. Fortunately, I also had the chance to visit several glaciers in the Alps during this period. Upon completing the three-month internship, I chose to return voluntarily to the Institute of Geosciences and Environment (IGE) in Grenoble to continue the work I had initiated during my bachelor internship.

Engaging in further modeling, iterations, and reviews, which extended into my PhD fellowship, these efforts culminated in the publication of our paper in 2020. This transformative internship experience paved the way for my future in glaciology, prompting me to pursue a double-diploma program that led me to a research-focused master degree in Grenoble, where I deepened my understanding of climate and glaciers.

The Cryosphere, 14, 3979–3994, 2020
https://doi.org/10.5194/tc-14-3979-2020

The Cryosphere Open Access EGU

Numerical modeling of the dynamics of the Mer de Glace glacier, French Alps: comparison with past observations and forecasting of near-future evolution

Vincent Peyaud[1], **Coline Bouchayer**[1,2], **Olivier Gagliardini**[1], **Christian Vincent**[1], **Fabien Gillet-Chaulet**[1], **Delphine Six**[1], **and Olivier Laarman**[1]

[1]Univ. Grenoble Alpes, CNRS, IRD, Grenoble INP, IGE, 38000 Grenoble, France
[2]The Njord Center, Department of Geosciences, University of Oslo, 0316 Oslo, Norway

Correspondence: Vincent Peyaud (vincent.peyaud@univ-grenoble-alpes.fr)

Received: 18 March 2020 – Discussion started: 28 April 2020
Revised: 20 August 2020 – Accepted: 6 September 2020 – Published: 13 November 2020

Abstract. Alpine glaciers are shrinking and rapidly loosing mass in a warming climate. Glacier modeling is required to assess the future consequences of these retreats on water resources, the hydropower industry and risk management. However, the performance of such ice flow modeling is generally difficult to evaluate because of the lack of long-term glaciological observations. Here, we assess the performance of the Elmer/Ice full Stokes ice flow model using the long dataset of mass balance, thickness change, ice flow velocity and snout fluctuation measurements obtained between 1979 and 2015 on the Mer de Glace glacier, France. Ice flow modeling results are compared in detail to comprehensive glaciological observations over 4 decades including both a period of glacier expansion preceding a long period of decay. To our knowledge, a comparison to data at this detail is unprecedented. We found that the model accurately reconstructs the velocity, elevation and length variations of this glacier despite some discrepancies that remain unexplained. The calibrated and validated model was then applied to simulate the future evolution of Mer de Glace from 2015 to 2050 using 26 different climate scenarios. Depending on the climate scenarios, the largest glacier in France, with a length of 20 km, could retreat by 2 to 6 km over the next 3 decades.

1 Introduction

Mountain glacier mass balances show a strong sensitivity to climate change and can thus be used to assess the impact of climate change in remote areas (Oerlemans, 2001; Zemp et al., 2019). During the 20th century, all alpine glaciers showed a strong recession (Zemp et al., 2015). This observed trend is expected to continue in the future under a warming climate (IPCC, 2019) with important impacts on watershed hydrology (Huss and Hock, 2018; Brunner et al., 2019), tourism and hydropower resources (e.g., Welling et al., 2015; Stewart et al., 2016), accompanied by the emergence of new risks (e.g., Kääb et al., 2018) and sea-level rise (Hock et al., 2019; Marzeion et al., 2020). Properly assessing these future impacts requires the development of modeling tools capable of describing the processes driving these glacier changes.

Numerical ice flow models with different degrees of complexity have been developed to forecast glacier evolutions. The first studies of individual glaciers (e.g., Huybrechts et al., 1989; Letréguilly and Reynaud, 1989; Stroeven et al., 1989; Greuell, 1992) were constrained to flow line models related to the local driving stress, while studies on a regional scale (since Haeberli and Hölzle, 1995) focused on empirical approaches in which ice dynamics is not explicitly taken into account and glacier evolution is based on parameterizations calibrated with either equilibrium-line altitude (ELA) models (e.g., Zemp et al., 2006), extrapolations of observed geometry changes (e.g., Huss et al., 2008; Huss, 2012; Huss and Hock, 2018), or volume and length–area scalings (e.g., Marzeion et al., 2012; Radić et al., 2014). Process-based

models were also developed to integrate simple dynamics (e.g., Le Meur and Vincent, 2003; Clarke et al., 2015; Zekollari et al., 2019; Maussion et al., 2019). These studies suggest a glacier volume loss from 65 % to 94 % in Central Europe by the end of the century depending on the climate scenario (IPCC, 2019; Marzeion et al., 2020). However, the Fourth Intergovernmental Panel on Climate Change (IPCC) Assessment Report (Solomon et al., 2007) and other studies (e.g., Vincent et al., 2014) emphasize the need for a new generation of glacier models that accurately describe the ice flow dynamics to correctly forecast individual glacier evolution. Today, such three-dimensional physical models are widely available. Indeed, with the improvement of computational resource performance, running a model describing the Stokes ice flow solution for the complex three-dimensional geometry of a whole glacier has become much more affordable (e.g., Réveillet et al., 2015; Jouvet and Huss, 2019; Gilbert et al., 2020). Among such models, Elmer/Ice (Gagliardini et al., 2013) has already been used for a number of glacier applications (e.g., Gagliardini et al., 2011; Réveillet et al., 2015; Gilbert et al., 2020) and will be used for this study.

However, very few glacier datasets are available to make a detailed comparison between observed and modeled fluctuations at the multi-decadal scale. Mer de Glace offers a rare opportunity to compare state-of-the-art model results with a large dataset containing observed thickness changes, ice flow velocities and snout fluctuations over a nearly continuous 40-year period thanks to the GLACIOCLIM observatory monitoring program (Vincent, 2002; Vincent et al., 2014; Berthier et al., 2004, 2005, 2014; Berthier and Vincent, 2012). In addition, running simulations on this glacier provides the opportunity to fulfill the need of capturing with a full Stokes ice flow model the local complex ice dynamics of a glacier that presented a large advance before the 1980s, followed by a rapid retreat over 3 decades.

In this paper, the performance of the Elmer/Ice ice flow model is first assessed in terms of its ability to reconstruct these past multi-decadal fluctuations in the tongue of Mer de Glace. A thorough comparison makes it possible to explore the sources of discrepancies between the reconstruction and the observations. In a second step, prognostic simulations are performed to simulate the evolution of the glacier until 2050 under different climate scenarios.

2 Study site and glaciological data

Mer de Glace (45°55′ N, 6°57′ E) and the Géant glacier form the largest glacier in the French Alps which covers an area of 32 km^2. It is located in the Mont Blanc massif (Fig. 1) and is monitored as part of the GLACIOCLIM observatory (https://glacioclim.osug.fr/, last access: 3 November 2020). The upper accumulation area, named Géant glacier, reaches 4300 m a.s.l. (above sea level). From this accumulation region, the ice flows at a speed of up to 500 m yr^{-1} (Millan et al., 2019) through a narrow, steep portion (an icefall between 2700 and 2400 m a.s.l.) before feeding Mer de Glace that covers the lower, 7 km long section above the terminus located at 1534 m a.s.l. in 2018. As shown in Fig. 1, Mer de Glace has a single tributary glacier which is named Leschaux glacier.

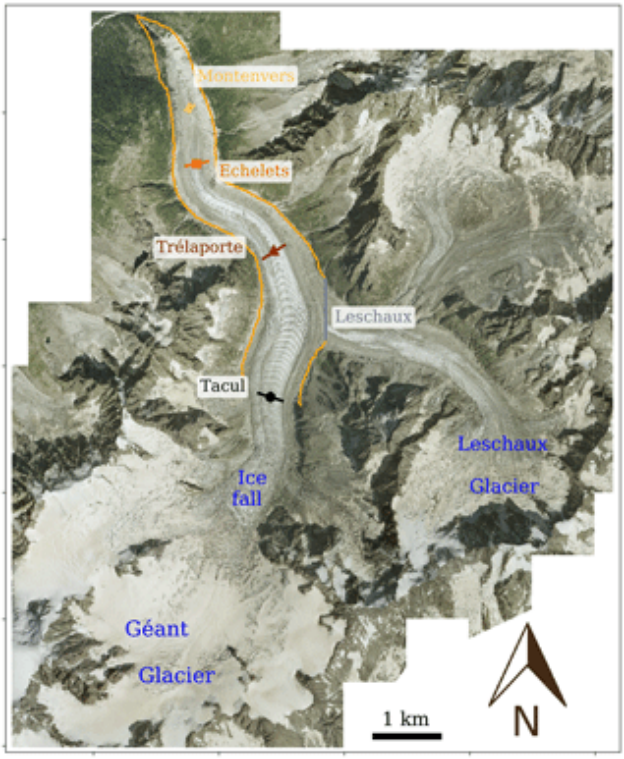

Figure 1. Map of Mer de Glace (orthophoto acquired in 2008 ©RGD74). The orange contour delimits the area modeled in this study. The location of the four cross sections (Tacul, Trélaporte, Echelets and Montenvers) and the Leschaux gate are indicated by the colored lines. The Tacul and Leschaux gates represent boundary gates where data are used to force the model, whereas the three other profiles represent internal gates where data are used to validate the model.

Several surface digital elevation models (DEMs) are available for different times in the past. The first map was produced in 1905 by Vallot (1905) using the classical topographic method. Another DEM was made by the Institut Géographique National (IGN) in 1979, and two were made by the Laboratory of Glaciology of Grenoble in 2003 and 2008 using aerial photographs (Vincent et al., 2014). A surface velocity field was derived from SPOT-5 (Système Probatoire d'Observation de la Terre) in 2003. Moreover, continuous field measurements have been performed at the lower part of the glacier (below 2300 m a.s.l.) from a network of stakes that have been monitored continuously since 1979 at four different elevations: the Tacul (2148 m a.s.l. in 2018), Trélaporte (1937 m a.s.l.), Echelets (1725 m a.s.l.) and Montenvers (1627 m a.s.l.) cross sections (see Fig. 1).

Surface elevation has been measured systematically each year since 1979 along these four cross sections. Surface mass balance and annual surface velocity observations are also available at these cross sections, although they are not continuous between 1979 and 1994 except for observations at the Tacul cross section, which are continuous over the whole period. The bedrock topography was determined below 2300 m a.s.l. using mechanical borehole drillings, seismic soundings (Süustrunk, 1951; Vallon, 1961, 1967; Gluck, 1967) and radar measurements (2018; not published).

Given the lack of bedrock topography measurements in the upper part of the glacier (above the ice fall of Géant glacier) and the absence of measurements of bedrock topography for Leschaux glacier, the model domain was restricted to the lower part of the glacier from the Tacul cross section down to the snout. Here, we assume that the contribution of the Géant and Leschaux glaciers to Mer de Glace can be represented as specified flux conditions on the boundary of the Mer de Glace model.

3 Methods

3.1 Ice flow model

Mer de Glace ice flow dynamics are modeled with the Elmer/Ice open-source finite-element model (Gagliardini et al., 2013). This model has been applied to simulate real and artificial mountain glaciers (e.g., Farinotti et al., 2017; Gilbert et al., 2020).

The three-dimensional velocity field $\boldsymbol{u} = (u, v, w)$ and p, the isotopic pressure, are solutions to the Stokes equations that express conservation of momentum and conservation of mass for an incompressible fluid. We use the viscous isotropic nonlinear Glen's law (Glen, 1955) to link the deviatoric-stress tensor to the strain-rate tensor. The Glen's exponent is $n = 3$, and, assuming temperate ice, the rheological parameter A has a constant value ($A = 158\,\mathrm{MPa}^{-3}\,\mathrm{yr}^{-1}$; Paterson, 1994). Indeed, the ice of the lower part of Mer de Glace glacier is most likely temperate (Lliboutry et al., 1962).

The upper surface of the glacier is a free surface of elevation z_s (m) that evolves with time according to the following kinematic equation:

$$\frac{\partial z_\mathrm{s}}{\partial t} + u_\mathrm{s}\frac{\partial z_\mathrm{s}}{\partial x} + v_\mathrm{s}\frac{\partial z_\mathrm{s}}{\partial y} - w_\mathrm{s} = b(z_\mathrm{s}, t)\,, \tag{1}$$

where the surface mass balance $b(z,t)$, in ice equivalent thickness ($\mathrm{m\,yr}^{-1}$), is a function of surface elevation and time, and $\boldsymbol{u}_\mathrm{s} = (u_\mathrm{s}, v_\mathrm{s}, w_\mathrm{s})$ denotes the surface velocity vector. As the finite element mesh cannot have a null thickness, a lower limit of 1 m above the bedrock elevation is applied to z_s in Eq. (1).

3.2 Boundary conditions

Three types of boundary conditions are applied at the base, on the upper surface and on the two upstream gates of Tacul and Leschaux.

On the lower surface, a basal sliding is applied, as described in Sect. 3.2.1. On the upper surface, the surface mass balance (SMB) required in the free surface equation (Eq. 1) is derived either from observations when available or based on a positive degree day (PDD) model forced by climate simulations for the future. The two methods are explained in detail in Sect. 3.2.2.

The model domain does not cover the whole glacial catchment (see Fig. 1). Measurements of the bed are very sparse upstream of the Tacul gate and nonexistent on the Leschaux glacier. Modeling the whole glacier with a simple interpolation or a reconstructed bedrock would introduce large uncertainties. The large dataset of observations of thickness and centerline velocity collected at the Tacul cross section allows a good constraint on the flux passing through the gate. Observations at Leschaux cross section are limited, but, as presented in Sect. 3.2.3, the ice flow is much lower and has therefore a lower influence on the glacier evolution. Thus, in this study, the evolution of Mer de Glace is driven by two flux boundary conditions applied at the Tacul and Leschaux gates that prescribe the ice flux from the upstream accumulation areas of the glacier. The flux coming from the upper part of the glacier through the Tacul gate boundary condition is imposed from observations (thickness and central horizontal velocity at the Tacul gate) from the past and the estimated flux in the future. A similar method based on a flux is applied at the junction with Leschaux glacier. The implementation of an ice flux at these two gates for hindcast and forecast simulations differs slightly and is described in detail in Sect. 3.2.3.

Our simulations cover the period 1979–2050. The hindcast simulation covers the period 1979–2015 for which surface mass balances, surface velocities and elevation changes are available yearly at the four cross sections of Tacul, Trélaporte, Echelets and Montenvers (Fig. 1). The dataset at the Tacul cross section is used to specify the flux on this artificial boundary of the glacier domain, while the three others are used to evaluate the model over the hindcast period. For the forecast simulations from 2015 until 2050, results from climate simulations are used to simulate the future flux evolution at the boundary of the glacier domain.

Sections 3.2.2 and 3.2.3 describe in detail the respective boundary conditions for the two steps (hindcast and forecast) defined at the surface (mass balance) and at the Tacul and Leschaux gates (ice flux from the accumulation areas), respectively.

3.2.1 Basal conditions

At the base, ice cannot penetrate into the bed so the velocity component normal to the bed is null. As Mer de Glace is a

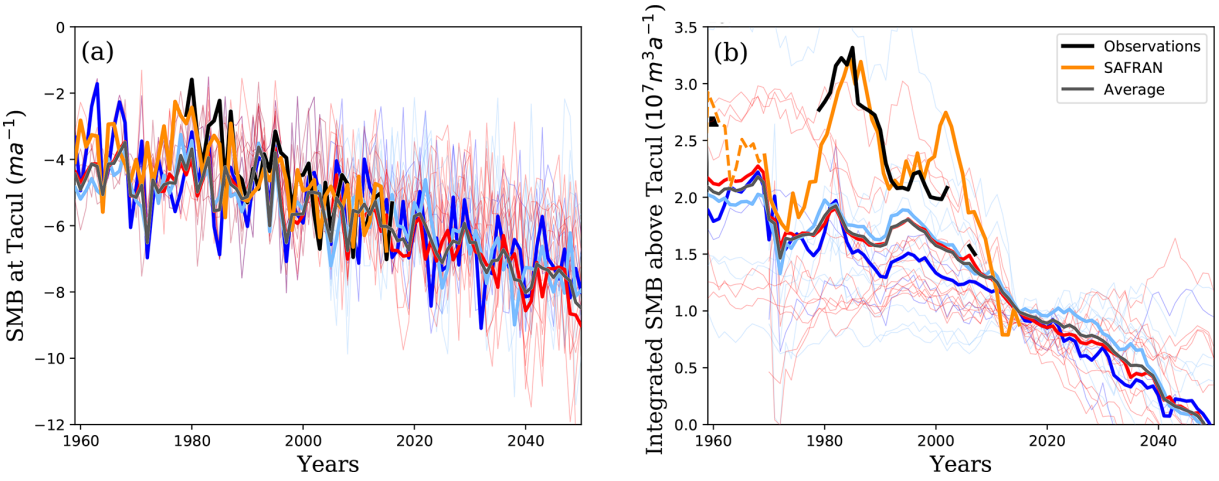

Figure 2. Evolution with time from 1960 to 2050 of **(a)** the surface mass balances (SMBs) at the Tacul gate and **(b)** the integrated surface mass balance above the Tacul gate. Observations are presented in black and values inferred from SAFRAN in orange. The others climate scenarios are plotted in dark blue (RCP 2.6), blue (RCP 4.5) and red (RCP 8.5); the average values for each scenario are highlighted by thick curves. Note that for the past period 1960–2015, the integrated surface mass balance above the Tacul gate in **(b)** does correspond to the flux at this gate and that "observations" are not from direct observations but are actually estimated from surface velocity and elevation following the method used in Berthier and Vincent (2012). All integrated surface mass balances for the forecast simulations are normalized to the 2015 observed mass balance.

temperate glacier, a certain amount of sliding on its bed is expected. A linear friction law relating the basal shear stress $\boldsymbol{\tau}_\mathrm{b}$ to the basal velocity $\boldsymbol{u}_\mathrm{b}$ is applied on the lower boundary:

$$\boldsymbol{\tau}_\mathrm{b} + \beta \boldsymbol{u}_\mathrm{b} = 0\,. \tag{2}$$

The time-independent basal friction parameter distribution $\beta(x, y)$ is inferred using an inverse method described in Gillet-Chaulet et al. (2012). This method relies on the computation of the adjoint of the Stokes system and the minimization of a cost function that measures the mismatch between modeled and observed velocities using the surface topography and surface velocities measured in August 2003 (Berthier et al., 2004). The value of the basal friction parameter is kept constant in both past and future simulations.

3.2.2 Surface mass balance

For the hindcast simulation, surface mass balance is derived from observations acquired during the historical period 1979–2015 (Fig. 2a; Six and Vincent, 2014). The surface mass balance at a given elevation is reconstructed according to an empirical relation with the one observed at the Tacul cross-section gate for the same year according to the following:

$$b(z_\mathrm{s}, t) = b_\mathrm{TAC}(t) + k_\mathrm{b}\,[z_\mathrm{s}(t) - z_{\mathrm{s\,TAC}}(t)]\,, \tag{3}$$

where $b_\mathrm{TAC}(t)$ is the annual surface mass balance measured (hindcast) or evaluated (forecast) at the Tacul altitude $z_{\mathrm{s\,TAC}}$. The vertical gradient $k_\mathrm{b} = \partial b/\partial z$ was estimated using the yearly measurements at the four profiles from 1995 to 2015 (see Fig. S1 in the Supplement). A mean value of $k_\mathrm{b} = 0.9\,\mathrm{m\,yr^{-1}}\,(100\,\mathrm{m})^{-1}$ is obtained with a standard deviation of $0.2\,\mathrm{m\,yr^{-1}}\,(100\,\mathrm{m})^{-1}$. Despite a strong variability from year to year (Fig. S1 in the Supplement and Rabatel et al., 2005), a constant surface mass balance gradient of $k_\mathrm{b} = 0.9\,\mathrm{m\,yr^{-1}}\,(100\,\mathrm{m})^{-1}$ is adopted for hindcast and forecast simulations.

For future simulations, the surface mass balance at the Tacul gate in Eq. (3) is inferred from a series of 26 downscaled and adjusted regional climate projections of the EURO-CORDEX program (Jacob et al., 2014). The adjustment was performed using the ADAMONT method (Verfaillie et al., 2017) using the SAFRAN (Système d'analyse fournissant des renseignements atmosphériques à la neige) reanalysis (Durand et al., 2009) as an observation reference, as described in Verfaillie et al. (2018). The 26 climate projections used here span the three representative concentration pathways (RCPs) (see Table S1 in the Supplement). Each RCP refers to a radiative forcing scenario considered by the IPCC and depending on the future volume of greenhouse gases emitted. They are labeled for the radiative forcing values by the year 2100 (RCP 2.6, RCP 4.5 and RCP 8.5 corresponding to 2.6, 4.5 and $8.5\,\mathrm{W\,m^{-2}}$, respectively).

A degree day model (Braithwaite, 1995; Hock, 2003), known for its simplicity and relatively good performance (Réveillet et al., 2017), is used to evaluate the surface melt at the Tacul gate from the air temperature. Surface melting is proportional to the sum of positive degree days (PDDs; i.e., the sum of daily mean temperatures above the melting point over a given period of time) assuming different melt factors for snow and ice. These melt factors, here expressed in

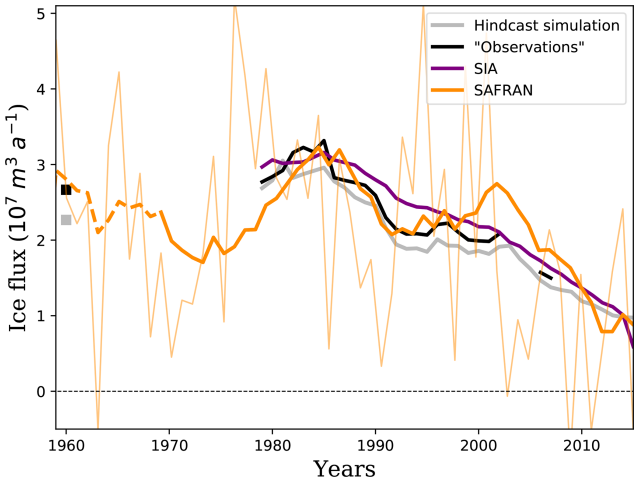

Figure 3. Ice flux through the Tacul gate from 1979 to 2015 based on a previous estimate (Berthier and Vincent, 2012; in black), from the shallow ice approximation (SIA) using only observed ice thicknesses at the Tacul gate (purple), as imposed for the hindcast simulations (gray; see text) and compared to the yearly SAFRAN surface mass balance integrated upstream of the Tacul gate (thin orange) and its 11-year running mean (thick orange).

ice thickness equivalent, are 0.0048 m°C^{-1} d^{-1} for snow and 0.0053 m°C^{-1} d^{-1} for ice, as calibrated by Réveillet et al. (2017) for Mer de Glace. The surface accumulation is the sum of the solid precipitation (snow) and winter liquid precipitation (rain); it is assumed that during winter any rain that falls freezes and remains in the snow pack. Previous works (e.g., Gerbaux et al., 2005; Réveillet et al., 2017; Vionnet et al., 2019) show that precipitation is underestimated in some reanalysis datasets. A comparison of precipitation simulated by SAFRAN reanalysis (Durand et al., 2009) with the annual surface mass balance at Tacul between 1979 and 2015 and with the observed winter accumulation data available after 1994 in the accumulation area (see Supplement) indicates that the SAFRAN precipitation must be increased by 63 % to best fit the observations, which is in good agreement with Réveillet et al. (2017). The same method is then repeated for the climate scenarios adopted for this study. For each scenario, the correction factor for precipitation is evaluated over the past period 1979–2015. On average, simulated precipitation must be increased by 70 % to fit observations with only slight differences from one scenario to another. The value of 70 % is therefore applied to all scenarios. The surface mass balance at the Tacul gate obtained after 2015 with the PDD model and the corrected precipitation from the 26 different climate scenarios constitute the forcing data for the 26 forecast simulations. The same relation as for the hindcast simulation (Eq. 3) is then used to infer the spatial distribution of the surface mass balance.

3.2.3 Flux through the Tacul gate

To account for the artificial boundaries at the Tacul and Leschaux gates, normal ice velocities over these boundaries and changes in surface elevation are imposed as Dirichlet boundary conditions for the free surface equations (Eq. 1). The treatment is different for hindcast and forecast simulations but also for Tacul and Leschaux, given that Leschaux has much less data.

In all cases, we assume that the form of the vertical profile of the horizontal velocity normal to the flux gate is given by the shallow ice approximation (SIA; Hutter, 1981). From the results of the inversion of basal friction performed over the whole domain using the 2003 observed surface velocity, we further assume a constant and uniform ratio between sliding and surface velocities of 1/3 at both gates ($r_{\mathrm{slid}} = u_{\mathrm{b}}/u_{\mathrm{s}} = 1/3$). The vertical profile of the normal velocity at the gate is evaluated as

$$u(z) = r_{\mathrm{slid}} u_{\mathrm{s}} + u_{\mathrm{d}}(z)\,, \tag{4}$$

in which the deformational velocity is either imposed knowing u_{s} (hindcast simulations at Tacul),

$$u_{\mathrm{d}}(z) = (u_{\mathrm{s}} - u_{\mathrm{b}})\left(\frac{z - z_{\mathrm{b}}}{H}\right)^{n+1}\,, \tag{5}$$

or evaluated using the diagnostic formulation for SIA (forecast at Tacul),

$$u_{\mathrm{d}}(z) = 2A(\rho_i g \nabla H)^n (z - z_{\mathrm{b}})^{n+1}\,. \tag{6}$$

In the above equations, z_{b} is the bedrock elevation, whereas H denotes ice thickness. In Eq. (6), the surface slope ∇H is the 2003 value and is held constant with time.

The transverse profile of surface velocity is assumed to follow the 2003 SPOT5 surface velocity at the Tacul cross section (see Fig. 7b in Berthier and Vincent, 2012): it is null on the side and increases linearly from both sides of the glacier to reach a maximum central value uniform over a constant width of 400 m.

For the hindcast simulation, this maximum central value, denoted as $u_{\mathrm{s\,TAC}}$, is given from observations, as is also the case for the ice thickness $h_{\mathrm{s\,TAC}}$. Knowing both the surface velocity, $u_{\mathrm{s}} = u_{\mathrm{s\,TAC}}$, and ice thickness, $H = h_{\mathrm{s\,TAC}}$, in Eq. (5) and assuming the above transverse velocity profile, the total flux through the gate can be estimated (see Fig. 2b). Despite the differences in the methods to estimate the ice flux at the gate, our inferred flux is consistent with the previous estimation of Berthier and Vincent (2012) (see Fig. 3) who assumed constant ratios of 0.8 between the width-averaged and observed centerline surface velocities and of 0.9 between depth-averaged and width-averaged surface velocities. The assumptions on transverse and vertical velocity profiles with $r_{\mathrm{slid}} = 1/3$ that we use in our modeling lead, respectively, to ratios of 0.75 and 0.85, which are very close to the

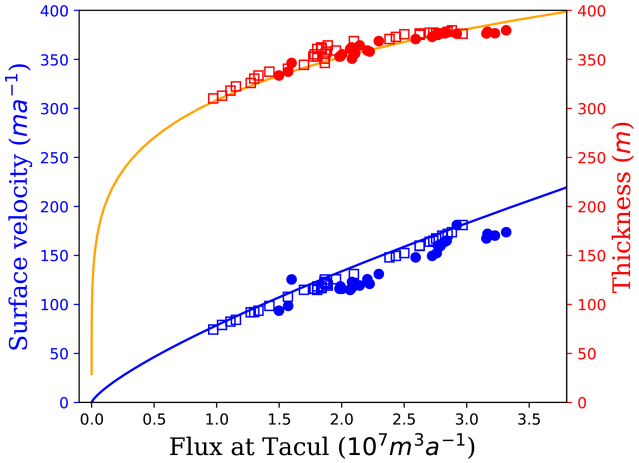

Figure 4. Surface velocity (blue) and thickness (red) at the Tacul gate as a function of the flux through the gate. The curves are the analytical solutions obtained using the SIA (Eq. 6), and the squares correspond to the flux integrated by Elmer/Ice using observed surface velocity, ice thickness and a velocity distribution given by Eqs. (4) and (5). The circles are the fluxes estimated by Berthier and Vincent (2012).

ones adopted by Berthier and Vincent (2012), explaining the closeness of the two approaches.

For the forecast simulations, u_s and H are unknown. Instead, the flux is directly evaluated from the integrated surface mass balance above the Tacul gate (see Fig. 2b) and then used to determine the value of H and the velocity distribution at the gate from Eq. (6). Ice flux through the gate is assessed by integrating, upstream of the Tacul gate, the surface mass balance given by the climate scenarios. For steady state conditions, the ice flux should be equal to the sum of the surface mass balance obtained over the whole area of the upper part. In reality, the glacier being in a highly unsteady state, this condition is not fulfilled. To estimate the relationship between ice flux at the gate and surface mass balance upstream of the gate, we use the observations made between 1979 and 2015 and the reconstructed surface mass balance using SAFRAN reanalyses (Durand et al., 2009). It is found that the observed ice flux at the Tacul gate is best estimated by averaging the surface mass balance integrated upstream of the gate over the 11 preceding years (Fig. 3). This duration corresponds approximately to the time period for the ice to flow from the lowest part of the accumulation area through the ice fall and reach the Tacul gate. The glacier has retreated for the last 3 decades and is expected to continue in the next decades. As the glacier regime will be similar in the future, it is furthermore assumed that this relationship will remain valid in the future.

The inferred relationships between ice flux, velocity and thickness at the Tacul gate are shown in Fig. 4. This figure also presents these relations for the available observations (1979–2015). Their comparison confirms the validity of the empirical relations used above. As shown in Fig. 2b, some scenarios lead to a negative integrated surface mass balance above the Tacul gate, which could result in a very small or even null flux at the gate when integrated over 11 years. To avoid a physically meaningless and overly large decrease in H (a zero flux would imply an instantaneous decrease in H to zero), the annual decrease in H at the Tacul gate is bounded by the local annual surface mass balance because the modeled thickness changes cannot be more negative than ablation. Moreover, to ensure the physical consistency of this boundary condition over the whole simulation period, surface velocity and thickness cannot be null. In applying this second condition, the minimal thickness in our simulation is always greater than 70 m. For surface velocity, a minimal condition of $10\,\mathrm{m\,yr^{-1}}$ is applied.

The same protocol is repeated for the Leschaux boundary condition. Unfortunately, the ice flow velocities through the Leschaux gate are only available for the year 2003 from satellite data (Berthier and Vincent, 2012). For other years, we assume that the ratio $u_{s\,\mathrm{TAC}}(t)/u_{s\,\mathrm{TAC}}(2003)$ obtained from Tacul observations is similar for the Leschaux gate. Note that in 2003, the surface velocity at the Leschaux gate was low ($9\,\mathrm{m\,yr^{-1}}$) compared to the velocity at the Tacul gate ($140\,\mathrm{m\,yr^{-1}}$). Its maximum ice thickness (175 m) was half of that of the Tacul gate (360 m), while their widths are similar (≈ 1000 m). The corresponding flux is consequently 2 orders of magnitude lower, and its effect on Mer de Glace flow is negligible during the period of interest. Therefore, for the forecast simulations, we simply assume that the thickness linearly decreases between the 2015 thickness and a null thickness in 2050. The velocity profile is then directly given by Eq. (6) without estimating a flux from the upstream accumulation.

4 Results

Figures 5 and 6 show, respectively, the reconstructed surface velocity and elevation and the front position for the whole period. Results from the hindcast simulation are compared to the observations over the period 1979–2015. After this validation stage, the forecast simulations explore the range of possible evolutions corresponding to the 26 EURO-CORDEX climate scenarios.

4.1 Hindcast simulation

For the validation of the hindcast simulation, the results of the model are compared with the centerline ice velocities (Fig. 5a) and observed surface elevation changes at the four cross sections (Fig. 5b). Note that at the highest profile (Tacul), the observations are used to impose the ice flux on this boundary of the model domain, explaining the perfect match between observations and model outputs. The valida-

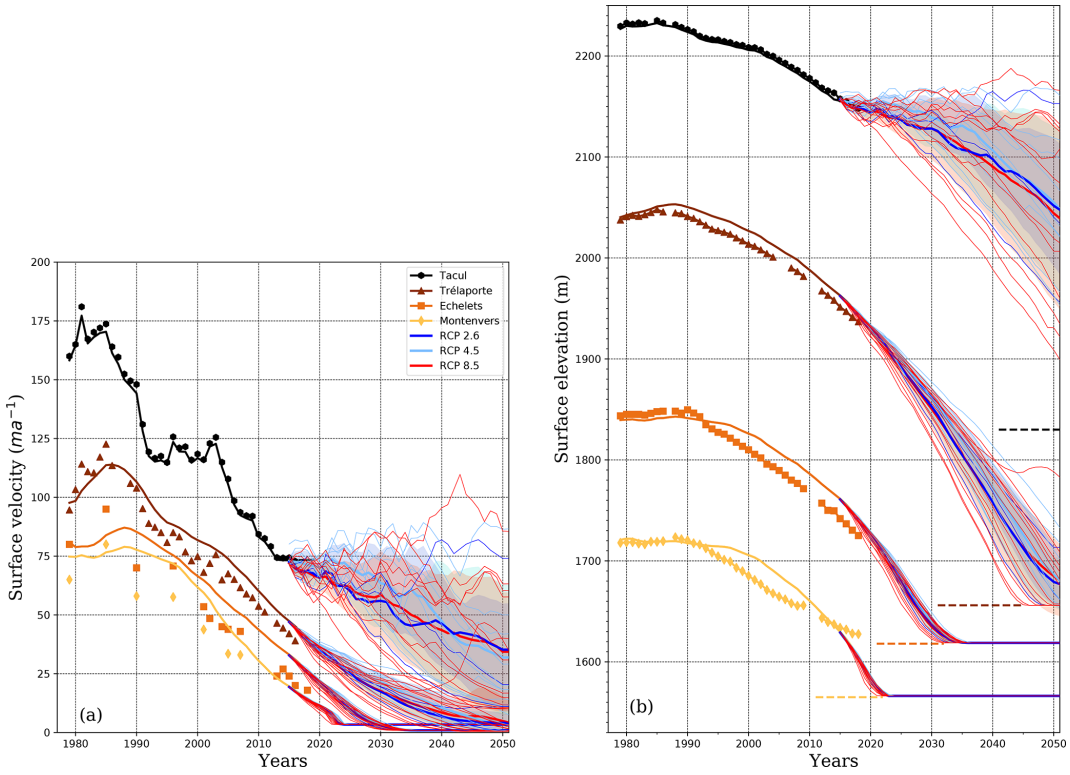

Figure 5. **(a)** Surface velocity and **(b)** surface elevation for all prognostic simulations. Hindcasts at the four profiles are shown by black (Tacul), brown (Trélaporte), orange (Echelets) and yellow (Montenvers) curves, and the symbols are the corresponding observations. Forecasts are shown in dark blue (RCP 2.6), blue (RCP 4.5) and red (RCP 8.5), with the average forecasts represented by thick curves with 1σ uncertainty bands (colored area). Dashed lines indicate the bedrock elevation for the four profiles.

tion is therefore only discussed for the three lower profiles of Trélaporte, Echelets and Montenvers.

The overall agreement of the model with the observations at the three lowest profiles was obtained without any tuning of the model parameters except the inversion of the friction coefficient using the 2003 velocity and surface elevation dataset. The model is capable of reproducing the thickening phase in the first years of the simulation period with increasing ice velocity and ice thickness, as well as the subsequent thinning phase with decreasing surface elevation and velocity. Despite this overall agreement, small differences are observed for both surface elevation and velocity.

For example, the peaks of calculated surface elevation and velocities are reached with a delay of about 3 years at Trélaporte. In the lower cross sections, Echelets and Montenvers, the surface elevation did not show a significant increase between 1979 and 1990. In general, the lower the profile is, the larger the delay will be between the onset of the decrease in the simulated compared to observed surface elevations. For the three lower cross sections, the modeled glacier is in general too thick over the last 25 years of the period compared to observations with a maximum difference of up to 25 m for Montenvers, the lowest cross section. For this cross section, this overestimation decreases in the last years before 2015, eventually becoming an underestimation. In general, the hindcast shows that the response time of thickness and velocities is too long, indicating that the modeled glacier does not respond quickly enough to the flux changes observed at the Tacul gate. The possible causes for this response delay are presented in the Discussion.

Despite these local differences in surface elevation and velocity, the general trend of snout retreat is very well reproduced by the model over the whole hindcast period (Fig. 6). The simulated front is almost stable between 1979 and 1990 and starts to retreat slowly 5 years before the observed retreat in 1995. Over the period 1995–2015, the rapid observed retreat of the ice front is well reproduced with a retreat rate of 30 m yr^{-1} compared to 35 m yr^{-1} for the observations.

Comparisons of area and volume evolution with the few available DEMs show good agreement (Fig. S3 in the Supplement). Figure 5 shows that hindcast thicknesses are slightly overestimated, and this trend is also visible in the volume evolution. The volume decrease between 1979 and 2003 (14 % of the initial volume) is underestimated by 30 %. Extent reduction (10 % of the initial area) is also underestimated by 25 %.

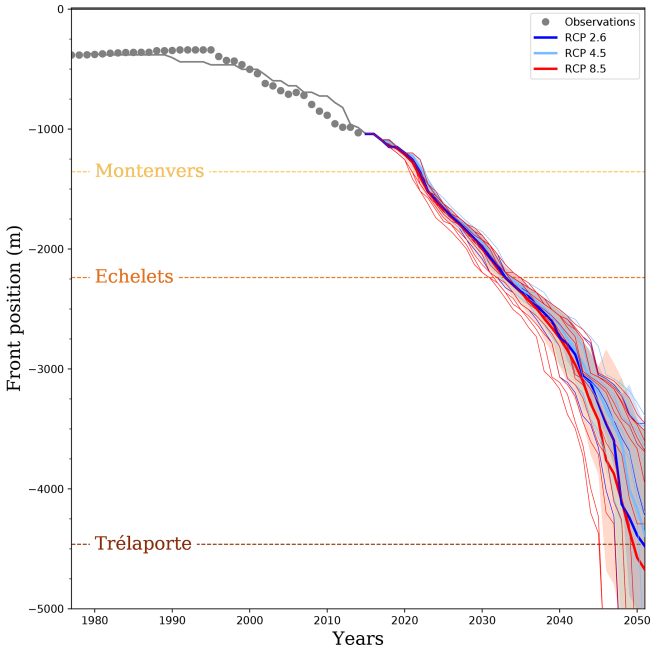

Figure 6. Evolution of the front position (along a flow line defined by the front fluctuation). The hindcast is in gray, and the squares represent observations. Forecasts are shown in dark blue (RCP 2.6), blue (RCP 4.5) and red (RCP 8.5) with average forecasts represented by thick curves with 1σ uncertainty bands.

4.2 Forecast simulations

The forecast simulations were carried out using the surface mass balance calculated from the 26 climate scenarios obtained in the framework of the EURO-CORDEX program (Fig. 2). Note that all representative concentration pathways (RCPs 2.6, 4.5 or 8.5) lead to a very similar mean decrease in surface mass balance by 2050 at the Tacul gate (see Fig. 2a), with almost double the amount of ice lost by 2050 compared to 1960. Large differences between the pathway scenarios appear only after 2050 (not shown). As a direct consequence, the same trend is observed for the integrated surface mass balance above the Tacul gate (see Fig. 2b). Even if a few individual scenarios from all RCPs can lead to stable or even increasing integrated surface mass balance above the Tacul gate by 2050, the general trend for all three RCPs is a decrease in surface mass balance, and ice flux at the Tacul gate drops close to zero by 2050 in some scenarios.

All forecast simulations show significant thinning and slowing downstream of the Tacul gate (Fig. 5). At Trélaporte and Echelets gates, differences in thickness changes are within the range of ± 20 and ± 10 m, respectively, until 2030. Between 2020 and 2030, the thinning at Echelets gate is from 8.0 to 8.8 m yr^{-1} (compared to the 5.0 m yr^{-1} observed between 2005 and 2015). After 2030, the simulations show much larger differences induced only by the differences in surface mass balance obtained from the different climate scenarios. Note that each climate scenario influences both the ice flux through the Tacul gate and the surface mass balance over the modeled domain. At the Tacul gate, depending on the climate scenario, the surface elevation could be either stable or could decrease by 250 m by 2050. For the most pessimistic climate model (RCP 8.5), the ice thickness at the Tacul gate is only ≈ 80 m in 2050, whereas the most optimistic scenario leads to a thickness slightly greater than that observed in 2015 (330 m).

However, these strong differences in ice thickness and ice flux at the Tacul gate lead to much smaller absolute differences in thinning and ice flow velocity downstream of the gate; the lower the cross section is, the smaller the differences in the different scenarios will be. For instance, modeled thinning at Trélaporte only varies in a range of 2 m yr^{-1} between 2030 and 2040, compared to differences as large as 9 m yr^{-1} at the Tacul gate over the same period. Despite some scenarios indicating stable conditions at the Tacul gate, surface elevation and ice flow velocity at the three lowest profiles decrease until 2050 for all climate scenarios, indicating conditions far from steady state for the present glacier.

Our modeling results make it possible to estimate the retreat of the snout over the next decades (Fig. 6). The observed rate of retreat was 35 m yr^{-1} for the hindcast period 1995–2015. According to the forecast simulations, the terminus of Mer de Glace will retreat at rates varying from 60 to 85 m yr^{-1} between 2020 and 2030, 65 to 95 m yr^{-1} for the period 2030–2040, and more than 90 m yr^{-1} after 2040. As a consequence, the Montenvers cross section could be free of ice by 2023 and the Echelets cross section by sometime between 2031 and 2035, depending on the climate scenario (Fig. 6). For the most pessimistic scenarios, the terminus could be close to the Tacul gate by 2050.

Finally, we define a mean reference scenario constructed as the average of all 26 climate scenarios. Figure 7 presents the evolution of the ice thickness and the glacier extent for this mean reference scenario. It also illustrates the variability in glacier extent induced by the different climate scenarios up until 2050 by showing the minimum and maximum extent obtained with the 26 different scenarios for the years 2015, 2025, 2040 and 2050. This mean reference scenario is further used to study the relative contribution of ice flux at the Tacul gate and surface mass balance of the glacier tongue in the Discussion section.

5 Discussion

The model reproduces the evolution of the glacier over the past 4 decades relatively well. However, the observed timing and amplitude of changes are not perfectly reproduced and are increasingly inaccurate as the distance to the Tacul gate increases.

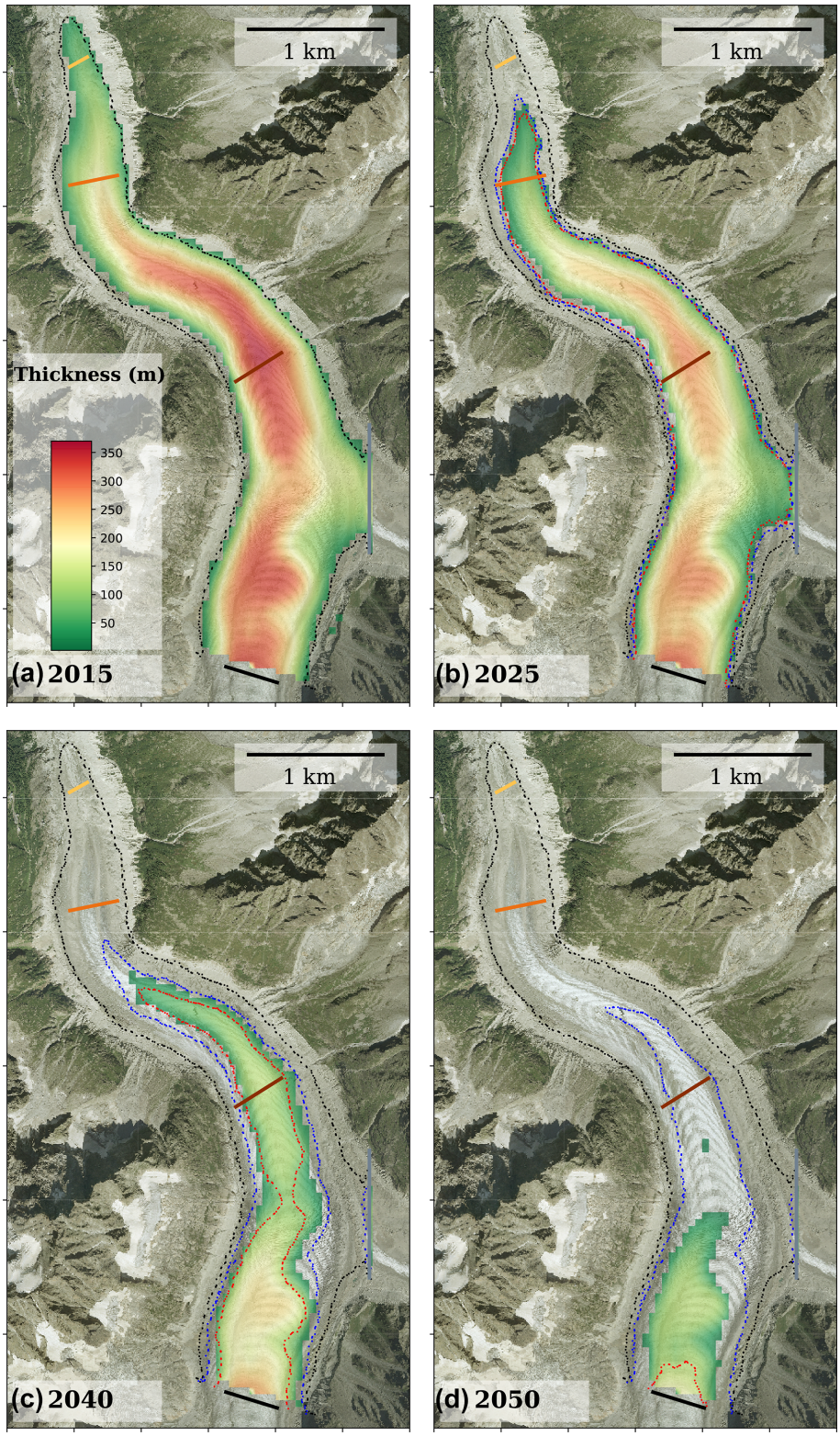

Figure 7. Ice thickness and glacier extension **(a)** at the end of the hindcast simulation in 2015 and for the mean reference forecast simulation for the years **(b)** 2025, **(c)** 2040 and **(d)** 2050. The climate scenario for the mean reference forecast simulation is the average of all 26 climate scenarios. Extensions of the most optimistic and most pessimistic scenarios are plotted in dark blue and red, respectively. The initial glacier extension in 2015 is plotted in black. The background image is the orthophoto from 2008 (©RGD74).

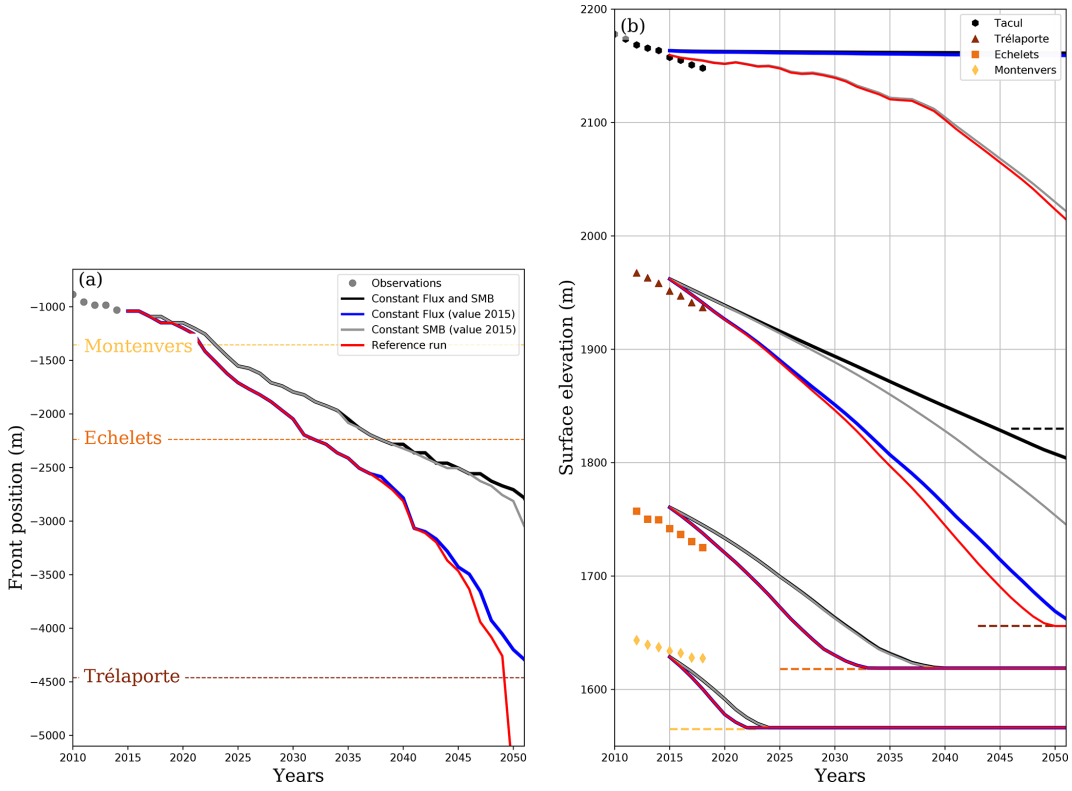

Figure 8. Sensitivity experiment for the mean reference scenario assuming the mean surface mass balance of all scenarios. Evolution of **(a)** the glacier front and **(b)** the surface elevation for this mean reference scenarios (red), assuming a constant surface mass balance (gray, value from year 2015), assuming a constant flux at the Tacul gate (blue, value from year 2015) and assuming that both surface mass balance and flux at the Tacul gate are constant and equal to their 2015 values (black). Dashed lines indicate in **(a)** the position along the retreat line and in **(b)** the bedrock elevation for the gates. For the two lowest gates of Echelets and Montenvers, the red and blue curves are superimposed.

In particular, the modeled glacier underestimates the early growth and thins a few years too late. Consequently the glacier is too thick and velocity too high after 1990, resulting in a flux that is increasingly too high at the profiles of Trélaporte, Echelets and Montenvers. For the hindcast period, there is a relatively high level of confidence in the applied surface mass balance and imposed flux at the Tacul gate, both being directly derived from a continuously maintained network of stakes over the whole glacier. According to Thibert et al. (2008), we can expect uncertainties on ablation estimated from a network of stakes on the order of $0.15\,\mathrm{m\,yr^{-1}}$ in ice equivalent thickness, which is low relative to the mean ablation measured on the tongue of Mer de Glace (from 5 to $12\,\mathrm{m\,yr^{-1}}$). Other uncertainties arise from the linear extrapolation of ablation over the tongue (Eq. 3) based on measurements in an area of clean ice. Indeed, debris cover below Echelets gate has increased in recent decades and may have locally decreased ablation by up to 3 m (Fig. 3b in Berthier and Vincent, 2012). This probably explains our overestimation of the thinning rate at the Montenvers profile after 2000 (see Fig. 5b). While other studies proposed a model for the debris cover evolution and its influence (Jouvet et al., 2011), it is difficult to estimate how the debris cover will evolve above Echelets gate and influence the future retreat of Mer de Glace. Nevertheless, to test the sensitivity to the linear vertical gradient k_b (Eq. 3), we performed the simulations with a lower gradient $k_\mathrm{b} = 0.7\,\mathrm{m\,yr^{-1}}\,(100\,\mathrm{m})^{-1}$. This value corresponds to the averaged gradient inferred from SAFRAN reanalysis and to the minimal gradient inferred from the climatic scenarios. For this gradient, we still assume the same surface mass balance at Tacul gate's altitude than for the gradient $k_\mathrm{b} = 0.9\,\mathrm{m\,yr^{-1}}\,(100\,\mathrm{m})^{-1}$. The lower gradient gives an ice ablation that is reduced by $1.2\,\mathrm{m\,yr^{-1}}$ at the front. The results are available in the Supplement (see Fig. S4). The lower gradient leads to higher discrepancies in thickness and front retreat during the hindcast. Compared to the chosen gradient, $k_\mathrm{b} = 0.9\,\mathrm{m\,yr^{-1}}\,(100\,\mathrm{m})^{-1}$, the forecast evolutions with the lower vertical gradient modestly limit the glacier thinning: Montenvers and Echelets gates are ice free after 5 years, and in 2050 the tongue is 250 to 500 m longer.

The bedrock elevation, of which measurement density has greatly improved due to a recent radar campaign over the modeled area (unpublished), is also well constrained with an estimated average uncertainty of 10 m (Vincent et al., 2009). Moreover, velocities are not systematically over or underestimated during the hindcast period, which might be an in-

dication of a missing transient process in our simulation. The sensitivity of the results to the value of the rate factor in Glen's law has not been explored, but one should expect that a different value would only affect the ratio between ice deformation and basal sliding. Moreover, the glacier being temperate, this value should be uniform and constant and cannot therefore explain the transient discrepancy between the model and the observations. Consequently, the major process explaining these discrepancies is likely basal friction and its evolution from year to year which is not accounted for in the model. Indeed, the basal conditions are inverted from the 2003 dataset and kept constant over the whole simulation. Changes in glacier geometry and surface runoff have likely induced changes in basal conditions over the 4 decades. Inferring these changes would require contiguous surface DEMs and surface velocity maps, which are not available for dates other than 2003.

Regarding the glacier retreat, Berthier and Vincent (2012) estimated that over the period 1979–2008, two-thirds of the increase in the thinning rates observed in the lowest part of Mer de Glace was caused by reduced ice fluxes (and consequently emergence velocities) at the Tacul gate and one-third by increasing surface ablation. In other words, they estimated that the retreat of the glacier front was more influenced by changes at high elevations than local changes. With a comprehensive ice flow description for the last 4 decades and for the future, the relative contribution to glacier retreat of local vs. higher elevation changes can be quantified. As shown below, the results of our hindcast are consistent with the results of Berthier and Vincent (2012) over the period 1979–2008.

For the future, we perform a set of sensitivity experiments to test the influence of the artificial flux condition at the Tacul gate using the mean reference scenario corresponding to the mean of the 26 scenarios (e.g., mean surface mass balance and mean flux at the Tacul gate). The trends obtained for this mean reference scenario apply also to most of the other individual scenarios presented above. We perform 3 additional simulations assuming either a constant surface mass balance with the value from the year 2015, a constant flux at the Tacul gate (value from year 2015), or that both surface mass balance and flux at the Tacul gate are constant and equal to their 2015 values. Figure 8 presents the front and surface elevation evolutions for the four experiments. The experiment with only decreasing surface mass balance is close to the mean reference scenario. In comparison, simulations with a constant SMB give similar trajectories with limited thinning and front retreat. Differences due to the Tacul gate flux are mainly visible close to Trélaporte gate and are limited downstream. Contrary to the past trends, Fig. 8a clearly indicates that the future retreat of the glacier front will be influenced more by local changes (i.e., changes in surface mass balance over the lowest part of the glacier) than by changes in flux from the upstream area (i.e. flux at the Tacul gate). It is only after 2045, when the front approaches the Tacul gate, that its retreat starts to be largely influenced by changes in

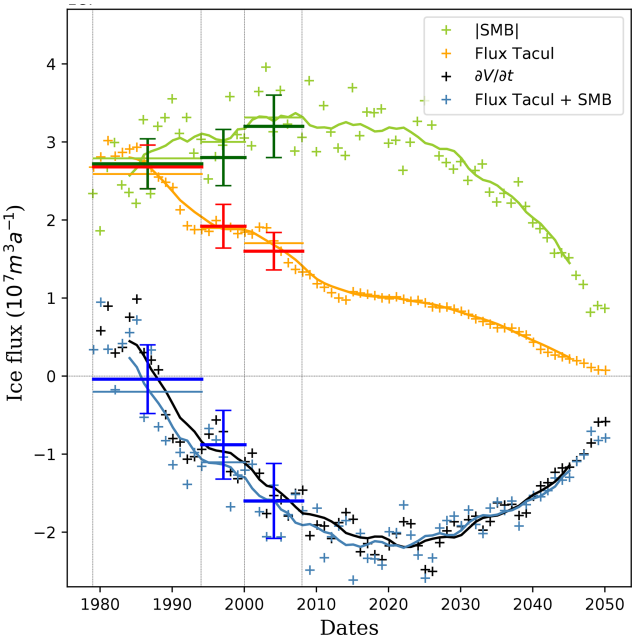

Figure 9. Sensitivity experiment for the mean reference scenario assuming the mean surface mass balance of all scenarios. Evolution with time of the absolute value of the integrated surface mass balance (green, real value always negative), integrated flux at the Tacul gate (orange, always positive) and changes in volume of the glacier tongue (black) in cubic meters of ice per year. The blue curve represents the sum of the two fluxes and is almost equal to the change in volume. For each quantity, crosses represent annual values, whereas the line is a 10-year running average. The bars with error bars in dark colors are the estimates of the same quantities by Berthier and Vincent (2012) for the three periods delimited by the vertical gray lines. Horizontal lines using the same colors as the curves represent the averages of the different quantities over the same periods.

the upstream flux. The same trend is visible for surface elevation changes at the two lowest profiles of Echelets and Montenvers where changes in surface elevation are mostly influenced by the local surface mass balance (Fig. 8b). For the intermediate profile of Trélaporte, the influence from the flux at the Tacul gate is visible, but the local surface mass balance still dominates the observed decrease in surface elevation over the whole studied period.

Integrated surface mass balance, flux through the Tacul gate and volume changes for the mean reference simulation are plotted in Fig. 9. When surface mass balance is integrated over the glacier downstream of the Tacul gate, we can estimate the relative contributions over time of the surface mass balance and the flux at the Tacul gate to the total change in volume of the glacier tongue. As depicted in Fig. 9, surface mass balance and flux at the Tacul gate were almost equal (in absolute values) over the period 1979–1994, and the glacier tongue of Mer de Glace was very close to equilibrium, explaining an almost stationary front position over this period (Fig. 6). Nevertheless, since that period, both terms have

started to decrease but not at the same rate, explaining the two-thirds contribution of flux at the Tacul gate observed by Berthier and Vincent (2012) over the period 1979–2008 and confirmed by our results. Whereas the flux at the Tacul gate has been decreasing at an almost constant rate since the mid-1980s, the rate of decrease in the tongue-integrated surface mass balance is evolving with time. As shown in Fig. 9, the tongue-integrated surface mass balance is currently reaching its minimum and is expected to increase in the future. As a consequence, the volume lost from the tongue of Mer de Glace is currently reaching its maximum and should start to decrease in the future. Indeed, even if larger melt rates are expected in the future, the tongue-integrated surface mass balance is increasing toward zero due to the decrease in the glacier tongue area. This explains why the surface mass balance over the glacier tongue is increasingly dominating changes in ice volume downstream of the Tacul gate relative to ice flux through the gate.

Because the model domain was restricted to the glacier area downstream of the Tacul gate, it was not possible to conduct simulations after 2050 for most of the scenarios. Indeed, after this date, the ice thickness at Tacul rapidly decays to zero. The choice of adopting a restricted domain for the modeling was dictated by the lack of measurements of bedrock elevation upstream. Prognostic simulations over a longer period would therefore require bedrock topography to be determined by additional mapping and/or inference using an inverse method (e.g., Fürst et al., 2018; Farinotti et al., 2019). Nevertheless, as shown by our results, the evolution of the glacier tongue is not sensitive to the boundary condition imposed at the Tacul gate. Therefore, including the upper part of the glacier in the modeled domain would not likely change the results for the studied period but would allow simulations beyond 2050.

Most studies simulating the three-dimensional geometry of a mountain glacier generally compare reconstructions with length, area or volume observations when DEMs are available (Jouvet et al., 2011; Zekollari et al., 2014). Our study allows in addition a yearly comparison of thickness and velocity changes at different locations of the glacier. The iconic status of Mer de Glace and facilities of the Électricité De France for hydropower resources and Compagnie du Mont Blanc for tourist activities justify a specific study with a state-of-the art model. It suggests that tourist facilities should be modified.

Vincent et al. (2014) used a parameterized model calibrated with past thickness changes and the surface mass balance inferred from its sensitivity to atmospheric warming to simulate the future fluctuations of Mer de Glace. They found that Mer de Glace will retreat by 1200 m by 2040 with a warming trend of $0.04\,^{\circ}\mathrm{C\,yr^{-1}}$. In a new estimation using, as the present study, the EURO-CORDEX projections adjusted with the ADAMONT method, Vincent et al. (2019) found retreats of 1 to 3 km by 2050. Zekollari et al. (2019) used an SIA model to reconstruct the evolution of all glaciers located in the Alps. They used a EURO-CORDEX ensemble scenario. They found that Mer de Glace will retreat by 2 to 6 km between 2017 and 2050, which is close to our results. On a decadal timescale, retreats with the parameterized model are smaller than retreats obtained with ice flow models. It could be related to the lack of the dynamics in the parameterized model. Another explanation is that parameterized models take into account the local thickness and surface mass balance changes given that they are based on in situ observations.

The future evolution of the glacier can also be related to its response time which has been a subject of interest of several studies. The response times of glaciers are affected by several predictors such as the glacier size, the glacier SMB and glacier slope, which is the main driver. Recently, Zekollari et al. (2020) used large-scale glacier modeling to investigate the response time in the European Alps. For Mer de Glace, the relationship proposed by the authors between average surface slope, elevation range and the response time gives a response time of 60 years, which is typical of the range of European Alps glaciers (50 ± 28 years). Our sensitivity experiments confirm this result. Indeed, the future simulation performed with stationary flux at Tacul and surface mass balance after 2015 shows that Mer de Glace will reach a steady state after 70 years and a front retreat of 4.1 km.

Finally, Jouvet and Huss (2019) lead forecast simulations for the Great Aletsch glacier, the largest glacier in the European Alps, with a full Stokes model and the EURO-CORDEX ensemble. Their results are close to those of Zekollari et al. (2019). They predict a glacier retreat of around 5 km between 2017 and 2050, which is similar to the Mer de Glace forecasts.

6 Conclusions

In this study, the Elmer/Ice ice flow model was applied to simulate the past and future evolution of the lower part of Mer de Glace. Given that the bedrock elevation remains unknown in the upper part of the glacier, we specified the ice fluxes at the Tacul and Leschaux gates which are the upper limits of the tongue. These ice fluxes were obtained from monitored cross-section surface area and ice flow velocities for hindcast. For forecasts, they were assessed from the simulated surface mass balance in the accumulation zone.

The simulation of the glacier tongue for the period 1979 to 2015 was driven by (i) surface mass balance measurements and (ii) the ice flux at the Tacul and Leschaux gates, which were obtained directly from the observed surface area and ice flow velocities. Ice flow modeling results were compared to detailed and continuous observations of surface elevation, surface velocity and snout fluctuations over 4 decades during which the glacier experienced both a period of increase and a long period of decay. To our knowledge, a comparison to data in this detail is unprecedented. We found that our

modeling using Elmer/Ice is able to reproduce the general behavior of the glacier. For example, the early growth of the glacier occurring between 1979 and 1990 is correctly reconstructed. However, the elevation increase is underestimated in the lower part of the tongue. After 1990, the modeling results are in agreement with observations. We suspect that the small differences between the model and the observations arise from the constant basal friction parameter imposed over the hindcast period. Additional uncertainties in the surface mass balance of the tongue are likely related to the sparse debris cover.

Using 26 climate scenarios, the model was run forward to simulate the evolution of the glacier tongue until 2050. There were major differences in the ice fluxes calculated at the Tacul gate from all these scenarios; however, changes in velocity and elevation at the lowest part of the glacier, as well as the retreat of the glacier front, were shown to be relatively independent of this upstream flux. Indeed, our sensitivity study indicates that the future changes at the lowest cross sections of the tongue are mainly influenced by the local surface mass balance, which depends on the distance from the upper gate where the ice flux is prescribed. This also explains why the upper cross section of Trélaporte is more sensitive to the upstream flux condition at Tacul. Because of the decreasing surface area, the rate of volume loss from the glacier downstream of the Tacul gate is currently reaching a maximum and will continue decreasing in the future. The glacier snout could retreat by 2 to 6 km over the next 3 decades and be close to the Tacul gate by 2050.

Forecast simulations over a longer period would require extension of the model domain upstream of the Tacul gate, which is hindered by the unknown bedrock topography. Radar measurements in the upper part of Mer de Glace and/or inverse modeling are therefore required to estimate the bedrock topography in this area before realistic forecast simulations of Mer de Glace can be extended beyond 2050.

Code availability. Elmer/Ice code is publicly available through GitHub (https://github.com/ElmerCSC/elmerfem, last access: 3 November 2020, Gagliardini et al., 2013).

Supplement. The supplement related to this article is available online at: https://doi.org/10.5194/tc-14-3979-2020-supplement.

Author contributions. VP, CV, CB and OG designed the experiments. VP, CB and FG-C performed the numerical modeling. OL, DS, and CV performed the geophysical and geodetic measurements. VP led the writing of the paper with contribution from all coauthors.

Competing interests. The authors declare that they have no conflict of interest.

Acknowledgements. We thank Samuel Morin and Deborah Verfaillie (Centre d'Etude de la Neige, Météo France/CNRS) who produced the climate scenarios used in this study (ADAMONT simulations, https://opensource.umr-cnrm.fr/projects/adamont, last access: 3 November 2020). Remote field measurements were obtained thanks to the support of the TOSCA program of the French Space Agency (CNES). Glaciological data were obtained from the GLACIOCLIM database, https://glacioclim.osug.fr/ (last access: 3 November 2020). This study was supported by Électricité de France and Compagnie du Mont Blanc. We thank all collaborators past and present for their thorough measurements of mass balance, thickness and velocity changes, as well as bedrock topography, for Mer de Glace over all these decades. We thank the editor Andreas Vieli and the three anonymous reviewers for their judicious comments and suggestions that greatly improved the quality of the initial paper.

Review statement. This paper was edited by Andreas Vieli and reviewed by three anonymous referees.

References

Berthier, E. and Vincent, C.: Relative contribution of surface mass-balance and ice-flux changes to the accelerated thinning of Mer de Glace, French Alps, over 1979-2008, J. Glaciol., 58, 501–512, https://doi.org/10.3189/2012JoG11J083, 2012.

Berthier, E., Arnaud, Y., Baratoux, D., Vincent, C., and Rémy, F.: Recent rapid thinning of the "Mer de Glace" glacier derived from satellite optical images, Geophys. Res. Lett., 31, L17401, https://doi.org/10.1029/2004GL020706, 2004.

Berthier, E., Vadon, H., Baratoux, D., Arnaud, Y., Vincent, C., Feigl, K. L., Rémy, F., and Legresy, B.: Surface motion of mountain glaciers derived from satellite optical imagery, Remote Sens. Environ., 95, 14–28, https://doi.org/10.1016/j.rse.2004.11.005, 2005.

Berthier, E., Vincent, C., Magnússon, E., Gunnlaugsson, Á. Þ., Pitte, P., Le Meur, E., Masiokas, M., Ruiz, L., Pálsson, F., Belart, J. M. C., and Wagnon, P.: Glacier topography and elevation changes derived from Pléiades sub-meter stereo images, The Cryosphere, 8, 2275–2291, https://doi.org/10.5194/tc-8-2275-2014, 2014.

Braithwaite, R. J.: Positive degree-day factors for ablation on the Greenland ice sheet studied by energy-balance modelling, J. Glaciol., 41, 153–160, https://doi.org/10.3189/S0022143000017846, 1995.

Brunner, M. I., Gurung, A. B., Zappa, M., Zekollari, H., Farinotti, D., and Stähli, M.: Present and future water scarcity in Switzerland: Potential for alleviation through reservoirs and lakes, Sci. Total Environ., 666, 1033–1047, https://doi.org/10.1016/j.scitotenv.2019.02.169, 2019.

Clarke, G. K. C., Jarosch, A. H., Anslow, F. S., Radić, V., and Menounos, B.: Projected deglaciation of western Canada in the twenty-first century, Nat. Geosci., 8, 372–377, https://doi.org/10.1038/ngeo2407, 2015.

Durand, Y., Laternser, M., Giraud, G., Etchevers, P., Lesaffre, B., and Mérindol, L.: Reanalysis of 44 yr of climate in the French Alps (1958–2002): Methodology, model

validation, climatology, and trends for air temperature and precipitation, J. Appl. Meteorol. Clim., 48, 429–449, https://doi.org/10.1175/2008JAMC1808.1, 2009.

Farinotti, D., Brinkerhoff, D. J., Clarke, G. K. C., Fürst, J. J., Frey, H., Gantayat, P., Gillet-Chaulet, F., Girard, C., Huss, M., Leclercq, P. W., Linsbauer, A., Machguth, H., Martin, C., Maussion, F., Morlighem, M., Mosbeux, C., Pandit, A., Portmann, A., Rabatel, A., Ramsankaran, R., Reerink, T. J., Sanchez, O., Stentoft, P. A., Singh Kumari, S., van Pelt, W. J. J., Anderson, B., Benham, T., Binder, D., Dowdeswell, J. A., Fischer, A., Helfricht, K., Kutuzov, S., Lavrentiev, I., McNabb, R., Gudmundsson, G. H., Li, H., and Andreassen, L. M.: How accurate are estimates of glacier ice thickness? Results from ITMIX, the Ice Thickness Models Intercomparison eXperiment, The Cryosphere, 11, 949–970, https://doi.org/10.5194/tc-11-949-2017, 2017.

Farinotti, D., Huss, M., Fürst, J. J., Landmann, J., Machguth, H., Maussion, F., and Pandit, A.: A consensus estimate for the ice thickness distribution of all glaciers on Earth, Nat. Geosci., 12, 168–173, https://doi.org/10.1038/s41561-019-0300-3, 2019.

Fürst, J. J., Navarro, F., Gillet-Chaulet, F., Huss, M., Moholdt, G., Fettweis, X., Lang, C., Seehaus, T., Ai, S., Benham, T. J., Benn D. I., Björnsson H., Dowdeswell J. A., Mariusz Grabiec, G., Kohler, J., Lavrentiev, I., Lindbäck, K., Melvold, K., Pettersson, R., Rippin, D., Saintenoy, A., Pablo Sánchez-Gámez, P., Schuler, T. V., Sevestre, H., Vasilenko, E., and Braun, M. H.: The Ice-Free Topography of Svalbard, Geophys. Res. Lett., 45, 11–760, https://doi.org/10.1029/2018GL079734, 2018.

Gagliardini, O., Gillet-Chaulet, F., Durand, G., Vincent, C., and Duval, P.: Estimating the risk of glacier cavity collapse during artificial drainage: The case of Tête Rousse Glacier, Geophys. Res. Lett., 38, L10505, https://doi.org/10.1029/2011GL047536, 2011.

Gagliardini, O., Zwinger, T., Gillet-Chaulet, F., Durand, G., Favier, L., de Fleurian, B., Greve, R., Malinen, M., Martín, C., Råback, P., Ruokolainen, J., Sacchettini, M., Schäfer, M., Seddik, H., and Thies, J.: Capabilities and performance of Elmer/Ice, a new-generation ice sheet model, Geosci. Model Dev., 6, 1299–1318, https://doi.org/10.5194/gmd-6-1299-2013, 2013.

Gerbaux, M., Genthon, C., Etchevers, P., Vincent, C., and Dedieu, J.: Surface mass balance of glaciers in the French Alps: distributed modeling and sensitivity to climate change, J. Glaciol., 51, 561–572, https://doi.org/10.3189/172756505781829133, 2005.

Gilbert, A., Sinisalo, A., Gurung, T. R., Fujita, K., Maharjan, S. B., Sherpa, T. C., and Fukuda, T.: The influence of water percolation through crevasses on the thermal regime of a Himalayan mountain glacier, The Cryosphere, 14, 1273–1288, https://doi.org/10.5194/tc-14-1273-2020, 2020.

Gillet-Chaulet, F., Gagliardini, O., Seddik, H., Nodet, M., Durand, G., Ritz, C., Zwinger, T., Greve, R., and Vaughan, D. G.: Greenland ice sheet contribution to sea-level rise from a new-generation ice-sheet model, The Cryosphere, 6, 1561–1576, https://doi.org/10.5194/tc-6-1561-2012, 2012.

Glen, J. W.: The creep of polycrystalline ice, P. R. Soc. A, 228, 519–538, 1955.

Gluck, S.: Détermination du lit rocheux sous la Mer de Glace par séismique-réflexion, CR Acad. Sci., 264, 2272–2275, 1967.

Greuell, W.: Hintereisferner, Austria: mass-balance reconstruction and numerical modelling of the historical length variations, J. Glaciol., 38, 233–244, https://doi.org/10.3189/S0022143000003646, 1992.

Haeberli, W. and Hölzle, M.: Application of inventory data for estimating characteristics of and regional climate-change effects on mountain glaciers: a pilot study with the European Alps, Ann. Glaciol., 21, 206–212, https://doi.org/10.1017/S0260305500015834, 1995.

Hock, R.: Temperature index melt modelling in mountain areas, J. Hydrol., 282, 104–115, https://doi.org/10.1016/S0022-1694(03)00257-9, 2003.

Hock, R., Bliss, A., Marzeion, B., Giesen, R. H., Hirabayashi, Y., Huss, M., Radić, V., and Slangen, A. B. A.: GlacierMIP – A model intercomparison of global-scale glacier mass-balance models and projections, J. Glaciol., 65, 453–467, https://doi.org/10.1017/jog.2019.22, 2019.

Huss, M.: Extrapolating glacier mass balance to the mountain-range scale: the European Alps 1900–2100, The Cryosphere, 6, 713–727, https://doi.org/10.5194/tc-6-713-2012, 2012.

Huss, M. and Hock, R.: Global-scale hydrological response to future glacier mass loss, Nat. Clim. Change, 8, 135–140, https://doi.org/10.1038/s41558-017-0049-x, 2018.

Huss, M., Farinotti, D., Bauder, A., and Funk, M.: Modelling runoff from highly glacierized alpine drainage basins in a changing climate, Hydrol. Process., 22, 3888–3902, https://doi.org/10.1002/hyp.7055, 2008.

Hutter, K.: The effect of longitudinal strain on the shearstress of an ice sheet: in defence of using stretched coordinates, J. Glaciol., 27, 39–56, https://doi.org/10.3189/S0022143000011217, 1981.

Huybrechts, P., de Nooze, P., and Decleir, H.: Numerical modelling of glacier d'Argentière and its historic front variations, in: Glacier Fluctuations and Climatic Change, edited by: Oerlemans, J., 373–389, https://doi.org/10.1007/978-94-015-7823-3_24, 1989.

IPCC: High Mountain Areas, in: IPCC Special Report on the Ocean and Cryosphere in a Changing Climate, Cambridge University Press, available at: https://www.ipcc.ch/srocc (last access: 3 November 2020), 2019.

Jacob, D., Petersen, J., Eggert, B., Alias, A., Christensen, O. B., Bouwer, L. M., Braun, A., Colette, A., Déqué, M., Georgievski, G., Georgopoulou, E., Gobiet, A., Menut, L., Nikulin, G., Haensler, A., Hempelmann, N., Jones, C., Keuler, K., Kovats, S., Kröner, N., Kotlarski, S., Kriegsmann, A., Martin, E., van Meijgaard, E., Moseley, C., Pfeifer, S., Preuschmann, S., Radermacher, C., Radtke, K., Rechid, D., Rounsevell, M., Samuelsson, P., Somot, S., Soussana, J.-F., Teichmann, C., Valentini, R., Vautard, R., Weber, B., and Yiou, P.: EURO-CORDEX: new high-resolution climate change projections for European impact research, Reg. Environ. Change, 14, 563–578, https://doi.org/10.1007/s10113-013-0499-2, 2014.

Jouvet, G. and Huss, M.: Future retreat of Great Aletsch Glacier, J. Glaciol., 65, 869–872, https://doi.org/10.1017/jog.2019.52, 2019.

Jouvet, G., Huss, M., Funk, M., and Blatter, H.: Modelling the retreat of Grosser Aletschgletscher, Switzerland, in a changing climate, J. Glaciol., 57, 1033–1045, https://doi.org/10.3189/002214311798843359, 2011.

Kääb, A., Leinss, S., Gilbert, A., Bühler, Y., Gascoin, S., Evans, S. G., Bartelt, P., Berthier, E., Brun, F., Chao, W.-A., Farinotti, D., Gimbert, F. Guo, W., Huggel, C., Kargel, J. S., Leonard, G.

J., Tian, L., Treichler, D., and Yao, T.: Massive collapse of two glaciers in western Tibet in 2016 after surge-like instability, Nat. Geosci., 11, 114–120, https://doi.org/10.1038/s41561-017-0039-7, 2018.

Le Meur, E. and Vincent, C.: A two-dimensional shallow ice-flow model of Glacier de Saint-Sorlin, France, J. Glaciol., 49, 527–538, https://doi.org/10.3189/172756503781830421, 2003.

Letréguilly, A. and Reynaud, L.: Past and Forecast Fluctuations of Glacier Blanc (French Alps), Ann. Glaciol., 13, 159–163, https://doi.org/10.3189/S0260305500007813, 1989.

Lliboutry, L., Vallon, M., and Vivet, R.: Étude de trois glaciers des Alpes Françaises, in: Union Géodésique et Géophysique Internationale, Association Internationale d'Hydrologie Scientifique, Commission des Neiges et des Glaces, Colloque d'Obergurgl, 10–18 September 1962, 145–59, 1962.

Marzeion, B., Jarosch, A. H., and Hofer, M.: Past and future sea-level change from the surface mass balance of glaciers, The Cryosphere, 6, 1295–1322, https://doi.org/10.5194/tc-6-1295-2012, 2012.

Marzeion, B., Hock, R., Anderson, B., Bliss, A., Champollion, N., Fujita, K., Huss, M., Immerzeel, W., Kraaijenbrink, P., Malles, J.-H., Maussion, F., Radìc, V., Rounce, D. R., Sakai, A., Shannon, S., van de Wal, R., and Zekollari, H.: Partitioning the Uncertainty of Ensemble Projections of Global Glacier Mass Change, Earths Future, 8, e2019EF001470, https://doi.org/10.1029/2019EF001470, 2020.

Maussion, F., Butenko, A., Champollion, N., Dusch, M., Eis, J., Fourteau, K., Gregor, P., Jarosch, A. H., Landmann, J., Oesterle, F., Recinos, B., Rothenpieler, T., Vlug, A., Wild, C. T., and Marzeion, B.: The Open Global Glacier Model (OGGM) v1.1, Geosci. Model Dev., 12, 909–931, https://doi.org/10.5194/gmd-12-909-2019, 2019.

Millan, R., Mouginot, J., Rabatel, A., Jeong, S., Cusicanqui, D., Derkacheva, A., and Chekki, M.: Mapping Surface Flow Velocity of Glaciers at Regional Scale Using a Multiple Sensors Approach, Remote Sens.-Basel, 65, 2498, https://doi.org/10.3390/rs11212498, 2019.

Oerlemans, J.: Glaciers and climate change: a meteorologist's view., A. A. Balkema Publishers, 2001.

Paterson, W. S. B.: The Physics of Glaciers, 3rd edn., Elsevier Science Ltd, 1994.

Rabatel, A., Dedieu, J.-P., and Vincent, C.: Using remote-sensing data to determine equilibrium-line altitude and mass-balance time series: validation on three French glaciers, 1994–2002, J. Glaciol., 51, 539–546, https://doi.org/10.3189/172756505781829106, 2005.

Radić, V., Bliss, A., Beedlow, A. C., Hock, R., Miles, E., and Cogley, J. G.: Regional and global projections of twenty-first century glacier mass changes in response to climate scenarios from global climate models, Clim. Dynam., 42, 37–58, https://doi.org/10.1007/s00382-013-1719-7, 2014.

Réveillet, M., Rabatel, A., F., G.-C., and Soruco, A.: Simulations of changes to Glaciar Zongo, Bolivia (16° S), over the 21st century using a 3-D full-Stokes model and CMIP5 climate projections, Ann. Glaciol., 56, 89–97, https://doi.org/10.3189/2015AoG70A113, 2015.

Réveillet, M., Vincent, C., and Six, D. Rabatel, A.: Which empirical model is best suited to simulate glacier mass balances?, J. Glaciol., 63, 39–54, https://doi.org/10.1017/jog.2016.110, 2017.

Six, D. and Vincent, C.: Sensitivity of mass balance and equilibrium-line altitude to climate change in the French Alps, J. Glaciol., 60, 867–878, https://doi.org/10.3189/2014JoG14J014, 2014.

Solomon, S., Qin, D., Manning, M., Averyt, K., and Marquis, M.: Climate change 2007 – the physical science basis: Working group I contribution to the fourth assessment report of the IPCC, vol. 4, Cambridge University Press, 2007.

Stewart, E. J., Wilson, J., Espiner, S., Purdie, H., Lemieux, C., and Dawson, J.: Implications of climate change for glacier tourism, Tourism Geogr., 18, 377–398, https://doi.org/10.1080/14616688.2016.1198416, 2016.

Stroeven, A., van de Wal, R., and Oerlemans, J.: Historic front variations of the Rhone Glacier: simulation with an ice flow model, in: Glacier Fluctuations and Climate Change, edited by: Oerlemans, J., Springer, Dordrecht, 391–405, 1989.

Süustrunk, A. E.: Sondage du glacier par la méthode sismique, Houille Blanche, No. spécial A, 309–318, https://doi.org/10.1051/lhb/1951010, 1951.

Thibert, E., Blanc, R., Vincent, C., and Eckert, N.: Glaciological and volumetric mass-balance measurements: error analysis over 51 years for Glacier de Sarennes, French Alps, J. Glaciol., 54, 522–532, https://doi.org/10.3189/002214308785837093, 2008.

Vallon, M.: Épaisseur du glacier du Tacul (massif du Mont- Blanc), CR Acad. Sci., 252, 1815—1817, 1961.

Vallon, M.: Contribution à l'étude de la Mer de Glace., Ph.D. thesis, Université de Grenoble, 1967.

Vallot, J.: Tome I à VI, in: Annales de l'Obsevatoire météoprologique, physique et glaciaire du Mont Blanc (altitude 4,358 métres), G Steinheil, Paris, 1905.

Verfaillie, D., Déqué, M., Morin, S., and Lafaysse, M.: The method ADAMONT v1.0 for statistical adjustment of climate projections applicable to energy balance land surface models, Geosci. Model Dev., 10, 4257–4283, https://doi.org/10.5194/gmd-10-4257-2017, 2017.

Verfaillie, D., Lafaysse, M., Déqué, M., Eckert, N., Lejeune, Y., and Morin, S.: Multi-component ensembles of future meteorological and natural snow conditions for 1500 m altitude in the Chartreuse mountain range, Northern French Alps, The Cryosphere, 12, 1249–1271, https://doi.org/10.5194/tc-12-1249-2018, 2018.

Vincent, C.: Influence of climate change over the 20th Century on four French glacier mass balances, J. Geophys. Res., 107, 4375, https://doi.org/10.1029/2001JD000832, 2002.

Vincent, C., Soruco, A., Six, D., and Le Meur, E.: Glacier thickening and decay analysis from 50 years of glaciological observations performed on Glacier d'Argentière, Mont Blanc area, France, Ann. Glaciol., 50, 73–79, https://doi.org/10.3189/172756409787769500, 2009.

Vincent, C., Harter, M., Gilbert, A., Berthier, E., and Six, D.: Future fluctuations of Mer de Glace, French Alps, assessed using a parameterized model calibrated with past thickness changes, Ann. Glaciol., 55, 15–24, https://doi.org/10.3189/2014AoG66A050, 2014.

Vincent, C., Peyaud, V., Laarman, O., Six, D., Gilbert, A., Gillet-Chaulet, F., Berthier, E., Morin, S., Verfaillie, D., Rabatel, A., Jourdain, B., and Bolibar, J.: Déclin des deux plus grands glaciers des Alpes françaises au cours du XXI siècle: Argentière et Mer de Glace, La Météorologie, 106, 49–58, https://doi.org/10.4267/2042/70369, 2019.

Vionnet, V., Six, D., Auger, L., Dumont, M., Lafaysse, M., Quéno, L., Réveillet, M., Dombrowski-Etchevers, I., Thibert, E., and Vincent, C.: Sub-kilometer Precipitation Datasets for Snowpack and Glacier Modeling in Alpine Terrain, Front. Earth Sci., 7, 182, https://doi.org/10.3389/feart.2019.00182, 2019.

Welling, J. T., Árnason, Þ., and Ólafsdottír, R.: Glacier tourism: A scoping review, Tourism Geogr., 17, 635–662, https://doi.org/10.1080/14616688.2015.1084529, 2015.

Zekollari, H., Fürst, J. J., and Huybrects, P.: Modelling the evolution of Vadret da Morteratsch, Switzerland, since the Little Ice Age and into the future, J. Glaciol., 60, 1155–1168, https://doi.org/10.3189/2014JoG14J053, 2014.

Zekollari, H., Huss, M., and Farinotti, D.: Modelling the future evolution of glaciers in the European Alps under the EURO-CORDEX RCM ensemble, The Cryosphere, 13, 1125–1146, https://doi.org/10.5194/tc-13-1125-2019, 2019.

Zekollari, H., Huss, M., and Farinotti, D.: On the Imbalance and Response Time of Glaciers in the European Alps, Geophys. Res. Let., 47, e2019GL085578, https://doi.org/10.1029/2019GL085578, 2020.

Zemp, M., Haeberli, W., Hoelzle, M., and Paul, F.: Alpine glaciers to disappear within decades?, Geophys. Res. Lett., 33, L13504, https://doi.org/10.1029/2006GL026319, 2006.

Zemp, M., Frey, H., Gärtner-Roer, I., and Nussbaumer, S. U.": Historically unprecedented global glacier decline in the early 21st century, J. Glaciol., 61, 745–762, https://doi.org/10.3189/2015JoG15J017, 2015.

Zemp, M., Huss, M., Thibert, E., Eckert, N., McNabb, R., Huber, J., Barandun, M., Machguth, H., Nussbaumer, S. U., Gärtner-Roer, I., Thomson, L., Paul, F., Maussion, F., Kutuzov, S., and Cogley, J. G.: Global glacier mass changes and their contributions to sea-level rise from 1961 to 2016, Nature, 568, 382–386, https://doi.org/10.1038/s41586-019-1071-0, 2019.

A.2 Glacier surges controlled by the close interplay between subglacial friction and drainage (in review, 2023)

During the early stages of my doctoral research, my primary emphasis was on the theoretical aspects of glacier surges, aiming to comprehend Dr. Thøgersen's work and potentially adapt the model from his 2019 publication (Thøgersen et al., 2019) for soft-bed glaciers. My main goal was to establish a theoretical connection between basal friction and subglacial hydrology in this specific context. Although my research direction moved away from achieving this specific goal, the process involved extensive exploration, equation development, encountering obstacles, and multiple restarts. Through this journey, I gained insights into the physical theories and the contemporary mathematical framework that seeks to elucidate glacier surges.

Drawing upon my theoretical understanding of surge processes and my background in glaciology, I engaged with Dr. Thøgersen paper, contributing ideas and offering feedback throughout the research process. This paper has undergone, and perhaps still continues to experience, a lengthy journey. Originally, we submitted it to *Nature* in 2021, only to face rejection. The editor advised us to reiterate the submission in *Nature Geosciences*, but unfortunately, it was rejected once again. Determined to find the right fit, we reformatted the entire manuscript to adhere to the *Journal of Geophysical Research: Earth Surfaces*'s template. This time, the manuscript has been rejected for re-submission due to a mathematical error in the equations.

During this process, Dr. Thøgersen left academia, which lead the reviews on hold for approximately a year. Recently, Dr. Gilbert and Prof. Schuler delved back into the code, addressing the problems. We are currently still working on the manuscript for an imminent re-submission.

Appendix B

Dissemination inside academia and beyond

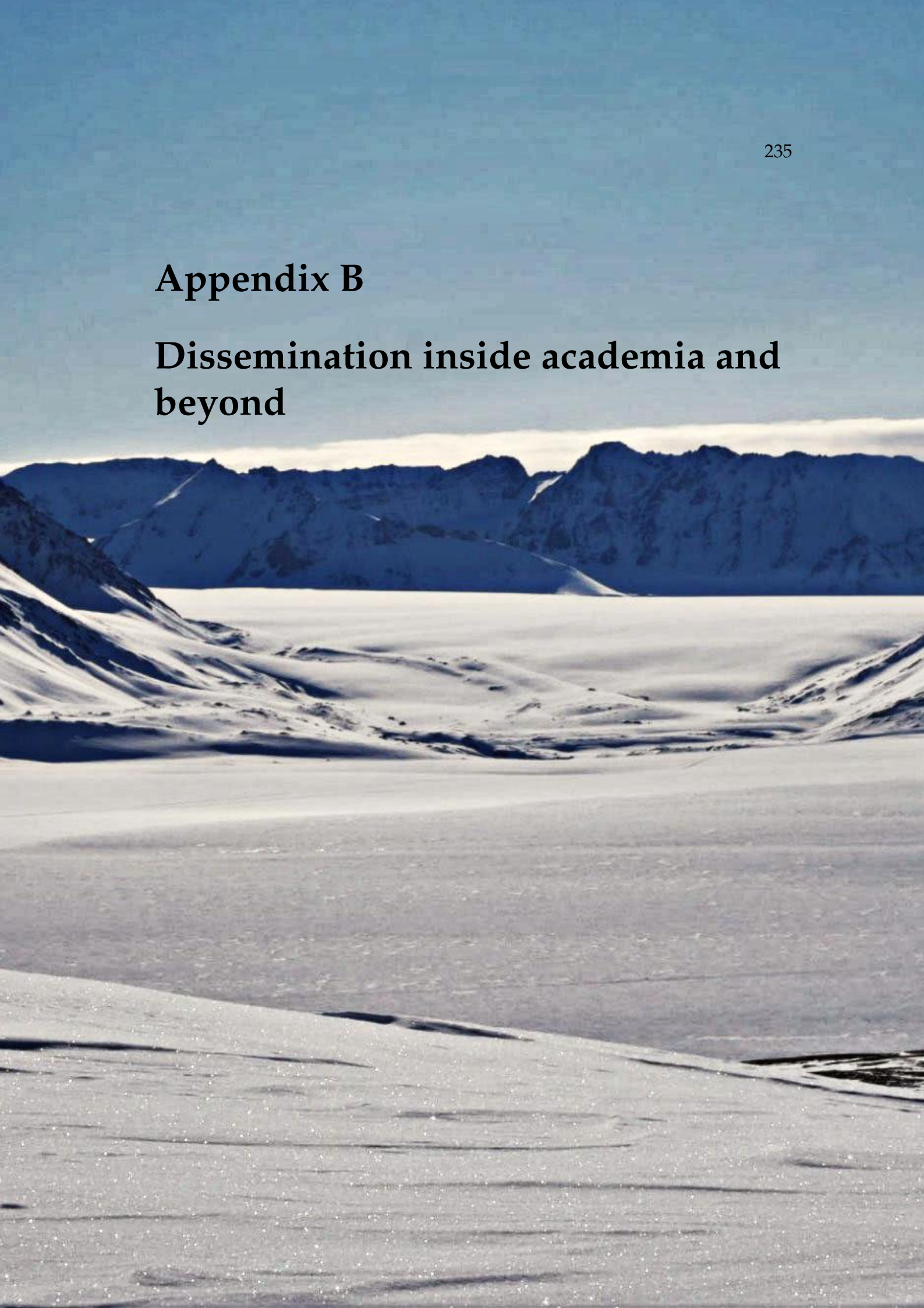

B.1 Talks

- Bouchayer, C., U. Nanni, L. Schmidt, P.M. Lefeuvre, John Hult, F. Renard and T.V. Schuler. Multi-scale variations of subglacial hydro-mechanical conditions. EarthFlows, Oslo, Norway. June 2023.
- Bouchayer, C., Aiken, J., Thøgersen, K., Renard, F. and Schuler, T. Surging potential and probabilistic map of surging for Svalbard glaciers. IGS Nordic Branch meeting, Oslo, Norway. November 2021
- Bouchayer, C., Aiken, J., Thøgersen, K., Renard, F. and Schuler, T. Why do glaciers surge? Understanding the controlling parameters using machine learning and simulations. EarthFlows, Oslo, Norway. December 2020
- Bouchayer, C., Aiken, J., Thøgersen, K., Renard, F. and Schuler, T. Surging potential and probabilistic map of surging for Svalbard glaciers. AGU Fall Meeting, New Orleans, USA. December 12-18 2021.

B.2 Posters

- Bouchayer, C., U. Nanni, L. Schmidt, P.M. Lefeuvre, John Hult, F. Renard and T.V. Schuler. Exploring the changes in the ice-till coupling of a surge-type glaciers. IGS Symposium on maritime glaciers, Juneau, USA. July 2022
- Bouchayer, C., U. Nanni, L. Schmidt, P.M. Lefeuvre, John Hult, F. Renard and T.V. Schuler. Observing the on-going destabilisation of Kongsvegen, an Arctic surge-type glacier. AGU Fall Meeting, Chicago, USA. December 2022
- Bouchayer, C., Aiken, J., Thøgersen, K., Renard, F. and Schuler, T. Why do glaciers surge? Svalbard Science conference, Oslo, Norway. November 2021.

B.3 Service

- Co-convener of the AGU session 'C43B: Nonlinear Responses of the Cryosphere: Glacier Surges and Other Abrupt Changes and Instabilities' - AGU Fall Meeting, Chicago, USA. December 2022

B.4 Outreach

- 'Accessing the inaccesible, the hidden secrets of glacier stability' - French Institute in Norway. October 2022

- 'A year on ice' - Pint of Science Festival, on youtube. May, 2021.
- 'Un an en Antarctique' - APECS France Polar Week, on zoom, for kids between 7 and 12 years old. November 2020